



VNIVERSITAT  
ID VALÈNCIA

VNIVERSITAT  
ID VALÈNCIA



**BIOTECMED**

Estructura de Recerca Interdisciplinar  
en Biotecnologia i Biomedicina

## **PROGRAMA DE POSTGRADO EN BIOMEDICINA Y BIOTECNOLOGÍA**

### **TYPE IV PILI AND THEIR ROLE IN VIRULENCE IN**

### ***Vibrio vulnificus***

Memoria presentada por

**Francisco Xavier Silva Hernández**

para optar al grado de Doctor con mención internacional

por la Universidad de Valencia

Dirigida por

**Dra. Carmen Amaro González**

Valencia, 2021





VNIVERSITAT  
D VALÈNCIA

VNIVERSITAT  
D VALÈNCIA



BIOTECMED

Estructura de Recerca Interdisciplinar  
en Biotecnologia i Biomedicina

La Dra. Carmen Amaro González, catedrática del departamento de Microbiología y Ecología y directora del grupo de Patógenos Acuáticos del Estructura de Recerca Interdisciplinar en Biotecnologia i Biomedicina (ERI BIOTECMED), ambos de la Universidad de Valencia, certifica que D. Francisco Xavier Silva Hernández ha realizado bajo su dirección el trabajo titulado “Type IV pili and their role in virulence in *Vibrio vulnificus*” y autoriza la lectura y defensa de la misma para optar al grado de Doctor en Ciencias Biológicas por la Universidad de Valencia.

Y para que así conste a los efectos oportunos, firma la presente en Valencia, 2021.

Fdo. Carmen Amaro González







VNIVERSITAT  
DE VALÈNCIA



BIOTECMED

Estructura de Recerca Interdisciplinària  
en Biotecnologia i Biomedicina

La Dra. Eva Sanjuan, investigadora del departamento de Microbiología y Ecología y miembro del grupo de Patógenos Acuáticos del Estructura de Recerca Interdisciplinària en Biotecnologia i Biomedicina (ERI BIOTECMED), ambos de la Universidad de Valencia, certifica que D. Francisco Xavier Silva Hernández ha realizado bajo su tutela el trabajo titulado “Type IV pili and their role in virulence in *Vibrio vulnificus*” y autoriza la lectura y defensa de la misma para optar al grado de Doctor en Ciencias Biológicas por la Universidad de Valencia.

Y para que así conste a los efectos oportunos, firma la presente en Valencia, 2021.

Fdo. Eva Sanjuan



“Theory is when you know everything but nothing works. Practice is when everything works but no one knows why. In our lab, theory and practice are combined: nothing works and no one knows why.” **Albert Einstein**

“Somewhere, something incredible is waiting to be known.” **Carl Sagan**

“I may not have gone where I intended to go, but I think I have ended up where I needed to be.” **Douglas Adams**

“Goddamit paco, you are an idiot”. **Dr. Hannes Campo**



# Acknowledgments

So, yeah, writing in Spanglish because F... it, I already wrote 170 pages in English, so who cares. Antes que nada, agradezco a mi mama, por que lo he dicho y seguiré diciendo que, sin ella no soy nada y todo lo que he logrado hasta ahora, ha sido por su apoyo y ella es la roca sobre la que me he apoyado durante toda mi vida, muchas gracias ma, ya sabes que te quiero de aquí al infinito. También le doy gracias a mi familia, mi Abue por todo su amor incondicional y su comida, mis tíos, y a todos mis primos que la mayoría ya tiene trabajo y algunos hijos, pero yo soy el raro que sigue estudiando y sin trabajo, jejeje.....

Ahora mi carnal, orgullosamente Dr. Cancino, chake, que me hemos disfrutado la carrera juntos y sufrido el doctorado aun mas. Gracias por toda la ayuda, pedas, consejos y amistad, mas que amistad, ahora es un hermano. Ya hemos vivido juntos como por 7 años o algo así jaja. También agradezco a la bandai, bandera, basuca, bambalina allá en México, que siempre es divertido despertarse y ver 14335 mensajes en whatsapp de pura mamada jajaja. Román my BFFEAEUTEOT, Chebibi y Monica y nuestros épicos momentos de peda en Madrid, Pepis jalando buena música always, Aldo el amigo mas noble (y otaku) que vas a poder tener, Tokayo (que ahora va a ser padre, MUCHISISIMAS FELICIDADES!!!), mi buen amigo de la infancia Fernando que pronto será un famoso perfumero en Paris, Limón el cítrico favorito de todos y Bulos que se perdió por la España profunda, pero siempre esta presente. Aunque llevamos ya separados muchos años y a veces no hablamos por la diferencia horaria y por la misma distancia, creo que esta amistad ya va a durar para siempre, y espero que así sea y la mantengamos hasta que se acabe el mundo, que seguro será pronto. Los quiero amiguis, con puteria ;\*.

También agradezco a todos los demás amigos que andan allá en México como los Pugs y sus encarecidas discusiones interesante en el grupo, Mariel su hermana y mis demás amigos de la infancia, saluditos a ellos también.

Now, HOW COULD I NOT MENTION MY DEAR FRIEND DR. CAMPO, holy shit who would had thought I would find my exact duplicate in Valencia and he is from Belgium. I'm black he is white, vanilla and chocolate, I'm total chaos and he probably has Asperger's, who knows.

Fiercely intelligent, amazing friend and very geeky, I would have probably not enjoyed my years in Valencia as much without this majestic golden boi and his well-endowed, girthy and VAST knowledge of Belgian beers and lord of the rings. P.D. Don't make him angry, he IS very scary. Love you bro, we will be reunited again, eventually.

Now obviously can't forget Mr. Bob my other PhD friend, which knows that doing the thesis is THE BEEEEEEEEEEEEEST, thanks for all your science communications and party hard times (before the married life). Huge thanks also to Nick and Sara for their epic hospitality and amazing bad movie nights (before covid), John and Germain also, for showing from time to time.

MUCHISIMAS GRACIAS para la Dra. Carla Hernandez-Cabanyero por aguantarme todos estos años con mis tonterías en el lab y junto con Amparo por ayudarme con los experimentos de anguilas que tanto nos encantan. Sin ellas esta tesis seguro que no hubiera sido posible.

Muchas gracias a todo mis demás compis del lab, que ya se que aunque no parece, soy bastante amigable, jaja. Muchas gracias a Miguel, mi senpai, que aunque a veces me daba miedo, aprendí mucho de él cuando aun era un tontito de primer año de doctorado. Muchísimas gracias a mis colaboradores de Taiwan donde pase uno de los mejores meses de mi vida, Huge thanks to Dr. Chun-tee and the entire lab of the Dr Lien-I Hor. Also INFINITE THANKS to Dr. Dean Rowe-Magnus and for the opportunity to go to Bloomington and save this thesis from crashing and burn with an epic mutation protocol for our dear *V. vulnificus* strain.

Lastly but not least, muchas gracias a mi tutora Eva por responder a todas mis preguntas y estar siempre para ayudar, revisar la tesis y demás y por supuesto a la jefa jefaza Carmen por ser esa chispa de locura que mantiene el laboratorio, por su confianza en mi y por darme tantas oportunidades al estar en este equipo de investigación.

Y bueno, que mas queda que, cerrar estos 5+ años que llevo aquí, rompiéndome la cabeza, llorando, bebiendo, frustrándome, riendo y, sobre todo, investigando. Muchas gracias a todos los que pasaron por mi vida durante estos años, y en especial a CONACYT por financiarme este titulo. Perdón si no los mencione pero mi cerebro ya no da para mas, entiéndanme :P.

## Resumen

Las bacterias del género *Vibrio*, compuesto por más de 100 especies, están presentes en la gran mayoría de los ecosistemas acuáticos alrededor del mundo. Estas bacterias son gram-negativas, aeróbicas y anaeróbicas facultativas, y cuentan con al menos un flagelo polar. Se pueden encontrar tanto como un organismo de vida libre en el agua, como habitando superficies bióticas y abióticas en forma de agregaciones inmóviles llamadas biofilms. Una gran cantidad de especies pertenecientes a este género son patógenas para los humanos, dentro de las cuales, las tres más importantes son, *V. cholerae*, *V. parahaemolyticus*, y *V. vulnificus*, debido a su elevada tasa de incidencia y gravedad de las infecciones causadas por ellos.

*V. vulnificus* es considerado como un agente zoonótico de gran importancia para la salud pública. Esta especie fue descrita en los años 70 por diversos estudios, debido a que fue encontrada al mismo tiempo en pacientes septicémicos en los Estados Unidos, y en aislados de anguilas pertenecientes a granjas de acuicultura en Japón. Inicialmente esta bacteria fue clasificada dentro de un género totalmente diferente, pero consecuentes pruebas relacionadas con sus características fenotípicas y metabólicas lo llevaron a ser clasificado dentro de el género *Vibrio* y finalmente denominado como *V. vulnificus* en 1979. Tras varios análisis genómicos, se demostró que los aislados procedentes de pacientes septicémicos y anguilas enfermas eran de la misma especie, aunque demostraban algunas diferencias fenotípicas. Esto llevó a los autores de dichos análisis a proponer una clasificación de la especie en 3 biotipos diferenciados por sus características metabólicas y especificidad de hospedador. Dentro de estos biotipos, el biotipo 2 (Bt2) agrupaba varias cepas aisladas de anguilas, las cuales contaban con características serológicas casi idénticas, y por lo cual fueron designadas como serovar E (SerE). Con el paso del tiempo, se describieron otras serovares provenientes de anguilas, aunque estas resultaron ser menos virulentos para las mismas anguilas y para ratones, y por consiguiente, la SerE fue denominada como un agente causante de la vibriosis humana, el cual tenía la capacidad de infectar tanto humanos como peces, convirtiéndolo en un complejo zoonótico clonal. Esta habilidad infectiva hacia peces es concedida por el plásmido de virulencia pVvBt2, el cual se

encuentra en todas las cepas de este biotipo, y confiere los mecanismos necesarios para resistir al sistema inmune de los peces.

Debido a la alta heterogeneidad de la especie, esta clasificación de biotipos esta siendo revisada actualmente y se han propuesto, tras varios análisis genómicos, la implementación de una nueva taxonomía basada en 5 linajes diferentes, incluyendo una patovariedad denominada *piscis*, cuya característica representativa es la posesión del pVvbt2. Esta patovariedad incluye todos los aislados virulentos para peces, incluyendo el complejo zoonótico clonal, cuya cepa representativa es la CECT 4999, comúnmente denominada R99 en las colecciones de laboratorio. Esta cepa fue aislada en 1999 a partir de anguilas europeas enfermas, y es la cepa usada en este estudio. Su genoma consta de dos cromosomas, uno de un tamaño relativamente grande y otro más pequeño, en el cual se encuentran la mayor parte de los genes relacionados con virulencia. Por otro lado, el plásmido cuenta con una gran cantidad de genes identificados previamente, así como varias proteínas hipotéticas, y como ya se menciono antes, los genes necesarios para infectar a peces.

*V. vulnificus* es capaz de causar una variedad de sintomatologías, que en conjunto se denominan vibriosis, tanto en peces como en humanos. Esta enfermedad está caracterizada por diferentes síntomas que varían dependiendo de la ruta de entrada e infección del patógeno. Algunas de las manifestaciones clínicas causadas por la vibriosis son, necrosis, gastroenteritis, fascitis y en el peor de los casos, septicemia fulminante, la cual conlleva la muerte. En humanos la vibriosis se puede contraer mediante la ingesta de mariscos contaminados, o mediante la exposición de heridas a agua o animales marinos portadores de la bacteria. Personas que padecen enfermedades crónicas como cirrosis, hepatitis, cáncer e inmunodeficiencias son 80 veces mas propensos a sufrir una septicemia fulminante causada por *V. vulnificus*. Cabe resaltar que, las patologías del hígado causan elevados niveles de hierro en la sangre, y se ha demostrado que esta característica es sumamente favorable para las infecciones causadas por este patógeno. Afortunadamente, las infecciones causadas por *V. vulnificus* son relativamente raras, sin embargo, en los Estados Unidos, se ha estimado que mas de 80,000 personas contraen vibriosis cada año, de las cuales aproximadamente 500 casos resultan en hospitalizaciones y 100 de ellos en muerte. Esto ocurre debido a que, existen co-



morbilidades que afectan al resultado de la infección. En peces, la vibriosis puede ocurrir en dos modalidades causadas por la SerE, la modalidad de agua dulce y de agua salobre. Los signos clínicos mas comunes asociados a la vibriosis de peces son lesiones externas en el abdomen, ano, opérculo, úlceras y abdomen inflamado, mientras que internamente se presenta inflamación intestinal, palidez del hígado e inflamación del riñón. Igual que en humanos, los casos septicémicos en peces presentan una gran probabilidad de muerte.

Este patógeno es capaz de causar una septicemia fulminante debido a sus diversos factores de virulencia, que le confieren a la capacidad de infectar a peces y humanos a través de diversos mecanismos. Desafortunadamente, estos factores de virulencia aun no se conocen en su totalidad, por lo que actualmente siguen siendo estudiados. La producción de vibriosis por este patógeno es un proceso multifactorial que se logra mediante la acción sinérgica de diversos mecanismos celulares, los cuales permiten a la bacteria ser motil, adherirse a diferentes superficies, producir biofilms, sobrevivir la acción bactericida del sistema inmunitario, adquirir hierro dentro del hospedador y producir enzimas citotóxicas y citolíticas. En peces, la patovar *piscis*, mediante el pVvbt2, produce dos importantes proteínas, la Ftbp y la Fpcrp, que confieren la habilidad de secuestrar el hierro de la sangre, y de resistir las acciones bactericidas del complemento y la fagocitosis respectivamente. En general, el factor de virulencia mas importante de *V. vulnificus* es la capsula, debido a que se ha demostrado que variantes acapsulados de la especie son avirulentos, y el polisacárido de la cápsula es el único factor esencial necesario para la resistencia del complemento en sangre humana. Por otro lado, en anguilas, la cápsula resulta ser esencial solamente para la vibriosis transmitida a través del agua y dirigida a la colonización de las branquias.

Sin embargo existen otros factores de virulencia que influyen de forma importante el curso de la infección causada por *V. vulnificus*. Añadidos al polisacárido de la cápsula, los lipopolisacárido también influyen en la letalidad causada por las infecciones de vibriosis que surgen por el consumo de marisco contaminado. Esto se debe a que la cápsula ayuda en gran medida a que la bacteria se proteja de el ambiente hostil y ácido encontrado en el tracto digestivo. De igual forma, la bacteria secreta diversas enzimas y toxinas que están involucradas en daño celular. Una de las mas importantes es la toxina RtxA1, que está directamente

relacionada con la producción de sepsis y citotoxicidad. Otras toxinas, como la VvhA y la VvpE, también están involucradas en citotoxicidad y daño celular, y se hipotetiza que aunque individualmente no tienen un efecto importante en la virulencia, ejercen un efecto aditivo o de soporte hacia otras toxinas mas importantes como la RtxA1, incrementando así la acción toxica de la bacteria. Otro importante factor de virulencia es la capacidad de adquisición de hierro dentro del hospedador, que le permite a la bacteria superar la inmunidad nutricional que se presenta dentro del hospedador. La adquisición de hierro es un fator critico para la patogenicidad de *V. vulnificus*. Para esto, la bacteria cuenta con dos sistemas generales de captación de hierro, un sideróforo con su receptor, y un receptor de hemina. Estos mecanismos le permiten al patógeno secuestrar el hierro del hospedador, como se demostró en un estudio donde al ser irrumpidos, la bacteria perdió totalmente su virulencia en ratones. Sin embargo, esto no sucede en anguilas, debido a la existencia de un tercer sistema de captación de hierro especifico para peces, el ya mencionado Ftbp, codificado en el plásmido de virulencia.

La relación entre el hierro y la virulencia de *V. vulnificus*, abarca diferentes mecanismos de patogenicidad como toxinas y enzimas que le permiten sobrevivir a los efectos del sistema inmune. Sin embargo, existen otro tipo de mecanismos físicos en forma de apéndices bacterianos, que también participan en la virulencia de la bacteria. El mas conocido de estos apéndices es el flagelo, el aparato de motilidad mas importante para diversos géneros de bacterias. Este organelo permite a las células bacterianas moverse a altas velocidades hacia quimio atrayentes como, potenciales hospedadores o gradientes de nutrientes en el ambiente. Sin embargo, el flagelo también es usado por diversos patógenos como mecanismo de supervivencia, de colonización y de invasión hacia sus hospedadores. No obstante, también existen otros tipos de apéndices involucrados en la patogenicidad en *Vibrios* y en otras especies bacterianas, estos son los pelos o “pili”. Los pili bacterianos son organelos filamentosos que están presentes en la superficie de diversas bacterias gram negativas. Estos apéndices cuentan con una gran cantidad de funciones tales como; intercambio génico entre células, adhesión, evasión del sistema inmune, agregación bacteriana y producción de biofilms. Entre estos apéndices, se encuentra una familia especial llamada Pili tipo IV. Esta multifuncional familia de pili, además de ejercer las funciones ya mencionadas, también está involucrada en motilidad.

Esta habilidad es posible gracias a la característica única que poseen estos apéndices de extenderse y retraerse. Este mecanismo crea un “arpón” bacteriano que impulsa la bacteria y le permite moverse en diversas superficies. Esta habilidad también le permite a la bacteria movilizarse hacia otras células para comenzar la formación de biofilms y colonizar así otras superficies.

Dentro de la familia de los Pili tipo IV, existen dos tipos de pili con diversas características especiales, los cuales están involucrados directamente en la formación de biofilms y en cierta manera en la virulencia: los MSHA pili y los Tad pili. Los MSHA pili (pili sensitivo a manosa de hemaglutinación) han sido estudiados extensamente en patógenos como *V. cholerae*, sin embargo no se ha descrito mucho en *V. vulnificus*. Estos apéndices están involucrados en la adhesión inicial a sustratos en el ambiente acuático, y son necesarios para la persistencia de la bacteria en el medio ambiente. De igual forma, también son esenciales para la formación de biofilms. Ninguna función del pelo MSHA en torno a virulencia había sido descrita hasta hace poco, cuando se describió el papel que desempeñan en la colonización del intestino de ratones. Estos apéndices tienen que ser reprimidos y destruidos para evitar que el sistema inmune los reconozca y emita una señal que alerte al sistema inmune. Sin embargo, estos estudios solo se han realizado en *V. cholerae* y las funciones patogénicas de este pili aun no han sido descritas en su totalidad para otras especies. Los Tad pili, por sus siglas en inglés, *Tight adherence*, se diferencian de los demás por ser notablemente pequeños y no estar asociados con motilidad celular. Sin embargo, los Tad pili desempeñan importantes funciones en patogénesis, así como también en producción de colonias rugosas, adhesión y formación de biofilms. Estos apéndices han sido relacionados con el aparato de secreción celular Tipo II debido a su estructura y proteínas relacionadas con su biosíntesis que presentan cierta homología con los de estos sistemas de secreción. Los Tad pili se encuentran codificados por los *tad* loci, los cuales se encuentran dentro de los genomas de diversos *Vibrios* y, sorprendentemente, varias de estas especies presentan más de un *tad* loci. *V. vulnificus* cuenta con 3 *tad* loci distintos que se han denominado de la siguiente manera: *tad-1*, *tad-2* y *tad-3*. Independientemente de las funciones ya mencionadas que ejercen los Tad pili, solo se han descrito un puñado de funciones específicas relacionadas a *tad-3*, el cual está involucrado en la persistencia ambiental y la

resistencia que confiere a los biofilms ante fuerzas mecánicas exteriores, como corrientes acuáticas. Sin embargo, un estudio reciente ha propuesto la hipótesis que, aunque individualmente los *tad* loci no participan mayoritariamente en producción de biofilms y virulencia, es necesario que los tres sean expresados para conferir un mecanismo de evasión hacia el sistema inmune del hospedador.

En conclusión, *V. vulnificus* es un patógeno zoonótico de gran importancia sanitaria a nivel mundial. Esto lo convierte en un sujeto de estudio altamente importante para poder elucidar los mecanismos de patogénesis que lo convierten en un patógeno peligroso, no solo para la salud pública, sino también para la acuicultura que sufre grandes pérdidas por brotes infecciosos de vibriosis. Estos factores de virulencia funcionan de forma sinérgica para lograr una evasión del sistema inmune y un ataque al hospedador efectivo, el cual es sorprendentemente rápido. Es por esto que el estudio de dichos factores nos ayudara a comprender integralmente la patogénesis producida por esta bacteria y por tanto a combatirla de una mejor manera.

**El primer objetivo general** de el presente trabajo fue descubrir si los Pili tipo IV del complejo zoonótico clonal estaban controlados por hierro. Esto surgió debido a que en nuestro estudio transcriptómico anterior, varios genes involucrados en dos sistemas de Pili tipo IV (*MSHA* y *Tad*), estaban siendo diferencialmente expresados por hierro. Por consiguiente, al observar que el genoma de *V. vulnificus* contaba con tres genes distintos de *mshA*, los cuales supuestamente codificarían para la principal subunidad estructural de dicho pelo, nuestro **segundo objetivo general** fue averiguar si las dos copias extras de *mshA* estaban involucradas en la formación de biofilms y adhesión a superficies. Para esto, generamos diversos mutantes knock-out de estos genes en la cepa representativa del complejo zoonótico clonal y los testamos individualmente para observar sus capacidades de adhesión y producción de biofilms. Finalmente, el **tercer objetivo general** fue determinar las funciones, si es que existen, de los dos sistemas de Pili tipo IV en la virulencia del complejo zoonótico clonal. Esto se abordó mediante la obtención de cepas mutantes para los genes de la subunidad mayor de los *tad* loci. Tras haber obtenido todos los mutantes necesarios, procedimos a observar la capacidad de producción y las estructuras de biofilms de toda las cepas, cuantificando su producción mediante diversas

metodologías. Finalmente, pusimos a prueba la capacidad de virulencia ante anguilas a través de diferentes ensayos *in vivo* y *ex vivo*.

Para cumplir nuestros objetivos generales, diseñamos y ejecutamos el siguiente esquema experimental:

1. Para observar qué genes están influenciados por hierro, hemos analizado el perfil transcriptómico de la cepa representativa del complejo zoonótico clonal al crecerla en presencia y ausencia de hierro.
2. Para obtener los mutantes de los genes seleccionados a partir del análisis transcriptómico, los cuales incluyen a los sistemas MSHA, Tad pili y su peptidasa, y el flagelo, probamos varios protocolos de mutación bacteriana, y finalmente diseñamos un protocolo de mutación. Esto con el fin de encontrar y utilizar la metodología más eficaz para la producción de diversos mutantes simples y compuestos en el complejo zoonótico clonal de *V. vulnificus*.
3. Para averiguar las funciones en virulencia de los genes seleccionados, efectuamos diversas pruebas *in vivo*, *in vitro* y *ex vivo*. En estos experimentos testamos las capacidades de infección, colonización, virulencia, adhesión y producción de biofilms. Para esto, aplicamos diversas metodologías y tecnologías como; microscopia confocal, microscopia de fluorescencia, infecciones por baño e intraperitoneales, entre otras.

Después de obtener la extensa librería de mutantes necesarios y concluido satisfactoriamente las extensas pruebas fenotípicas e infecciones con animales, hemos obtenido los siguientes resultados.

**El método de mutagénesis basado en pTfoX y transformación natural es el más efectivo para crear mutantes en el complejo zoonótico clonal.** Después de probar diversos métodos para la generación de mutaciones en la cepa de R99, y de diseñar un protocolo nuevo utilizando la enzima de digestión NotI, con el cual pudimos obtener un mutante con dominio de glicosiltransferasa llamado *s/t*, hemos llegado a la conclusión que usar el plásmido pTfoX es la forma más eficiente de deletar genes. Mediante la inducción artificial de la transformación natural, que en las especies del género *Vibrio* está regulada por el gen *tfoX*, y el uso de PCR's anidadas, la construcción e inserción de un constructo artificial de mutación en el genoma del

complejo zoonótico clonal resultó ser altamente eficiente. Este método es suficientemente estable y reproducible para obtener diversos mutantes en poco tiempo. Este proceso puede ser manipulado fácilmente para obtener dobles, e incluso triples mutantes, al variar la implementación de casetes de resistencia a antibióticos.

***V. vulnificus* tiene tres copias distintas de la subunidad mayor del pelo MSHA en su genoma, pero solo uno de ellos es funcional.** El complejo zoonótico clonal, así como varias otras especies pertenecientes al género *Vibrio*, cuentan con tres genes *mshA* codificados en su genoma. Sin embargo, solo uno de ellos se encuentra dentro de un locus funcional, previamente descrito, que está encargado de la biosíntesis de los MSHA pili. Hasta donde sabemos, este es el primer trabajo donde se estudian los dos genes *mshA* extra que se encuentran en el genoma de *V. vulnificus*. Con fines de esta investigación, los hemos denominado *mshA-1*, *mshA-2* y *mshA-3*. Al comparar las secuencias y estructuras proteicas de los tres genes, es evidente que, aunque conservan cierta homología en su secuencia, son significativamente diferentes entre sí. Aunado a esto, tras hacer un estudio filogenético, se observó que los genes *mshA-2* y *mshA-3* están bastante conservados en diversas especies de *Vibrios*, mientras que el *mshA-1* se encuentra en un clúster donde se observa más heterogeneidad entre sus secuencias. Esto podría indicar que, de ser el único gen funcional, sus tareas podrían variar de cierta forma dependiendo de cada especie y de su ambiente específico. Tras poner a prueba las cepas mutantes de los 3 genes sobre sus capacidades de producción de biofilms y analizando los resultados mediante de microscopía confocal y tinción con cristal violeta, fue evidente que solo el gen *mshA-1* estaba involucrado en la formación de biofilms. Esto se comprobó debido a que la delección de los otros genes no afectó en absoluto a este mecanismo. Además, al probar la adhesión a superficies bióticas tras una prueba utilizando caparazones de crustáceo como sustrato, solo el mutante de *mshA-1* resultó ser ineficiente en su adhesión. Finalmente, al probar la influencia de los pili MSHA en la virulencia del complejo zoonótico clonal, observamos que estos pili influyen de manera significativa la adhesión a branquias de las anguilas, ya que al estar incapacitados mediante la delección de *mshA-1*, la bacteria fue deficiente en infección por el medio acuático. Curiosamente, el mutante en este gen no fue deficiente en la infección intraperitoneal, ni tampoco fue más sensible al suero

humano ni de anguila. Estos resultados nos indican que, solamente el gen *mshA-1* está involucrado en la producción de los MSHA pili, y por consiguiente, es el único gen involucrado en la producción de biofilm y adhesión a superficies. De igual forma, en este estudio describimos por primera vez el papel que juegan los pili MSHA en la virulencia de anguilas en el complejo zoonótico clonal.

**El flagelo juega un papel significativo en la virulencia del complejo zoonótico clonal y en el crecimiento de la bacteria.** Tras obtener un mutante en el flagelo al delecionar el gen *flgE* que codifica para la proteína hook que ancla el filamento flagelar a la bacteria, observamos un cambio significativo en el crecimiento celular. Al parecer, al perder el flagelo, la bacteria tiende a producir una mayor población y biomasa al llegar a la fase estacionaria. Esta diferencia se observó al comparar el crecimiento total del mutante con el de la R99 a través de absorbancia y recuento en placa. Curiosamente, no se observaron diferencias en el crecimiento durante las primeras 8 horas, solo se observaron tras una incubación *overnight* (18 horas). Sin embargo, aunque el mutante exhibió un crecimiento mayor, este exceso de crecimiento no afectó la producción de biofilms, debido a que los niveles de biomasa producidos eran comparables con los de la cepa mutante si se discriminaban las células bacterianas no adheridas. Por otro lado, el mutante de flagelo resultó ser deficiente en la virulencia para anguilas cuando estas se infectan a través del medio acuático. Este resultado era de esperarse, ya que al ser inmóviles, las bacterias no tienen la capacidad de ser atraídas ni de moverse hacia el hospedador o las branquias, las cuales son el principal portal de entrada hacia el organismo. Sin embargo, al inyectar el mutante por la vía intraperitoneal, no hubo diferencia alguna entre la virulencia de este de la cepa salvaje. Estos resultados difieren con los obtenidos en una investigación previa, donde el flagelo resultó ser necesario para una colonización eficiente por *V. cholerae* del intestino de ratón. No obstante, al ser una especie diferente, una comparativa estricta no puede realizarse, así como se debe tener en cuenta la gran diferencia existente entre hospedadores. Esto puede influir de manera significativa en la forma en que la bacteria sortea los obstáculos del ambiente interno del hospedador, como por ejemplo, la complejidad y protección mucosa que existe en los intestinos de ratones, que no son similares a los intestinos de anguilas.

**La peptidasa VvpD juega un papel importante en la virulencia del complejo zoonótico clonal.**

Estudios previos en *P. aeruginosa*s han demostrado que la peptidasa PILD es necesaria para la biogénesis de los Pili tipo IV y es la encargada de modificar las prepilinas y convertirlas en pili funcionales, así como para la secreción extracelular. El homólogo de esta peptidasa en *V. vulnificus* es la VvpD, y nuestros resultados demuestran que es necesaria para la secreción extracelular tanto de la hemolisina como de la proteasa. De igual forma, hemos confirmado que esta peptidasa es necesaria para la virulencia de anguilas, ya que el mutante de *vvpD* es totalmente avirulento tanto en infección por vía intraperitoneal como por agua. El mutante de la peptidasa también es más susceptible al suero de anguila que al suero humano, lo cual indica que, tal vez esta peptidasa está involucrada en la secreción de alguna enzima o proteína que confiere resistencia a la bacteria contra suero de anguila. Finalmente, la delección de esta enzima, como se ha demostrado en trabajos anteriores, afecta el crecimiento de la bacteria. De igual manera, las cepas deficientes en la peptidasa presentan una formación aberrante de biofilm y menor producción del mismo, lo cual era de esperar, debido a que esta enzima está encargada del correcto funcionamiento de los Tad pili y estos están relacionados con adhesión y biofilm.

**Los tres *tad* loci deben ser funcionales para influenciar la producción de biofilm y virulencia en el complejo zoonótico clonal.**

Diversos estudios genéticos han demostrado la presencia de estos pili en varias bacterias gram negativas, un ejemplo muy claro es en el género *Vibrionaceae*. Se ha descrito que varias especies pertenecientes a este género contienen más de un locus *tad*, y en el caso de *V. vulnificus*, existen tres distintos. Después de probar las capacidades de producción de biofilm de cada *tad* loci de manera individual y en combinación, incluyendo un triple mutante, llegamos a la conclusión que los tres *tad* loci deben ser funcionales para que, de manera sinérgica, desempeñen un papel en la producción de biofilms. Anteriormente se había descrito que uno de los *tad* loci, el *tad-3*, estaba relacionado con la capacidad de la bacteria de crear biofilms robustos y resistentes ante fuerzas mecánicas exteriores provenientes del ambiente que coloniza. Sin embargo, en nuestro estudio, el locus *tad-3* no mostró ninguna relación con la producción de biofilms, esto podría deberse a dos



razones: la primera, es que la cepa utilizada en el estudio anterior es una cepa clínica conocida por ser virulenta para humanos. La segunda razón podría ser que el gen *flp* encargado de procesar la subunidad mayor del pelo estaba sobre expresado, debido a que la cepa usada era una descendiente de la cepa clínica y presentaba un incremento cuatro veces mayor en la producción de biofilms. De igual forma, para que los *tad* loci influenciases la virulencia del complejo zoonótico clonal, deben ser funcionales. Esto fue comprobado al hacer diferentes ensayos de virulencia en los cuales únicamente el triple mutante demostró ser deficiente en la colonización de anguilas. Sin embargo, el triple mutante únicamente fue deficiente en la adhesión inicial a las agallas, sin mostrar ningún impedimento para invasión y colonización de otros órganos. Curiosamente, el triple mutante pareció no presentar impedimento alguno en virulencia al ser inyectado por la vía intraperitoneal. Este resultado es diferente al obtenido en una investigación anterior, donde un mutante triple de los *tad* loci en una cepa clínica de *V. vulnificus*, resultó ser menos virulenta para ratones. De igual forma en el mismo estudio, el triple mutante mostró una resistencia menor al complemento del suero de ratón. Independientemente de los resultados anteriores, nuestro triple mutante no mostró deficiencia alguna en crecimiento tanto en suero de humano como de anguila, y no existieron diferencias entre la cepa parental y la mutante frente a la actividad de macrófagos humanos.

En conclusión, nuestros resultados arrojan nueva información que relaciona nuevas funciones de dos sistemas de Pili tipo IV, así como al flagelo, a producción de biofilms y virulencia en el complejo zoonótico clonal de *V. vulnificus*. Esto sugiere que, aunque se tengan registros pasados de funciones de sistemas similares, estos pueden cambiar y/o expandirse dependiendo de la especie y nicho donde se encuentren, lo cual implica que la existencia de diversos mecanismos celulares con funciones diferenciales entre especies e incluso entre cepas. Por este motivo una generalización en bacterias o el nombramiento de una especie tipo que represente a toda un género, como *V. cholerae*, debería de reconsiderarse al menos en torno a mecanismos complejos como lo son los de virulencia.



## INDEX

<b>RESUMEN</b>	<b>11</b>
<b>ABBREVIATIONS</b>	<b>27</b>
<b>INTRODUCTION</b>	<b>29</b>
<b>1.- <i>Vibrio vulnificus</i>: multi host pathogen</b>	<b>31</b>
1.1.- Phylogeny	31
1.2.- Natural reservoirs and epidemiology	34
<b>2.- Vibriosis</b>	<b>36</b>
<b>3.- Human vibriosis</b>	<b>37</b>
<b>4.- Fish vibriosis</b>	<b>39</b>
<b>5.- Virulence determinants</b>	<b>40</b>
5.1.- Capsule polysaccharide	41
5.2.- Lipopolysaccharides	42
5.3.- Toxins and enzymes	43
5.4.- Host immune evasion	47
5.5.- Iron acquisition	48
<b>6.- Bacterial appendages</b>	<b>51</b>
6.1.- The flagellum	51
6.2.- Bacterial pili	55
6.3.- Type IV pili	56
6.4.- The MSHA pili	62
6.5.- Tight adherence pili	65
<b>7.- Biofilm</b>	<b>68</b>
<b>8.- References</b>	<b>77</b>
<b>HYPOTHESIS AND OBJECTIVES</b>	<b>91</b>
<b>GENERAL METHODOLOGY</b>	<b>95</b>
<b>1.- Obtention of mutants in the zoonotic clonal-complex</b>	<b>97</b>
<b>2.- <i>In silico</i> analysis</b>	<b>100</b>

2.1.- MSHA major pilin subunit genes analysis and alignments	100
2.2.- MSHA proteins analysis	100
<b>3.- Bacterial strains, growth and media conditions</b>	<b>100</b>
<b>4.- Maintenance of animals and serum/blood cells obtention</b>	<b>103</b>
<b>5.- Transcriptomic analysis and Rt-qPCR</b>	<b>103</b>
<b>6.- Microarray data analysis</b>	<b>104</b>
6.1.- Data validation by Rt-qPCR	104
<b>7.- Development of a new directed-mutagenesis protocol adapted to the zoonotic clonal-complex of <i>V. vulnificus</i></b>	<b>104</b>
7.1.- Protocols assessed	104
<b>8.- Mutant complementation</b>	<b>112</b>
<b>9.- <i>In vitro</i> assays</b>	<b>112</b>
9.1.- Biofilm formation and quantification	112
<b>10.- <i>Ex vivo</i> assays</b>	<b>113</b>
10.1.- Resistance and growth in serum	113
10.2.- Hemagglutination test	113
10.3.- Proteolytic and hemolytic activity	113
10.4.- Infection experiments with cell lines	114
10.5.- Adhesion to crab shells as biotic surfaces	114
<b>11.- <i>In vivo</i> assays</b>	<b>115</b>
11.1.- Virulence and co-colonization	115
<b>12.- Scanning electron microscopy</b>	<b>115</b>
<b>13.- Statistical analysis</b>	<b>116</b>
<b>14.- Ethical statement</b>	<b>116</b>
<b>15.- References</b>	<b>117</b>
<b>RESULTS</b>	<b>121</b>
<b>1.- Transcriptomic study in iron rich and poor media</b>	<b>123</b>
<b>2- Microarray validation</b>	<b>125</b>

<b>3.- Development of a mutation protocol for the zoonotic clonal-complex</b>	<b>126</b>
3.1.- Obtention of a non-motile mutant	126
3.2.- Obtention of the <i>s/t</i> mutant	126
3.3.- TfoX-induced transformation as the standard technique for mutagenesis in the zoonotic clonal complex	127
<b>4.- MSHA pilus and eel virulence</b>	<b>127</b>
4.1.- The zoonotic clonal-complex of <i>Vibrio vulnificus</i> harbors three distinct copies of the MSHA major pilin subunit gene	127
4.2.- <i>Ex vivo</i> and <i>in vitro</i> assays	132
4.3.- <i>In vivo</i> assays	136
<b>5.- Prepilin peptidase virulence for eels</b>	<b>138</b>
5.1.- <i>In vitro</i> assays	138
5.2.- <i>Ex vivo</i> and <i>in vivo</i> experiments	139
<b>6.- Tad pili and eel virulence</b>	<b>140</b>
6.1.- <i>In vitro</i> assays	140
6.2.- The Tad pili and their role in virulence	143
<b>7.- Flagellum and virulence for eels</b>	<b>145</b>
7.1.- <i>In vitro</i> assays	146
7.2.- <i>In vivo</i> assays	149
<b>8.- References</b>	<b>150</b>
<b>DISCUSSION AND CONCLUSIONS</b>	<b>153</b>
<b>1.- Discussion</b>	<b>155</b>
<b>2.- Conclusions</b>	<b>169</b>
<b>3.- References</b>	<b>171</b>
<b>APENDIX</b>	<b>177</b>



## ABBREVIATIONS

+Fe	Supplemented with 100 $\mu$ M FeCl <sub>3</sub>
+Tf	Supplemented with 10 $\mu$ M human apo-transferrin
Abs <sub>x</sub>	Absorbance at x nm
Amp	Ampicillin
Bp	Base pairs
Bt	Biotype
C	Clinical
cDNA	Complementary DNA
CFU	Colony forming units
Chr	Chromosome
CM9	M9 broth supplemented with 0.2% casamino acids
CM	Chloramphenicol
DNA	Deoxyribonucleic acid
E	Environmental
ECPs	Extracellular products
FC	Fold change
Fpcrp	Fish phagocytosis and complement resistance protein
Ftbp	Fish transferrin binding protein
Fur	Ferric uptake regulator
HMW	High molecular weight
Ilk-8	Proinflammatory cytokine
i.p.	Intra-peritoneal
IPTG	Isopropyl $\beta$ -D-1-thiogalactopyranoside
IROMP	Iron regulated outer membrane protein
Km	Kanamycin
L	Lineage
LB	Luria Bertani broth
LBA	Luria Bertani broth + 2% agar
LD <sub>50</sub>	Lethal dose 50
LPS	Lipopolysaccharide
MARTX	Multifunctional autoprocessing repeat in toxin
MCs	Monocyte cells
MOI	Multiplicity of infection
MS	Minical salts medium
MSg	Minimal salts medium + 10% glycerol
MSHA	Mannose-sensitive hemagglutination

mRNA	Messenger RNA
NO	Nitric oxide
NT	Non tested
OM	Outer membrane
OMP	Outer membrane protein
ORF	Open reading frame
PAMP	Pathogen-associated molecular pattern
PBS	Phosphate buffered saline
pR99	R99 strain pVvBt2
pv.	Pathovar
pVvBt2	<i>V. vulnificus</i> pv. <i>piscis</i> virulence plasmid
R99	<i>V. vulnificus</i> pv. <i>piscis</i> SerE wild-type representative strain (CECT4999 strain)
RNA	Ribonucleic acid
RNAseq	RNA sequencing
RT-qPCR	Reverse-transcription quantitative polymerase chain reaction
SCSIE	Servei Central de Suport a la Investigació (Experimental Central Service for Experimental Research)
Ser	Serotype
Sm	Streptomycin
TLR	Toll-like receptor
TNF	Tumor necrosis factor
Tp	Trimethoprim
TPH-1	Human peripheral blood MCs
tRNA	Transfer RNA
TSA	Tryptone soy agar
VBNC	Viable but nonculturable
vps	Vibrio polysaccharide
vs	Versus





# **INTRODUCTION**

---



## 1.- *Vibrio vulnificus*: a multi-host pathogen

### 1.1- Phylogeny and taxonomy overview

The genus *Vibrio* is ubiquitous to the water ecosystems around the world and is composed by approximately of 150 species. They are gram-negative bacteria that can have straight or curved shapes, and are motile by at least one polar flagellum. They are chemoorganotrophs, and facultative anaerobes, having both respiratory and fermentative metabolisms. These bacteria are found both as free-living planktonic bacteria in the water column and sessile cells which form biofilms on biotic and abiotic surfaces (Ill *et al.*, 2015; Tonon *et al.*, 2015). Approximately a dozen *Vibrio* species are known to cause disease in humans, but several other species are responsible for disease in marine organisms, including fish, coral and aquatic invertebrate like mollusks and crustaceans. Among the human pathogens, *V. cholerae*, *V. parahaemolyticus*, and *V. vulnificus* are the most important ones, both in incidence and severity of cases. The last one is considered a zoonotic agent (Amaro and Biosca, 1996). The impact of this group of bacteria in aquatic life (mainly farmed species) and human health justifies the monitoring and study of this diverse group (Toranzo *et al.*, 2005).

*V. vulnificus* was first described in 1975, by Hollis *et al.*, (1976) from septicemic patients in the United States. The clinical isolates were halophilic vibrios that distinguished themselves from the rest by their ability to ferment lactose. These lactose-positive isolates were named *Beneckea vulnifica* (Reichelt *et al.*, 1976). Some time later, J. J. Farmer 3<sup>rd</sup> proposed to transfer the species to the genus *Vibrio*, and rename it as *Vibrio vulnificus* (Farmer, 1979). In parallel, a series of strains were isolated from diseased eels (*Anguilla japonica* and *A. anguilla*) in farms of Shintoku, an island in Japan, which prevailed in brackish and warm waters during the summer. These isolated strains were classified as *Vibrio anguillarum* type B or *V. anguillcida*, although their phenotypic features were more akin to *V. fischeri* (Muroga *et al.*, 1976). Later, DNA hybridizations demonstrated that the eel and human isolates belonged to the same species, although they differed in some phenotypic traits, such as indole production and predilection for different hosts. This led to a proposal of a subdivision of the species into two biotypes: Biotype 1 (Bt1), which comprised isolates similar to the ones used in the description of the species, and

included human and environmental isolates, and Biotype 2 (Bt2) that clustered indole negative eel-isolates (Tison *et al.*, 1982). These eel isolates were serologically identical, thus this new serovar was designated as serovar E (SerE) in 1996 (Biosca *et al.*, 1996). This serovar was confirmed as a causative agent of human vibriosis, when it was confirmed that a human clinical isolate from the ATCC (American Type Culture Collection) belonged to this specific serovar and was virulent for eels (Amaro and Biosca, 1996). A third Biotype (Bt3) was described by Bisharat *et al.*, and included strains isolated from wound and bacteremia of patients who had been in contact with inland cultured tilapia. All these strains showed biochemical and genetical properties not found in the other strains (Bisharat *et al.*, 1999).

Over the time, new serovars were isolated from diseased eels (Høi *et al.*, 1998; Fouz and Amaro, 2003), however these serovars were less virulent for eels and avirulent for mice, which made the first described SerE the only zoonotic variant of the species (Fouz *et al.*, 2010). The capability of the Bt2 to infect humans and fish lies within the possession of a virulence plasmid (pVvBt2) present in all the strains of this biotype that confers the means to resist and escape the innate immunity of fish (Lee *et al.*, 2008; Valiente, Lee, *et al.*, 2008; Amaro *et al.*, 2015; Roig *et al.*, 2018).

*V. vulnificus* is a highly heterogeneous bacterial species, thus the subdivision into subtypes does not represent the real relationship among the strains. To find out these relationships, several sequence-based analyses (e.g., MLSA; Multi-Locus Sequence Analysis) were performed by different laboratories (Koton *et al.*, 2015; López-Pérez *et al.*, 2019). In those studies, the species was divided into two lineages in relation with their human pathogenic potential but not with the biotype, this were the Clinical (C) and Environmental (E) lineages. The Clinical lineage grouped most human clinical isolates, and the Environmental grouped most environmental isolates, including Bt2 strains from diseased eels, however, the positioning of Bt3 in either lineage changed depending on the phylogenetic approach used (Bisharat *et al.*, 2005; Cohen *et al.*, 2007). Furthermore, another MLST analysis, revealed a polyphyletic origin of the Bt2 strains, and proposed the reclassification of this group into a pathovar that contains all the strains with fish-pathogenic potential (Sanjuán *et al.*, 2011). The authors also performed

and e-burst analysis that confirmed that all SerE strains constituted a clonal-complex that infects fish and can infect humans (unpublished results).

Later, a robust phylogenetic study was performed by Roig *et al.*, (2018) from the analysis of 80 genomes from strains belonging to the three biotypes isolated worldwide from clinical (human and animal) and environmental samples. The authors concluded that the species was subdivided into five supported lineages that did not correspond with the current biotypes (**Figure 1**). Lineage 1 (L1) included the most dangerous strains for public health, mostly isolated from human blood, together with some environmental isolates, all of them classified as Bt1. Lineage 2 (L2) was formed by a mixture of Bt1 and Bt2 strains from various sources, including diseased fish from fish farms. Lineage 3 (L3) was composed exclusively of Bt3 strains also linked to fish farms, and lineage 4 (L4) and 5 (L5) included a few clinical and environmental strains from specific geographical areas that were previously classified as Bt1. Interestingly, Bt2 strains appeared inside L2 distributed in three serovar-related groups, one of which was the zoonotic clonal-complex. This study also revealed that a 75% of the genes involved in virulence for humans were present in the core genome, which suggested that all the strains of the species should be considered potentially virulent for humans, regardless the lineage or biotype. The analysis of congruence of the phylogenetic trees corresponding to the chromosomes and pVvBt2 showed that, the evolutionary history of chromosomes and plasmids was different. This suggested that the plasmid had been acquired several times by different clones, probably through the aquaculture environment. Finally, the authors proposed the substitution of the current classification of biotypes into a classification of phylogenetic lineages and a pathovar including all fish-virulent and the zoonotic clonal-complex, the *pv. piscis*.

The representative strain of the zoonotic clonal-complex, is the CECT 4999 strain, denominated R99 in the laboratory collection. This strain was first isolated in 1999 from an European eel (Roig *et al.*, 2018) and is the strain used in this study. The genome of this strain has been sequenced and closed, it consists of two chromosomes (ChrI and ChrII) that codify for a total of 4533 coding regions (ORF), and the virulence plasmid pR99. Over 80% of the ORF's of the plasmid show significant homology to previously identified genes, while the rest correspond

to hypothetical proteins. The greater part of the virulence-related genes are mainly located in the second chromosome, but the genes that allow the bacteria to infect fish are located within the pR99.

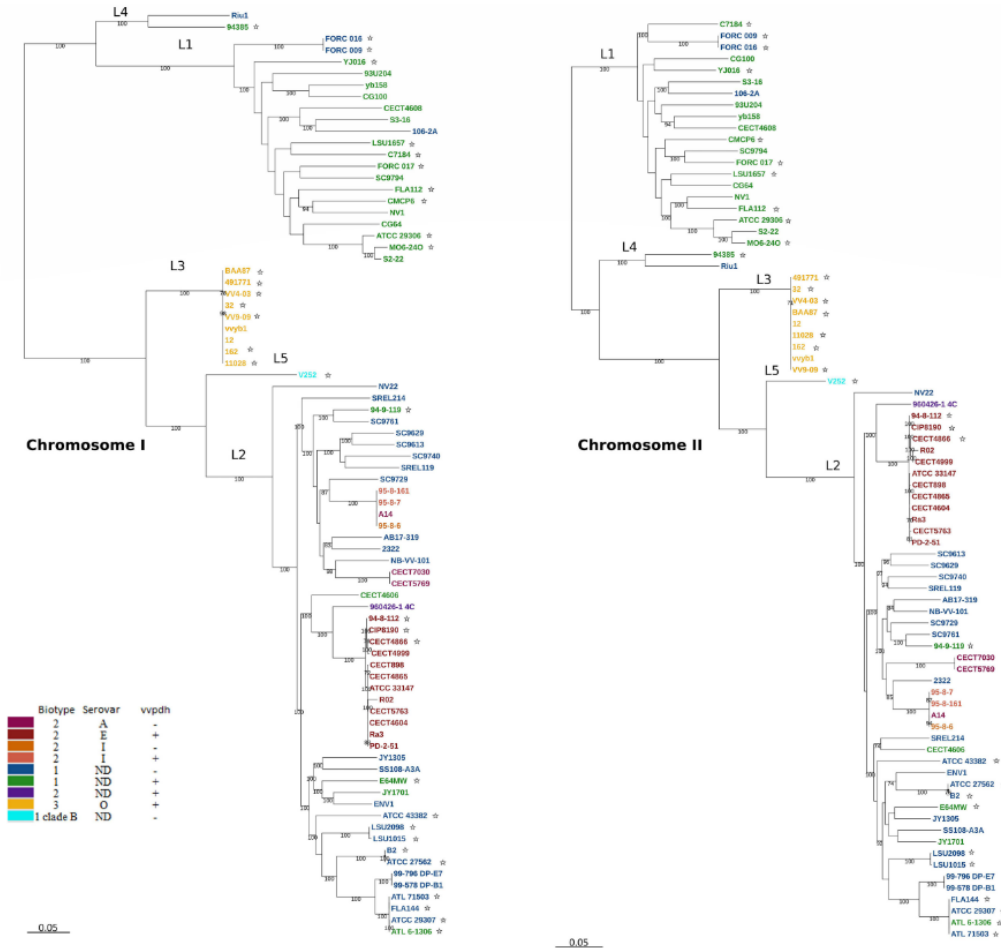


**Fig.1. Phylogenetic tree constructed by analyzing core genomes of all three biotypes.** The phylogeny based on single nucleotide polymorphisms in the core genome of the species. Image taken from Roig *et al.*, (2018).

## 1.2.- Natural reservoirs and epidemiology

The two most important environmental factors for the survival and persistence of *V. vulnificus* in the environment are temperature and salinity (Oliver, 2013; Takemura *et al.*, 2014). This pathogen is an obligate halophilic, so it inhabits estuarine or brackish waters with

moderate salinities of 1-2% NaCl (Wetz *et al.*, 2014; Oliver, 2015) and coastal waters around the globe within tropical and subtropical areas, preferring warm waters ranging from 10 to 30°C (Oliver, 2015; Baker-Austin and Oliver, 2018). Although the optimal temperature for growth is above 18°C, and virulence in fish is boosted around 25°C (Amaro *et al.*, 1995; Jones and Oliver, 2009; Hernández-Cabanyero and Amaro, 2020), the bacteria can survive below 9°C by entering the viable but not culturable state (VBNC) where the cells are still alive but would not be able to grow, form colonies or biofilms, and their metabolic processes are halted (Oliver, 2015). This state proves to be favorable for surviving potential lethal environmental threats that metabolically active bacteria would not be able to. The dynamics between salinity and temperature dictate the presence and persistence of the bacteria in the environment, for example, the temperature threshold of *V. vulnificus* is lower in high salinity waters, while it can thrive in a wider range of water temperature when salt concentrations are less than 1%, (Oliver, 2015).

Temperature is a critical factor that influences the presence of vibrios in the water column, recent changes in the climate due to global warming are changing the distribution and incidence of these pathogens around the world. Several studies have shown a direct relation in changes in geographical distribution, incidence of vibrio populations and vibriosis cases with the increase of water temperatures in several regions. (Baker-Austin *et al.*, 2013, 2017; Oliver, 2015; Heng *et al.*, 2017; Semenza *et al.*, 2017). This change in habitat distribution is not a recent trend and has been documented as far back as 1998, in a study where several *V. vulnificus* infections were reported in Denmark after unusually warm temperatures happened over the summer (Høi *et al.*, 1998). More recently, during the unusually warmer summers of 2003 and 2006, there was a surge in vibrio wound infections linked to recreational activities in the Baltic sea area (Baker-Austin *et al.*, 2013). Surprisingly, in colder places at locations as far as 160 km from the arctic circle, a significant increase of *Vibrio* infections had been recorded in recent years, approximately 89 cases of vibriosis were reportedly linked to a heatwave in the summer of 2014 which caused an unprecedented rise in water temperatures in northern Scandinavia (Baker-Austin *et al.*, 2016).

These ecology studies shed light on the recent changing geographical distribution of *Vibrio*, which seems to be caused by global warming and the heating of water bodies around the world. These increases in global temperature are causing increasing numbers of infections in areas where vibriosis was already prevalent (Baker-Austin *et al.*, 2010; Oliver, 2015). Because of the link between the increase of water temperature, global warming, and rise in vibrio populations, these species are considered a biological marker for climate change, which should encourage the monitoring of temperature and bacterial presence in the water column, in order to prevent a rise in infections of these potentially fatal pathogens (Baker-Austin *et al.*, 2017; Deeb *et al.*, 2018).

As mentioned before, this pathogen can switch between free-living planktonic lifestyle, and sessile biofilm communities associated with a plethora of aquatic environment components such as, zooplankton, sediments and algae. However, its main reservoir can be narrowed down to crustacean carapaces, fish mucosal surfaces and filtering organisms like bivalves (Oliver, 2015). Within the diverse grouping of the species, there exists a clear relation between the type of strain and its preferred habitat and route of infection (Roig *et al.*, 2018). The zoonotic clonal-complex has only been recuperated from diseased fish and from few clinical samples coming from wound infections caused by handling infected animals, but it has never been linked to shellfish-borne vibriosis (Amaro *et al.*, 2015). However, water filtering organisms can accumulate high concentrations of free-swimming lifestyle strains, which may end up being consumed by humans and constituting a completely different route of infection (López-Pérez *et al.*, 2019).

## **2.- Vibriosis**

*V. vulnificus* is capable to cause disease in humans and fish, collectively known as vibriosis. The disease has several ranges of severity and different symptoms determined by the type of infection and route of entry of the pathogen. This species, is one of the few members from the *Vibrio* family that can cause severe and possibly lethal clinical manifestations like gastroenteritis, tissue necrosis, fasciitis and, in the worst cases, fulminant septicemia (Jones and



Oliver, 2009; Baker-Austin and Oliver, 2018; Yun and Kim, 2018). Interestingly, *V. vulnificus* differs from other vibrios by its capacity to infect its host via different entry points. In fish it can enter through the gills, anus, and fins, meanwhile in humans, infection can begin through ingestion, and contact with broken skin and wounds (Marco-Noales Ester *et al.*, 2001; Baker-Austin and Oliver, 2018). This not only differentiates *V. vulnificus* from other species, but the point of entry can dictate the outcome and progression of the infection, which in the most severe cases, results in death by sepsis (Amaro and Biosca, 1996; Amaro *et al.*, 2015). Unlike other vibrios, *V. vulnificus* is a zoonotic agent as it can be transmitted from diseased fish to humans, and it must be considered an important worldwide public health problem that needs to be controlled by the implementation of more stringent monitoring and preventive measures.

### **3.- Human vibriosis**

*V. vulnificus* can infect humans via ingestion of contaminated seafood or through exposure of broken skin and wounds to water or any aquatic organism harboring the bacteria. In the first case, the bacteria causes either mild gastroenteritis or primary septicemia, in the second case, the pathogen can cause either severe wound infections or secondary septicemia (Strom and Paranjpye, 2000). Patients with predisposing health conditions are 80 times more prone to develop sepsis (Horseman and Surani, 2011), and around 90% of reported cases of *V. vulnificus* infections had one or more underlying chronic diseases (Jones and Oliver, 2009; Oliver, 2015). Liver diseases like cirrhosis and hepatitis, cancer and immunodeficiencies, are the most prominent underlying ailments that are present in a great percentage of fatal cases (Haq and Dayal, 2005; Yun and Kim, 2018). Chronic liver pathologies are characterized by elevated iron levels in serum, which has been shown to increase the ability of *V. vulnificus* to survive and grow in human serum (Bogard and Oliver, 2007; Pajuelo *et al.*, 2016; Yun and Kim, 2018; Hernández-Cabanyero and Amaro, 2020).

Unlike illnesses caused by other *Vibrio* species, the gastrointestinal illness caused by *V. vulnificus* may be the most unreported (Daniels, 2011), in fact, the CDC estimates that only a 5% of this type of infections are reported (Skovgaard, 2007). This is because the infection is usually

self-limited and only in the most severe cases requires hospitalization. Wound infections, which are often necrotizing, are usually acquired when an open wound is exposed to warm seawater or while handling fish or seafood contaminated with *V. vulnificus*. In most cases, lesions rapidly develop cellulitis and, in severe situations, they evolve into necrotizing fasciitis (**Figure 2**) and systemic disease, which causes secondary septicemia after the diseases spreads through the bloodstream (Jones and Oliver, 2009; Oliver, 2015; Yun and Kim, 2018).

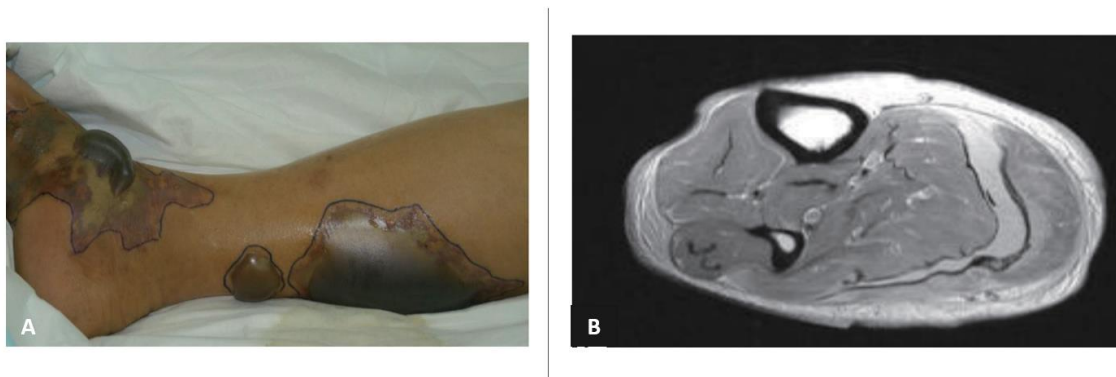


**Fig.2. Clinical manifestations of patients suffering from *V. vulnificus* infection.** (A) Typical skin lesions of vibriosis showing hemorrhage and serous bullae on the lower leg of a patient. (B) Magnetic resonance image showing necrotizing fasciitis on the lower leg of a patient. Image taken from Yun and Kim (2018).

The most significant *V. vulnificus* illness is a primary septicemia caused by the ingestion of raw seafood and is characterized by chills, fever, nausea, diarrhea, and abdominal pain. In most cases, unusual bullae filled with hemorrhagic fluid appear in arms and legs, requiring tissue debridement (Jones and Oliver, 2009; Oliver, 2015; Yun and Kim, 2018). In this case, the fatality is higher than 50% (Oliver, 2013, 2015). In the past decade, the annual incidence of *V. vulnificus* infections in the US increased by 41%. This increase tendency has been observed on other countries like Taiwan and Korea, (Yun and Kim, 2018). Normally, vibriosis infections are relatively rare (Oliver, 2013), which gives a “positive” outlook for the disease, because, even though half of the patients hospitalized die of fulminant septicemia, the overall number of vibriosis cases is substantially low. In the United States, it is estimated that every year, more than 80,000 people contract vibriosis, which leads to approximately 500 hospitalizations and 100 deaths (Oliver, 2015). This occurs due to the need for aforementioned pre-existing conditions and several other host characteristics that influence the onset of the infection (Haq

and Dayal, 2005; Horseman and Surani, 2011; Baker-Austin and Oliver, 2018). The majority of reported cases around the world including USA, North Korea and Taiwan come from older males over the age of 40 ( $\pm 85\%$ ), this may suggest a higher susceptibility for men to *V. vulnificus* infections (Haq and Dayal, 2005; Jones and Oliver, 2009; Yun and Kim, 2018). Although it is not clear why vibriosis is more prevalent in males, a study in Taiwan involving rats showed that estrogen had a protective function against sepsis by *V. vulnificus* (Yun and Kim, 2018).

#### 4.- Fish vibriosis

*V. vulnificus* causes disease in several species of aquatic animals, however, its main hosts are teleost fish that inhabit brackish warm waters, such as the Nile tilapia and the European eel (Tison *et al.*, 1982; Fouz and Amaro, 2003; Woo *et al.*, 2020). Vibriosis outbreaks are more common in waters over 25°C, and for this reason, this type of vibriosis is called warm water vibriosis (WWV) (Amaro *et al.*, 1995). The infection can occur in two modalities, the *brackish water modality*, caused by the SerE, and the *freshwater modality*, caused by the rest of the serovars (Roig and Amaro, 2007). In the first case, the pathogen preferentially colonize the gills, while in the latter, the intestine. From both locations, is possible for the bacterium to invade the bloodstream and cause death by septicemia.

Clinical signs associated with fish vibriosis are similar to those described for humans, since they both commonly result in a septicemia with a high probability of death by sepsis (Amaro *et al.*, 2015; Oliver, 2015). Externally, this manifest as lesions in the abdomen, hemorrhages in the anus, reddening of the operculum, bloated belly and ulcers (**Figure 3A**). Internally, inflammation of the intestine, discoloration of the liver and inflamed kidney (Amaro *et al.*, 2015). Although the clinical signs are generally similar in sickened eels, there is a rare but specific clinical manifestation caused by the freshwater vibriosis that clearly differentiates the two modalities, non-zoonotic strains cause a severe degradation of the jaw (**Figure 3B**), that only happens in a very few percentage of infected individuals (Haenen *et al.*, 2014; Amaro *et al.*, 2015).

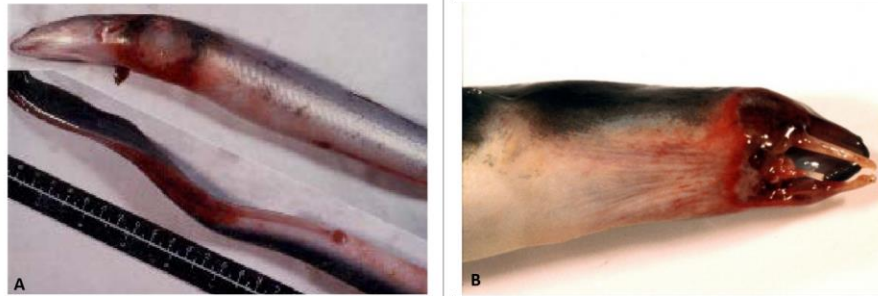


**Fig.3. Clinical manifestations of warm water vibriosis in diseased eels.** (A) Brackish modality vibriosis caused by the zoonotic clinal complex showing typical clinical signs of ulcers and hemorrhage. (B) Vibriosis caused by a non-zoonotic strain of the pathovar, showing the specific jaw degradation of this types of infection. Images taken from Biosca *et al.*, (1991) and Haenen *et al.*, (2014).

### 5.- Virulence determinants

*V. vulnificus* possesses several putative virulence factors that allow the bacteria to produce disease in fish and humans through different mechanisms. These factors have been studied throughout the years, however, the virulence is not yet completely understood. Production of disease by this pathogen seems to be a multifactorial process that involves a synergetic effort of different cellular mechanisms (Strom and Paranjpye, 2000). A great variety of virulence factors had been studied over the past years, which confer a wide range of functions that allows the survival, growth and colonization of this pathogen in its host (T. Williams *et al.*, 2014; Oliver, 2015; Heng *et al.*, 2017; Baker-Austin and Oliver, 2018; Yun and Kim, 2018). As we commented before, the majority of the human virulence-related genes were found to be in 75% of the stains, even though they did not share the same origin (Roig and Amaro, 2007). These factors grant several abilities to the bacteria that are instrumental in its pathogenicity, abilities like motility, attachment to different surfaces, production of biofilm, survival in serum, iron acquisition, the production of enzymes and induction of cellular damage by cytotoxicity. These mechanisms are readily available encoded within the bacterial genome, and tightly regulated by a complex net of global regulators such as SmcR, waiting in place for the moment the bacterium makes first contact with the host (Hyun *et al.*, 2007).

The pv. *piscis* is capable of infecting fish due to its particular characteristic of harboring the virulence plasmid pVvBt2 (Lee *et al.*, 2008). The plasmid encodes two iron-regulated outer

membrane proteins; a fish transferrin binding protein (Ftbp) that binds to transferrin of several *Teleostei* fish species (unpublished results), and the Fpcrp (Fish phagocytosis and complement resistance protein), that provides resistance to fish complement and phagocytosis (Hernández-Cabanyero *et al.*, 2019). Both proteins are optimally produced under iron restriction, especially in fish serum, and the Ftbp is even more favorably induced at temperatures over 25°C, which shows that resistance to fish innate immunity is controlled by environmental parameters, iron and temperature (Hernández-Cabanyero and Amaro, 2020). Remarkably, almost identical homologues of *ftbp* are present in the virulence plasmids of other fish pathogenic species such as *V. harveyi* and *Photobacterium damsela*, suggesting that horizontal gene transfer of virulence determinants is frequent in the artificial environment presented by fish farms, environments that favor the emergence of new virulent clones.

### **5.1.- Capsule polysaccharide**

The production of capsule polysaccharide (CPS) has been appointed as the main responsible for the virulence in *V. vulnificus* (Oliver, 2015), as non-encapsulated variants, denominated “translucent”, are almost avirulent, while encapsulated “opaque” variants of the same strain remain highly virulent (Simpson *et al.*, 1987; Wright *et al.*, 1990; T. Williams *et al.*, 2014). Most of the *V. vulnificus* isolates are capsulated, and different capsular types have been found among clinical and environmental isolates (Chen *et al.*, 2003). A recent study that combines TIS (Transposon-Insertion-Sequencing) with directed mutagenesis has demonstrated that CPS is the only virulence factor essential to resist human complement in blood (Carda-Diéguez *et al.*, 2018). Interestingly, capsule biosynthesis is controlled by iron, being optimally produced at high iron concentrations (Pajuelo *et al.*, 2016).

In eels, the capsule is not essential for virulence through the intraperitoneal (i.p.) route, since the translucent variants remained virulent, nevertheless, the loss of capsule did increase the infectivity dose, which suggests that the capsule exerts a role in virulence (Amaro *et al.*, 1995). On the other hand, the capsule seems to be required for virulence through water, the natural route for fish infection, since the translucent variants were completely avirulent in the

water infection assays. The non-capsulated strains colonized the gills *in vivo* in a less effective manner than the opaque ones, preventing the bacteria to reach the minimal concentrations needed for a successful infection (**Figure 4**) (Valiente, Jiménez, *et al.*, 2008; Amaro *et al.*, 2015). Thus, the capsule appears to be a factor needed for efficient colonization of gills, rather than needed for the specific invasion of eels.

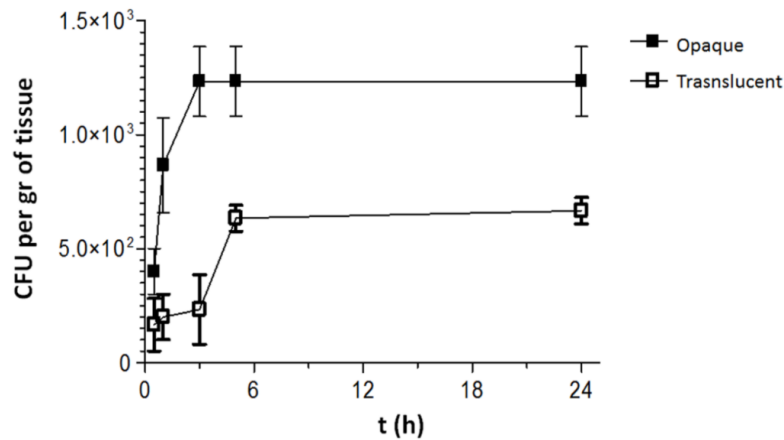


**Fig.4. Gill colonization in *V. vulnificus*.** The two variants of the zoonotic clonal-complex, opaque and translucent, recovered after immersion challenge. Less CFU of the non-capsulated strains were recuperated from the gills after the infection assay, which implies that a role of the capsule in a successful initial colonization. Image taken from Amaro *et al.*, (2015).

## 5.2.- Lipopolysaccharide

One virulence factor is believed to be involved in the fatal outcome of infections caused by consumption of contaminated water or shellfish, the lipopolysaccharide (LPS). Lipid A of LPS<sub>Vv</sub> is an endotoxin that, in large quantities, causes swift death in mice, while its inhibition results in zero casualties (Oliver, 2013, 2015). To sort the perils of the digestive system, *V. vulnificus* produces certain enzymes which increase the acidic tolerance of the cells after exposure to lower pH levels, and surprisingly, the LPS also plays a role in this acidic resistance. Thanks to these and other mechanisms, the cell can enter a state of nutrient starvation that confers cross-protective effect against oxidative stress (Eun Rhee *et al.*, 2002; Jones and Oliver,

2009). In case of fish, the lipid A of LPS<sub>Vv</sub> does not act as an endotoxin (Iliev *et al.*, 2005), instead, the high molecular weight (HMW) part of the O-antigen of LPS<sub>Vv</sub> confers partial protection against the complement (Amaro and Biosca, 1996). Again, LPS biosynthesis is controlled by iron and temperature, as the production of HMW-O-antigen is optimal at low iron concentrations and temperatures over 25°C (Pajuelo *et al.*, 2016; Hernández-Cabanyero *et al.*, 2019; Hernández-Cabanyero and Amaro, 2020).

### 5.3.- Toxins and enzymes

Recent studies have demonstrated that in addition to the CPS, the RtxA toxin is essential for the pathogenesis of *V. vulnificus* (Oliver, 2015). This toxin belongs to a family of toxins called MARTX (Multifunctional Autoprocessing Repeat in Toxin) with roles in virulence that involve invasion, cytotoxicity and cell death (Kim *et al.*, 2008; Kwak *et al.*, 2011). The RtxA1 toxins are high molecular weight proteins segmented in “modules”, the external modules form pores in the membrane of the target eukaryotic cells in order for the central module, which contains the effector domain of the toxin, to enter into the cytosol (Gavin and Satchell, 2015). This toxin is controlled by a complex regulatory network where various regulatory proteins and receptors act in synergy to promote the expression of RtxA1 in response to signals from the host environment (Lee *et al.*, 2020). Interestingly, since RtxA1 is a modular protein, several variants with several types of effector domains can be produced by *V. vulnificus* strains. A study made by Satchell *et al.*, (2011) showed that four variants of the RtxA1 toxins from clinical isolates had distinct effector domains and evolved from different recombination events by integrating DNA from plasmids and other *rtxA* genes from different species of vibrios. These results show the marked heterology that can arise in this toxin, which implies a possibility for the potential emergence of novel RtxA proteins with different degrees of toxicity among the *V. vulnificus* strains.

The zoonotic clonal-complex carries two copies of its own variant of the RtxA1 toxin, one in the ChrII and the other in the pVvBt2 (Roig *et al.*, 2011; Lee *et al.*, 2013). This toxin is denominated RtxA1<sub>3</sub>, although it differs in structure and mechanisms from the RtxA1 secreted

by other strains belonging to the L1 (**Figure 5**). In fish, RtxA<sub>13</sub> is secreted the moment it comes in contact with the host eukaryotic cells, and is involved in the lyse of phagocytes, inflammation and damage in the colonized gills, which promotes the entrance into the bloodstream (Callol *et al.*, 2015). In mice and eels, it has been shown that this toxin is involved in an early inflammatory response, and is essential for virulence (Murciano *et al.*, 2017).

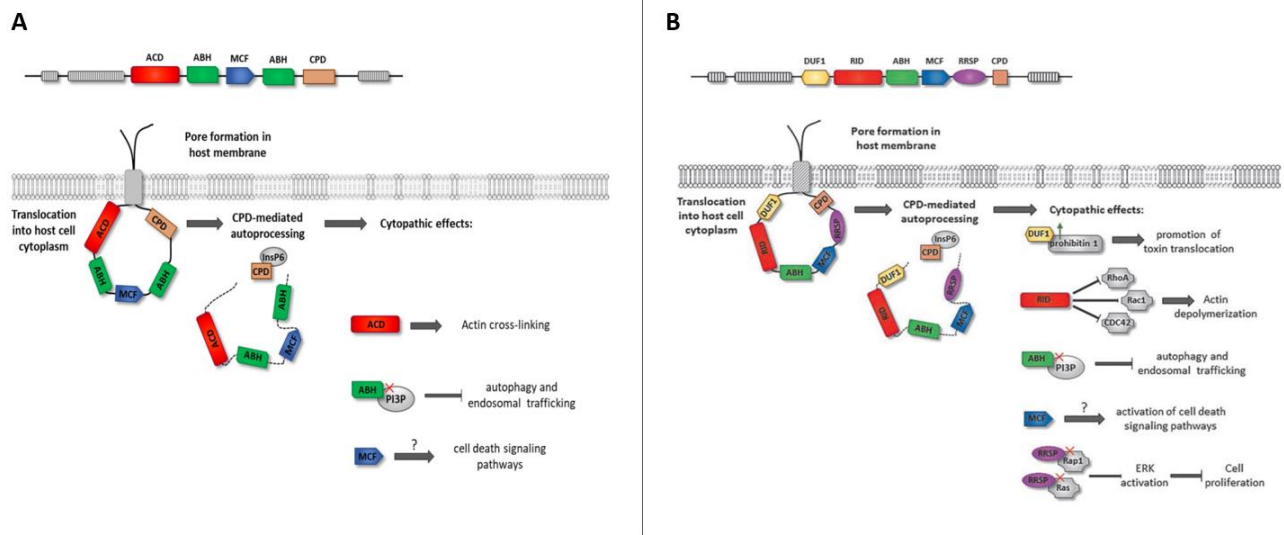


**Fig.5. *V. vulnificus* RtxA1 and RtxA<sub>13</sub> toxins structures.** When the toxin is secreted, the external module targets the cell membrane forming a pore that allows the central module and the toxin effector to enter the cytosol and cause cell death and tissue damage. (A) RtxA1 conserved external modules and variant internal module, the effector domains are coded in different colors. Image taken from Ph.D. thesis of Hernandez-Cabanyero (2019). (B) Zoonotic clonal-complex RtxA<sub>13</sub> toxin conserved external structure and internal module, the effector domains are coded in different colors. Image taken from Hernández-Cabanyero and Amaro (2020).

Although the RtxA toxins are important for initial contact and early stages of invasion, they are not the only contributors to tissue damage and invasion of blood and other organs in humans and fish. The Vvha toxin is an hemolysin that was first described in 1981 to cause lysis in mammalian erythrocytes (Kreger and Lockwood, 1981), and appeared to work cooperatively with RtxA1 to promote tissue damage (Jones and Oliver, 2009; Hor and Chen, 2013; Hernández-Cabanyero *et al.*, 2019). The gene encoding this protease (*vvhA*) was shown to have a high homology with a cytolyisin of *V. cholerae* El Tor strain (Yamamoto *et al.*, 1990). After thorough



research, it was stated that, in a concentration-dependent manner this hemolysin was cytotoxic for eukaryotic cells, and had the capacity of causing necrosis or apoptosis in several cell types. In addition, the toxin was lethal to mice and was capable of inducing several lethal clinical manifestations, like pulmonary ailments and cellulitis when the purified protein was injected (Hor and Chen, 2013).

The specific role of this cytolyisin in the virulence and pathogenesis of *V. vulnificus* is not known. Firstly, infections in mice showed that there was no difference in lethality between the knock-out mutant of VvhA and the wild type: infected mice continue to suffer necrosis and tissue damage, which would imply that the bacterium retains its cytotoxicity when it comes in contact with host cells. So it could be concluded that VvhA is not the only factor responsible for tissue damage, and therefore is not essential for virulence. However, in eels, it does have a role since it has been shown recently that mutants deficient in this hemolysin are deficient in virulence through water, which indicates that this toxin could act in the early stages of infection in these animals (Hernández-Cabanyero *et al.*, 2019). In fact, a recent study reinforced the idea that this hemolysin plays an important role in the induction of cytotoxicity by forming pores in the cellular membrane and activating the inflammatory response, although the authors concluded that due to the lack of results in mice, it could not be assigned a specific role in human infection (Yuan *et al.*, 2020).

Another study described a more direct involvement of the VvhA toxin in human virulence, the VvhA operon was expressed when the bacteria came into contact with the blood and macrophages of mice, and the IscR regulator, which contains a Fe-S cluster, promoted its expression in response to nitrosative stress and iron starvation (Choi *et al.*, 2020). At the same time, Hernández-Cabanyero *et al.* (2019) proved that this hemolysin was expressed in human and fish serum during both excess and restriction of iron, thus the expression of this toxin should be subject to a complex regulatory system, in which iron and nitrosative stress could intervene together with other signals.

Overall, VvhA alone does not cause any significant damage to the host, but it might be an additive toxic force to RtxA1 which could enhance the cytotoxicity, tissue damage and

facilitate the entry of the bacteria into the bloodstream (Hor and Chen, 2013; Hernández-Cabanyero *et al.*, 2019).

Besides cytotoxicity and hemolysis, *V. vulnificus* also exhibits a strong elastase activity conferred by a metalloprotease denominated VvpE, whose virulent characteristics had been studied in animal models (Jeong *et al.*, 2000). This enzyme belongs to the thermolysin family, which is an homologue of the hemagglutinin/protease secreted by *V. cholerae*, and its expression is coactivated through two transcriptional regulators, the cAMP receptor protein (CRP) and the SmcR (Jeong *et al.*, 2003; Benitez and Silva, 2017). This protease helps in the detachment of *V. cholerae* from its host intestinal epithelium, and appears to be regulated by *quorum sensing* (Kim *et al.*, 2013). Other functions attributed to VvpE are tissue necrosis, cutaneous lesions, vascular permeability, and traits of bullous lesions that manifest during septicemia (Jones and Oliver, 2009). In addition, VvpE can degrade multiple proteins like laminin, elastin, collagen, intestinal mucus, and most importantly, iron containing molecules like transferrin proteins and hemoglobin (Miyoshi *et al.*, 1999). Degradation of these proteins help in the release of free iron into the bloodstream, which should favor *V. vulnificus* growth and virulence, but research has shown no direct relation between this lytic activity and iron assimilation from human transferrin (Shin *et al.*, 2005). Even though this protease has lytic characteristics that should be related to the pathogenesis, VvpE deficient mutants had no difference in virulence against wild type strains in murine models (Shao and Hor, 2000; Kim *et al.*, 2007). Nonetheless, other studies imply a common role for this metalloprotease in survival, either in the environment or in hosts since the *vvpE* gene is highly conserved among the species (Valiente, Lee, *et al.*, 2008). Interestingly, the VvpE of the zoonotic clonal-complex has a unique role in colonization in fish. Protease mutants were avirulent during immersion challenges, but retained their infective capabilities when i.p. infections were performed (Valiente, Lee, *et al.*, 2008).

#### 5.4.- Host immune evasion

Once *V. vulnificus* has colonized organs and entered the bloodstream through tissue damage, necrosis and the activity of the various enzymes, it must evade the immune response to continue the infection. Vibriosis can happen at breakneck speeds, as humans can display symptoms of infection as little as 7 hours after ingestion of contaminated shellfish (Jones and Oliver, 2009), while in eels, extensive hemorrhages in internal organs and death by sepsis can happen in less than 48 hours (Valiente and Amaro, 2006; Amaro *et al.*, 2015). To understand the underlying mechanisms that provoke this, studies have described how the pathogen interacts with the first line of defense of the host, the innate immune response, either humoral or cellular. These two responses are deeply intertwined, and both serve as initiation and induction to one another, meaning that, there is no actual first responder, but an intertwined net of simultaneous processes. The humoral component is comprised of several bactericidal and bacteriostatic proteins, some of them form part of the serum complement, which are proteins activated by the presence of pathogens in blood and react in chain in order to destroy or mark the foreign bodies for phagocytosis (T. Williams *et al.*, 2014).

Phagocytes comprise the cellular component of the innate response and their role is to destroy pathogens by recognizing PAMPs (pathogen associated molecular patterns), however, *V. vulnificus* can evade these bacterial killers thanks to its capsule envelope (Amaro *et al.*, 1995; T. Williams *et al.*, 2014). Toll like receptors (TLR) also play a role in phagocytosis of this pathogen, although only a couple of them are able to bind to certain *V. vulnificus* PAMPs, for example, TLR2 binds to the surface lipoprotein encoded by *lipA* and TLR5 binds to flagellin and jointly activate the production of a proinflammatory cytokine (ILK-8), which is involved in the inflammatory response and its a major activator of neutrophils (Jones and Oliver, 2009). Neutrophils phagocyte foreign bacteria, and are one of the first immune components to respond to infection. A study performed with blood from patients with liver disease, showed that survival of *V. vulnificus* is related to a lower activity of neutrophils (Hor *et al.*, 1999), while other study showed an increase of neutrophil numbers in the peritoneal cavity after infection with the pathogen (Jones and Oliver, 2009).

Another type of phagocytes involved in the defense against *V. vulnificus* are the macrophages, however, their numbers are vastly reduced via induced apoptosis during the course of the infection. With the reduced presence of macrophages, neutrophils alone are not able to manage the ongoing infection, which suggests a primary role of the macrophages against *V. vulnificus*, while the neutrophils would serve as an auxiliary force (Jones and Oliver, 2009). The classical complement cascade also induces phagocytosis of *V. vulnificus*, mainly by polymorphonuclear leukocytes (Musher *et al.*, 1986). Macrophages secrete cytokines to recruit additional phagocytes to the site of infection, and in turn, exacerbate the inflammatory response produced by the same cytokines. Interleukin 1, 6 and 8, and the tumor necrosis factor alpha (TNF- $\alpha$ ) are constantly being secreted during complement activation and phagocytosis. This storm of cytokines could generate fatal consequences to the host, as a sustained immune response, incited by a successful invasion and infection by *V. vulnificus*, will create a feed-forwarding loop of inflammatory processes leading to a systemic inflammatory shock and death of the host (Shin *et al.*, 2002; Murciano *et al.*, 2015).

### **5.5.- Iron acquisition**

The humoral innate response has two very important bactericidal components: transferrin and lactoferrin, which form part of one of the most conserved and effective immune mechanisms among animals, the nutritional immunity (Hood and Skaar, 2012).

Iron is a co-factor for various enzymes and is necessary for the correct functioning of essential physiological processes such as DNA replication, and general metabolism. Iron can be found in several forms inside the host: forming complexes with heme, being part of proteins like hemoglobin, and sequestered by human transferrin or lactoferrin in blood and other body secretions (Hood and Skaar, 2012). Iron is also required for growth by every bacterial pathogen, for this reason, animals have evolved to limit access of free iron in their bloodstream, thus bacteria have had to come up with various mechanisms of iron uptake in order to colonize and infect their target hosts (Hood and Skaar, 2012). Iron availability is critical for *V. vulnificus* pathogenesis, iron concentrations in the host had been shown to influence the lethality and

effectiveness of infection, and high levels of non-transferrin bound iron are needed for *V. vulnificus* growth (Bogard and Oliver, 2007). Since iron is being restricted by the nutritional immunity of the host, *V. vulnificus* must use two non-specific iron uptake systems, the siderophore vulnibactim with its receptor VuuA, and the HupA haem receptor in order to sequester some of the host's iron (Elena G. Biosca *et al.*, 1996; Pajuelo *et al.*, 2014).

Interestingly, If both iron uptake systems are impaired, virulence in mice is completely lost, but not the virulence in eels, which suggests the existence of a third specific iron uptake system solely for eels or fish. Using a ferric regulation assay (FURTA), a candidate responsible for this specific iron uptake mechanism was identified, this was the fish transferrin binding protein (Ftbp) formerly denominated as Vep20 (Pajuelo *et al.*, 2014), which was found to be a specific receptor for the transferrin of eel and other teleost fish (Pajuelo *et al.*, 2015). This iron regulated outer membrane protein (IROMP) is encoded in the pVvBt2, and together with the Fpcrp (Hernández-Cabanyero *et al.*, 2019), are the main responsible for the pathogenesis in fish, (Sanjuán *et al.*, 2011; Amaro *et al.*, 2015; Hernández-Cabanyero *et al.*, 2019; Hernández-Cabanyero and Amaro, 2020).

The lifecycle of *V. vulnificus*, including the pv. *piscis* and the zoonotic clonal-complex is tightly dependent on the availability of the iron in its host, this dictates the severity of the consequent vibriosis infection in either humans or fish (**Figure 6**). It is important to know how these mechanisms work, even more if this specific virulence determinant can be the difference between a sole wound or gastrointestinal infection, or necrotizing fasciitis and fulminant septicemia. However, even though the relation between iron and *V. vulnificus* encompasses the mechanisms of virulence used for the survival of the innate immune response, there are still several other “physical” factors that are synergistically involved in pathogenicity, such as, motility, adhesion, and the diverse bacterial appendages that confer these abilities, which in turn, form part of the process of formation and persistence of biofilms.

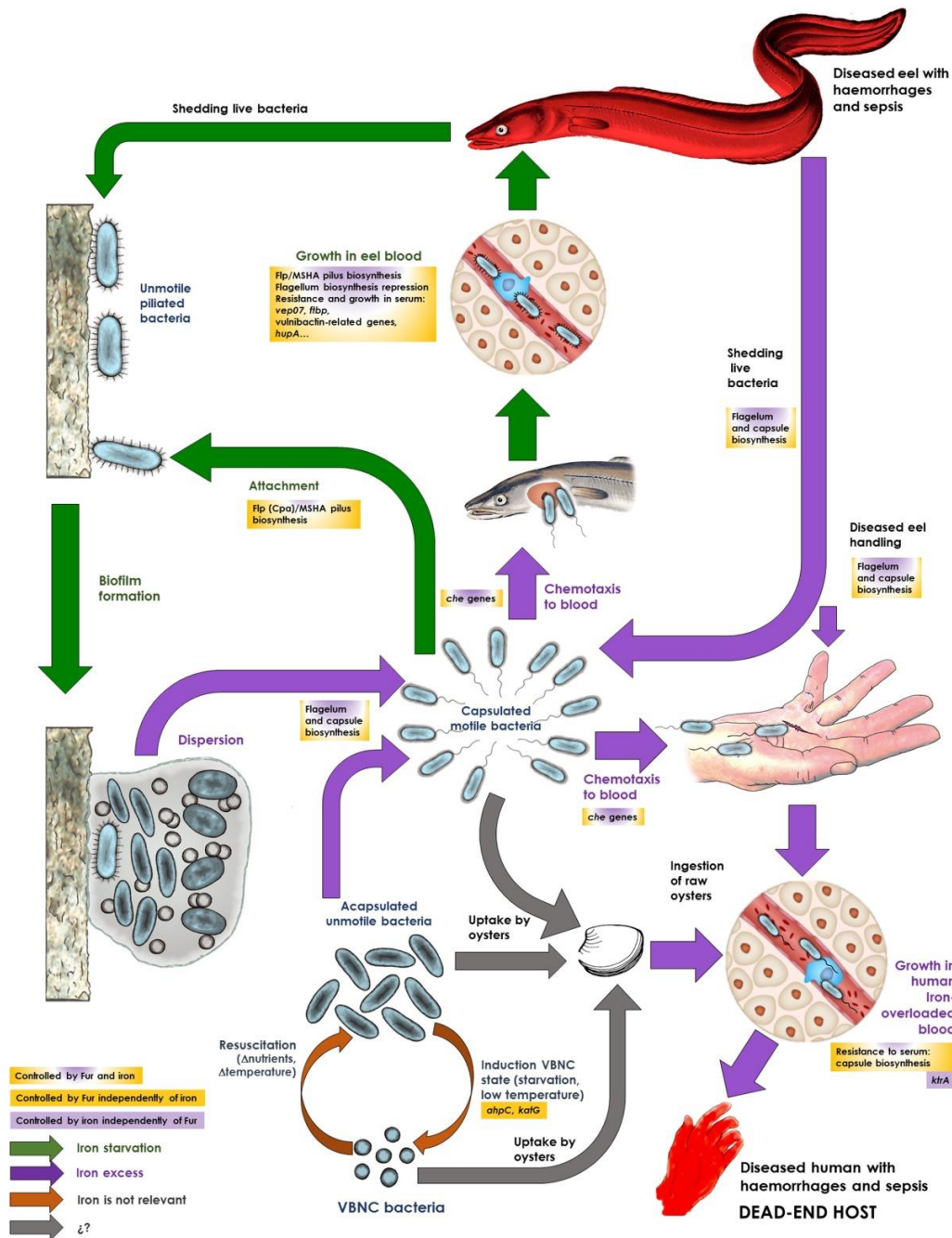


**Fig.6. Iron and life cycle of *V. vulnificus*.** This figure summarizes the life cycle of *V. vulnificus* and the influence of iron in the strategy for survival and infection. Genes regulated by iron are involved in metabolism, colonization, motility, resistance to the innate immune system and toxins. *V. vulnificus* is taken up and concentrated by filtering organisms that could be ingested by humans and cause disease, another route of infection is through contact with eels (zoonosis). The pathogen is attracted to blood or mucus from a susceptible host, where it attaches and starts colonization, this can be potentiated by warmer temperatures and elevated iron concentrations. *V. vulnificus* is shed from diseased eels into water, where it can survive as a free-living organism or in biofilms attached to biotic or abiotic surfaces, it can also enter the VBNC state. Image taken from Pajuelo *et al.*, (2016).

## **6.- Bacterial appendages**

The ability to move is often taken for granted, but is one of the most useful and widespread tools of survival employed by almost all organisms of the planet, including microorganisms. Motility is as, or even more important, than attachment when it comes to pathogenesis and survival of many bacteria. Bacterial cells need a physical way to reach their desired host or adhesion target, either by water or through slow but steady movement in solid surfaces. For this purpose, cells are equipped with different structures that vary in length, function and number, these bacterial appendages differ between species but are highly conserved among many pathogens as they are essential for virulence. The most common and well known of them all is the flagellum, which grants incredible movement capabilities in liquids called swimming motility. On the other hand, another type of filamentous structures clearly distinguishable from flagella called fimbriae or pili, can be found on the surface of many gram-negative and gram-positive bacteria. Pili play an essential role in the attachment and adhesion to biotic and abiotic surfaces, to their hosts, and even other bacteria. They also confer a wide array of other indispensable abilities such as; formation of biofilm, DNA uptake, twitching and swarming motility, which are a form of individual and group “crawling” movements used to traverse semi-solid surfaces.

### **6.1.- The Flagellum**

Cellular movement has always been an important and ancient trait of bacteria, this behavior is influenced by chemotaxis and chemical stimulation, which allows them to reach different destinations for colonization and nutrient scavenging (Josenhans and Suerbaum, 2002). Swimming motility is a high speed movement influenced by external stimulus and is prominently achieved by a specialized rotating organelle, the flagellum (Aizawa, 2014). This is a well conserved and complex protein structure present in a wide variety of bacterial species. This appendage is, in most cases, outside of the cell and is a highly specialized mechanism imbued within the cell envelope, normally located in the proximal end of the cell. The flagellum apparatus constitutes an exporting mechanism within the bacterial membrane towards the

extracellular milieu (Macnab, 1999), and has been compared to the Type III secretion system. The flagella machinery consists of three parts: the basal body (rotary motor), the hook (universal joint), and the filament (helical propeller). This filament is conformed by flagellin subunits that form a central channel (Figure 7).

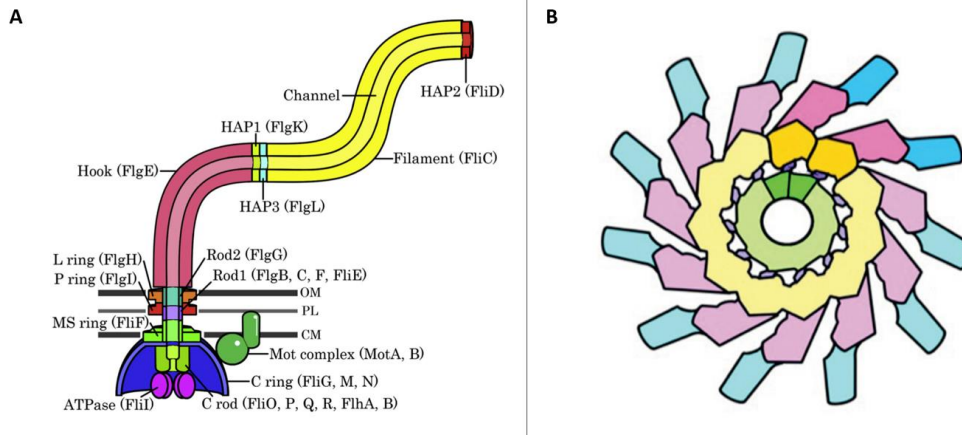


**Fig.7. Structure of the flagellum gram-negative bacteria.** (A) The three main components and proteins of the flagellum: the basal body, hook and filament. The basal body structure spans through the layers of the cell envelope where the flagellar filament is attached to by the hook. Hap, hook associated protein; OM, outer membrane; PL, peptidoglycan layer; CL, cell membrane. (B) Helical structure of the flagellin filament. Four domains comprise the filament architecture, creating a helical structure with a central channel. The domains are identified by different color; Hap, hook associated protein; OM, outer membrane; PL, peptidoglycan layer; CL, cell membrane. Image adapted from Aizawa (2014).

The basal body of the flagellum serves as the motor that makes the rotation and movement of the flagellum possible, this movement is directly linked to molecular signals released by the sensing of different chemical gradients in the environment, which dictate the behavior to either approach or retreat from the signal source (Armitage, 1999). The possession of a flagellar apparatus creates a considerable energetic tax upon the bacteria, a large amount of metabolic energy generated from a proton motor force is needed to synthesize the components of the motor apparatus and to create the power needed for movement (Josenhans and Suerbaum, 2002). The high expense of having and using flagella may seem detrimental for bacteria, but the benefits completely outweigh the costs, since these structures are used by



pathogens as a motility system to survive, invade and colonize their specific hosts. In addition to this, flagella are also essential tools for adapting to rapid environmental changes, and avoiding lysis events, evasion of predators and respond to nutrient fluctuations in the environment.

Motility is completely necessary for the initial infection for different pathogens, flagella is essential for the chemoattraction to the host tissues and can also serve as adhesin during the start of colonization, which eventually leads to the signaling cascade for the transcriptional initiation of other virulence factors, in addition non-flagellated bacteria were less virulent for their hosts (Josenhans and Suerbaum, 2002). Furthermore, non-fimbriate and flagellated but non-motile bacteria were still recovered from internal organs in concentrations comparable to their respective wild type strains (Allen-Vercoe and Woodward, 1999).

Each major structural component of the flagellum is assembled in a hierarchical manner initiated by the insertion of a Type III export apparatus into the cytoplasmic membrane, which secretes components in the correct order to form the basal body and hook, ending with secretion of large amounts of flagellin protein to form the filament. In a similar fashion, the transcription of the flagellar genes occurs in stages, where components of the flagellum that are needed in early assembly (e.g., export components) are transcribed earlier than other components (e.g., flagellin). In *V. cholerae*, the  $\sigma^{54}$ -dependent transcriptional activator FlrA is the sole class I gene, and its activation is required for expression of the class II genes that encode the export apparatus proteins (FlhAB, FliHIJOPQR), the C ring (FligMN), and FlrC, which is a second  $\sigma^{54}$ -dependent activator. Class III genes comprised the genes corresponding to the basal body, the hook (FlgE) and part of the T ring (MotX), and its expression is dependent on the product of the *fliC* gene together with the factor  $\sigma^{54}$ . Finally, the Class IV genes are transcribed by RNA polymerase with the alternate  $\sigma^{28}$  sigma factor (FliA), which in turn is a Class II gene; Class IV genes are those that code for flagellins (FlaBCDE), motor components, chemotaxis proteins, and methyl-accepting chemoreceptors (MCPs). Interestingly the FlaA, the major flagellin subunit, is transcribed as a Class III gene, even though this is a structural component of the filament (Echazarreta and Klose, 2019).

The flagellum has been described as an important virulence factor required for the invasion of the host. In *V. cholerae* flagellar motility is necessary for passing through the thick mucin barrier of the mucosa that protects the intestinal epithelium. At the site of colonization, FliA, is activated at the same time that the *quorum sensing* master regulator HapR gets repressed, and virulence genes related to intestinal colonization are expressed (Freter and Jones, 1976; Liu *et al.*, 2008). This implies a link between motility and *quorum sensing* in *V. cholerae*, as the flagellar synthesis regulates the expression of HapR in order to produce an efficient colonization of the host and kickstarts the expression of several virulence factors (Liu *et al.*, 2008). In fact, non-motile strains showed to be less efficient than wild type strains in mice intestinal colonization. Flagellar motility could facilitate bacterial attachment to the protective mucus layer when in cooperation with the N-acetylglucosamine-binding protein and the colonization factor GbpA, which has been reported to mediate bacterial adherence to intestinal mucin (Wong *et al.*, 2012). *V. cholerae* cells use flagella to penetrate mucin layers, but lose them during the process; in this pathogen, motility has been described as required to reach the crypts of the proximal small intestine, but not the distal regions protected by a thicker mucus barrier. Penetration of the mucus barrier could be as well facilitated by flagellum-independent locomotion and/or the activity of mucolytic enzymes (Liu *et al.*, 2008; Silva and Benitez, 2016).

*V. cholerae* is an important bacterial model to study the flagellum, however, the studies published in *V. vulnificus* are scarce. The *flg* operon was proposed to be a virulence determinant in *V. vulnificus*, as a transposon insertion that disrupted the flagellar basal body rod gene (*flgC*) produced non-motile cells, and showed a significant decrease in adhesion and lethality for mice (Kim and Rhee, 2003). Another study obtained aflagellated bacteria by means of the generation of mutants in the hook protein FlgE, which anchors the flagellum filament to the base of the cell, rendering the strain immobile and deficient in virulence in mice and adhesion to glass wool (Lee *et al.*, 2004).

Motility and adhesion are two mechanisms that are jointly regulated in many bacteria, once the cells have reached their desired substrate, adhesion can commence. For this, the bacteria undergoes transcriptomic changes that cause a great reduction of motility in order to achieve irreversible adhesion, and in the case of pathogens, the start of colonization and

invasion of the host, where other factors such as iron availability can influence the role of the flagellar apparatus (Pajuelo *et al.*, 2016). However, once inside the host, the pathogen should express other mechanisms specifically tailored for survival and pathogenesis inside the host environment, such as bacterial pili, toxins and enzymes (Josenhans and Suerbaum, 2002).

## 6.2.- Bacterial pili

Pili are multiple fimbrial structures formed by various polymerized monomer subunits called pilin. These filamentous organelles are present in the surface of all gram-negative bacteria (Sauer *et al.*, 2000; Craig *et al.*, 2004), and recently, a different type of pili, made by isopeptidic bonds, has been described in gram-positive bacteria (Barocchi and Telford, 2014). Many classes of pili are known, distinguished by their structure and function, the most important ones include; adhesion to different surfaces (included host cell in the case of bacterial pathogens), exchange of genetic material between cells (conjugative pili), evasion of the immune system, formation of cellular aggregations, and biofilm production (Barocchi and Telford, 2014). Through pili, the pathogen comes in contact with the host cells, and consequentially, a complex cascade of signals are induced through the cell-to-cell contact, which will determine the outcome of the colonization and infection (Sauer *et al.*, 2000). Despite their particular structures, variations in composition and function, these filaments have a common preserved trait amongst different gram-negative bacteria, this feature is an adhesive tip protruding from the end of the filament. The adhesive tip and assembly-disassembly motion of the structural pilins, enable the bacteria to perform different functions such as, DNA uptake, transformation, transfer of effector proteins and different types of motility (Barocchi and Telford, 2014). For example, twitching motility and social gliding uses a special type of pilin which makes the movement of the cell possible by using the pili as a sort of molecular anchor or grappling hook (**Figure 8**) (O'Toole and Kolter, 1998b). This mechanism of movement is slow, but works perfectly for the formation of adhesive colonies, and is used by several gram-negative bacteria like *Neisseria gonorrhoeae* and *P. aeruginosa* (Aizawa, 2014).

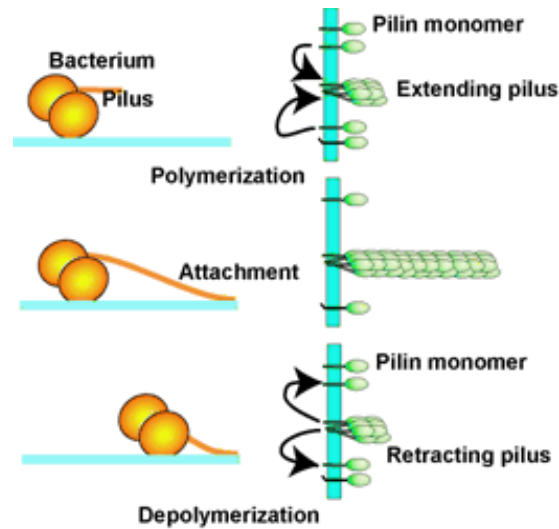


**Fig.8. Molecular mechanisms behind twitching motility.** Pilin monomers being extended and retracted via polymerization to achieve twitching motility, by using the adhesive tip at the end of the polymer the bacteria can pull itself thorough solid surfaces. Image taken from [www.uni-muenster.de](http://www.uni-muenster.de)

There are several known types of pili; the chaperone-usher pili, the toxin co-regulated pili (TCP), the Type III secretion needle, the Type IV pili, and the Type V pili (Barocchi and Telford, 2014; Hospenthal *et al.*, 2017). Next, we will focus on the Type IV pili, which are the ones studied in this thesis.

### 6.3.- Type IV pili

The toxin-coregulated pilus of *V. cholerae* and the MSHA pili belong to a very conserved, widespread and multifunctional family of pilins, the Type IV pili. These pili are the only types of pili that regulate motility (Ottow, 1975), moreover, they are involved in many bacterial processes, providing the ability to adhere to many chemically-diverse surfaces, promote bacterial aggregation, biofilm formation and virulence (Burrows, 2012). These appendages are extraordinarily thin and flexible filaments of no more than 9nm in width, which form bundles with each other (**Figure 9**). These pili are present in a vast quantity of bacterial species, and are the only type of bacterial pili found in both gram-positive and gram-negative bacteria (Wall and Kaiser, 1999; Berry and Pelicic, 2015; Craig *et al.*, 2019).

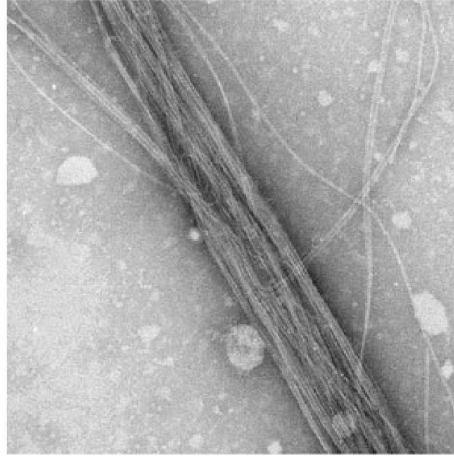


**Fig.9. Morphology of the Type IV pili.** Transmission electron microscopy image of a common bundle of Type IV pili of *Neisseria meningitidis*. Image taken from Pelicic (2008).

As mentioned before, Type IV pili are involved in a wide variety of functions, they enable bacteria to adhere to various surfaces and host cells, invasion of the host, electron transfer, DNA uptake, twitching and gliding motility, and are distinct from other types of pili thanks to their polar location (Wall and Kaiser, 1999; Barocchi and Telford, 2014; Hospenthal *et al.*, 2017). One of the most remarkable and unique characteristics of the Type IV pili, is their ability to extend and retract through polymerization and deconstruction of their pilin subunits achieved through cytoplasmic ATPases (Maier *et al.*, 2002; Mattick, 2002; Hospenthal *et al.*, 2017). These properties allow the bacteria to perform twitching motility which is a communal movement that involves cell to cell contact, interestingly, isolated cells normally do not participate in this type of motility. In *P. aeruginosa* twitching motility can be observed as it starts at the center of the colony and moves towards the outside, while forming distinctive characteristic clusters (Mattick, 2002; Murray and Kazmierczak, 2008). This kind of motility can be used by the bacteria to either bring together cells in order to form biofilms when the nutrients are scarce, or direct colonies to expand and colonize other surfaces during periods of nutrient-rich conditions (O'Toole and Kolter, 1998a).

By promoting the grouping and aggregation of bacterial cells, Type IV pili also influences attachment to different surfaces and interaction between its neighboring bacteria. The interactions are mediated by a complex net of regulatory systems and by intimate contact

through retraction of their Type IV pili. This behavior leads to aggregation, production of microcolonies and the eventual formation of biofilms, where DNA exchange is promoted between cells (Mattick, 2002; Berry and Pelicic, 2015). Type IV pili adhesion properties permit non-specific attachment of the bacteria to several different surfaces where they can start the aggregation and biofilm production, this is achieved by a nonspecific adhesion enabled by their adhesive subunit at the end the pilus (Skerker and Berg, 2001). In addition, these pili can bind to specific receptors of the epithelium and other types of cell tissue of different mammals, giving them a role in invasion and colonization, as well as establishing them as an important virulence factor (Merz and So, 2000). Although these pili are divided in subfamilies that differ in structure and components (see below), they share a typical architecture and a general molecular machinery which is composed of several subcomplexes that involve a great number of proteins and subunits, all required for a functional system (**Figure 10**) (Hospenthal *et al.*, 2017).

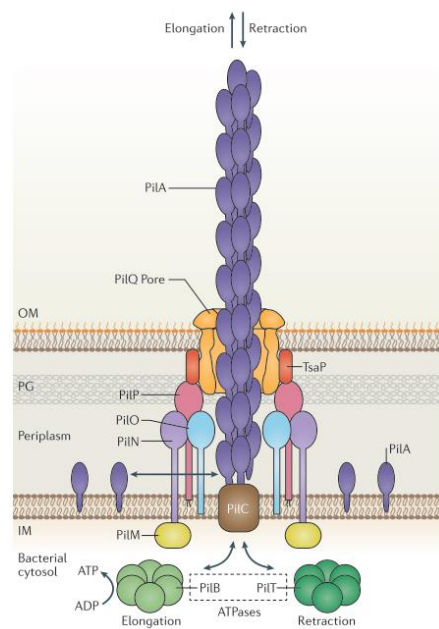


**Fig.10. The general Type IV pili machinery for retraction and elongation.** The different components of the Type IV pili system. Pilins are translocated into the inner membrane and polymerized into growing pilus, this machinery is composed of the outer membrane secretin subcomplex (not shown), the alignment subcomplex (PilM–PilN–PilO–PilP), and the inner membrane motor subcomplex (PilC–PilB–PilT). The energy for elongation and retraction is generated by ATP hydrolysis by PilT and PilB. Image taken from Hospenthal *et al.*, (2017).

Briefly, the pilin subunits are inserted into the inner membrane where their signal peptide is cleaved and methylated by a prepilin peptidase, then they are incorporated into the base of the pilus. Mature pilins keep spawning into the inner membrane to be added to the growing filament, this process is powered by the motor subcomplex composed of the inner membrane protein PilC and the ATPases PilB and PilT. These ATPases enable the elongation and consequential retraction of the filament through an outer membrane subcomplex, a pore where the pilus passes through (Barocchi and Telford, 2014; Berry and Pelicic, 2015; Hospenthal *et al.*, 2017). In summary, the Type IV pili and its biogenesis components are formed by a group of core proteins; the major pilin, a peptidase for processing the pilin subunits, ATPases that power the assembly, and an outer membrane protein that functions as an exit window of the pilus. This machinery shares common origins and structure with the archaeal flagella and the type II secretion system (Leighton *et al.*, 2015). The Type II secretion system is a widely distributed system amongst bacteria as it exports proteins and protein complexes from the inside of the cell towards the outer membrane in order to be released or remain associated with the bacterial surface (Cianciotto, 2005).

Although the pilin subunits of Type IV pili vary in structure and length, they always conserve a type III N-terminal signal sequence (Pelicic, 2008; Giltner *et al.*, 2012). The N-terminus is a highly conserved transmembrane segment that comprises a positively charged signal followed by a glycine, which is the cleavage site for one dedicated prepilin peptidase that varies between species. The mature pilin protein contains a highly conserved, extended, and hydrophobic N-terminal  $\alpha$ -helical region, that forms the core of the pilus fiber, followed by a globular C-terminal domain that is exposed on the outside surface. As the globular domain is highly variable, it provides diverse binding properties to several surfaces (Giltner *et al.*, 2012; Berry and Pelicic, 2015). Type IV pili are further subdivided into two types (Type IVa and Type IVb) based on the length of their leader sequence and mature pili, interestingly, they can be both expressed simultaneously in some species. Type IVa pilins have a short (5–6 residues) leader peptide, whereas Type IVb pilins commonly have a longer (13–30 residues) leader peptide, while the final mature pilin can be either longer (180–208 residues) or considerably shorter (40–50 residues) than mature Type IVa pilins (150–160 residues) (Giltner *et al.*, 2012).

Type IVa are a relatively homogeneous class and are widely distributed, even found in eukaryotic cells, this subfamily includes the Mannose-sensitive hemagglutinin (MSHA) pili. The Type IVb is more diverse and, although they share the same genetic organization as IVa, they are encoded by a fewer number of genes clustered into operons (**Table 1**). Each class has specific assembly systems that differentiate them in a more robust way (Burrows, 2012) (**Figure 11**).

**Table 1. Type IV pilin proteins and subunits in different bacterial species.**

Component	Pilin proteins		
<b>Type IVa pili</b>	<i>Pseudomonas aeruginosa</i>	<i>Neisseria spp.</i>	<i>Vibrio cholerae</i> (MSHA <sup>1</sup> )
<b>Major subunit</b>	PilA	PilE	MshA
<b>Core minor subunits</b>	FimU, PilV, PilW, PilX	PilH, PilI, PilJ, PilK	MshA, MShC, MshD, MshO
<b>Noncore minor subunit</b>	PilE	PilX (PilL), PilV, ComP	
<b>Prepilin peptidase</b>	PilD	PilD	VcpD
<b>Type IVb pili</b>	<b>EPEC<sup>2</sup> (bundle-forming pili)</b>	<i>Vibrio cholerae</i> (Tcp <sup>3</sup> )	<b>R64 thin pili</b>
<b>Major subunit</b>	BfpA	TcpA	PilS
<b>Core minor subunits</b>	BfpI, BfpJ, BfpK	TcpB	PilV
<b>Prepilin peptidase</b>	BfpP	TcpJ	PilU
<b>Tad pili</b>	<i>Aggregatibacter actinomycetemcomitans</i>	<i>Caulobacter crescentus</i>	<i>Pseudomonas aeruginosa</i>
<b>Major pilin subunit</b>	Flp	PilA	Flp
<b>Core minor subunits</b>	TadE, TadF	-----	TadF
<b>Prepilin peptidase</b>	TadV	CpaA	FppA
<b>Type II pseudopili</b>	<i>Klebsiella oxytoca</i>	<i>Vibrio cholerae</i>	<i>Pseudomonas aeruginosa</i>
<b>Major subunit</b>	PulG	EpsG	XcpT
<b>Core minor subunit</b>	PulH, PulI, PulJ, PulK	EpsH, EpsI, EpsJ, EpsK	XcpU, XcpV, XcpW, XcpX
<b>Prepilin peptidase</b>	PulO	VcpD	XcpA

<sup>1</sup>Mannose-sensitive hemagglutinin pili.

<sup>2</sup>Enteropathogenic *E. coli*.

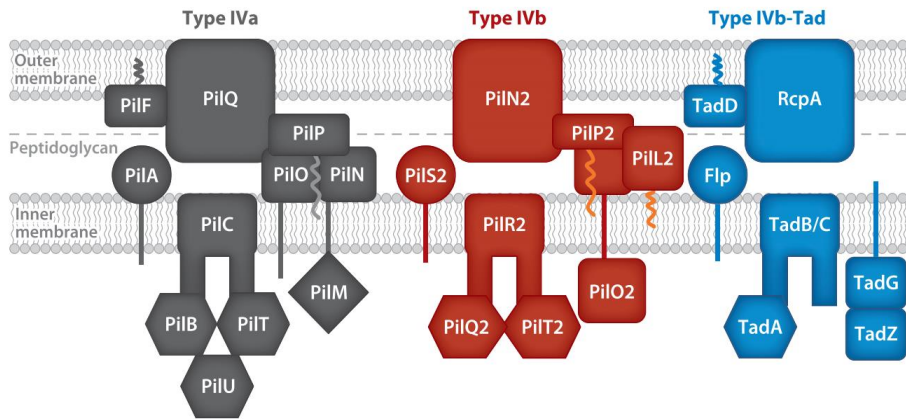
<sup>3</sup>Toxin-coregulated pili

Table adapted from Glitner *et al.*, (2012)

Type IVa pili do not form bundles and have short leader peptides, their pilin length is around 150-160aa and are anchored in the cell envelope. These pili permit the movement of the cells by the adhesive properties of the pilus and the towing motion created by the extension and retraction of the filaments, they are also involved in twitching motility and biofilm production (**Figure 10**) (Pelicic, 2008; Chang *et al.*, 2016). The adhesive capabilities and fully functionality of Type IVa pili were found to be necessary for the establishment and structure of biofilms in *P. aeruginosa*, since nonpiliated cells formed deficient biofilms (O'Toole and Kolter, 1998a; Burrows, 2012). Their biogenesis requires up to 40 genes scattered



throughout all their genome, although the MSHA pili differs in this trait, since all its complete assembly machinery genes are clustered into one single locus (Craig *et al.*, 2004; Giltner *et al.*, 2012; Roux *et al.*, 2012). Interestingly, the proteins that form the Type IVa pilins conserve a greater homology amongst themselves than with any other Type IV pilins (Craig *et al.*, 2004; Pelicic, 2008; Roux *et al.*, 2012).



**Fig.11. Different types of assembly systems of Type IV pili.** The structure and location in the cell envelope of the assembly systems is shown with their respective components. The major pilin subunits are PilA, PilS2 and Flp, several differences in the components of the system clearly mark the difference between these subfamilies of the Type IV pili. Image taken from Burrows (2012).

The Type IVb pili are less known and are not associated with motility, but they are involved in self-aggregation, biofilm formation, adhesion to eukaryotic cells, secretion and transmission of endogenous DNA for conjugation (Giltner *et al.*, 2012; Roux *et al.*, 2012). Their pili machinery is encoded by drastically fewer genes in comparison to those of the Type IVa pili, and are clustered in tightly regulated operons comprising 11-14 genes, that were most likely acquired through horizontal gene transfer (Roux *et al.*, 2012). The average length of their filament can vary depending on its subunits, which can make the pilus either long or extremely short (40-50aa), but whatever the case, they retain a very conserved morphology (Pelicic, 2008). This subfamily is divided even further into the Tad pili, a type of small pili (7-8kDa) that are present in both gram-negative and positive bacterial species (Giltner *et al.*, 2012). This

subtype of Type IV pili have their own unique set characteristics and biogenesis machinery (**Figure 11**) (Pelicic, 2008; Imam *et al.*, 2011).

The discovery and numbers of these pili are steadily increasing with the advent of more genome sequencing and analyses, and in a similar fashion, additional functions are being discovered. However, many of the processes involved still need to be identified. For this reason, only two main Type IV pili were studied in this work, and they will be thoroughly described below, these are the MSHA pili and Tad pili.

#### **6.4.- The MSHA pili**

The mannose-sensitive hemagglutinin (MSHA) pili was first classified by observing that hemagglutination was mediated by a specific pili in *V. cholerae* El tor strains (Jonson *et al.*, 1991). These appendages are essential for biofilm formation in biotic and abiotic surfaces, as well as motility and environmental persistence, and it is present in all *V. cholerae* El Tor strains (Marsh *et al.*, 1996; Marsh and Taylor, 1998a; Chiavelli *et al.*, 2001). The MSHA belongs to the Type IVa pili subfamily and has the peculiar characteristic of being organized in one single locus (**Figure 12**) in contrast to all the other pili under this classification (Marsh *et al.*, 1996; Giltner *et al.*, 2012; Roux *et al.*, 2012). In *V. Cholerae* the MSHA locus is 16.7kb in length and composed of 17 contiguous open reading frames containing the structural and secretory operons, including the major pilin subunit *mshA*, which is the main structural component of the pilus (Marsh and Taylor, 1998a).

The MSHA pili has been extensively researched in several *V. cholerae* strains, which led to a clear understanding of its role in biofilm production and attachment to biotic and abiotic surfaces (Thelin and Taylor, 1996; Chiavelli *et al.*, 2001). Knockout mutants of the MSHA pili exhibit impaired biofilm production and a severe hindrance in initial attachment (Watnick *et al.*, 1999; Chiavelli *et al.*, 2001; Jones *et al.*, 2015), they also show a reduction in the time they spent orbiting, a type of movement necessary to irreversibly attach to the substrate. This in turn increases the aimless roaming of the bacteria due to unrepressed flagellar activity, which

prevents pili interactions with potential target surfaces for adhesion (Utada *et al.*, 2014; Jones *et al.*, 2015; Sinha-Ray and Ali, 2017; Pu *et al.*, 2018).

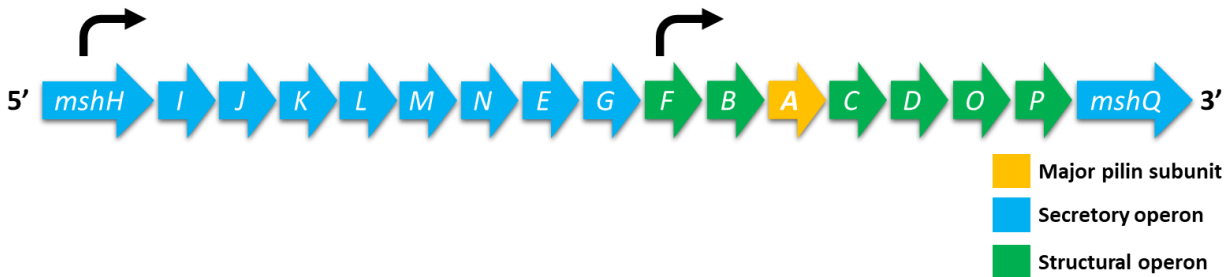


**Fig.12. Representation of the MSHA locus in *V. cholerae*.** The MSHA locus is comprised of two operons spanning 17 genes. The distinct operons and the major pilin subunit are color coded, the black arrows indicate the promoters for each operon. Imagen adapted from Marsh and Taylor (1998).

Floyd *et al.*, (2020) found out that these pilus are located in the lateral surfaces of the bacteria and are capable of retraction (**Figure 13**). They also described that the attachment to the substrate is regulated by c-di-GMP and the retraction and extension of the pilus is aided by PilT, but mainly pushed by interactions between another ATPase with high affinity receptors for c-di-GMP, the MshE (Nakhamchik *et al.*, 2008). Mutants in this ATPase and its union domain are incapable of extending the MSHA pili into the extracellular space. If functional, these mechanical movements stimulate near-surface motility patterns and aid in initial surface attachment. After cell division and proliferation of the already attached cells, this newly formed bacteria can either remain attached, aid in the microcolony formation or return to a planktonic state (Floyd *et al.*, 2020). The longer the cells remain attached, the higher the concentration of c-di-GMP will become, which will induce the production of extracellular matrix components and promote biofilm formation (Nakhamchik *et al.*, 2008; Chodur and Rowe-Magnus, 2018; Floyd *et al.*, 2020).

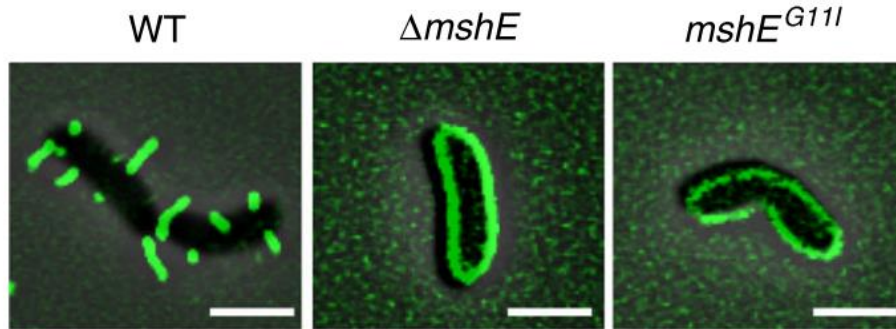


**Fig.13. The MSHA pili are distributed laterally alongside the cell envelope of *V. cholerae*.** Fluorescent images of MSHA pili of different strains of *V. cholerae*. The MSHA pili can be observed protruding from the lateral surface of the cell in the wild type, while in the *mshE* mutant, they remain retracted within the cell. A similar phenotype occurs in the *mshE*<sup>G11I</sup> mutant, which lacks the c-di-GMP domain of the MshE ATPase. Image taken from Floyd *et al.*, (2020).

Although MSHA pili play an essential role in environmental survival and adhesion to different surfaces, little has been described for its involvement in organ colonization or any other type of virulence traits. Several studies in mice had shown that the MSHA pili of *V. cholerae* is not necessary for a successful colonization of the intestine (Attridge *et al.*, 1996; Thelin and Taylor, 1996; Watnick *et al.*, 1999; Zampini *et al.*, 2003; Pruzzo *et al.*, 2008). However, another study in *V. cholerae* showed that the MSHA pilus must be repressed *in vivo* by ToxT, a transcriptional regulator, in order to successfully colonize mice intestines (Hsiao *et al.*, 2006). The authors explained that this repression is critical for host colonization, because this pili is identified by the S-IgA immunoglobulin in the mucosa, and inhibits the adhesion and colonization mediated by other virulence factors, like the TCP. Interestingly, MSHA repression seems to begin 12-h after initial infection, but these pili might be also expressed in latter stages of infection, as antibodies had been found in blood of recovering cholerae patients (Hang *et al.*, 2003). These results indicate that inhibition of the MSHA pilus is necessary for the initial evasion of the innate immune system (Hsiao *et al.*, 2006).

In a more recent study, the same authors described that the MSHA pili is degraded by the ToxT-regulated pre-pilin peptidase TcpJ. This peptidase recognizes the major pilin subunit of the MshA pili and degrades it, inhibiting the polymerization of a functional pilus (Hsiao *et al.*, 2008). Moreover, the authors hypothesized that the MSHA are dynamic structures capable of

retracting, thus a constant supply of pilus subunits is needed in order to pili to assemble and disassemble. As mentioned before, Floyd *et al.*, recently confirmed that the MSHA pilus is a dynamic extendable and retractable system, and its activity is directly controlled by c-di-GMP (Floyd *et al.*, 2020). Nevertheless, all these studies had only been performed on *V. cholerae*, and knowledge about the function and presence of this particular pilus in other species is relatively limited. Interestingly, *V. vulnificus*, contains the MSHA locus and the major pilin subunit gene *mshA* encoded within its genome, but does not have homologues of either ToxT or TcpJ. In addition, some of *V. vulnificus* isolates harbor more than one *mshA* encoded in their genome, and the role in virulence of those genes, if any, remains unknown.

### 6.5.- Tight adherence pili

It was observed that fresh clinical isolates of the periodontal pathogen *Aggregatibacter actinomycetemcomitans* produced long, filamentous fibrils, which were required to form a tenacious and structurally strong biofilm. These fibril are composed of bundles of individual pilus strands eventually denominated Flp (Fimbrial low molecular-weight protein) pili (Inoue *et al.*, 1998). Through transposon mutagenesis, the identification of a 14-gene segment, designated the *tad* (tight adherence) locus was possible (**Figure 14**). The *tad* genes encode a macromolecular transport system that is required for the biogenesis of the Flp pili (Kachlany *et al.*, 2000, 2001), including its major pilin subunit, the Flp-1. The only *tad* gene that is not required for the Flp-pilus expression in *A. actinomycetemcomitans* is the *flp-2* gene, which was predicted to encode a second pilin, but does not seem to be expressed by the bacteria (Tomich *et al.*, 2007).

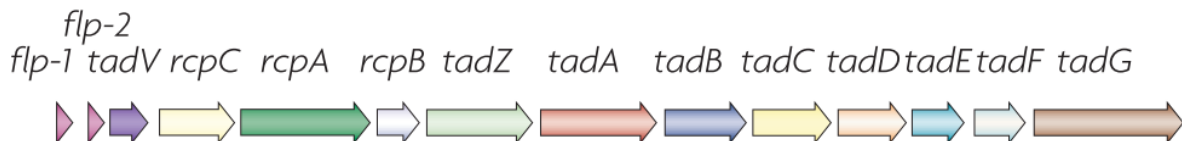


**Fig.14. Configuration of the Tad locus of *Aggregatibacter actinomycetemcomitans*.** The major pilin subunit is coded by the genes *flp-1*, while *flp-2* is predicted to code for a second pilin but is not required for the pilus expression. Image taken from Tomich *et al.*, (2007).

The Tad pili are a special type of appendage that differs from other Type IV pili because of their remarkably small size, which consists of approximately 50-80aa in length, and in this species their need of the specific prepilin peptidase TadV, for the processing of its subunits (De Bentzmann *et al.*, 2006; Burrows, 2012). These pili are not associated with motility since they lack an homologue of the ATPase in charge of pilus retraction observed in other Type IV pili, but there is growing evidence of their involvement in pathogenesis, colonization, adhesion, microcolony formation, biofilm production, rugose colony phenotype and several other functions (Tomich *et al.*, 2007; Roux *et al.*, 2012; Pu and Rowe-Magnus, 2018; Pu *et al.*, 2018; Duong-Nu *et al.*, 2019).

The structure of this pilus is made up by Flp monomers attached together through strong hydrophobic interactions mediated by their N-terminal domains forming a prepilin. This prepilin is then processed by TadV, which is essential for the correct assembly and functioning of the pilus (Tomich *et al.*, 2006). After the newly formed pilus is polymerized, it is anchored to the cell by TadG, a protein that was previously thought to be the major pilin subunit of the Tad pilus, but it is now classified as a component of the biogenesis apparatus (Wang and Chen, 2005). Two other Tad proteins are also essential for the correct Flp pilus expression, these are TadE and TadF, which are considered to be pseudopilins because of their pilin-like features and are also processed by TadV (Kachlany *et al.*, 2001). Pseudopilins in the Type II secretion system form a pilus-like structure called the “pseudopilus” that functions as a pump that secretes substrates into the outer membrane (Sandkvist, 2001). Like their analogous proteins in this secretion system, TadE and TadF are processed and inserted in the bacterial membrane, where they form structures akin to pseudopili in the periplasmic space (Tomich *et al.*, 2007). These proteins represent a novel class of pseudopilins since they do not present similarities to other Type IV pili or Type II secretion system proteins, but they do share similar functions (Tomich *et al.*, 2006).

The *tad* genes are present in several gram-negative and gram-positive bacteria, including some important human pathogens like *Yersinia pestis*, *Mycobacterium tuberculosis*

and *Bordetella pertussis*, representative agents of serious infectious diseases for humans. (Tomich *et al.*, 2007; Burrows, 2012). However, these pili seem to belong to a less widespread family, that is genetically more homogenous in terms of gene conservation and organization than the rest of the Type IVb pili (Tomich *et al.*, 2007). Another exclusive characteristic of the Tad pili, is the lack of homologs of its four core minor pilins, phylogenetic analyses suggest that an ancient divergence occurred between the homologous components of the Type II secretion system and the Type IV pili. This suggests that the Tad pili system should be considered as a new major secretion system (Tomich *et al.*, 2007).

Several *Vibrio* genomes possess more than one *tad* locus, the clinical strain CMPC6 of *V. vulnificus* harbors three distinct loci (**Figure 15**); *tad-1*, which is expressed under iron limited conditions, *tad-2* expressed in artificial sea water and *tad-3*, denominated “iam” (Initial attachment), which is essential for the first steps of substrate attachment in the environment, auto-aggregation and resistance against mechanical clearance (Pu and Rowe-Magnus, 2018; Pu *et al.*, 2018; Duong-Nu *et al.*, 2019). In *A. actinomycetemcomitans* the individual *tad* genes are clustered in a single locus, and they are expressed by a promoter region upstream of their *flp* genes. This promoter is in charge of transcribing all of the *tad* genes from *flp* to *tadD* (Haase *et al.*, 2003). Mutants in this promoter changed their colony morphology from rugose to smooth, which is characterized for being non-adherent and defective in biofilm production (Wang *et al.*, 2005). In *V. vulnificus* *tad-3* is involved in rugose colony formation and this phenotype is only fully achieved through the contribution of Tad pili (Pu and Rowe-Magnus, 2018). This implies that any mutation or alteration of the *tad* locus can lead to less adherent cells and colonies instead of other cellular mechanisms also involved in this process, highlighting the importance of Tad pili mediated adhesion.

These loci seem to be widely spread among several virulent *V. vulnificus* strains, suggesting a role in pathogenesis (Gulig *et al.*, 2010; Morrison *et al.*, 2012). To prove this, a recent study evaluated how each operon contributed to *V. vulnificus* pathogenesis by creating individual, double and a triple complete locus deletions of the Tad pili systems in the CMPC6

strain (Duong-Nu *et al.*, 2019). The results showed that *tad-1* seemed to be more involved, but not essential, in adhesion to host cells, which correlates with its expression under iron restrictive conditions, as this mimics the environment inside of a host. However, no other significant change was observed in individual or double loci mutants. When the authors deleted all three loci, the bacteria became susceptible to complement-mediated bacteriolysis and had deficient biofilm formation, adhesion, impaired invasive capabilities in mice, and a defective production of the RtxA1 toxin. This suggests that all three *tad* operons are required for full *V. vulnificus* virulence, moreover, by helping in the evasion of the immunity system, the *tad* loci should confer a “stealth” mechanism that grants *V. vulnificus* the ability to hide from phagocytes and avoid being killed (Duong-Nu *et al.*, 2019).

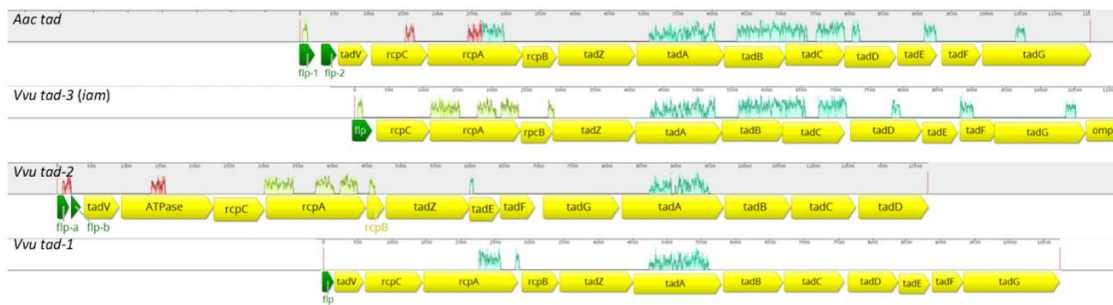


**Fig.15. The three *tad* loci found in the genome of *V. vulnificus* CMPC6.** A comparison of the components of the distinct *tad* loci in the genome of a clinical strain of *V. vulnificus* with the one of *A. actinomycetemcomitans*. The *tad-3* locus was denominated iam (Initial attachment) for its role in the attachment and avoidance of mechanical clearance in the environment. Image taken from Pu and Rowe-Magnus (2018).

## 7.- Biofilm

Bacteria have the remarkable ability to adhere to various surfaces, and with this “simple” action, a community of bacteria can start growing into a highly regulated and complex structure called biofilms, that not only shields them from many environmental factors, but promotes further colonization of more surfaces and general growth (Toole *et al.*, 2000). Biofilms are remarkable bacterial aggregations visible to the naked eye. This type of bacterial community development has been steadily studied by microbiologists since the 1970’s, and



during this time it was determined that biofilms constitute an important percentage of all the bacterial biomass in the planet (Costerton *et al.*, 1978). Sometime later, scientist began to understand that this sticky aggregation of bacteria was not just a clump of cells, but a complex community with specific characteristics, that could adhere to very specific surfaces. A common example of this are the plaque forming bacteria that attaches to the teeth of different dentistry patients (Costerton *et al.*, 1999).

After several advances in microscopy and other fields of science, and conjoint efforts of disciplines such as ecology, mathematics, and microbiology, the biofilm structure finally was thoroughly studied. (Costerton *et al.*, 1999). At first it was believed that biofilms were a single one-dimensional “smudge” of bacterial growth, but after the advent of more complex microscopy technologies, the real structure composed of a matrix of enclosed microcolonies was discovered. Within two decades of research, biofilm was defined as a structured community of bacterial cells encased in a polymeric matrix with adherent capabilities to biotic and abiotic surfaces. The cells that conform this aggregation are capable of expressing different genes than the free living planktonic cells, this differential expression shows a complex level of differentiation that is conducted by sophisticated cell to cell signaling systems and cellular specialization. This type of bacterial organization is remarkable and unique, since it involves the formation of a coordinated multicellular system organized by different individual prokaryotic cells, instead of a larger and more complex eukaryote organism (Stoodley *et al.*, 2002).

Production of a mature biofilm is crucial for bacterial survival in different settings and locations, normally, this would make them very diverse and specialized to their specific niche, nonetheless, the visible appearance of biofilms are surprisingly similar, meaning the existence of a common and conserved structure among numerous bacterial species (Hall-Stoodley *et al.*, 2004). Even so, there are several differences among different bacterial biofilms, for example, biofilms in periodontitis patients are thicker and their architecture allows every distinct microcolony to remain anchored to the surface of the teeth and enables each individual cell manage the shearing forces of the buccal environment. This type of biofilm structure allows an easier nutrient distribution to singular cells, and helps develop biofilms with considerable thickness and complexity (Stoodley *et al.*, 2002). The process of biofilm formation has been

proposed to be in five differential stages (**Figure 16**); Initial attachment, production of extracellular polysaccharide (EPS), development of the biofilm architecture, maturation and dispersion (Stoodley *et al.*, 2002; Hall-Stoodley *et al.*, 2004).

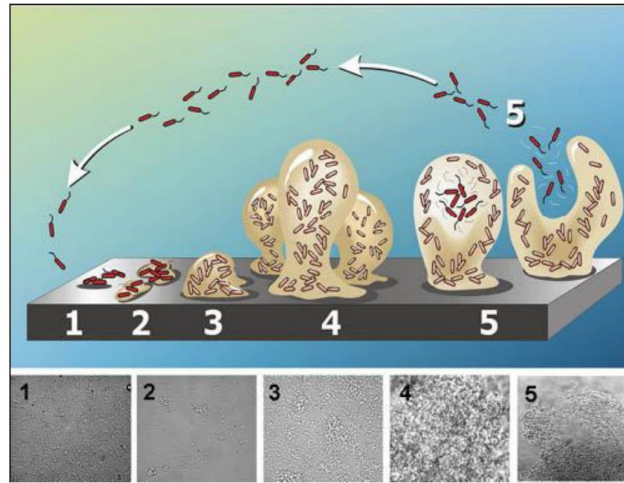


**Fig.16. Five-stage process of biofilm development.** (1) Initial attachment to biotic or abiotic surfaces. (2) Secretion of EPS. (3) Initiation of biofilm structure. (4) Maturation of the biofilm structure and microcolonies. (5) Dispersion. Image taken from [www.the-scientist.com](http://www.the-scientist.com)

Biofilm production starts when bacteria sense environmental cues which dictates the transition into sessile living from swimming planktonic lifestyles, which leads to the initiation and regulation of the initial attachment. These environmental factors vary among different bacteria, which have multiple genetic pathways to govern this behavior (Toole *et al.*, 2000). *V. cholerae* strains defective in EPS are deficient in initial attachment, early biofilm production and have aberrant biofilm structures during the infective process (Watnick and Kolter, 1999), while similar mutants in *P. aeruginosa* showed no impairment in initial attachment. This suggest that, despite the mechanisms employed for the production of biofilm, common traits are shared among species, however, specific functions may still be different, and their importance may not be comparable among all species (Toole *et al.*, 2000).

The initial attachment to surfaces begins by preparing the substrate by covering it with a thin bacterial film in order to absorb any organic and inorganic debris that could obstruct the adhesion, and to neutralize the surface charge that could repel the attachment of the bacteria

(Mahami and Adu-Gyamfi, 2011). The consequent biofilm formation is a process that can take up to 10 days, and can occur by three different forms: movement of already attached cells by surface motility of Type IV pili (O'Toole and Kolter, 1998a), self-replication of already attached cells, and recruitment of free living cells from the environment. There is no set level of contribution for any of these mechanisms in the production of biofilm, since the process depends on the overall conditions of the environment that the bacteria are colonizing (Stoodley *et al.*, 2002).

Once the bacterial cells are associated with the surface, the change into irreversible attachment starts by shifting the weak interaction forces of the cells to the substratum into permanent adhesion by extracellular products such as EPS. The production of EPS not only cements the bacteria in place, but also prevents desiccation in environmental biofilms, and could also enhance antimicrobial resistance by binding to harmful molecules and preventing them from reaching the cells (Mahami and Adu-Gyamfi, 2011). Other types of extracellular products can be secreted to aid in this step in biofilm formation, for example, in *P. aeruginosa* alginate is produced, which is involved in biofilm production in pulmonary infections (Stoodley *et al.*, 2002), and in *Staphylococcus epidermis* adhesins bond the cells together and enhance microcolony formation and maturation of the biofilm (Gerke *et al.*, 1998). In the transition to irreversible attachment, other cellular mechanisms are actively involved, such as twitching motility (O'Toole and Kolter, 1998b; Mattick, 2002).

The third stage of biofilm development; the maturation step, involves the growth of the attached bacteria and the production of microcolonies that will lead to the final biofilm structure (Mahami and Adu-Gyamfi, 2011). Once the attached cells start to grow and produce microcolonies, the bacteria needs to adapt to this novel "pluricellular" lifestyle, and undergo metabolic changes in order to generate a complex architecture for the redistribution of cells away from the substrate (Davies *et al.*, 1998; Toole *et al.*, 2000). Biofilm maturation stage is a heavily regulated process that entails radical morphological and genetic changes in order for the bacteria to survive and adapt to this new lifestyle. Studies in several different species showed that, in mature biofilms gene expression changes drastically in comparison to planktonic bacteria. In *P. aeruginosa* almost 50% of its genes were upregulated (Sauer *et al.*,

2002), these differentially expressed proteins are involved in metabolism, LPS-biosynthesis, membrane transport and secretion, protective mechanisms, DNA translation, metabolism and gene regulation (Greenberg *et al.*, 2001). In *V. cholerae*, down-regulation of motility is crucial for the transition from planktonic to sessile lifestyle and induction of the extracellular matrix biosynthesis. Furthermore, in the mature biofilm nutrient flow and waste disposal are mediated by limited diffusion, which favors the induction of *quorum sensing* and stationary growth phase (Silva and Benitez, 2016).

To form a matured biofilm, the cells envelop themselves in EPS and other exocellular products, recruit new free-living cells and become able to resist external antimicrobial elements. This stage leads to the final step of biofilm development, the dispersion, which will allow the bacteria the subsequent colonization of other substrates. Although dispersal of bacterial cells can be produced by detachment due to external forces like fluid shear, mechanical clearance of the water flow, and degradation of the EPS, bacteria can detach themselves from the biofilm through three different methods; swarming, clumping and surface dispersal (Hall-Stoodley *et al.*, 2004). These dispersal strategies can be influenced by nutrient level fluctuations or *quorum sensing*, but biofilms can also fragment themselves in order to further colonize the environment or host organs (in case of pathogenic species). These sheared clumps can quickly revert to the planktonic lifestyle and quickly boost the dispersal of the bacteria (Mahami and Adu-Gyamfi, 2011).

Biofilms are well known bacterial structures characterized for their resilience and adaptative properties, as well as being a survival mechanism against antibiotic agents, either biological or chemical (Hall-Stoodley *et al.*, 2004; Silva and Benitez, 2016). Nosocomial infections are persistent threats to human health, and a very high percentage of these infections have been attributed to biofilms dwellings in hospital surfaces or inside medical equipment (Mah and O'Toole, 2001). Since the advent of antibiotics, few studies had been published and focused about how biofilms are affected by this compounds. Bacteria inside biofilms are protected against antimicrobial agents, this agents are unable to penetrate the entire depth of the biofilm, this is a concerning issue, given the fact that many of the infections

that affect human health are produced by commensal bacterial species known for producing resistant biofilms, like *S. epidermidis* and *P. aeruginosa* (Costerton *et al.*, 1999).

Even though bacterial cells produce antigens that stimulate the production of antibodies, these immune defenses are not prepared to kill the bacteria within biofilms, and can cause collateral damage in the surrounding tissue, which translates into biofilm infections that cannot be cleared by the immune system (Costerton *et al.*, 1999). This biofilm infection strategy has been described in *V. cholerae* when colonizing the intestine lumen of mammals (Silva and Benitez, 2016). The most effective way to deal with these biofilm-borne infections is to surgically remove the contaminated tissue, because while attached, biofilms serve as a perpetual and prolific factory of motile cells that fuel the course of the infection (Spormann *et al.*, 2004).

Several *Vibrio* species are pathogens, and can cause serious disease via various infection routes (Strom and Paranjpye, 2000). *V. cholerae* utilizes biofilms to ensure a successful growth in the aquatic environment and in the host, where biofilm aggregates were shown to be more infectious (Faruque *et al.*, 2006). *V. parahaemolyticus*, is known to form biofilms in seafood, this pathogen is a well-known causative agent of massive food-related poisoning outbreaks (Rajkowski, 2009; Han *et al.*, 2016). However, there is no doubt that biofilm production is a fundamental part of the vibrio pathogenesis and virulence, but biofilm is also essential for its life cycle, as it confers a wide arrange of mechanisms for environmental survival. For example, biofilm production by *V. harveyi* is involved in the mutualistic symbiosis between the bacteria and its particular host, the *Eupryma scolopes*, where it provides the mollusk its characteristic bioluminescence by colonizing the light organ (Ruby and Asato, 1993; Yip *et al.*, 2007). Biofilm production allows species such as *V. vulnificus* to colonize carapaces of plankton and shellfish in order to persist in the aquatic environment (Yildiz and Visick, 2009).

The production of biofilm is of utmost importance for the *Vibrionaceae* family, as they use this ability to survive and colonize in their respective niches, however, there are several differences entailing biofilm biosynthesis, regulation and functions that sets them apart from other bacteria (Yildiz and Visick, 2009; Sun *et al.*, 2013). One of the most prevalent components

in vibrio biofilms is the extracellular matrix composed of different polysaccharides, which encases the aggregates of bacterial cells, and enables them to attach to specific substrates. The genes responsible for the production of EPS and CPS are prevalent in several species of vibrio, and their expression is related to the morphology of the colonies and biofilm (Yildiz and Visick, 2009). This means that the expression of polysaccharides is tightly controlled among vibrio species, in *V. vulnificus* a complex regulatory network consisting of three transcriptional regulators; BrpT, BrpS and BrpR, create a feedback loop that controls the regulation of the *cabABC* operon. This operon is necessary for the production of robust biofilms and rugose colony morphology (Park *et al.*, 2015; Hwang *et al.*, 2020).

In *V. cholerae*, biofilm formation is dependent of its specific exopolysaccharide (VPS, *Vibrio* polysaccharide), which is encoded in two loci, and denominated as *vps*. This *vps* locus is conserved and present through several other vibrio species genomes and, in most cases, is also responsible for biofilm production (Yildiz and Schoolnik, 1999). In *V. vulnificus*, this is denominated as *wcr*, and few is known about it apart from its role in colony morphology. This locus bares great homology to the *cps* locus of *V. parahaemolyticus* which produces CPS instead of EPS and is required for opaque colony morphology (Enos-berlage and McCarter, 2000; Smith and Siebeling, 2003). An exception to the generally conserved *vps* locus, is the 18 gene cluster of the polysaccharide biosynthesis genes (*syp*) of *V. fischeri*, which is involved in colony morphology and pellicle formation. Interestingly, these genes are not found in *V. cholerae* but are conserved in *V. vulnificus*. (Yildiz and Visick, 2009). Even though there are several loci and homologues of polysaccharide genes among the *Vibrionaceae* family, they have not been profoundly studied, and roles between species might even be detrimental for biofilm formation or even contradictory while compared to one another. Moreover, distinct *Vibrio* species produce different EPS, which implies a great diversity of biofilm composition, structures and components (Yildiz and Visick, 2009).

The complexity of the biofilm needs to be tightly regulated for a successful biosynthesis. To achieve this, several species rely on *quorum sensing*, which regulates several virulence determinants (Waters and Bassler, 2005). In *V. vulnificus* and *V. fischeri*, the *quorum sensing* regulators SmcR and LitR are involved in the formation of opaque colonies, and when

disrupted, biofilm formation is severely affected (Hyun *et al.*, 2007). On the other hand, mutation in the regulator homologue HapR of *V. cholerae*, increases *vps* expression (essential for development of three-dimensional biofilm structures) and rugosity in colonies, which implies that, this regulator is an inhibitor of biofilm production in this pathogen (Yildiz *et al.*, 2004). Moreover, repression of HapR also enhances colonization of the mice intestine and incites expression of virulence factors (Liu *et al.*, 2008). Another type of regulation for biofilm comes from the ubiquitous second messenger c-di-GMP, which is produced by diguanylate cyclases (DGCs) and degraded by phosphodiesterases (PDEs) (Jenal *et al.*, 2017). This molecule controls the transition from motile to sessile lifestyle in several bacteria, when it is present in high levels it induces biofilm production and inhibits flagellar motility (Romling and Amikam, 2006; Jones *et al.*, 2015). Interestingly, several *Vibrio* species contain larger amounts of DGCs and PDEs with predicted sensory domains, which suggests the importance of c-di-GMP in this genus, and it has been proposed to allow them the capacity to adapt to different environments (Galperin *et al.*, 2001). In *V. cholerae*, c-di-GMP decreases motility and induces biofilm production by regulating the *vps* locus, similar regulatory effects can also be observed in *V. parahaemolyticus* (Yildiz and Visick, 2009). On the other hand, little is known about the role of c-di-GMP in *V. vulnificus*. In this species, DGCs induce capsule production, but does not affect motility (Nakhamchik *et al.*, 2008).

Motility in vibrios seems to have several more roles in the production of biofilm than in other bacterial species, in *V. cholerae*, when the flagella is impaired, there is a reduction in attachment to the host substrate and altered biofilm development (Watnick and Kolter, 1999; Watnick *et al.*, 2010). In addition, evidence shows that the flagellar motor could also be involved in interactions with surfaces and subsequent adhesion for biofilm production (Lauriano *et al.*, 2004). A similar characteristic was observed in *V. parahaemolyticus* where the flagellar motor mediates transition from sessile to motile cells in order to facilitate for locomotion in solid surfaces or viscous environments (Kawagishi *et al.*, 1996). In another study, a role of flagellum in the biofilm of *V. vulnificus* was described, it showed that mutants in flagella were deficient in attachment to abiotic surfaces and produced less biofilm *in vitro* (Lee *et al.*, 2004).

As flagella, pili also participates in biofilm formation and promotes cell-surface interactions. In *V. cholerae* several Type IV pili contribute to biofilm production, one of these pili, the MSHA pilus, has shown to be of significant importance for initial attachment and aggregation for planktonic cells in O1 El Tor and O139 strains (Watnick *et al.*, 1999; Chiavelli *et al.*, 2001). In *V. parahaemolyticus*, the MSHA pilus is also involved in biofilm formation, where it works in junction with the chitin regulated pilus (ChiRP), another Type IV pili, to adhere to chitinous particles (Shime-hattori *et al.*, 2006). Not only these pili are needed for biofilm, but also the enzymes in charge in processing their pilin proteins which transform them into functional, mature pili. In *V. vulnificus*, an homologous of the Type IVa prepilin peptidase PilD (VvpD) is necessary for attachment to oysters, and mutants in this enzyme showed deficient adhesion to both biotic and abiotic surfaces (Paranjpye *et al.*, 1998, 2007). Everything considered, although the *Vibrio* genus exploits various pili to promote adhesion and biofilm production, their function and relevance in the biofilm biosynthesis may vary from species to species, and would be influenced by diverse environmental cues and host responses.

However, despite extensive studies about biofilm species like *V. cholerae* and *V. fischeri* little has been studied about biofilms in another important human pathogen, *V. vulnificus*. Apart from general mechanisms shared among vibrios, and their involvement in colonization of plankton and shellfish, there is a big gap of knowledge regarding the specific role of biofilm in this species (Yildiz and Visick, 2009). The few studies focused in *V. vulnificus* biofilms mention the relation between the capsule and its inhibitory effect in biofilm production in humans (Joseph and Wright, 2004). In the case of the zoonotic clonal-complex, the biofilm has been suggested to be a survival strategy between outbreaks, as it could be detected on the body surface of surviving eels, which act as carriers (Marco-Noales Ester *et al.*, 2001).

In conclusion, these studies spanning different species of vibrios, highlight the vast difference between all the biofilm mechanisms of each individual species, even though they belong to the same genus. This boils down to the fact that there can not be a single “reference” species in place to serve as a common guideline in either the complex role of biofilms or any other type of virulence and cellular mechanisms.



## 8.- References

1. Aagesen, A.M. and Häse, C.C. (2012) Sequence Analyses of Type IV Pili from *Vibrio cholerae*, *Vibrio parahaemolyticus*, and *Vibrio vulnificus*. *Microb Ecol* **64**: 509–524.
2. Aizawa, S.I. (2014) *Flagella*, Elsevier Ltd.
3. Allen-Vercoe, E. and Woodward, M.J. (1999) The role of flagella, but not fimbriae, in the adherence of *Salmonella enterica* serotype Enteritidis to chick gut explant. *J Med Microbiol* **48**: 771–780.
4. Amaro, C. and Biosca, E.G. (1996) *Vibrio vulnificus* biotype 2, pathogenic for eels, is also an opportunistic pathogen for humans. *Appl Environ Microbiol* **62**: 1454–1457.
5. Amaro, C., Biosca, E.G., Fouz, B., Alcaide, E., and Esteve, C. (1995) Evidence that water transmits *Vibrio vulnificus* biotype 2 infections to eels. *Appl Environ Microbiol* **61**: 1133–1137.
6. Amaro, C., Sanjuán, E., Fouz, B., Pajuelo, D., Lee, C.-T., Hor, L.-I., and Barrera, R. (2015) The Fish Pathogen *Vibrio vulnificus* Biotype 2: Epidemiology, phylogeny, and virulence factors involved in warm-water vibriosis. *Microbiol Spectr* **3**:
7. Armitage, J.P. (1999) *Bacterial tactic responses*, Elsevier Masson SAS.
8. Attridge, S.R., Manning, P.A., Holmgren, J., and Jonson, G. (1996) Relative significance of mannose-sensitive hemagglutinin and toxin-coregulated pili in colonization of infant mice by *Vibrio cholerae* El Tor. **64**: 3369–3373.
9. Baker-Austin, C. and Oliver, J.D. (2018) *Vibrio vulnificus* : new insights into a deadly opportunistic pathogen. *Environ Microbiol* **20**: 423–430.
10. Baker-Austin, C., Stockley, L., Rangdale, R., and Martinez-Urtaza, J. (2010) Environmental occurrence and clinical impact of *Vibrio vulnificus* and *Vibrio parahaemolyticus*: A European perspective. *Environ Microbiol Rep* **2**: 7–18.
11. Baker-Austin, C., Trinanes, J., Gonzalez-Escalona, N., and Martinez-Urtaza, J. (2017) Non-cholera vibrios: The microbial barometer of climate change. *Trends Microbiol* **25**: 76–84.
12. Baker-Austin, C., Trinanes, J.A., Salmenlinna, S., Löfdahl, M., Siitonen, A., Taylor, N.G.H., and Martinez-Urtaza, J. (2016) Heat wave–associated vibriosis, Sweden and Finland, 2014. *Emerg Infect Dis* **22**: 1216–1220.
13. Baker-Austin, C., Trinanes, J.A., Taylor, N.G.H., Hartnell, R., Siitonen, A., and Martinez-Urtaza, J. (2013) Emerging *Vibrio* risk at high latitudes in response to ocean warming. *Nat Clim Chang* **3**: 73–77.
14. Barocchi, Michèle A. and Telford, John L. (2014) *Bacterial pili: structure, synthesis and role in disease*, Advances i. Barocchi, M. A. and Telford, J. L. (eds) Wallingford: CABI.

15. Benitez, J.A. and Silva, A.J. (2017) *Vibrio cholerae* hemagglutinin(HA)/protease: an extracellular metalloprotease with multiple pathogenic activities. *Toxicon* **115**: 55–62.
16. De Bentzmann, S., Aurouze, M., Ball, G., and Filloux, A. (2006) FppA, a novel *Pseudomonas aeruginosa* prepilin peptidase involved in assembly of type IVb pili. *J Bacteriol* **188**: 4851–4860.
17. Berry, J.L. and Pelicic, V. (2015) Exceptionally widespread nanomachines composed of type IV pilins: The prokaryotic Swiss Army knives. *FEMS Microbiol Rev* **39**: 134–154.
18. Biosca, Elena G., Fouz, B., Alcaide, E., and Amaro, C. (1996) Siderophore-mediated iron acquisition mechanisms in *Vibrio vulnificus* biotype 2. *Appl Environ Microbiol* **62**: 928–935.
19. Biosca, Elena G, Oliver, J.D., Amaro, C., Carolina, N., and Carolina, N. (1996) Phenotypic characterization of *Vibrio vulnificus* biotype 2, a lipopolysaccharide-based homogeneous serogroup within *Vibrio vulnificus* Downloaded from <http://aem.asm.org/> on December 7, 2020 at UNIVERSITAT DE VALENCIA. *Appl Environ Microbiol* **62**: 918–927.
20. Bisharat, N., Agmon, V., Finkelstein, R., Raz, R., Ben-Dror, G., Lerner, L., et al. (1999) Clinical, epidemiological, and microbiological features of *Vibrio vulnificus* biogroup 3 causing outbreaks of wound infection and bacteraemia in Israel. *Lancet* **354**: 1421–1424.
21. Bisharat, N., Cohen, D.I., Harding, R.M., Falush, D., Crook, D.W., Peto, T., and Maiden, M.C. (2005) Hybrid *Vibrio vulnificus*. *Emerg Infect Dis* **11**: 30–35.
22. Bogard, R.W. and Oliver, J.D. (2007) Role of iron in human serum resistance of the clinical and environmental *Vibrio vulnificus* genotypes. *Appl Environ Microbiol* **73**: 7501–7505.
23. Burrows, L.L. (2012) *Pseudomonas aeruginosa* twitching motility: Type IV pili in action. *Annu Rev Microbiol* **66**: 493–520.
24. Callol, A., Pajuelo, D., Ebbesson, L., Teles, M., MacKenzie, S., and Amaro, C. (2015) Early steps in the European eel (*Anguilla anguilla*)-*Vibrio vulnificus* interaction in the gills: Role of the RtxA13 toxin. *Fish Shellfish Immunol* **43**: 502–509.
25. Carda-Diéguez, M., Silva-Hernández, F.X., Hubbard, T.P., Chao, M.C., Waldor, M.K., and Amaro, C. (2018) Comprehensive identification of *Vibrio vulnificus* genes required for growth in human serum. *Virulence* **9**: 981–993.
26. Chang, Y.W., Rettberg, L.A., Treuner-Lange, A., Iwasa, J., Søgaaard-Andersen, L., and Jensen, G.J. (2016) Architecture of the type IVa pilus machine. *Science (80- )* **351**:
27. Chen, C., Wu, K., Chang, Y., Chang, C., Tsai, H., Liao, T., et al. (2003) Comparative genome analysis of *Vibrio vulnificus*, a marine pathogen. *Genome Res* **13**: 2577–2587.
28. Chiavelli, D.A., Marsh, J.W., and Taylor, R.K. (2001) The Mannose-Sensitive Hemagglutinin of *Vibrio cholerae* promotes adherence to zooplankton. *Appl Environ Microbiol* **67**: 3220–3225.

29. Chimento Tonon, L.A., Silva, B.S. de O., Moreira, A.P.B., Valle, C., Alves, N., Cavalcanti, G., et al. (2015) Diversity and ecological structure of vibrios in benthic and pelagic habitats along a latitudinal gradient in the Southwest Atlantic Ocean. *PeerJ* **2015**: 1–20.
30. Chodur, D.M. and Rowe-Magnusa, D.A. (2018) Complex control of a genomic island governing biofilm and rugose colony development in *Vibrio vulnificus*. *J Bacteriol* **200**:
31. Choi, G., Jang, K.K., Lim, J.G., Lee, Z.W., Im, H., and Choi, S.H. (2020) The transcriptional regulator IscR integrates host-derived nitrosative stress and iron starvation in activation of the *vvhBA* operon in *Vibrio vulnificus*. *J Biol Chem* **295**: 5350–5361.
32. Cianciotto, N.P. (2005) Type II secretion: A protein secretion system for all seasons. *Trends Microbiol* **13**: 581–588.
33. Cohen, A.L. V, Oliver, J.D., Depaola, A., Feil, E.J., and Boyd, E.F. (2007) Emergence of a virulent clade of *Vibrio vulnificus* and correlation with the presence of a 33-kilobase genomic island. *Appl Environ Microbiol* **73**: 5553–5565.
34. Costerton, J.W., Gessey, G.G., and Cheng, K.J. (1978) How the bacteria stick. *Sci Am* 86–95.
35. Costerton, J.W., Stewart, P.S., and Greenberg, E.P. (1999) Bacterial biofilms: A common cause of persistent infections. *Science (80- )* **284**: 1318–1322.
36. Craig, L., Forest, K.T., and Maier, B. (2019) Type IV pili: dynamics, biophysics and functional consequences. *Nat Rev Microbiol* **17**: 429–440.
37. Craig, L., Pique, M.E., and Tainer, J.A. (2004) Type IV pilus structure and bacterial pathogenicity. *Nat Rev Microbiol* **2**: 363–378.
38. Daniels, N.A. (2011) *Vibrio vulnificus* oysters: Pearls and perils. *Clin Infect Dis* **52**: 788–792.
39. Davies, D.G., Parsek, M.R., Pearson, J.P., Iglewski, B.H., Costerton, J.W., and Greenberg, E.P. (1998) The involvement of cell-to-cell signals in the development of a bacterial biofilm. *Science (80- )* **280**: 295–298.
40. Deeb, R., Tufford, D., Scott, G.I., Moore, J.G., and Dow, K. (2018) Impact of climate change on *Vibrio vulnificus* abundance and exposure risk. *Physiol Behav* **41**: 2289–2303.
41. Duong-Nu, T.-M., Jeong, K., Hong, S.H., Puth, S., Kim, S.Y., Tan, W., et al. (2019) A stealth adhesion factor contributes to *Vibrio vulnificus* pathogenicity: Flp pili play roles in host invasion, survival in the blood stream and resistance to complement activation. *PLOS Pathog* **15**: 1–29.
42. Echazarreta, M.A. and Klose, K.E. (2019) *Vibrio* flagellar synthesis. *Front Cell Infect Microbiol* **9**: 1–11.
43. Enos-berlage, J.L. and McCarter, L.L. (2000) Relation of capsular polysaccharide production and colonial cell organization to colony morphology in *Vibrio*

- parahaemolyticus*. *J Bacteriol* **182**: 5513–5520.
44. Eun Rhee, J., Haeng Rhee, J., Youl Ryu, P., and Ho Choi, S. (2002) Identification of the *cadBA* operon from *Vibrio vulnificus* and its influence on survival to acid stress. *FEMS Microbiol Lett* **208**: 245–251.
  45. Farmer, J.J. (1979) *Vibrio* (“Benecke”) *vulnificus*, the bacterium associated with sepsis, septicaemia, and the sea. *Lancet* **314**: 903.
  46. Faruque, S.M., Biswas, K., Udden, S.M.N., Ahmad, Q.S., Sack, D.A., Nair, G.B., and Mekalanos, J.J. (2006) Transmissibility of cholera : *In vivo*-formed biofilms and their relationship to infectivity and persistence in the environment. *PNAS* **103**:
  47. Floyd, K.A., Lee, C.K., Xian, W., Nametalla, M., Valentine, A., Crair, B., et al. (2020) c-di-GMP modulates type IV MSHA pilus retraction and surface attachment in *Vibrio cholerae*. *Nat Commun* **11**: 1–16.
  48. Fouz, B. and Amaro, C. (2003) Isolation of a new serovar of *Vibrio vulnificus* pathogenic for eels cultured in freshwater farms. *Aquaculture* **217**: 677–682.
  49. Fouz, B., Llorens, A., Valiente, E., and Amaro, C. (2010) A comparative epizootiologic study of the two fish-pathogenic serovars of *Vibrio vulnificus* biotype 2. *J Fish Dis* **2000**: 383–390.
  50. Freter, R. and Jones, G.W. (1976) Adhesive Properties of *Vibrio cholerae* : Nature of the Interaction with Intact Mucosal Surfaces. *Infect Immun* **14**: 246–256.
  51. Galperin, M.Y., Nikolskaya, A.N., and Koonin, E. V (2001) Novel domains of the prokaryotic two-component signal transduction systems. *FEMS Microbiol Lett* **203**: 11–21.
  52. Gavin, H.E. and Satchell, K.J.F. (2015) MARTX toxins as effector delivery platforms. *Pathog Dis* **73**:
  53. Gerke, C., Kraft, A., Süßmuth, R., Schweitzer, O., and Götz, F. (1998) Characterization of the N-Acetylglucosaminyltransferase activity involved in the biosynthesis of the *Staphylococcus epidermidis* polysaccharide intercellular adhesin. *J Biol Chem* **273**: 18586–18593.
  54. Giltner, C.L., Nguyen, Y., and Burrows, L.L. (2012) Type IV pilin proteins: versatile molecular modules. *Microbiol Mol Biol Rev* **76**: 740–772.
  55. Greenberg, E.P., Whiteley, M., Banger, M.G., Bumgarner, R.E., Parsek, M.R., Teitzel, G.M., and Lory, S. (2001) Gene expression in *Pseudomonas aeruginosa* biofilms. *Nature* **413**: 860–864.
  56. Gulig, P.A., Crécy-Lagard, V. de, Wright, A.C., Walts, B., Telonis-Scott, M., and McIntyre, L.M. (2010) SOLiD sequencing of four *Vibrio vulnificus* genomes enables comparative genomic analysis and identification of candidate clade-specific virulence genes. *BMC Genomics* **11**:

57. Haase, E.M., Stream, J.O., and Scannapieco, F.A. (2003) Transcriptional analysis of the 5' terminus of the flp fimbrial gene cluster from *Actinobacillus actinomycetemcomitans*. *Microbiology* **149**: 205–215.
58. Haenen, O.L.M., Fouz, B., Amaro, C., Isern, M.M., Zrncic, S., Mikkelsen, H., et al. (2014) Vibriosis in aquaculture. Tampere , Finland , 4 th September 2013. *Bull Eur Ass Fish Pathol* **34(4)**:
59. Hall-Stoodley, L., Costerton, J.W., and Stoodley, P. (2004) Bacterial biofilms: From the natural environment to infectious diseases. *Nat Rev Microbiol* **2**: 95–108.
60. Han, N., Rahaman, F., Kabir, I., and Ha, S. (2016) Biofilm formation by *Vibrio parahaemolyticus* on food and food contact surfaces increases with rise in temperature. *Food Control* **70**: 161–166.
61. Hang, L., John, M., Asaduzzaman, M., Bridges, E.A., Vanderspurt, C., Kirn, T.J., et al. (2003) Use of *in vivo*-induced antigen technology ( IVIAT ) to identify genes uniquely expressed during human infection with *Vibrio cholerae*. *PNAS* **100**: 8508–8513.
62. Haq, S.M. and Dayal, H.H. (2005) Chronic liver disease and consumption of raw oysters: A potentially lethal combination - A review of *Vibrio vulnificus* septicemia. *Am J Gastroenterol* **100**: 1195–1199.
63. Heng, S.P., Letchumanan, V., Deng, C.Y., Ab Mutalib, N.S., Khan, T.M., Chuah, L.H., et al. (2017) *Vibrio vulnificus*: An environmental and clinical burden. *Front Microbiol* **8**:
64. Hernández-Cabanyero, C. and Amaro, C. (2020) Phylogeny and life cycle of the zoonotic pathogen *Vibrio vulnificus*. *Environ Microbiol*.
65. Hernández-Cabanyero, C., Lee, C. Te, Tolosa-Enguis, V., Sanjuán, E., Pajuelo, D., Reyes-López, F., et al. (2019) Adaptation to host in *Vibrio vulnificus*, a zoonotic pathogen that causes septicemia in fish and humans. *Environ Microbiol* **21**: 3118–3139.
66. Høi, Lise, Dalsgaard, I., Paola, A.D.E., and Siebeling, R.J. (1998) Heterogeneity among isolates of *Vibrio vulnificus* recovered from Eels ( *Anguilla anguilla* ) in Denmark. *Appl Environ Microbiol* **64**: 4676–4682.
67. Høi, L., Larsen, J.L., Dalsgaard, I., and Dalsgaard, A. (1998) Occurrence of *Vibrio vulnificus* biotypes in Danish marine environments. *Appl Environ Microbiol* **64**: 7–13.
68. Hollis, D.G., Weaver, R.E., Baker, C.N., and Thornsberry, C. (1976) Halophilic *Vibrio* species isolated from blood cultures. *J Clin Microbiol* **3**: 425–431.
69. Hood, M.I. and Skaar, E.P. (2012) Nutritional immunity: transition metals at the pathogen–host interface. *Nat Rev Microbiol* **10**: 525–537.
70. Hor, L.I., Chang, T.T., and Wang, S.T. (1999) Survival of *Vibrio vulnificus* in whole blood from patients with chronic liver diseases: Association with phagocytosis by neutrophils and serum ferritin levels. *J Infect Dis* **179**: 275–278.

71. Hor, L.I. and Chen, C.L. (2013) Cytotoxins of *Vibrio vulnificus*: Functions and roles in pathogenesis. *Biomed* **3**: 19–26.
72. Horseman, M.A. and Surani, S. (2011) A comprehensive review of *Vibrio vulnificus*: An important cause of severe sepsis and skin and soft-tissue infection. *Int J Infect Dis* **15**: e157–e166.
73. Hospenthal, M.K., Costa, T.R.D., and Waksman, G. (2017) A comprehensive guide to pilus biogenesis in Gram-negative bacteria. *Nat Rev Microbiol* **15**: 365–379.
74. Hsiao, A., Liu, Z., Joelsson, A., and Zhu, J. (2006) *Vibrio cholerae* virulence regulator-coordinated evasion of host immunity. *PNAS* **103**: 14542–14547.
75. Hsiao, A., Toscano, K., and Zhu, J. (2008) Post-transcriptional cross-talk between pro- and anti-colonization pili biosynthesis systems in *Vibrio cholerae*. *Mol Microbiol* **67**: 849–860.
76. Hwang, S.H., Park, J.H., Lee, B., and Choi, S.H. (2020) A regulatory network controls cabABC expression leading to biofilm and rugose colony development in *Vibrio vulnificus*. *Front Microbiol* **10**: 1–13.
77. Hyun, L.J., Rhee, J.E., Park, U., Ju, H.-M., Lee, B.C., Kim, T.S., et al. (2007) Identification and Functional Analysis of *Vibrio vulnificus* SmcR, a Novel Global Regulator. *J Microbiol Biotechnol* **17**: 325–334.
78. Ill, J.J.F., Brenner, F.W., Cameron, D.N., Birkhead, K.M., Control, D., and Janda, J.M. (2015) *Vibrio*, Bergey's M. John Wiley & Sons, Inc.
79. Iliev, D.B., Roach, J.C., Mackenzie, S., Planas, J. V., and Goetz, F.W. (2005) Endotoxin recognition: In fish or not in fish? *FEBS Lett* **579**: 6519–6528.
80. Imam, S., Chen, Z., Roos, D.S., and Pohlschröder, M. (2011) Identification of surprisingly diverse type IV Pili, across a broad range of gram-positive bacteria. *PLoS One* **6**:.
81. Inoue, T., Tanimoto, I., Ohta, H., Kato, K., Murayama, Y., and Fukui, K. (1998) Molecular characterization of low-molecular-weight component protein, Flp, in *Actinobacillus actinomycetemcomitans* fimbriae. *Microbiol Immunol* **42**: 253–258.
82. Jenal, U., Reinders, A., and Lori, C. (2017) Cyclic di-GMP: second messenger extraordinaire. *Nat Rev Microbiol* **1**–14.
83. Jeong, H.S., Lee, M.H., Lee, K.H., Park, S.J., and Choi, S.H. (2003) SmcR and Cyclic AMP receptor protein coactivate *Vibrio vulnificus* vvpE encoding elastase through the RpoS-dependent promoter in a synergistic manner. *J Biol Chem* **278**: 45072–45081.
84. Jeong, K.C., Jeong, H.S., Rhee, J.H., Lee, S.E., Chung, S.S., Starks, A.M., et al. (2000) Construction and phenotypic evaluation of a *Vibrio vulnificus* vvpE mutant for elastolytic protease. *Infect Immun* **68**: 5096–106.
85. Jones, C.J., Utada, A., Davis, K.R., Thongsomboon, W., Zamorano Sanchez, D., Banakar,

- V., et al. (2015) C-di-GMP regulates motile to sessile transition by modulating MshA pili biogenesis and near-surface motility behavior in *Vibrio cholerae*. *PLoS Pathog* **11**: 1–27.
86. Jones, M.K. and Oliver, J.D. (2009) *Vibrio vulnificus*: Disease and pathogenesis. *Infect Immun* **77**: 1723–1733.
  87. Jonson, G., Holmgren, J., and Svennerholm, A.M. (1991) Identification of a mannose-binding pilus on *Vibrio cholerae* El Tor. *Microb Pathog* **11**: 433–441.
  88. Josenhans, C. and Suerbaum, S. (2002) The role of motility as a virulence factor in bacteria. *Int J Med Microbiol* **291**: 605–614.
  89. Joseph, L.A. and Wright, A.C. (2004) Expression of *Vibrio vulnificus* capsular polysaccharide inhibits biofilm formation. *J Bacteriol* **186**: 889–893.
  90. Kachlany, S.C., Planet, P.J., DeSalle, R., Fine, D.H., Figurski, D.H., and Kaplan, J.B. (2001) Flp-1, the first representative of a new pilin gene subfamily, is required for non-specific adherence of *Actinobacillus actinomycetemcomitans*. *Mol Microbiol* **40**: 542–554.
  91. Kawagishi, I., Imagawa, M., Imae, Y., McCarter, L., and Homma, M. (1996) The sodium-driven polar flagellar motor of marine *Vibrio* as the mechanosensor that regulates lateral flagellar expression. *Mol Microbiol* **20**: 693–699.
  92. Kim, C.M., Park, R.Y., Chun, H.J., Kim, S.Y., Rhee, J.H., and Shin, S.H. (2007) *Vibrio vulnificus* metalloprotease VvpE is essentially required for swarming. *FEMS Microbiol Lett* **269**: 170–179.
  93. Kim, S.M., Park, J.H., Lee, H.S., Kim, W. Bin, Ryu, J.M., Han, H.J., and Choi, S.H. (2013) LuxR homologue smcr is essential for *Vibrio vulnificus* pathogenesis and biofilm detachment, and its expression is induced by host cells. *Infect Immun* **81**: 3721–3730.
  94. Kim, Y.R., Lee, S.E., Kook, H., Yeom, J.A., Na, H.S., Kim, S.Y., et al. (2008) *Vibrio vulnificus* RTX toxin kills host cells only after contact of the bacteria with host cells. *Cell Microbiol* **10**: 848–862.
  95. Kim, Y.R. and Rhee, J.H. (2003) Flagellar basal body flg operon as a virulence determinant of *Vibrio vulnificus*. *Biochem Biophys Res Commun* **304**: 405–410.
  96. Koton, Y., Gordon, M., Chalifa-Caspi, V., and Bisharat, N. (2015) Comparative genomic analysis of clinical and environmental *Vibrio vulnificus* isolates revealed biotype 3 evolutionary relationships. *Front Microbiol* **5**: 1–10.
  97. Kreger, A. and Lockwood, D. (1981) Detection of extracellular toxin(s) produced by *Vibrio vulnificus*. *Infect Immun* **33**: 583–590.
  98. Kwak, J.S., Jeong, H.G., and Satchell, K.J.F. (2011) *Vibrio vulnificus* rtxA1 gene recombination generates toxin variants with altered potency during intestinal infection. *Proc Natl Acad Sci U S A* **108**: 1645–1650.
  99. Lauriano, C.M., Ghosh, C., Correa, N.E., and Klose, K.E. (2004) The Sodium-Driven

- Flagellar Motor Controls Exopolysaccharide Expression in *Vibrio cholerae*. *J Bacteriol* **186**: 4864–4874.
100. Lee, C. Te, Amaro, C., Wu, K.M., Valiente, E., Chang, Y.F., Tsai, S.F., et al. (2008) A common virulence plasmid in biotype 2 *Vibrio vulnificus* and its dissemination aided by a conjugal plasmid. *J Bacteriol* **190**: 1638–1648.
  101. Lee, C. Te, Pajuelo, D., Llorens, A., Chen, Y.H., Leiro, J.M., Padrós, F., et al. (2013) MARTX of *Vibrio vulnificus* biotype 2 is a virulence and survival factor. *Environ Microbiol* **15**: 419–432.
  102. Lee, J.H., Rho, J.B., Park, K.J., Kim, C.B., Han, Y.S., Choi, S.H., et al. (2004) Role of flagellum and motility in pathogenesis of *Vibrio vulnificus*. *Infect Immun* **72**: 4905–4910.
  103. Lee, Z.W., Hwang, S.H., Choi, G., Jang, K.K., Lee, T.H., Chung, K.M., et al. (2020) A MARTX toxin rtxA gene is controlled by host environmental signals through a CRP-coordinated regulatory network in *Vibrio vulnificus*. *MBio* **11**: 1–18.
  104. Leighton, T.L., Buensuceso, R.N.C., Howell, P.L., and Burrows, L.L. (2015) Biogenesis of *Pseudomonas aeruginosa* type IV pili and regulation of their function. *Environ Microbiol* **17**: 4148–4163.
  105. Liu, Z., Miyashiro, T., Tsou, A., Hsiao, A., Goulian, M., and Zhu, J. (2008) Mucosal penetration primes *Vibrio cholerae* for host colonization by repressing quorum sensing. *PNAS* **105**: 9769–9774.
  106. López-Pérez, M., Jayakumar, J.M., Haro-Moreno, J.M., Zaragoza-Solas, A., Reddi, G., Rodriguez-Valera, F., et al. (2019) Evolutionary model of cluster divergence of the emergent marine pathogen *Vibrio vulnificus*: From genotype to ecotype. *MBio* **10**: 1–18.
  107. Macnab, R.M. (1999) The bacterial flagellum: Reversible rotary propellor and type III export apparatus. *J Bacteriol* **181**: 7149–7153.
  108. Mah, T.F.C. and O'Toole, G.A. (2001) Mechanisms of biofilm resistance to antimicrobial agents. *Trends Microbiol* **9**: 34–39.
  109. Mahami, T. and Adu-Gyamfi, A. (2011) Biofilm-associated infections: public health implications. *Int Res J Microbiol (IRJM)* **2**: 375–381.
  110. Maier, B., Potter, L., So, M., Seifert, H.S., and Sheetz, M.P. (2002) Single pilus motor forces exceed 100 pN. *Proc Natl Acad Sci U S A* **99**: 16012–16017.
  111. Marco-Noales Ester, Milan, M., Fouz, B., Sanjuan, E., and Amaro, C. (2001) Transmission to Eels, Portals of Entry, and Putative Reservoirs of *Vibrio vulnificus* Serovar E (Biotype 2). *Appl Environ Microbiol* **67**: 4717–4725.
  112. Marsh, J.W., Sun, D., and Taylor, R.K. (1996) Physical linkage of the *Vibrio cholerae* mannose-sensitive hemagglutinin secretory and structural subunit gene loci: Identification of the mshG coding sequence. *Infect Immun* **64**: 460–465.



113. Marsh, J.W. and Taylor, R.K. (1998) Genetic and transcriptional analyses of the *Vibrio cholerae* mannose-sensitive hemagglutinin type 4 pilus gene locus. *J Bacteriol* **181**: 1110–1117.
114. Mattick, J.S. (2002) Type IV Pili and Twitching Motility. *Annu Rev Microbiol* **56**: 289–314.
115. Merz, A.J. and So, M. (2000) Interactions of pathogenic *Neisseriae* with epithelial cell membranes. *Annu Rev Cell Dev Biol* **16**: 423–457.
116. Miyoshi, S.I., Kawata, K., Tomochika, K.I., and Shinoda, S. (1999) The hemagglutinating action of *Vibrio vulnificus* metalloprotease. *Microbiol Immunol* **43**: 79–82.
117. Morrison, S.S., Williams, T., Cain, A., Froelich, B., Taylor, C., Baker-Austin, C., et al. (2012) Pyrosequencing-based comparative genome analysis of *Vibrio vulnificus* environmental isolates. *PLoS One* **7**: 1–15.
118. Murciano, C., Hor, L.I., and Amaro, C. (2015) Host-pathogen interactions in *Vibrio vulnificus*: Responses of monocytes and vascular endothelial cells to live bacteria. *Future Microbiol* **10**: 471–487.
119. Murciano, C., Lee, C. Te, Fernández-Bravo, A., Hsieh, T.H., Fouz, B., Hor, L.I., and Amaro, C. (2017) MARTX toxin in the zoonotic serovar of *Vibrio vulnificus* triggers an early cytokine storm in mice. *Front Cell Infect Microbiol* **7**: 1–19.
120. Muroga, K., Jo, Y., and Nishibuchi, M. (1976) Pathogenic *Vibrio* isolated from cultured eels. Characteristics and taxonomic status. *Fish Pathog* **11**: 141–145.
121. Murray, T.S. and Kazmierczak, B.I. (2008) *Pseudomonas aeruginosa* exhibits sliding motility in the absence of type IV pili and flagella. *J Bacteriol* **190**: 2700–2708.
122. Musher, D.M., Hansen, M. V., Goree, A., Gyorkey, F., Chapman, A.J., and Baughn, R.E. (1986) Emergence of bactericidal and opsonizing antibody to *Vibrio vulnificus* following bacterial infection. *J Clin Microbiol* **23**: 411–415.
123. Nakhamchik, A., Wilde, C., and Rowe-Magnus, D.A. (2008) Cyclic-di-GMP regulates extracellular polysaccharide production, biofilm formation, and rugose colony development by *Vibrio vulnificus*. *Appl Environ Microbiol* **74**: 4199–4209.
124. O’Toole, G.A. and Kolter, R. (1998a) Flagellar and twitching motility are necessary for.pdf. *Mol Microbiol* **30**: 295–304.
125. O’Toole, G.A. and Kolter, R. (1998b) Flagellar and twitching motility are necessary for *Pseudomonas aeruginosa* biofilm development. *Mol Microbiol* **30**: 295–304.
126. Oliver, J.D. (2015) The Biology of *Vibrio vulnificus*. *Microbiol Spectr* **3**: 1–10.
127. Oliver, J.D. (2013) *Vibrio vulnificus*: Death on the Half Shell. A Personal journey with the pathogen and its ecology. *Microb Ecol* **65**: 793–799.
128. Ottow, J.C. (1975) Ecology, physiology, and genetics of fimbriae and pili. *Annu Rev Microbiol* **29**: 79–108.

129. Pajuelo, D., Hernández-Cabanyero, C., Sanjuan, E., Lee, C.-T., Silva-Hernández, F.X., Hor, L.-I., et al. (2016) Iron and fur in the life cycle of the zoonotic pathogen *Vibrio vulnificus*. *Environ Microbiol* **18**: 4005–4022.
130. Pajuelo, D., Lee, C. Te, Roig, F.J., Hor, L.I., and Amaro, C. (2015) Novel host-specific iron acquisition system in the zoonotic pathogen *Vibrio vulnificus*. *Environ Microbiol* **17**: 2076–2089.
131. Pajuelo, D., Lee, C. Te, Roig, F.J., Lemos, M.L., Hor, L.I., and Amaro, C. (2014) Host-nonspecific iron acquisition systems and virulence in the zoonotic serovar of *Vibrio vulnificus*. *Infect Immun* **82**: 731–744.
132. Paranjpye, R.N., Johnson, A.B., Baxter, A.E., and Strom, M.S. (2007) Role of type IV pilins in persistence of *Vibrio vulnificus* in *Crassostrea virginica* oysters. *Appl Environ Microbiol* **73**: 5041–5044.
133. Paranjpye, R.N., Lara, J.C., Pepe, J.C., Pepe, C.M., and Strom, M.S. (1998) The type IV leader peptidase/N-methyltransferase of *Vibrio vulnificus* controls factors required for adherence to HEp-2 cells and virulence in iron- overloaded mice. *Infect Immun* **66**: 5659–5668.
134. Park, J.H., Jo, Y., Jang, S.Y., Kwon, H., Irie, Y., Parsek, M.R., et al. (2015) The cabABC operon is essential for biofilm and rugose colony development in *Vibrio vulnificus*. *PLoS Pathog* **11**: 1–32.
135. Pelicic, V. (2008) Type IV pili: e pluribus unum? *Mol Microbiol* **68**: 827–837.
136. Pruzzo, C., Vezzulli, L., and Colwell, R.R. (2008) Global impact of *Vibrio cholerae* interactions with chitin. *Environ Microbiol* **10**: 1400–1410.
137. Pu, M., Duriez, P., Arazi, M., and Rowe-Magnus, D.A. (2018) A conserved Tad pilus promotes *Vibrio vulnificus* oyster colonization. *Environ Microbiol* **20**: 828–841.
138. Pu, M. and Rowe-Magnus, D.A. (2018) A Tad pilus promotes the establishment and resistance of *Vibrio vulnificus* biofilms to mechanical clearance. *npj Biofilms Microbiomes* **4**:
139. Rajkowski, K.T. (2009) Biofilms in fish processing. In, Fratamico, P.M., Annous, B.A., and Nereus W. Gunther, I. (eds), *Biofilms in the Food and Beverage Industries*. Woodhead Publishing Series in Food Science, Technology and Nutrition, p. 600.
140. Reichelt, J.L., Baumann, P., and Baumann, L. (1976) Study of genetic relationships among marine species of the genera *Beneckea* and *Photobacterium* by means of *in vitro* DNA/DNA Hybridization. *Arch Microbiol* **110**: 101–120.
141. Roig, F.J. and Amaro, C. (2007) Phenotypic and genotypic characterization of a new fish-virulent *Vibrio vulnificus* serovar that lacks potential to infect humans Phenotypic and genotypic characterization of a new fish-virulent *Vibrio vulnificus* serovar that lacks potential to infect huma. *Microbiology* **153**: 1926–1934.

142. Roig, F.J., González-Candelas, F., and Amaro, C. (2011) Domain organization and evolution of multifunctional autoprocessing repeats-in-toxin (MARTX) toxin in *Vibrio vulnificus*. *Appl Environ Microbiol* **77**: 657–668.
143. Roig, F.J., González-Candelas, F., Sanjuán, E., Fouz, B., Feil, E.J., Llorens, C., et al. (2018) Phylogeny of *Vibrio vulnificus* from the analysis of the core-genome: Implications for intra-species taxonomy. *Front Microbiol* **8**: 1–13.
144. Romling, U. and Amikam, D. (2006) Cyclic di-GMP as a second messenger. *Curr Opin Microbiol* **9**: 218–228.
145. Roux, N., Spagnolo, J., and De Bentzmann, S. (2012) Neglected but amazingly diverse type IVb pili. *Res Microbiol* **163**: 659–673.
146. Ruby, E.G. and Asato, L.M. (1993) Growth and flagellation of *Vibrio fischeri* during initiation of the sepiolid squid light organ symbiosis. *Arch Microbiol* **159**: 160–167.
147. Sandkvist, M. (2001) Biology of type II secretion. *Mol Microbiol* **40**: 271–283.
148. Sanjuán, E., González-Candelas, F., and Amaro, C. (2011) Polyphyletic origin of *Vibrio vulnificus* Biotype 2 as revealed by sequence-based analysis. *Appl Environ Microbiol* **77**: 688–695.
149. Sauer, F.G., Mulvey, M.A., Schilling, J.D., Martinez, J.J., and Hultgren, S.J. (2000) Bacterial pili: molecular mechanisms of pathogenesis. *Curr Opin Microbiol* **3**: 65–72.
150. Sauer, K., Sauer, K., Camper, A.K., Camper, A.K., Ehrlich, G.D., Ehrlich, G.D., et al. (2002) *Pseudomonas aeruginosa* displays multiple phenotypes during development as a biofilm. *Society* **184**: 1140–1154.
151. Semenza, J.C., Trinanes, J., Lohr, W., Sudre, B., Löfdahl, M., Martinez-Urtaza, J., et al. (2017) Environmental suitability of vibrio infections in a warming climate: An early warning system. *Environ Health Perspect* **125**: 1–12.
152. Shao, C.P. and Hor, L.I. (2000) Metalloprotease is not essential for *Vibrio vulnificus* virulence in mice. *Infect Immun* **68**: 3569–3573.
153. Shime-hattori, A., Iida, T., Arita, M., Park, K., and Kodama, T. (2006) Two type IV pili of *Vibrio parahaemolyticus* play different roles in biofilm formation. *Fed Eur Microbiol Soc* **264**: 89–97.
154. Shin, S.H., Shin, D.H., Ryu, P.Y., Chung, S.S., and Rhee, J.H. (2002) Proinflammatory cytokine profile in *Vibrio vulnificus* septicemic patients sera. *FEMS Immunol Med Microbiol* **33**: 133–138.
155. Shin, S.H., Sun, H.Y., Park, R.Y., Kim, C.M., Kim, S.Y., and Rhee, J.H. (2005) *Vibrio vulnificus* metalloprotease VvpE has no direct effect on the iron-assimilation from human holotransferrin. *FEMS Microbiol Lett* **247**: 221–229.
156. Silva, A.J. and Benitez, J.A. (2016) *Vibrio cholerae* Biofilms and Cholera Pathogenesis.

*PLoS Negl Trop Dis* **10**: 1–25.

157. Simpson, L.M., White, V.K., Zane, S.F., and Oliver, J.D. (1987) Correlation between virulence and colony morphology in *Vibrio vulnificus*. *Infect Immun* **55**: 269–272.
158. Sinha-Ray, S. and Ali, A. (2017) Mutation in *flrA* and *mshA* genes of *Vibrio cholerae* inversely involved in vps-independent biofilm driving bacterium toward nutrients in lake water. *Front Microbiol* **8**: 1–13.
159. Skerker, J.M. and Berg, H.C. (2001) Direct observation of extension and retraction of type IV pili. *Proc Natl Acad Sci U S A* **98**: 6901–6904.
160. Skovgaard, N. (2007) Risk assessment of *Vibrio vulnificus* in raw oysters, interpretative summary and technical report. *Int J Food Microbiol* **119**: 358–359.
161. Smith, A.B. and Siebeling, R.J. (2003) Identification of genetic loci required for capsular expression in *Vibrio vulnificus*. *Infect Immun* **71**: 1091–1097.
162. Spormann, A.M., Thormann, K., Saville, R., Shukla, S., and Entcheva, P. (2004) Microbial biofilms. *Nanoscale Technol Biol Syst* 341–357.
163. Stoodley, P., Sauer, K., Davies, D.G., and Costerton, J.W. (2002) Biofilms as complex differentiated communities. *Annu Rev Microbiol* **56**: 187–209.
164. Strom, M.S. and Paranjpye, R.N. (2000) Epidemiology and pathogenesis of *Vibrio vulnificus*. *Microbes Infect* **2**: 177–188.
165. Sun, Y., Bernardy, E.E., Hammer, B.K., and Miyashiro, T. (2013) Competence and natural transformation in vibrios. *Mol Microbiol* **89**: 583–595.
166. Takemura, A.F., Chien, D.M., and Polz, M.F. (2014) Associations and dynamics of vibronaceae in the environment, from the genus to the population level. *Front Microbiol* **5**: 1–26.
167. Thelin, K.H. and Taylor, R.K. (1996) Toxin-coregulated pilus, but not mannose-sensitive hemagglutinin, is required for colonization by *Vibrio cholerae* O1 El Tor biotype and O139 strains. *Infect Immun* **64**: 2853–2856.
168. Tison, D.L., Nishibuchi, M., Greenwood, J.D., and Seidler, R.J. (1982) *Vibrio vulnificus* biogroup 2: new biogroup pathogenic for eels. *Appl Environ Microbiol* **44**: 640–6.
169. Tomich, M., Fine, D.H., and Figurski, D.H. (2006) The TadV protein of *Actinobacillus actinomycetemcomitans* is a novel aspartic acid prepilin peptidase required for maturation of the Flp1 pilin and TadE and TadF pseudopilins. *J Bacteriol* **188**: 6899–6914.
170. Tomich, M., Planet, P.J., and Figurski, D.H. (2007) The *tad* locus: Postcards from the widespread colonization island. *Nat Rev Microbiol* **5**: 363–375.
171. Toole, G.O., Kaplan, H.B., and Kolter, R. (2000) Biofilm formation as microbial development. *Annu Rev Microbiol* 49–79.

172. Toranzo, A.E., Magariños, B., and Romalde, J.L. (2005) A review of the main bacterial fish diseases in mariculture systems. *Aquaculture* **246**: 37–61.
173. Utada, A.S., Bennett, R.R., Fong, J.C.N., Gibiansky, M.L., Yildiz, F.H., Golestanian, R., and Wong, G.C.L. (2014) *Vibrio cholerae* use pili and flagella synergistically to effect motility switching and conditional surface attachment. *Nat Commun* **5**: 4913.
174. Valiente, E. and Amaro, C. (2006) A method to diagnose the carrier state of *Vibrio vulnificus* serovar E in eels: Development and field studies. *Aquaculture* **258**: 173–179.
175. Valiente, E., Jiménez, N., Merino, S., Tomas, J.M., and Amaro, C. (2008) *Vibrio vulnificus* biotype 2 serovar e gne but not galE is essential for lipopolysaccharide biosynthesis and virulence. *Infect Immun* **76**: 1628–1638.
176. Valiente, E., Lee, C.-T., Lamas, J., Hor, L.-I., and Amaro, C. (2008) Role of the virulence plasmid pR99 and the metalloprotease Vvp in resistance of *Vibrio vulnificus* serovar E to eel innate immunity. *Fish Shellfish Immunol* **24**: 134–141.
177. Wall, D. and Kaiser, D. (1999) Type IV pili and cell motility. *Mol Microbiol* **32**: 01–10.
178. Wang, Y. and Chen, C. (2005) Mutation analysis of the flp operon in *Actinobacillus actinomycetemcomitans*. *Gene* **351**: 61–71.
179. Wang, Y., Liu, A., and Chen, C. (2005) Genetic basis for conversion of rough-to-smooth colony morphology in *Actinobacillus actinomycetemcomitans*. *Infect Immun* **73**: 3749–3753.
180. Waters, C.M. and Bassler, B.L. (2005) Quorum Sensing : Communication in Bacteria. *Annu Rev Cell Dev Biol* **21**: 319–346.
181. Watnick, P.I., Fullner, K.J., and Kolter, R. (1999) A role for the mannose-sensitive hemagglutinin in biofilm formation by *Vibrio cholerae* El Tor. *J Bacteriol* **181**: 3606–3609.
182. Watnick, P.I. and Kolter, R. (1999) Steps in the development of a *Vibrio cholerae* El Tor biofilm. *Mol Microbiol* **34**: 586–595.
183. Watnick, P.I., Lauriano, C.M., Klose, K.E., and Croal, L. (2010) The absence of a flagellum leads to altered colony morphology, biofilm development and virulence in *Vibrio cholerae* O139. *Mol Microbiol* **39**: 223–235.
184. Wetz, J.J., Blackwood, A.D., Fries, J.S., Williams, Z.F., and Noble, R.T. (2014) Quantification of *Vibrio vulnificus* in an estuarine environment: A Multi-Year Analysis Using QPCR. *Estuaries and Coasts* **37**: 421–435.
185. Williams, T., Ayrapetyan, M., Ryan, H., and Oliver, J. (2014) Serum survival of *Vibrio vulnificus*: Role of genotype, capsule, complement, clinical origin, and *in situ* incubation. *Pathogens* **3**: 822–832.
186. Wong, E., Vaaje-Kolstad, G., Ghosh, A., Hurtado-Guerrero, R., Konarev, P. V., Ibrahim, A.F.M., et al. (2012) The *Vibrio cholerae* colonization factor GbpA possesses a modular

- structure that governs binding to different host surfaces. *PLoS Pathog* **8**: 1–12.
187. Woo, P.T.K., Leong, J.-A., and Buchmann, K. (2020) Vibriosis. In, *Climate change and infectious fish diseases*. Ontario, p. 471.
  188. Wright, A.C., Simpson, L.M., Oliver, J.D., and Morris, J.G. (1990) Phenotypic evaluation of acapsular transposon mutants of *Vibrio vulnificus*. *Infect Immun* **58**: 1769–1773.
  189. Yamamoto, K., Wright, A.C., Kaper, J.B., and Morris, J.G. (1990) The cytolysin gene of *Vibrio vulnificus*: Sequence and relationship to the *Vibrio cholerae* El Tor hemolysin gene. *Infect Immun* **58**: 2706–2709.
  190. Yildiz, F.H., Liu, X.S., Heydorn, A., and Schoolnik, G.K. (2004) Molecular analysis of rugosity in a *Vibrio cholerae* O1 El Tor phase variant. *Mol Microbiol* **53**: 497–515.
  191. Yildiz, F.H. and Schoolnik, G.K. (1999) *Vibrio cholerae* O1 El Tor : Identification of a gene cluster required for the rugose colony type , exopolysaccharide production, chlorine resistance, and biofilm formation. *PNAS* **96**: 4028–4033.
  192. Yildiz, F.H. and Visick, K.L. (2009) *Vibrio* biofilms : so much the same yet so different. *Cell Press* **17**: 109–118.
  193. Yip, E.S., Geszvain, K., Deloney-Marino, C.R., and Visick, K.L. (2007) The symbiosis regulator RscS controls the *syp* gene locus, biofilm formation and symbiotic aggregation by *Vibrio fischeri*. *Mol Microbiol* **62**: 1586–1600.
  194. Yuan, Y., Feng, Z., and Wang, J. (2020) *Vibrio vulnificus* hemolysin: biological activity, regulation of *vvhA* expression, and role in pathogenesis. *Front Immunol* **11**: 1–8.
  195. Yun, N.R. and Kim, D.M. (2018) *Vibrio vulnificus* infection: A persistent threat to public health. *Korean J Intern Med* **33**: 1070–1078.
  196. Zampini, M., Canesi, L., Betti, M., Ciacci, C., Tarsi, R., Gallo, G., and Pruzzo, C. (2003) Role for mannose-sensitive hemagglutinin in promoting interactions between *Vibrio cholerae* El Tor and mussel hemolymph. *Appl Environ Microbiol* **69**: 5711–5715.



# **HYPOTHESIS AND OBJECTIVES**

---

---





This work is part of the research carried out by the team “Pathogens in Aquaculture: Zoonotic and fish pathogens” (PAZFP) of the Institute of Biotechnology and Biomedicine (BIOTECMED) of the University of Valencia. One of the main objectives of PAZFP is to unravel the mechanisms that *V. vulnificus* uses to cause vibriosis, by using a combination of *omic and single-gene* methodologies applied to *in vitro*, *ex vivo* and *in vivo* experiments, that simulate human and animal vibriosis. This PhD project began with the discovery that iron regulates the expression of several genes encoding Type IV pili. It has been described that this class of pili has an amazing range of biological functions that are critical to the survival of the pathogen in the environment, and the success of bacterial infection as indicated in the introduction. In this scenario, the present PhD project was proposed under the title of “Type IV pili and their role in virulence in *V. vulnificus*”.

This work sought to fill the gap of knowledge about the functions and role in virulence of **Type IV pili in the zoonotic clonal-complex of the pathogen *V. vulnificus***. The hypothesis was that the MSHA and the Tad pili should have an important role in virulence, since several components of their biogenesis loci are differentially expressed according to iron availability, an environmental signal that governs the entire life cycle of the bacteria. To this end, we selected the representative strain of the zoonotic clonal-complex, analyzed its transcriptome under iron rich and poor conditions, and obtained a wide collection of in-frame mutants in selected genes related to Type IV pili. A series of *in vitro*, *ex vivo* and *in vivo* assays were then performed with these mutants in order to demonstrate their role in biofilm formation, virulence for eels through different routes and serum resistance.

Accordingly, the main objectives of this PhD were:

1. **Find out whether the Type IV pili of the zoonotic clonal-complex were regulated by iron.**
  - By analyzing the transcriptome of the selected strain under iron-rich and iron-poor conditions.

**2. Discover If the two extra copies of the major pilin subunits (*mshA*) and the Tad pili have a role in biofilm formation, as the *mshA* gene does in *V. cholerae* and other bacterial species.**

- By generating several mutant strains of the zoonotic clonal-complex with simple, double and triple deletions of the major pilin subunit genes.
- By individually testing the adhesion and biofilm production capabilities of all the mutants obtained through several phenotypic tests.

**3. To determine the involvement, if any, of two Type IV pili systems in the virulence of the zoonotic clonal-complex.**

- By obtaining simple, double and triple mutant strains deficient in the major pilin subunits of the MSHA pili and the *tad* loci.
- By observing the biofilm structures and production capabilities of the Type IV pili mutants through crystal violet staining and biomass quantification paired with confocal microscopy.
- By assessing the role in virulence of each *mshA* and *flp* gene in the virulence in eels through different *in vivo* infection assays and *in vitro* serum resistance.



# GENERAL METHODOLOGY

---



## 1.- Obtention of mutants in the zoonotic clonal-complex

To specifically understand the function of a gene encoded in a bacterial genome, we must first localize it in its genomic environment, find out if it resides inside a locus, if there are any operons involved in its transcription, and most importantly, obtain its complete sequence and predicted proteins that codes for. With the advent of genome sequencing technologies, the knowledge and availability of genomes of either eukaryotic or prokaryotic organisms has exponentially increased every year. Modern analysis techniques like DNA microarrays, proteomics, gene clustering, codon analysis, and many others methods had been essential for the assignment of roles to several unknown genes with no adjudicated functions (Baba *et al.*, 2006). Many hypothesis and predictions can be made through the interminable modern sequencing techniques and leading genomic technologies, but no definitive conclusion can be made until the consequences of the gene deletions are observed in a living system.

To achieve this, the deletion of individual genes, or disruptions of loci, are implemented to interrupt the correct translation of a target gene or genes. Several methods had been produced to obtain these results, however, in 1993 an efficient approach was described to create single gene deletions (Baudin *et al.*, 1993). This method enables the creation of a DNA construct through simple PCR amplifications that can be integrated into the genome by homologous recombination through several methods such as electroporation or conjugation, resulting in the effective deletion of the target gene. This popular method has been proved highly efficient and has been adapted to thousands of laboratories worldwide, while being used effectively in different bacteria with outstanding results. However, not all bacteria are suitable for easy genetic modification, such is the case of *V. vulnificus*, which is notoriously difficult to modify, this is due to its innate resistance to the artificial integration of DNA into its genome, thus creating a natural impediment for artificial transformation (Jayakumar *et al.*, 2020).

Several factors influence this particular trait in the zoonotic clonal-complex:

- It produces an additional and specific restriction/modification system that is not present in the rest of the studied strains of the species.

- It requires flanking regions beside the target gene of 1.5 kb or more, in order to achieve an efficient recombination.
- Cells are extraordinarily susceptible to osmotic changes, making the introduction of the large quantities of genetic material needed for electroporation very challenging.

Considering the inefficiency of electroporation, various methods of transformation for *V. vulnificus* revolved around bacterial conjugation and chitin-based natural transformation, which was first employed in *Vibrio cholerae* (Sun *et al.*, 2013; Klevanskaa *et al.*, 2014). However, the most utilized method for *V. vulnificus* mutagenesis is exceptionally time consuming and burdensome. Briefly, amplified flanking regions of the target gene are cloned into a suicide vector that will be introduced into the strain. The suicide vector forces the chromosomal recombination of foreign DNA into the bacteria in which the plasmid is unable to replicate. A second recombination event leads to the loss of the vector sequences and primes the bacteria to be selected through the plasmid-encoded *sacB*, a counter-selectable marker gene that codes for levansucrase, which converts sucrose to levans, a harmful metabolite for bacteria. Therefore, when the bacteria is grown in presence of sucrose, it undergoes defined genetic alterations leading to the loss of the sucrose marker and the wild type DNA sequences from the co-integrated molecule (Gulig *et al.*, 2009).

However, this method is time consuming, as it requires several sub-cloning steps into suicide vectors, which are difficult to introduce into *V. vulnificus*. In addition it requires large quantities of DNA and a laborious screening of hundreds of colonies for sucrose sensitivity. Alternatively, some researchers harnessed the natural transformation capabilities of these bacteria in hopes of obtaining another viable mutation protocol, however this process demands copious amounts of linearized plasmid and leads to significantly low efficiencies (Gulig *et al.*, 2009; Klevanskaa *et al.*, 2014).

In conclusion, the study of *V. vulnificus* biology had been hampered by a paucity of molecular tools. As the most effective genetic analyses are performed through in-frame deletion of single genes, the production of knock-out mutants in *V. vulnificus* was **the first and**

**most important milestone for this work**, which served as the core for the general experimental design (**Figure 1**). To this end, we tested several mutation protocols and created our own mutagenesis method, in order to rule out the most efficient one for obtaining the extensive battery of mutant needed to meet our objectives. This new protocol amalgams several proven effective techniques previously used in bacterial transformation and mutagenesis in vibrio species (Miller and Mekalanos, 1988; Baba *et al.*, 2006; Gulig *et al.*, 2009).

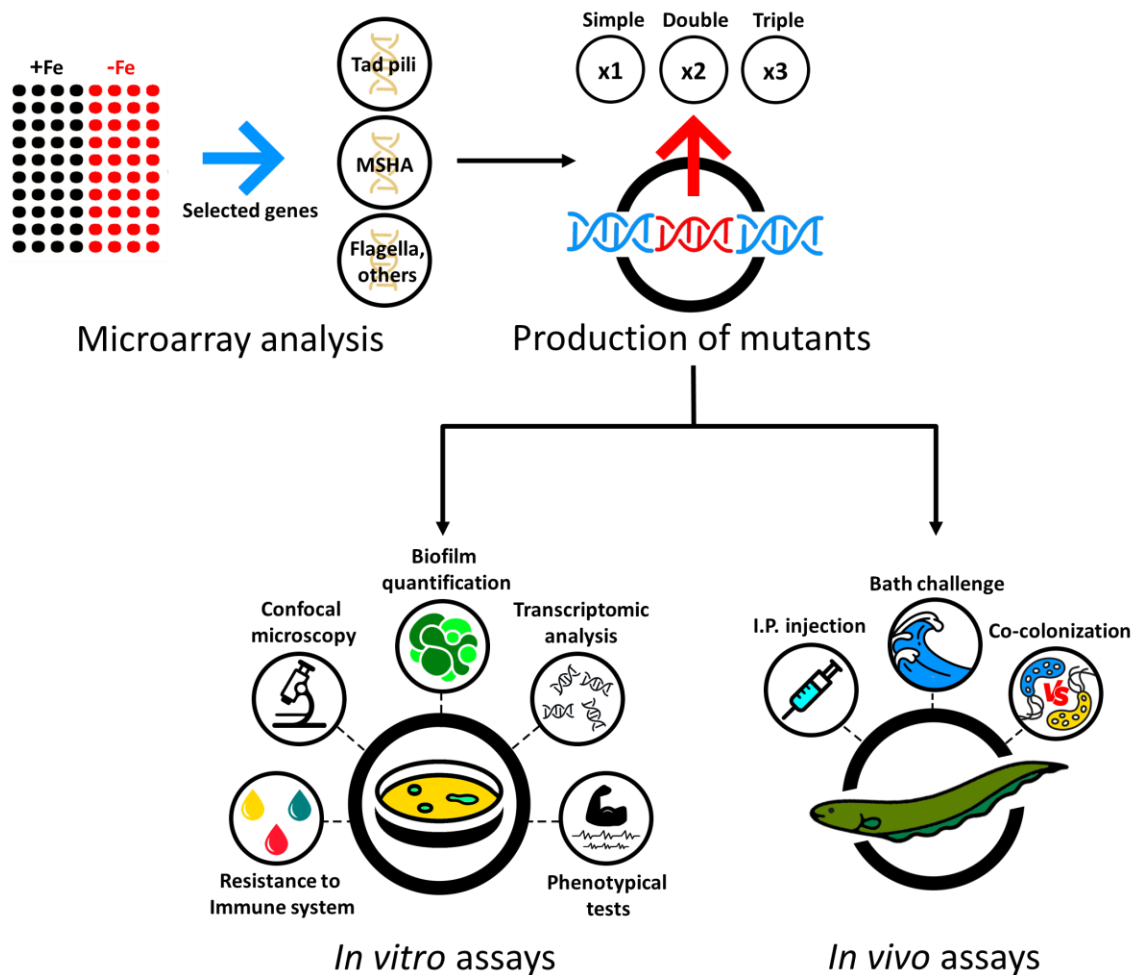


**Fig.1. General methodology followed throughout this work to fulfill our desired objectives.** Genes from two different Type IV pili systems and flagella were selected from our past microarray analysis in function of their iron stimulon (Pajuelo *et al.*, 2016). Single, double and triple mutants from these systems of the zoonotic clinal complex of *V. vulnificus* were generated, and the resulting strains were subjected to several *in vitro* and *in vivo* in order to assess their virulence capabilities.

## 2.- *In silico* analysis

2.1.- MSHA Major pilin subunit genes analysis and alignments. In the published genome of *V. vulnificus* R99 three different *mshA* genes are annotated. Homology search for the three proteins were carried out with BLAST (Altschul *et al.*, 1990). The gene sequences obtained were used to carry out the phylogenetic analysis using the MEGA X program. The evolutionary history was inferred by using the Maximum Likelihood method based on the Tamura 3-parameter model.

2.2.- MSHA proteins analysis. CLUSTAL W alignment of MshA protein sequences of *V. vulnificus* R99, *V. cholerae* El Tor FJ147 and *V. parahaemolyticus* RIMD 2210633 were performed and visualized in the Jalview 2.11.1.3<sup>®</sup> software. The prediction of the 3D structures of the MSHA proteins was performed with PHYRE 2 software. This tool develops template-based modeling in which the proteins are aligned to another of known structure based on patterns of evolutionary variation (Kelley *et al.*, 2015).

## 3.- Bacterial strains, growth and media conditions

All strains (**Table 1**) were actively grown at 28°C in the media: Luria-Betani broth (LB + 0.5% NaCl), TSA-1 (TSA [tryptone soy agar], 1% NaCl), CM9 (M9 broth (Miller, 1972) supplemented with 0.2% casamino acids), Minimal salts medium with glycerol (MS + 10% glycerol [MSg]) and LB-agar (LBA). For the genetic manipulation of the strains, the following antibiotic concentrations were used: ampicillin (Amp), 100 µg/ml; chloramphenicol (Cm), 20 µg/ml (*E. coli*) or 2 µg/ml (*V. vulnificus*); kanamycin (Km), 40 µg/ml (*E. coli*) or 150 µg/ml (*V. vulnificus*); and trimethoprim (Tp), 25 µg/ml (*V. vulnificus*). To analyze the effect of exogenous iron on growth, the following culture media were used: CM9 + Fe (CM9 supplemented with 100 µM FeCl<sub>3</sub>) and CM9 + Tf (CM9 supplemented with 10 µM of human apo-transferrin [Sigma-Aldrich]). In case of liquid cultures, 5 ml of medium was inoculated with overnight bacteria at a ratio 1:100 (v/v), and incubated with shaking (220 rpm, New Brunswick Scientific Agitator). For bacterial counting, the drop plate method on TSA-1 was used (Hoben and Somasegaran, 1982)



and OD<sub>625</sub> measurements were used to follow bacterial growth. All strains were kept in LB + 20% glycerol at -80 °C.

**Table 1. Species, strains and plasmids used in the study**

Species, strain, plasmid	Characteristics	Source
R99	<i>V. vulnificus</i> zoonotic clonal-complex representative strain CECT4999, (Roig <i>et al.</i> , 2018)	Diseased eel
R99 + <i>LacZ</i>	CECT4999 + pVSV103	Collection
R99 + pTfoX	CECT4999 + pTfoX	This study
$\Delta mshA-1$	CECT4999 <i>mshA-1</i> defective mutant	This study
$\Delta mshA-2$	CECT4999 <i>mshA-2</i> defective mutant	This study
$\Delta mshA-3$	CECT4999 <i>mshA-3</i> defective mutant	This study
$\Delta mshA-1/2$	CECT4999 <i>mshA-1</i> and <i>mshA-2</i> defective mutant	This study
$\Delta mshA-1/3$	CECT4999 <i>mshA-1/mshA-3</i> defective mutant	This study
$\Delta mshA-2/3$	CECT4999 <i>mshA-2/mshA-3</i> defective mutant	This study
$\Delta mshA-123$	CECT4999 <i>mshA-1</i> , <i>mshA-2</i> and <i>mshA-3</i> defective mutant	This study
<i>cmshA-1</i>	$\Delta mshA-1$ + pMMB207 carrying the <i>mshA-1</i> gene	This study
$\Delta mshA-1$ + GFP	CECT4999 <i>mshA-1</i> defective mutant + pVSV102	This study
$\Delta mshA-2$ + GFP	CECT4999 <i>mshA-2</i> defective mutant + pVSV102	This study
$\Delta mshA-3$ + GFP	CECT4999 <i>mshA-3</i> defective mutant + pVSV102	This study
$\Delta mshA-1/2$ + GFP	CECT4999 <i>mshA-1/mshA-2</i> defective mutant + pVSV102	This study
$\Delta mshA-1/3$ + GFP	CECT4999 <i>mshA-1/mshA-3</i> defective mutant + pVSV102	This study
$\Delta mshA-2/3$ + GFP	CECT4999 <i>mshA-2/mshA-3</i> defective mutant + pVSV102	This study
$\Delta mshA-123$ + GFP	CECT4999 <i>mshA-1/mshA-2/mshA-3</i> defective mutant + pVSV102	This study
<i>cmshA-1</i> + GFP	$\Delta mshA-1$ + pMMB207 carrying the <i>mshA-1</i> gene	This study
$\Delta flp-1$	CECT4999 <i>flp</i> ( <i>tad</i> locus-1) defective mutant	This study
$\Delta flp-2$	CECT4999 <i>flp</i> ( <i>tad</i> locus-2) defective mutant	This study
$\Delta flp-3$	CECT4999 <i>flp</i> ( <i>tad</i> locus-3) defective mutant	This study
$\Delta flp-1/2$	CECT4999 <i>flp</i> ( <i>tad</i> locus-1/ <i>tad</i> locus 2) defective mutant	This study
$\Delta flp-1/3$	CECT4999 <i>flp</i> ( <i>tad</i> locus-1/ <i>tad</i> locus 3) defective mutant	This study
$\Delta flp-2/3$	CECT4999 <i>flp</i> ( <i>Tad</i> locus-2/ <i>tad</i> locus 3) defective mutant	This study
$\Delta flp-123$	CECT4999 <i>flp</i> ( <i>Tad</i> locus-1/ <i>tad</i> locus 2/ <i>tad</i> locus 3) defective mutant	This study
$\Delta flp-1$ + GFP	$\Delta flp-1$ + pVSV102	This study
$\Delta flp-2$ + GFP	$\Delta flp-2$ + pVSV102	This study
$\Delta flp-3$ + GFP	$\Delta flp-3$ + pVSV102	This study
$\Delta flp-1/2$ + GFP	$\Delta flp-1/2$ + pVSV102	This study
$\Delta flp-1/3$ + GFP	$\Delta flp-1/3$ + pVSV102	This study

**Table 1. Species, strains and plasmids used in the study**

Species, strain, plasmid	Characteristics	Source
$\Delta flp-2/3$ + GFP	$\Delta flp-2/3$ + pVSV102	This study
$\Delta flp-123$ + GFP	$\Delta flp-123$ + pVSV102	This study
<i>cfp-1</i>	$\Delta flp-1$ + pMMB207 carrying the <i>flp</i> ( <i>tad</i> locus-1) gene	This study
<i>cfp-3</i>	$\Delta flp-3$ + pMMB207 carrying the <i>flp</i> ( <i>tad</i> locus-3) gene	This study
<i>cfp-1</i> + GFP	<i>cfp-1</i> + pVSV102	This study
<i>cfp-3</i> + GFP	<i>cfp-3</i> + pVSV102	This study
$\Delta flgE$	CECT4999 <i>flgE</i> deficient mutant	This study
$\Delta flgE$ + GFP	CECT4999 <i>flgE</i> deficient mutant + pVSV102	This study
<i>cfp-1</i>	$\Delta flgE$ + pMMB207 carrying the <i>flgE</i> gene	This study
<i>cfp-3</i> + GFP	<i>cfp-3</i> + pVSV102	This study
$\Delta flgE/mshA-1$	CECT4999 <i>flgE</i> and <i>mshA-1</i> double mutant	This study
$\Delta flgE/mshA-1$ + GFP	CECT4999 <i>flgE</i> and <i>mshA-1</i> double mutant + pVSV102	This study
$\Delta flgE/cmshA-1$	$\Delta flgE/mshA-1$ + pMMB207 carrying the <i>mshA-1</i> gene	This study
$\Delta flgE/cmshA-1$ + GFP	$\Delta flgE/mshA-1$ + pVSV102 + pMMB207 carrying the <i>mshA-1</i> gene	This study
$\Delta pilT$	CECT4999 <i>pilT</i> deficient mutant	This study
$\Delta vvpD$	CECT4999 <i>vvpD</i> deficient mutant	This study
$\Delta slt^*$	CECT4999 deficient in murein glycosyltransferase <i>slt</i> gene	This study
SM17 $\lambda$ pir	<i>E. coli</i> cloning strain and transposon donor, <i>pir</i> <sup>+</sup> , <i>tra</i> <sup>+</sup> , Sm <sup>R</sup> , Tmp <sup>R</sup>	(R. Simon, 1983)
SM17 $\lambda$ pir + GFP	SM17 $\lambda$ pir + pVSV102	This study
DH5 $\alpha$	<i>E. coli</i> highly efficient transformation strain with the <i>lacZM15</i> gene	(Hanahan, 1983)
Plasmids	Characteristics	Source
pMMB207	Complementation vector CnF <sup>R</sup>	Addgene
pTfoX	pMMB207 vector with inducible <i>tfoX</i> gene, Amp <sup>R</sup>	(Dalia <i>et al.</i> , 2014)
pVSV102	Vector with inducible green fluorescent protein (GFP) gene, Km <sup>R</sup>	(Dunn <i>et al.</i> , 2006)
pVSV103	Vector with inducible <i>lacZ</i> gene, Km <sup>R</sup>	(Dunn <i>et al.</i> , 2006)
pDM4	Suicide vector CnF <sup>R</sup>	(Milton <i>et al.</i> , 1996)
pGEM <sup>®</sup> -T easy	T/A Cloning vector, Amp <sup>R</sup>	Promega
pUC19	Cloning vector Amp <sup>R</sup>	New England Biolabs
pCVD442	Suicide vector, with <i>sacB</i> gene, Amp <sup>R</sup>	(Donnenberg and Kaper, 1991)

\*Wrongly annotated in the R99 pVvBt2 plasmid as PilT, the twitching motility ATPase.

Amp: Ampicillin

Sm: Streptomycin

Tmp: Trimethoprim

CnF: Chloramphenicol

Km: Kanamycin

#### **4.- Maintenance of animals and serum/blood cells obtention**

Non vaccinated farmed eels (*Anguilla anguilla*) were purchased from a local eel farm, and were maintained and handled by authorized personal in the facilities of the Central Service for Experimental Research (SCSIE) of the University of Valencia (Spain) following the ethic statement. Eel blood and serum were obtained as previously described (Biosca *et al.*, 1993; Lee *et al.*, 2013). Briefly, eel sera was aseptically obtained from healthy fish, the fish were bled by caudal fin puncture, and blood was allowed to clot. The separated sera was used immediately. Human serum was purchased from a commercial house (Sigma-Aldrich).

#### **5.- Transcriptomic analysis and RT-qPCR**

We analyzed the global response to iron in the zoonotic clonal-complex of *V. vulnificus* by using a previously generated mutant in the regulator of iron uptake (Fur) in the selected strain CECT 4999, and a previously designed microarray (Pajuelo *et al.*, 2016). The CECT 4999 specific microarray contained 4553 probes of 60 nucleotides in length, corresponding to the three replicons of the strain (ChrI, ChrII and pVvbt2), with 3 probes per target (GEO repository; accession number GPL19040). The bacterium and its derivative mutants were grown in CM9, CM9 + Fe and CM9 - Tf up to the mid-log phase of growth. Then, RNA was extracted by centrifuging 1ml of the cultures at 13000 rpm for 5 min, discarding the supernatant and resuspending the pellet in 500µl of NucleoZOL® (Macherey-Nagel). After 15 min of room temperature incubation, 400ul of RNAase-free water per 1ml of NucleoZOL® was added to the lysate. Samples were centrifuged for 15 min at 14,000 rpm and the supernatant was transferred to a fresh tube where 1 ml of isopropanol was added to precipitate de RNA. The mixture was incubated for 10 min at room temperature and centrifuged at maximum potency for another 10 min. The resulting supernatant was discarded and the pellet was washed twice with 75% of ethanol, finally the ethanol was removed and the RNA was treated with Turbo DNAase kit (Invitrogen) to remove the possible DNA contamination, and cleaned using the GeneJET® RNA Cleanup and Concentration Micro Kit (Thermo Fisher) following the manufacturer's

instructions. RNA was quantified with a Nanodrop ND-2000 and only samples with A260/A280 > 1.8 and A260/A230 > 2 were used.

## **6.- Microarray data analysis**

The data was analyzed with Genespring 14.5 GX software (Agilent technologies) using the 75% percentile normalization for the comparisons of iron overloaded CM9 vs iron deficient CM9. Student's t-test ( $P < 0.05$ ) was applied to observe transcriptomic profile differences between the conditions.

6.1.-Data validation by RT-qPCR. The same RNA samples used for the microarray analysis were analyzed by RT-qPCR to calculate the expression of the selected genes (primers listed in **Table 2**). To this end, cDNA was produced from 1  $\mu\text{g}$  of RNA using Maxima Reverse Transcriptase (Thermo Scientific) as described by the manufacturer. The qPCRs were carried out using Power SYBR<sup>®</sup> Green PCR Master Mix (Applied Biosystems) and the StepOne<sup>®</sup> Plus RT-PCR System (Applied Biosystems). Reactions were carried out in a final volume of 10  $\mu\text{l}$  (5  $\mu\text{l}$  2x Master Mix, 2  $\mu\text{l}$  DEPC H<sub>2</sub>O, 1  $\mu\text{l}$  cDNA, 1  $\mu\text{l}$  forward primer, 1  $\mu\text{l}$  reverse primer, both at a concentration of 100nM) and the settings consisted of 10 min of denaturalization at 95°C followed by 40 cycles of 15 seconds of denaturalization at 95°C and 1 min of annealing and extension at 62°C. The *recA* gene was used as standard and the fold induction ( $2^{-\Delta\Delta\text{Ct}}$ ) for each gene was calculated according to Livak and Schmittgen (2001).

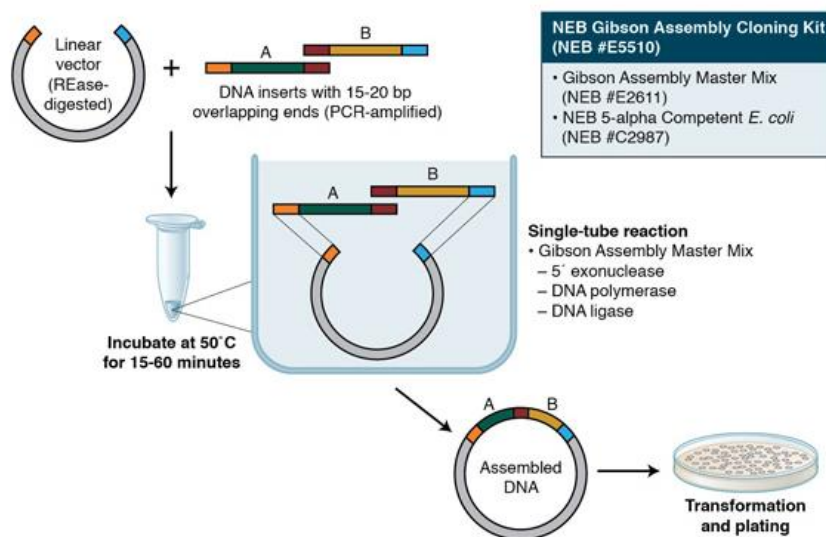
## **7.- Development of a new directed-mutagenesis protocol adapted to the zoonotic clonal-complex of *V. vulnificus***

7.1.- Protocols assessed: Five protocols were tested for obtaining the several knock-out mutants necessary for this work. The one selected was chosen for its efficiency and overall less time-consuming steps. Here we make a brief description of all these protocols. All primers utilized for the mutation protocols are listed in **Table 2**.

*Multi-vector cloning combined with natural transformation.* An 1.5 kb upstream and downstream region of the target gene of the R99 strain and a selected antibiotic cassette were amplified with complementing sticky ends. The fragments were cloned into the cloning vector pGEM®-T easy (Promega) to obtain pGene1 (upstream fragment), pGene2 (Downstream fragment), and pGene3 (antibiotic cassette), which were then introduced in electrocompetent *E. coli* Dh5 $\alpha$  cells. The plasmids were treated with restriction enzymes and the upstream fragment was cut and ligated into pGene2, forming pGene4 (upstream + downstream fragment). An antibiotic cassette and the pGene4 vector were digested with a compatible restriction enzyme to get complementary sticky ends in order to ligate the cassette into the plasmid and produce the pGene5 vector (upstream fragment + antibiotic + downstream fragment). Then, an overnight culture of the wild type strain was diluted 1:100 (v/v) in 3 ml of MS with sterile crab shell fragments of around 1 cm in circumference and incubated overnight at 28°C. After incubation, the supernatant was removed and the crab shells with any residual media were incubated again overnight at 28°C with 2 ml of fresh MS + 5 $\mu$ g of linearized pGene5 plasmid. Finally, the tubes were vigorously vortex for 30 seconds to dislodge any attached bacteria, the media was removed, centrifuged, resuspended in 100 ml PBS 1x and plated in LB + 1 plates with the proper antibiotic. Colonies were picked and re-streaked in fresh LB + 1 antibiotic to check for resistance.

*Gibson assembly directed mutagenesis combined with conjugation.* This protocol was used in our previous work (Carda-Diéguez *et al.*, 2018), to get mutants deficient in heme utilization in a strain of L1 (YJ016; formerly Bt1), in which DNA fragments of 500 bp flanking the target gene were enough for an effective recombination. In case of the R99 strain, we utilized fragments of 1.5 kb as commented before. In all cases, the DNA construct was obtained by ligating the PCR-products of the flanking sequences of the target gene and a Streptomycin (Sm) resistance cassette to the suicide vector pDM4 using Gibson assembly (**Figure 2**) (Gibson *et al.*, 2009). The vectors were transferred from *E. coli* SM10 to *V. vulnificus* by conjugation. To carry out the conjugation, *V. vulnificus* and an *E. coli* harboring the suicide plasmid with the mutation construct were grown overnight in LB-1 + 5mM MgCl<sub>2</sub>. Then, using the same media, cultures were grown in agitation for 5 hours at 28°C for *V. vulnificus* and 37°C for *E. coli*, cells were

washed three times and resuspended in 50µl of LB-1 + 5mM MgCl<sub>2</sub>. The strains were mixed together and the total volume was incubated on LBA-5mM MgCl<sub>2</sub> on a .45µm filter. The mix was incubated overnight at 37 °C, and the resulting bacterial lawn was scraped and spread via triple streak onto LBA with Cnf and Sm, and incubated at 28°C overnight. Isolated colonies were checked for conjugation by PCR and antibiotic resistance.

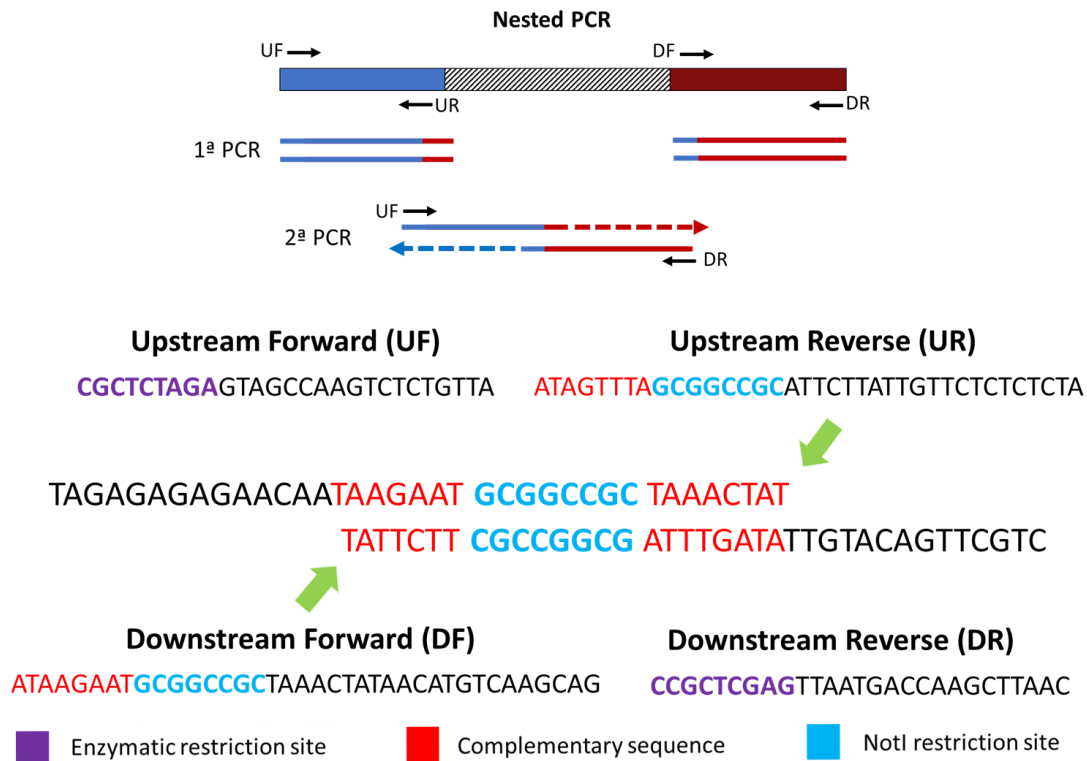
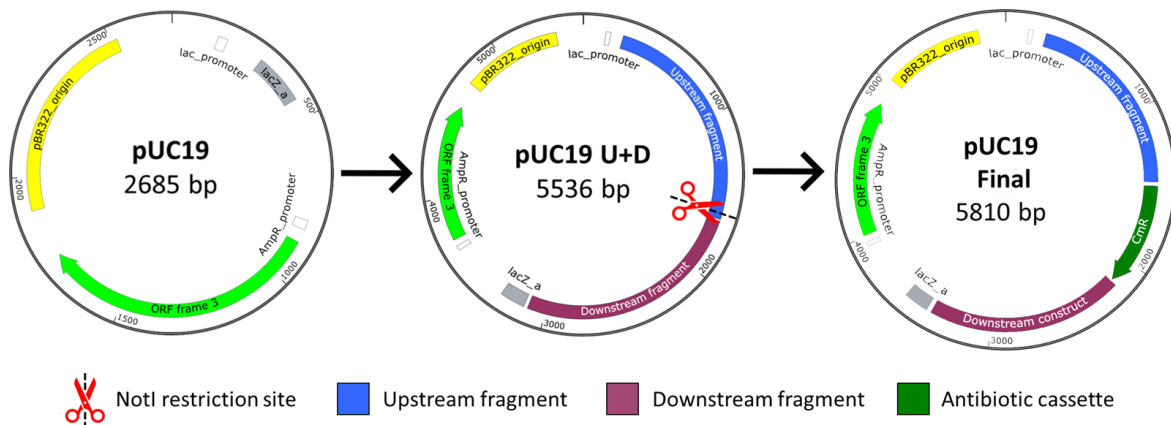


**Fig.2. Gibson assembly workflow.** This fusion method is based of three distinct enzymatic activities in a single reaction tube; an exonuclease, a DNA polymerase and a ligase. The reaction modifies de 5' end of the fragments in order to expose the complementary sequences for the annealing. After, the ligase seals the nicks and links of the DNA fragments and fuse them together. Image taken from <https://www.neb.com/applications/cloning-and-synthetic-biology/dna-assembly-and-cloning/gibson-assembly> on 8/12/2020.

Finally, sucrose-based counter-selection was performed (Donnenberg and Kaper, 1991), briefly, three random resistant colonies were grown overnight, the culture was diluted 1:100 in LB + 10% sucrose (wt/vol) and incubated again until they reached an OD<sub>600</sub> of 0.5. Then, 100 µl of a serial ten-fold dilution from each one were spread on LBA plates. “Watery” colonies (pale colonies that barely held the circular morphology) were checked by PCR for in-frame deletion.

*Triple ligation combined with conjugation.* This protocol was replicated as described previously (Shao and Hor, 2000), briefly, the DNA construct was obtained by amplifying around 1.5 kb of the flanking sequences of a target gene and cloned via triple ligation into the pGEM®-T easy vector (Promega). The vector was then transformed into *E. coli* DH5α to generate a recombinant fragment. Then, through restriction enzymes, this fragment was removed and cloned into the suicide vector pCV442, which was transformed into an *E. coli* S17-1λpir in order to be conjugated into R99 as previously described. Finally, sucrose selection was performed as before, and “watery” colonies were spotted in replicate in LBA and LBA + Amp. Colonies that grew on LBA, but not LBA + amp, were grown and checked for gene deletion through PCR and sequencing.

*NotI-Ligation combined with natural transformation.* This novel protocol was created to produce a faster and more effective alternative to mutagenesis when no results were obtained with the previous methods. An 1.5 kb upstream and downstream fragment were amplified using specially designed primers (**Table 2**). This generated complementary sequences between each other, each containing half of a restriction site recognized by the NotI enzyme (**Figure 3A**). The fragments were fused together through nested PCR and cloned into the pGEM®-T easy vector (Promega). The fused fragment was then transferred into the cloning vector pUC19. The antibiotic resistance cassette was cloned into the construct by using the new NotI restriction site created between the upstream and downstream regions (**Figure 3B**). Finally, the plasmid was linearized with a specific restriction enzyme that cuts on the opposite region from where the NotI site is located, creating long “protective” sequences that flank the mutation construct and prevent DNA degradation by nucleases. Large quantities of linearized plasmid (5-7μg) were incubated with the wild type strain overnight at 28°C in MS with crab shell fragments, and consequentially plated in LBA with a selected antibiotic. Mutant colonies are re-streaked in fresh LBA plates with antibiotic and checked through PCR.

**A****Synthesis of flanking fragments****B**

**Fig 3. Protocol created to produce knock-out mutants in *V. vulnificus* zoonotic clonal-complex.** This protocol was created in our laboratory as a reproducible technique to obtain mutants in the zoonotic clonal-complex of *V. vulnificus*. This technique melds together different methods such as natural transformation and synthesis of the mutation construct via nested PCR. (A) Nested PCR used to fuse together the upstream and downstream fragments and create the mutation construct. (B) puc19 vector progression as we incorporate the amplified fragments and the antibiotic cassette in order to be linearized for the natural transformation process.



*Natural transformation induced by pTfoX.* This protocol was modified from a previous work where it was used to generate mutants from the clinical strain CMPC6 of *V. vulnificus* (Chodur *et al.*, 2018). To increase the extremely low transformation frequency of the R99 strain, it was conjugated with the plasmid pTfoX, as detailed before. This plasmid carries the gene *tfoX* under the control of the inducible promoter  $P_{tac}$  (Dalia *et al.*, 2014). This gene is a positive regulator of the competence in vibrios and is activated when the bacteria comes in contact with chitin (Meibom *et al.*, 2005). Briefly, a nested PCR was performed utilizing specially designed primers (**Table 2**) to amplify 1-1.5 kb upstream and downstream fragments of the target gene, as well as the desired antibiotic resistance cassette (Tp, Km or Cm). The resulting products were stitched together to generate the mutation construct by a second PCR. The conjugated wild type strain was incubated overnight at 28°C in LB-1+ampicillin with .5M IPTG (Isopropyl  $\beta$ -D-1-thiogalactopyranoside) to induce natural transformation. Then, 500 $\mu$ l of Sea salt mix (Instant ocean™) (20 ppt) was mixed with 10 $\mu$ l of the overnight culture and 50 $\mu$ l of the nested PCR product. The mixture was incubated overnight at 28°C, 1 ml of LB-1 was then added and incubated for 6 hours in agitation before plating in LBA plates with the appropriate antibiotic. Colonies growing on the agar plates were then picked individually and grown overnight in LB-1 liquid media with the pertinent antibiotic. Finally, the cultures were plated in LBA with the corresponding antibiotic and individual colonies were tested by PCR. **This protocol was the only one that allowed us to get mutants in the zoonotic clonal-complex in a reproducible and efficient manner, therefore, it was finally the one selected.**

**Table 2. Primers used for mutation and complementation**

Product	Primer	Sequence	Size (bp)	Product
<i>ΔmshA-1</i>	MshA-1	CCTGTATAAGCAGGAATGGC	1200±	Upstream construct
	MshATmp-2	GTCGACGGATCCCCGGAATCATAGTGTCTCTCTCTA		
	MshACnf-2	AACCTCTTACGTGCCGATCACATAGTGTCTCTCTCTATG		
	MshATmp-3	GAAGCAGCTCCAGCCTACATAGAAAGTTAAGTGCCTT		
	MshACnf-3	AGTGGCAGGGCGGGCGTAGAAAGTTAAGTGCCTTA		Downstream construct
MshA-4	TCACTGCCGTCCATGTTGC			
<i>ΔmshA-2</i>	MshA2-1	CCAAATGAGAGAGCTTCTTCT	1200±	Upstream construct
	MshA2Tmp-2	GAAGCAGCTCCAGCCTACATAATCATAGACACTAGATAAGT		
	MshA2Km-2	GATGCTCGATGAGTTTTTCTAATAATCATAGACACTAGAT		
	MshA2Tmp-3	GTCGACGGATCCCCGGAATCATTTATTTCTCTATTTTTTAT		
	MshA2Km-3	GTAGAAAAGATCAAAGGATCTTCCATTTATTTCTCTATTT		Downstream construct
MshA2-4	CTCAAGAAATTTGCCATTTTCTA			
<i>ΔmshA-3</i>	MshA3-1	TATGGCGGGGCGATGAG	1200±	Upstream construct
	MshA3Tmp-2	GTCGACGGATCCCCGGAATCATCCGTA CTCCACTACTCA		
	MshA3Tmp-3	GAAGCAGCTCCAGCCTACATAGAACATTGACTCACCAACAA		Downstream construct
	MshA3-4	CATAACAATAATGGCGCAAATAG		
<i>cmshA-1</i>	MshA-Fx	AACAGAATTCGAGCTCGGTACATGAAAAGACAAGGCGGTTTC	468	Complementation
	MshA-Rx	TGATTTAATCTGTATCAGGCTGCTATTGCGCGCCGAAGC		
<i>ΔmshA-1 NotI</i>	MshaNotI-1	CGCTCTAGAGTAGCCAAGTCTCTGTTA	1200±	Upstream construct
	MshaNotI-2	ATAGTTTAGCGGCCGCATTCTTAT		
	MshaNotI-3	TAAGAATGCGGCCGCTAAACTAT		Downstream construct
	MshaNotI-4	CCGCTCGAGTTAATGACCAAGCTTAAC		
<i>ΔflgE T-Lig</i>	FlgE-UF	ATGAGAATTGATGGATTTAA	1500	Upstream construct
	FlgE-UR	GTCGACGGATCCCCGGAATCATCGTTACCTCTAAGCCAAAAGTT		
	FlgE-DF	GAAGCAGCTCCAGCCTACATAATGTGGGTAGTAAACTG		Downstream construct
	FlgE-DR	TTAGACTGGCATGTTCAATA		
<i>ΔSlt-NotI</i>	Slt-UF	CAAGAGATGAACTTTGAACATC	1200±	Upstream construct
	Slt-UR	GAGTTTAGCGGCCGCTATTCTTATACCACCATCAAAC		
	Slt-DF	AAGAATGCGGCCGCTAAACTATTTCCAC		Downstream construct
	Slt-DR	TGATCAAGAGAAGCCAGCAAA		
<i>ΔpilT</i>	PilT-1	AGCGGTTTGCACTTCTTC	1200±	Upstream construct
	PilT-2	GTCGACGGATCCCCGGAATCATTTATTTTCCCTTAAAAGACTT		
	PilT-3	GAAGCAGCTCCAGCCTACATAACTGAGGTCTGCAATGAG		Downstream construct
	PilT-4	CGCGTCTTCTCACTGATTT		
<i>cflgE</i>	cFlgE-F	AACAGAATTCGAGCTCGGTACATGTCATATGTATCTTTAAGCG	1305	FlgE hook gene
	cFlgE-R	TGATTTAATCTGTATCAGGCTGTTAACGAATCTGCAGAATGTTT		
<i>Δflp-1</i>	Flp1	TCACCACGTCGATCCAACG	1200±	Upstream construct
	Flp1Tmp-2	GTCGACGGATCCCCGGAATCATCATTACTCCTTT		
	Flp1Cnf-2	AACCTCTTACGTGCCGATCACATCATTACTCCTTTTTG		
	Flp1Tmp-3	GAAGCAGCTCCAGCCTACATAAACGTGAATCCAGAGATTGT		
	Flp1Cnf-3	AGTGGCAGGGCGGGCGTAAACGTGAATCCAGAGA		
Flp1-4	ATTGATTGCCAATCGCGAGC			

**Table 2. Continuation**

Product	Primer	Sequence	Size (bp)	Product
<i>Δflp-2</i>	Flp2-1	CATAGGAGCGGCTGCTTGT	1200±	Downstream construct
	Flp2Tmp-2	GTCGACGGATCCCCGGAATCATTAGCTGATAGCTCCGTC		
	Flp2km-2	GTAGAAAAGATCAAAGGATCTTCCATTAGCTGATAGCTC CG		
	Flp2Tmp-3	GAAGCAGCTCCAGCCTACATAGTCGCTGACGTTCCACTC		
	Flp2km-3	GATGCTCGATGAGTTTTTCTAATAGTCGCTGACGTTCCA C		
	Flp2-1	GGCTCGATTGACGATTTTTGC		
<i>Δflp-3</i>	Flp3-1	TATCAGTTAAGATCATCAAGTTAT	1200±	Upstream construct
	Flp3Tmp-2	GTCGACGGATCCCCGGAATCATATTATCCTCTTATTAAC		Downstream construct
	Flp3Tmp-3	GAAGCAGCTCCAGCCTACATAACATTTTCATACTCATTAAATG		
	Flp3-4	CGGCAATTTCTGGATCACCT		
<i>ΔvvpD</i>	PiID-1	ATTGGCCAAAACGCGGTGC	1200±	Upstream construct
	PiID-2	AGTGGCAGGGCGGGGCGTGATATGGCTTTAGTGAT		Downstream construct
	PiID-3	AACCTCTTACGTGCCGATCACATATAATCGTTGTTCTC		
	PiID-4	CATCGCAAAGCTGAGATGAAA		
<i>cf1p-1</i>	Flp1-F	AATTCACACAGGAAACAGAATTCGAGCTCGGTACATG CTGAAACAATTCATTAACGA	177	Complementation
	Flp1-R	TTCTGCGTTCTGATTAATCTGTATCAGGCTGTTACTCGC CTGCAGGGTTC		
<i>cf1p-3</i>	Flp3-F	AATTCACACAGGAAACAGAATTCGAGCTCGGTACATGT TTAACAAAGTTATGACAAAA	216	Complementation
	Flp3-R	TTCTGCGTTCTGATTAATCTGTATCAGGCTGTTAAGATT TAACAGTTTCTGCG		
pMMB207	pMMB207-F pMMB207-R	TTTGGCGGATGAGAGAAGATT GTACCGAGCTCGAATTCTGTT	9000±	Complementation
Trimethoprim	Tp-F	ATTCGGGGATCCGTCGAC	692	Antibiotic cassette
	Tp-R	TGTAGGCTGGAGCTGCTTC		
Chloramphenicol	Cf-F	TGATCGGCACGTAAGAGGTT	760	Antibiotic cassette
	Cf-R	CGCCCCGCCCTGCCACT		
Kanamycin	Km-F	GAAGATCCTTTGATCTTTTCTAC	937	Antibiotic cassette
	Km-R	TTAGAAAAACTCATCGAGCATC		
<i>mshA-1</i>	qPCRM1-F qPCRM1-R	ACAAGGCGGTTTCACCCTG CGCGCATCATCTGCAGAT	105	qRT-PCR
<i>mshA-2</i>	qPCRM2-F qPCRM2-R	AGCATCGGGATAGCCATAAAT TTATGGTGTCATTCTGCACA	115	qRT-PCR
<i>mshA-3</i>	qPCRM3-F qPCRM3-R	GAAGTAGTGGTGCATCGTC TTCTAGCCGTGCCACTTTG	105	qRT-PCR
<i>flp-1</i>	qPCRFlp1-F qPCRFlp1-R	ATGCTGAAACAATTCATTAACGA TTTCAGCGCAGAGATAAACAC	116	qRT-PCR
<i>flp-2</i>	qPCRFlp2-F qPCRFlp2-R	TCATTAACGATGAAAACGGCG TTTCAGCGCAGAGATAAACAC	123	qRT-PCR
<i>cf1p-3</i>	qPCRFlp3-F qPCRFlp3-R	ATGTTTAAACAAAGTTATGACAAAA TTGCAGACATTGCCACTGCA	112	qRT-PCR

## 8.- Mutant complementation

Complementation was performed by amplifying a linearized version of the pMMB207 vector as a backbone for ligating the target gene sequence via complementary 5' and 3' ends (primers listed in **Table 2**). Both PCR products were ligated using the In-fusion® HD Cloning kit (Takara), the resulting product was transformed into *E. coli* SM17-1 $\lambda$ pir by electroporation (R. Simon, 1983). Transformed cells were conjugated with the corresponding knock-out mutant using the same protocol as before, transformants were confirmed by PCR.

## 9.- *In vitro* assays

9.1.- Biofilm formation and quantification. The process of biofilm formation on plastic devices was tested by using the following methodologies:

*Observation and description with a confocal laser scanning microscope (CLSM)*. For confocal microscopy analysis, GFP (green fluorescent protein) tagged strains were used (**Table 1**). An overnight culture in CM9 + Km was used to inoculate 3 ml of MSg (1:50) with and without 4% D-mannose (wt/vol) on a 35 mm  $\mu$ -Dish® (Ibidi) plate. Strains were grown overnight at 28°C in static and the biofilm was visualized in a confocal microscope FV1000 (Olympus FluoView®). Each biofilm was scanned at three randomly selected positions on three biological replicates, and the Z stacks were generated by optical sectioning at each of these positions. Images of the biofilms were analyzed with the Imaris viewer® (Bitplane) software. The biofilm biovolume (total amount of space/biomass occupied by a biofilm), average thickness (thickness of each biofilm extending from the bottom to the top of the growth/viewing channel surface), and roughness coefficient (a measure of heterogeneity in biofilm architecture) were determined with COMSTAT 2.1® biofilm analysis software (Heydorn *et al.*, 2000). Biofilms were analyzed in two conditions: Filtered (quantification of the cells adhered to the substrate forming biofilm) and not filtered (quantification of total biomass present in the media).

*Quantification by absorbance*. Biofilm was quantified by a modified crystal violet staining method (Guo and Rowe-Magnus, 2010). Briefly, overnight CM9, and CM9 + Fe or CM9 -

Fe cultures were used to inoculate fresh media to an OD<sub>600</sub> of 0.5. Then, the cultures were placed into a 96-well microtiter plate (6 wells per strain) and left overnight for static growth at 30°C. After incubation, bacterial growth was measured at A<sub>600</sub> before carefully removing the media by aspiration and staining the biofilm of the plate walls with 150µl of 0.1% crystal violet for 30 min. Wells were rinsed with PBS (180µl) three times and the violet stain was solubilized with 150µl of 96% ethanol. The OD<sub>595</sub> of the solubilized biofilm was measured and the OD<sub>595</sub>/OD<sub>600</sub> ratio was calculated to determine the relative biofilm production.

## 10.- *Ex vivo* assays

10.1.- Resistance and growth in serum. Overnight cultures were adjusted to 1x10<sup>3</sup> CFU/ml in PBS, mixed at a 1:1 ratio with eel or human serum (Sigma-Aldrich), and incubated at 28°C (eel) or 37°C (human) for 4 hours. The survival ratio was determined after 4h of incubation as previously described by Lee *et al.*, (2013).

10.2.- Hemagglutination test. The hemagglutination capacity of the R99 and *mshA* mutant strains was tested by mixing them with fresh human erythrocytes (small quantities of human blood were donated by Valencian La Fe clinical hospital) with a bacterial suspension. Briefly, 500µl of fresh human blood was centrifuged at 3000 rpm for 5 min at 4°C, then 6µl of the red blood cells precipitant was carefully resuspended in 194µl of PBS 1x. Bacterial cells from a 5ml tube of an overnight culture were pelleted and washed twice and resuspended in 1 ml of PBS. Volumes of 20µl of both suspensions were mixed on a glass-slide and bacteria and red blood cells were mixed by gentle agitation for 1 min. Visible agglutination before 3 min was recorded as a positive result. Negative controls were bacteria or red blood cells mixed with PBS.

10.3.- Proteolytic and Hemolytic activity. The extracellular products (ECPs) from the R99 strain and its derivative mutants were obtained from 24 h cultures at 28°C on CM9 agar plates (1.5% agar [wt/vol]) according to Biosca and Amaro (1996). Proteolytic and hemolytic activities in ECPs were evaluated by seeding two-fold dilutions on agarose-caseine (1% wt/vol in PBS) casein (% non-fat milk) or agarose-erythrocytes (5%) (Defibrinated sheep blood, Sigma-Aldrich) plates. Positive enzymatic activity was confirmed by a defined translucent halo produced on the

agarose plates and PBS was used as negative control. The enzymatic activity was calculated as the inverse of the highest dilution giving a positive result on the plate.

10.4.- Infections experiments with cell lines. TPH-1 (human peripheral blood MCs) were maintained as suspension cells in Roswell Park Memorial Institute Medium (RPMI-1640, Sigma-Aldrich), and supplemented with 10% FBS (Fetal Bovine Serum, Sigma-Aldrich) plus 1% P/S solution (penicillin-streptomycin). Before the infection experiments, cells were seeded in tissue culture plates containing serum and antibiotic-free DMEM (Dulbecco's Modified Eagle's medium, Sigma-Aldrich) and incubated for 3 hours. Then, cells were infected with overnight cultures of *V. vulnificus* and *E. coli* cells, previously washed with PBS, at a MOI (multiplicity of infection; bacteria: human cell) of 10. Co-cultures were incubated at 37°C and 5% CO<sub>2</sub> up to 4h and sampled at different times points to quantify survival of the bacterial cells. Control experiments were performed by incubating *V. vulnificus* and *E. coli* without monocytes. Survival was determined by measuring the viable bacterial cells after each hour of incubation via drop plate counts on TSA-1 (Hoben and Somasegaran, 1982).

10.5.- Adhesion to crab shells as biotic surfaces. The capacity of adhesion to biotic surfaces was assessed by inoculating a 1:1000 dilution of a mild-exponential CM9 culture of R99 and derivative mutants into a 48-well tissue culture test plate (3 wells per strain) containing 1 ml of CM9 and a piece of sterile crab shell with an area of approximately 1 cm<sup>2</sup>. The strains were incubated for 5 hours at 28°C in static, then the supernatant was removed, and the shells were carefully washed three times with 1 ml of fresh PBS. Finally, the crab shells were transferred into a tube containing 1ml of fresh PBS, the tubes were vortexed vigorously for 20 seconds and the resultant supernatant was 10-fold diluted and plated for bacterial counts (CFU/ml). The same experiment was performed with GFP tagged strains to observe the bacteria adhered to the shells with a Olympus TH4-200 fluorescence inverted optical microscope at 600x magnification.

## 11.- *In vivo* Assays

11.1.- Virulence and co-colonization. Virulence of the strains was determined as LD<sub>50</sub> (Reed and Muench, 1938) by intra-peritoneal injection (i.p.) and immersion challenge, both performed by infecting the animals with the LD<sub>50</sub> dose of R99 pertinent to each way of infection (Amaro *et al.*, 1995; Hernández-Cabanyero *et al.*, 2019). Briefly, groups of 6 eels (20 grs) were infected with the LD<sub>50</sub> of R99 ( $1 \times 10^2$  for i.p. and  $1 \times 10^6$  for Immersion) and doses above and below this threshold of the selected Type IV mutant. For the immersion challenge, each group of eels were incubated one hour in infective baths containing the bacterial load. Mortalities were validated by recovering the bacteria from internal organs of diseased eels, and the LD<sub>50</sub> of the mutants was determined through serial bacterial 10-fold dilutions in PBS (Amaro *et al.*, 1995).

The co-colonization and invasion assays were performed by immersion of groups of 24 eels (40 g) in a mixed infective bath containing a R99 harboring a *lacZ* gene for white-blue colony and the selected Type IV pili mutant. Three live eels per group were randomly sacrificed at 1, 12, 24 and 72h, and samples of gills, liver, kidney and blood were pooled and plated for bacterial counts (CFU/organ). TSA-1 + X-gal plates were used for the bacterial count, in these plates, the blue colonies corresponding to the R99 (*lacZ*+) and the white ones to the mutant (*lacZ*-) strain were easily distinguished.

## 12.- Scanning Electron microscope

Bacteria were observed with the electron microscope from the SCSIE (Servicio central de soporte a la investigación experimental), to this end, flagellar mutants were left to sediment for 5 hours without agitation and the supernatant media was removed carefully with a pipette to avoid disturbing the bacterial aggregation. After fixation for 4 h in 2% glutaraldehyde, each sample was washed three times in PBS 1X and placed in 2% phosphate-buffered osmium, followed by three rinses in distilled water. The samples were then serially dehydrated in ethanol, and sent to critical-point drying with carbon oxide in a Autosamdri® 814 critical point dryer (tousimis) mounted on metal stubs, and consequentially coated with gold-palladium, in a

SC7640 SEM Sputter Coater (Quorum Technologies). The cells were observed in a S4800 FEG-SEM (Hitachi) at magnifications of x1500. Representative photographs were obtained.

### **13.- Statistical analysis**

All the experiments were performed by triplicate, the results are presented as means  $\pm$  SE (standard error), significance of differences ( $P < 0.05$ ) between the means was tested by unpaired student T-test. When comparison of two or more conditions was necessary, analysis of variance (ANOVA) was utilized. All analyses were performed using GraphPad Prism® version 6.04 for Windows.

### **14.- Ethic statement**

All assays involving animals were approved by the Institutional Animal Care and Use Committee and the local authority (Generalitat Valenciana), following European Directive 2010/63/EU and the Spanish law 'Real Decreto' 53/2013 and were performed in the SCSIE facilities by using the protocol 2019/VSC/PEA/0063 (colonization and invasion in eels). We also have a permission from Generalitat Valenciana to use eels for scientific research purposes.



## 15.- References

1. Altschul, S.F., Gish, W., Miller, W., Myers, E.W., and Lipman, D.J. (1990) Basic local alignment search tool. *J Mol Biol* **215**: 403–410.
2. Amaro, C., Biosca, E.G., Fouz, B., Alcaide, E., and Esteve, C. (1995) Evidence that water transmits *Vibrio vulnificus* biotype 2 infections to eels. *Appl Environ Microbiol* **61**: 1133–1137.
3. Baba, T., Ara, T., Hasegawa, M., Takai, Y., Okumura, Y., Baba, M., et al. (2006) Construction of *Escherichia coli* K-12 in-frame, single-gene knockout mutants: The Keio collection. *Mol Syst Biol* **2**:
4. Baudin, A., Ozier-kalogeropoulos, O., Denouel, A., Lacroute, F., and Cullin, C. (1993) A simple and efficient method for direct gene deletion in *Saccharomyces cerevisiae*. *Nucleic Acids Res* **21**: 3329–3330.
5. Biosca, E.G., Llorens, H., Garay, E., and Amaro, C. (1993) Presence of a capsule in *Vibrio vulnificus* biotype 2 and its relationship to virulence for eels. *Infect Immun* **61**: 1611–1618.
6. Carda-Diéguez, M., Silva-Hernández, F.X., Hubbard, T.P., Chao, M.C., Waldor, M.K., and Amaro, C. (2018) Comprehensive identification of *Vibrio vulnificus* genes required for growth in human serum. *Virulence* **9**: 981–993.
7. Chodur, D.M., Coulter, P., Isaacs, J., Pu, M., Fernandez, N., Waters, C.M., and Rowe-Magnus, D.A. (2018) Environmental calcium initiates a feed-forward signaling circuit that regulates biofilm formation and rugosity in *Vibrio vulnificus*. *Am Soc Microbiol* **9**: 1–14.
8. Dalia, A.B., Lazinski, D.W., and Camilli, A. (2014) Identification of a membrane-bound transcriptional regulator that links chitin and natural competence in *Vibrio cholerae*. *Mol Microbiol* **5**:
9. Sonnenberg, M.S. and Kaper, J.B. (1991) Construction of an *eae* deletion mutant of enteropathogenic *Escherichia coli* by using a positive-selection suicide vector. *Infect Immun* **59**: 4310–4317.
10. Dunn, A.K., Millikan, D.S., Adin, D.M., Bose, J.L., and Stabb, E. V (2006) New rfp- and pES213-derived tools for analyzing symbiotic *Vibrio fischeri* reveal patterns of infection and *lux* expression in situ. *Appl Environ Microbiol* **72**: 802–810.
11. Gibson, D.G., Young, L., Chuang, R.Y., Venter, J.C., Hutchison, C.A., and Smith, H.O. (2009) Enzymatic assembly of DNA molecules up to several hundred kilobases. *Nat Methods* **6**: 343–345.
12. Gulig, P.A., Tucker, M.S., Thiaville, P.C., Joseph, J.L., and Brown, R.N. (2009) USER friendly cloning coupled with chitin-based natural transformation enables rapid mutagenesis of *Vibrio vulnificus*. *Appl Environ Microbiol* **75**: 4936–4949.

13. Guo, Y. and Rowe-Magnus, D.A. (2010) Identification of a c-di-GMP-regulated polysaccharide locus governing stress resistance and biofilm and rugose colony formation in *Vibrio vulnificus*. *Infect Immun* **78**: 1390–1402.
14. Hanahan, D. (1983) Studies on transformation of *Escherichia coli* with plasmids. *J Mol Biol* **166**: 557–580.
15. Hernández-Cabanyero, C., Lee, C. Te, Tolosa-Enguis, V., Sanjuán, E., Pajuelo, D., Reyes-López, F., et al. (2019) Adaptation to host in *Vibrio vulnificus*, a zoonotic pathogen that causes septicemia in fish and humans. *Environ Microbiol* **21**: 3118–3139.
16. Heydorn, A., Nielsen, A.T., Hentzer, M., Sternberg, C., Givskov, M., Ersboll, B.K., and Molin, S. (2000) Quantification of biofilm structures by the novel computer program COMSTAT. *Microbiology* **146**: 2395–2407.
17. Hoben, H.J. and Somasegaran, P. (1982) Comparison of the pour, spread, and drop plate methods for enumeration of *Rhizobium* spp. in inoculants made from presterilized peat. *Appl Environ Microbiol* **44**: 1246–1247.
18. Jayakumar, J.M., Shapiro, O.H., and Almagro-Moreno, S. (2020) Improved Method for Transformation of *Vibrio vulnificus* by Electroporation. *Curr Protoc Microbiol* **58**: e106.
19. Kelley, L.A., Mezulis, S., Yates, C.M., Wass, M.N., and Sternberg, M.J.E. (2015) The Phyre2 web portal for protein modeling, prediction and analysis. *Nat Protoc* **10**: 845–858.
20. Klevanskaa, K., Bier, N., Stingl, K., Strauch, E., and Hertwig, S. (2014) PVv3, a new shuttle vector for gene expression in *Vibrio vulnificus*. *Appl Environ Microbiol* **80**: 1477–1481.
21. Lee, C. Te, Pajuelo, D., Llorens, A., Chen, Y.H., Leiro, J.M., Padrós, F., et al. (2013) MARTX of *Vibrio vulnificus* biotype 2 is a virulence and survival factor. *Environ Microbiol* **15**: 419–432.
22. Livak, K.J. and Schmittgen, T.D. (2001) Analysis of relative gene expression data using real-time quantitative PCR and the 2- $\Delta\Delta$ CT method. *Methods* **25**: 402–408.
23. Meibom, K.L., Blokesch, M., Dolganov, N.A., Wu, C.Y., and Schoolnik, G.K. (2005) Chitin induces natural competence in *Vibrio cholerae*. *Science (80- )* **310**: 1824–1827.
24. Miller, J.H. (1972) Experiments in molecular genetics. In, *Experiments in molecular genetics*. Cold Spring Harbor, N.Y.: Cold Spring Harbor Laboratory, p. 466.
25. Miller, V.L. and Mekalanos, J.J. (1988) A novel suicide vector and its use in construction of insertion mutations: Osmoregulation of outer membrane proteins and virulence determinants in *Vibrio cholerae* requires *toxR*. *J Bacteriol* **170**: 2575–2583.
26. Milton, D.L., O’Toole, R., Hörstedt, P., and Wolf-Watz, H. (1996) Flagellin A is essential for the virulence of *Vibrio anguillarum*. *J Bacteriol* **178**: 1310–1319.
27. Pajuelo, D., Hernández-Cabanyero, C., Sanjuan, E., Lee, C.-T., Silva-Hernández, F.X., Hor,

- L.-I., et al. (2016) Iron and fur in the life cycle of the zoonotic pathogen *Vibrio vulnificus*. *Environ Microbiol* **18**: 4005–4022.
28. R. Simon, U.P. and A.P. (1983) A Broad host range mobilization system for *in vivo* genetic engineering: Transposon mutagenesis in gram negative bacteria. *Nat Biotechnol* **1**: 784–791.
29. Reed, L.J. and Muench, H. (1938) A simple method of estimating fifty percent endpoints. *Am J Epidemiol* **27**: 493–497.
30. Roig, F.J., González-Candelas, F., Sanjuán, E., Fouz, B., Feil, E.J., Llorens, C., et al. (2018) Phylogeny of *Vibrio vulnificus* from the analysis of the core-genome: Implications for intra-species taxonomy. *Front Microbiol* **8**: 1–13.
31. Shao, C.P. and Hor, L.I. (2000) Metalloprotease is not essential for *Vibrio vulnificus* virulence in mice. *Infect Immun* **68**: 3569–3573.
32. Sun, Y., Bernardy, E.E., Hammer, B.K., and Miyashiro, T. (2013) Competence and natural transformation in vibrios. *Mol Microbiol* **89**: 583–595.





# RESULTS

---

---



## 1.- Transcriptomic study in iron rich and poor media

The genes studied in this work were selected from a transcriptomic analysis of differentially expressed genes of the zoonotic clonal-complex strain R99 under iron-excess and iron-poor conditions (Pajuelo *et al.*, 2016). Among the colonization-related genes under the control of iron, there were multiple genes belonging to two Type IV pili systems, a twitching motility located in the pVvbt2 and multiple genes related to flagellum (**Table 1**).

**Table 1. Genes of interest related to biofilm and virulence selected from the transcriptomic analysis.**

Name	Function	Location in the genome	Iron restriction stimulon (FC <sup>1</sup> )
<b>Chromosome I (3,394,464 bp)</b>			
<i>mshL</i>	Type II secretin	423,063	+2.47
<i>mshM</i>	ATPase	424,717	+31.93
<i>mshQ</i>	MSHA biogenesis protein	433,440	+18.68
<i>mshA-1</i>	MSHA major pilin subunit	430,790	0
<i>flp-2</i>	Tight adherence associated pilin	764,158	-17.94
<i>rcpC/cpaB</i>	Auxiliary inner membrane assembly protein	766,021	0
<i>rcpA/cpAC</i>	Flp secretin protein	767,021	0
<i>tadB</i>	Pilus assembly inner membrane protein	773,710	0
<i>tadD</i>	Cellulose biosynthesis and glycan metabolism	775,632	0
<i>flp-1</i>	Tight adherence associated pilin	1,370,446	+34.95
<i>rcpC/cpaB</i>	Auxiliary inner membrane assembly protein	1,371,072	+3.22
<i>rcpA/cpaC</i>	Flp secretin protein	1,371,914	+28.76
<i>tadB</i>	Pilus assembly inner membrane protein	1,376,281	+8.36
<i>tadD</i>	Cellulose biosynthesis and glycan metabolism	1,378,098	+7.44
<i>cpsD</i>	Capsular polysaccharide synthesis enzyme, sugar transferase	1,335,059	0
<i>cpsB</i>	Capsular polysaccharide synthesis protein	1,336,500	-35.98
<i>flgP</i>	Flagellar protein	2,473,594	-65.75
<i>flgO</i>	Flagellar protein	2,473,755	-14
<i>flgM</i>	Negative regulator of flagellin synthesis	2,476,071	-10.9
<i>flgL</i>	Flagellar hook-associated protein	2,478,292	-37.1
<i>flgK</i>	Flagellar hook associated protein	2,481,379	-48.6
<i>flgJ</i>	Flagellar protein	2,483,246	-19
<i>flgG</i>	Flagellar basal-body rod protein	2,484,072	-9.6
<i>flgE</i>	Flagellar hook protein	2,486,389	-8.8
<i>flgD</i>	Flagellar basal-body rod modification protein	2,487,127	-6.21
<i>flgC</i>	Flagellar basal-body rod protein	2,487,145	-37.1
<i>flgB</i>	Flagellar basal-body rod protein	2,487,566	-5.2
<i>flgA</i>	Flagellar basal-body P-ring formation protein	2,490,159	-19.41
<i>mshA-2*</i>	MSHA major pilin subunit	2,559,410	0
<i>capD</i>	Glucosyl-4 epimerase	3,118,103	+3.19

<sup>1</sup> FC: fold change value or range of fold change values for each individual gene.

\*Orphan major pilin subunit genes that do not belong to the MSHA locus

**Table 1. Continuation**

Name	Function	Location in the genome	Iron restriction stimulon (FC <sup>1</sup> )
<b>Chromosome II (1,700,225 bp)</b>			
<i>flp-3</i>	Tight adherence associated pilin	629,517	0
<i>rcpC/cpaB</i>	Auxiliary inner membrane assembly protein	629,796	0
<i>rcpA/cpAC</i>	Flp secretin protein	630,572	0
<i>tadB</i>	Pilus assembly inner membrane protein	634,819	0
<i>tadD</i>	Cellulose biosynthesis and glycan metabolism	636,697	0
<i>mshQ</i>	MSHA biogenesis protein	944,651	+32.92
<i>mshA-3*</i>	MSHA major pilin subunit	983,504	-7.67
<i>cpsB</i>	Capsular polysaccharide synthesis protein	437,612	0
<b>pVvbt2 (68,446 bp)</b>			
<i>pilT</i>	Twitching motility ATPase	pVvbt2 plasmid	+33.03

<sup>1</sup> FC: fold change value or range of fold change values for each individual gene.

\*Orphan major pilin subunit genes that do not belong to the MSHA locus

Interestingly, various genes of the MSHA locus were upregulated in iron restrictive conditions, except for the *mshA* gene. There are three *mshA* genes in the genome of the R99, as mentioned before, one belongs to the MSHA locus (*mshA-1*), and the other two are orphan genes. From the three, *mshA-1* and *mshA-2* were not iron-responsive, while *mshA-3* was downregulated under iron starvation. In addition a second *mshQ* (involved in the biogenesis of the pilus) was also upregulated in iron restriction conditions (**Table 1**). It has been reported that *V. vulnificus* harbors three *tad* loci in its genome, each one codifies for a complete machinery assembly system (Pu and Rowe-Magnus, 2018). We found out that several genes of the *tad-1* locus were upregulated under iron restriction, while regarding the other two loci, only the *flp-2* gene from the *tad-2* locus was downregulated (-17.94). In addition, several genes belonging to the flagellar biosynthesis mechanism were downregulated in iron restrictive conditions. The majority of these genes code for proteins related to the basal body of the flagellar machinery, including the hook protein (**Table 1**).

As we observed that Type IV pili and flagellum expression seemed to be regulated by iron, we selected the three distinct *mshA* genes, the three *flp* genes and *flgE* in order to get mutants impaired in pili and flagellum, to study their role in virulence and biofilm formation. In case of the pili, we obtained simple, double and triple in-frame deletion mutants. In case of the flagellum, we selected the *flgE* gene that encodes the hook protein to produce an immotile mutant that preserved its adhesive and immunogenic properties attributed to the flagellum



(Ballado *et al.*, 2001). All the mutants were tested through several *in vivo*, *ex vivo* and *in vitro* assays. Interestingly, the plasmid gene *pilT* was strongly upregulated under iron starvation. PilT is an ATPase involved in the retraction and elongation of the Type IV pilus, which allows some species the twitching motility. For this reason, a mutant of the plasmid gene *pilT* was also obtained.

Finally, we decided to include in the study a *vvpD* deficient mutant. This gene codes for a prepilin peptidase in charge of processing the Type IVa pilin precursors, which are pilin-like Type II secretion system proteins. This enzyme is necessary for the expression of surface pili, secretion of cytotoxin, metalloprotease and chitinase and, in *V. cholerae*, for the correct assembly of the MSHA pilus (Paranjpye and Strom, 2005).

## 2.- Microarray validation

The results obtained with the microarray analysis were validated by quantifying the transcription level of the genes by RT-qPCR (**Table 2**). In general, the results obtained with both techniques were consistent, but we observed some differences among the expressions of the three *mshA* pilins, being the most remarkable result that the *mshA-3* expression was downregulated in the microarray, whereas it seemed to be slightly upregulated when quantitative PCR was used.

**Table 2. Comparison of fold change values between the array and RT-qPCR in the selected genes. For the RT-qPCR, *recA* was used as the reference gene and the fold induction ( $2^{-\Delta\Delta Ct}$ ) for each gene was calculated.**

Gene	FC <sup>1</sup>	
	Array	RT-qPCR
	Microarray validation	
<i>mshA-1</i>	--	3.3 (+)
<i>mshA-2</i>	--	-5.5 (-)
<i>mshA-3</i>	-7.6 (-)	4.3 (+)
<i>flp-1</i>	34.9 (++)	28.6 (++)
<i>flp-2</i>	-17.9 (--)	-16.7 (--)
<i>flp-3</i>	--	-1.3 (-)
<i>pilT</i>	33 (++)	28.4 (++)

<sup>1</sup>FC: fold change values qualitative classification: -,  $-2 < X < -10$ ; --,  $-10 \leq X < -25$ ; =,  $-2 < X < 2$ ; +,  $2 \leq X < 10$ ; ++,  $10 \leq X < 35$

### 3.- Development of a mutation protocol for the zoonotic clonal-complex

To achieve the objectives of the thesis, a wide mutant collection needed to be created, and this was our first major drawback. As we mentioned before in the introduction section, the zoonotic clonal-complex of *V. vulnificus* is very resistant to genetic manipulation, producing a mutant can consume months of hard work. A considerable effort and amount of time was invested in testing several mutation protocols, most of them with unsatisfactory results. At the end, we were successful in obtaining several mutants with some of the described protocols before settling with the one we selected, which entails the artificial induction of the natural transformation capability of *V. vulnificus* by upregulating the *tfoX* gene.

3.1.- Obtention of a non-motile mutant. A non-motile mutant was obtained by deleting the *flgE* gene. The flagellar mutant was produced using the triple ligation protocol, this protocol was adapted from the laboratory of professor Lien-I Hor in Taiwan (Shao and Hor, 2000). The *flgE* gene codes for the hook protein which is part of the flagellar biosynthesis mechanism and anchors the flagellin filament into the cellular envelope of the bacteria (Ballado *et al.*, 2001). By deleting this gene we produced an aflagellated strain that still produced the flagellin filament but is incapable of incorporate to attach it to the cell.

3.2.- Obtention of the *s/t* mutant. This mutant was obtained through the NotI ligation protocol, which was designed in our laboratory. This method relies on the natural transformation, induced by the presence of chitin, which mimics one of the environmental reservoirs for this species (animals with exoskeleton of chitin), where DNA recombination occurs naturally. However, even though we obtained this mutant with this protocol, we observed an extremely low efficiency (1 positive mutant colony out of more than 500 tested). While obtaining the mutant, we observed that this gene was wrongly annotated in the pVvbt2 as an ATPase with the sequence reference WP\_017060513.1 and protein Id ASJ41555.1, but the real identity of this gene corresponds to a lytic glycosyltransferase domain-protein. Lytic transglycosylases are enzymes involved in peptidoglycan remodeling by creating space for the addition of new components, or for the assembly of proteins that need to span through the cell

wall (Lairson *et al.*, 2008). This new annotation forced us to exclude this gene from this thesis, nonetheless, it will form part of a further research.

3.3.- TfoX-induced transformation as the standard technique for mutagenesis in the zoonotic serovar of *V. vulnificus*. This protocol is based on the induction of natural transformation through the inducible expression of the *tfoX* gene encoded by the pTfoX vector. This method proved to be highly efficient in the deletion of target genes, thus we selected it as our principal mutation protocol. With this technique we were able to obtain 2-3 mutants in a week, with less time-consuming steps by using a quick and reliable nested PCR amplification that effortlessly fuses the mutant construct in one quick reaction. After optimizing all the conditions for this protocol, we were able to produce all the mutants pertaining in this work, such as the three distinct  $\Delta mshA$ , the three  $\Delta flp$  of their respective *tad* locus and pertinent double and triple mutants. To obtain the compound mutants, instead of using the wild type as the starting strain, a R99 with a previously obtained simple mutant that conserved the pTfoX plasmid was used. All mutants were tested by PCR and grown in LB-1 broth containing the appropriate combination of antibiotics. In all cases, growth curves of each mutant were compared against the wild type to confirm that the ability to grow was not impaired by the mutation.

#### 4.- MSHA pilus and eel virulence

4.1.- The zoonotic clonal-complex of *V. vulnificus* harbors three distinct copies of the MSHA major pilin subunit gene. The genome of the selected strain of the zoonotic clonal-complex contains three distinct *mshA* genes, all of which encode proteins with the characteristic conserved N-terminal region of the MSHA major pilin subunit. We have designated these proteins as *mshA-1* (vvect4999\_RS02145), *mshA-2* (vvect4999\_RS12730) and *mshA-3* (vvect4999\_RS20940). The *mshA-1* gene is the only one that belongs to a MSHA locus, which is located in the chromosome I, while *mshA-2* and *mshA-3* are orphan genes located in the chromosome I and II, respectively (**Figure 1**).

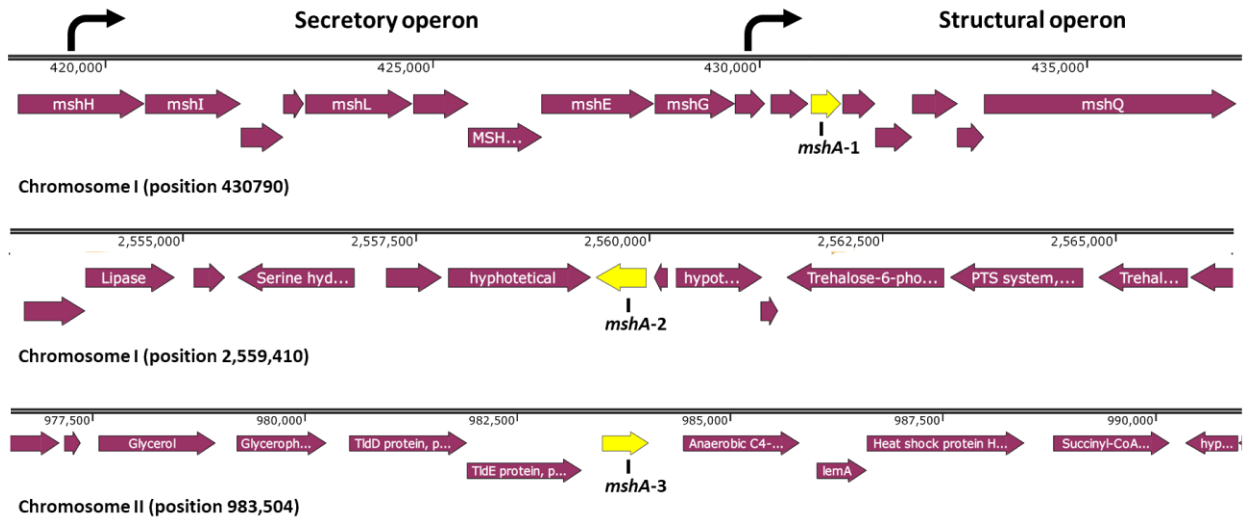


**Fig.1.** Schematic representation of the MSHA genes located in the genome of *Vibrio vulnificus*. The major MSHA pilin subunit gene (*mshA-1*) is located in a locus spanning 16.7 kb with 16 contiguous open reading frames, while *mshA-2* and *mshA-3* are orphan genes. The promoters required for the expression of the pilus are indicated by arrows. The other two genes do not belong to any loci. ORFs were drawn to scale using SnapGene® software.

We analyzed the presence and homology of *mshA* genes in a selection of genomes of other pathogenic *Vibrio* species, as well as genomes belonging to representative strains of the main *V. vulnificus* lineages (Table 3). All *V. vulnificus* strains of L2 contained all three *mshA* genes (*mshA<sub>VV</sub>* in this analysis), while most L1 strains (60%) showed only *mshA<sub>VV-1</sub>* and *mshA<sub>VV-3</sub>*, and all the lineage L3 strains lacked all *mshA* genes or homologues of these. All *V. cholerae* strains presented only the *mshA-1* gene, while all *V. parahaemolyticus* showed *mshA-1* and *mshA-3* genes (Table 3). Therefore, *mshA<sub>VV-2</sub>* appears to be exclusive to *V. vulnificus* and is mostly present in L2 strains. Finally, *mshA<sub>VV-1</sub>* showed the highest genetic variability while *mshA<sub>VV-2</sub>* and *mshA<sub>VV-3</sub>* were more conserved.

**Table 3. Sequence analysis and alignment to R99 of the three distinct *mshA* genes among different strains and species**

Species	Strains (Lineage) <sup>a</sup>	Genes					
		Length (bp)			Identity to R99 <sup>b</sup> (%)		
		<i>mshA</i> -1	<i>mshA</i> -2	<i>mshA</i> -3	<i>mshA</i> -1	<i>mshA</i> -2	<i>mshA</i> -3
<i>Vibrio vulnificus</i>	R99 (L2)	468	540	555	100	100	100
	ATCC 27562 (L2)	447	540	555	63.3	100	99.1
	CMCP6 (L1)	456	-	555	65.6	-	95.1
	ENV1 (L2)	471	540	555	66.6	100	99.3
	FORC_017 (L1)	471	537	549	67.1	54.7	94.1
	FORC_037 (L2)	492	540	555	63.9	99.8	94.1
	FORC_053 (L1)	510	540	555	66.7	98.9	94.1
	FORC_054 (L2)	471	540	555	66.4	100	99.5
	MO6-24/O (L1)	510	540	555	66.7	98.9	94.1
	YJ016 (L1)	471	-	555	67.1	-	94.2
	Vvyb1 (L3)	-	-	-	-	-	-
	12 (L3)	-	-	-	-	-	-
	11028 (L3)	-	-	-	-	-	-
	32 (L3)	-	-	-	-	-	-
	162 (L3)	-	-	-	-	-	-
<i>Vibrio cholerae</i>	El Tor FJ147	528	-	-	61.2	-	-
	HC1037	537	-	-	60.2	-	-
	N16961	537	-	-	60.2	-	-
<i>Vibrio parahaemolyticus</i>	FORC_004	468	-	528	66.3	-	62.1
	RIMD 2210633	498	-	537	60.4	-	61.9
	VPD14	498	-	537	60.4	-	61.9
<i>Shewanella ioihica</i>	ATCC 51908	492	-	-	55.1	-	-
<i>Shewanella woodyi</i>	PV-4	501	-	-	56.4	-	-

a. Phylogenetic Lineage of *V. vulnificus* according to Roig *et al.* (2018) and unpublished results.

b. Pairwise alignment was performed with the Geneious 7.1.9™ software using the Needleman–Wunsch algorithm.

To further compare the sequence similarities of the three *mshA* genes, we constructed a phylogenetic tree from all the analyzed sequences (**Figure 2**). The three genes clustered in three different groups within *V. vulnificus*, and did not correspond with lineage aggrupation. Furthermore, *mshA*-2 and *mshA*-3 of *V. vulnificus* were closer to the *mshA*-3 of *V. parahaemolyticus*, this probably occurred after an event of horizontal gene transfer and subsequent divergence. The analysis also confirmed the high homology of the *mshA*-2 and *mshA*-3 genes of all the species, except for the *mshA*-2 of the *V. vulnificus* FORC 017 strain. Interestingly, all the *mshA*-1 genes of *V. vulnificus* not only showed the highest variability among the different isolates, but were also grouped in one cluster together with the *mshA*-1 of *V. parahaemolyticus* and *V. cholerae*, also suggesting a common origin for this gene in these three species.

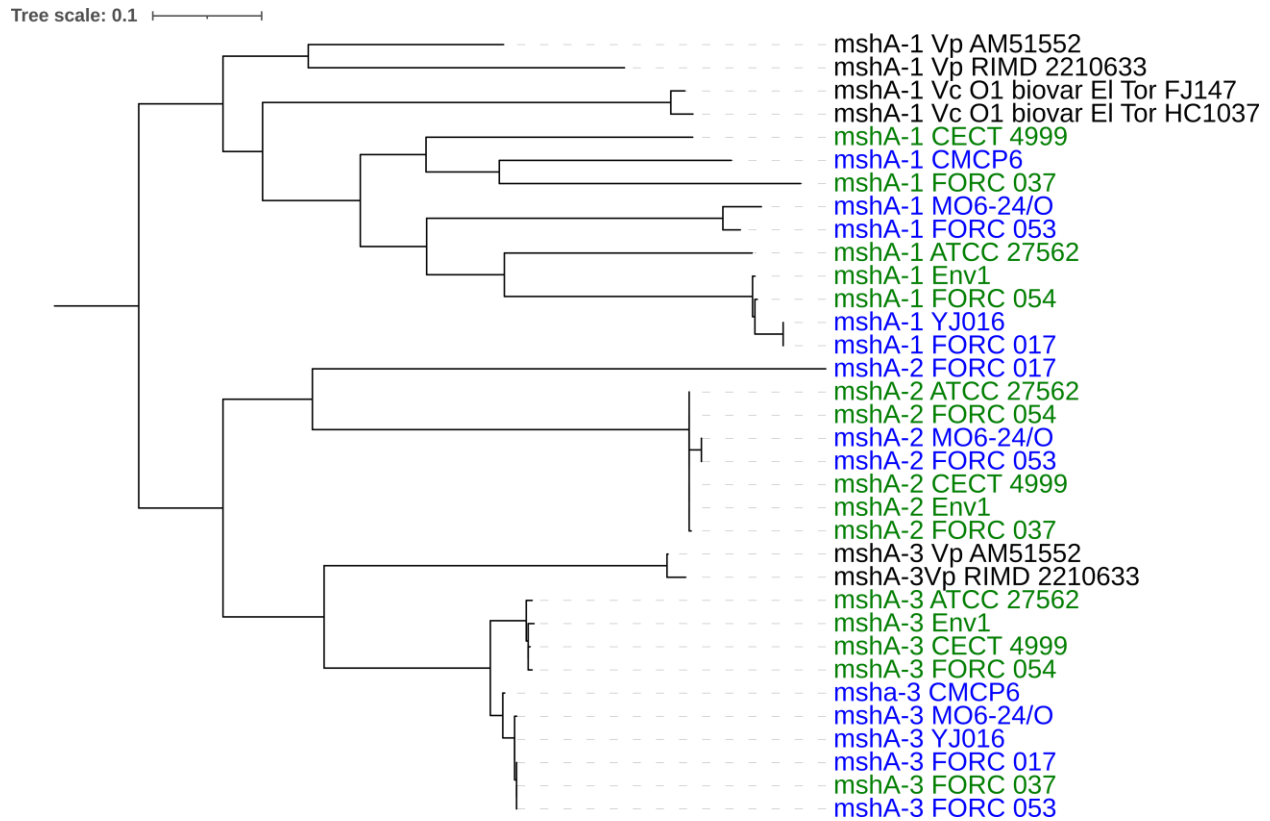


**Fig.2.** Phylogenetic tree of *mshA* genes. Maximum-likelihood tree derived from the sequence of the three genes in human pathogenic vibrios. Bootstrap support values higher than 80% are indicated in the corresponding nodes. Non *V. vulnificus* strains marked in black, strains belonging to L2 are marked in green, and strains from L1 are marked in blue.

PHYRE 2 was used for the prediction of the 3D structure of the three MSHA<sub>Vv</sub> proteins (**Figure 3A**), this tool develops template-based modeling in which the proteins are aligned to another of known structured based on patterns of evolutionary variation. Even though the DNA sequences of the proteins showed differences, their 3D model structures are strikingly similar. Their structures show homology to fimbriae, pili subunit proteins, and other prepilin-like proteins. We performed a clustalW alignment of the aminoacidic sequences of the *mshA* genes of *V. vulnificus* R99, *V. cholera* O1 El Tor FJ147 and *V. parahaemolyticus* RIMD 2210633 strains. It can be observed that the conserved N-terminal sequence (pilus core) of the prepilin which is similar in all of the sequences analyzed (**Figure 3B**).

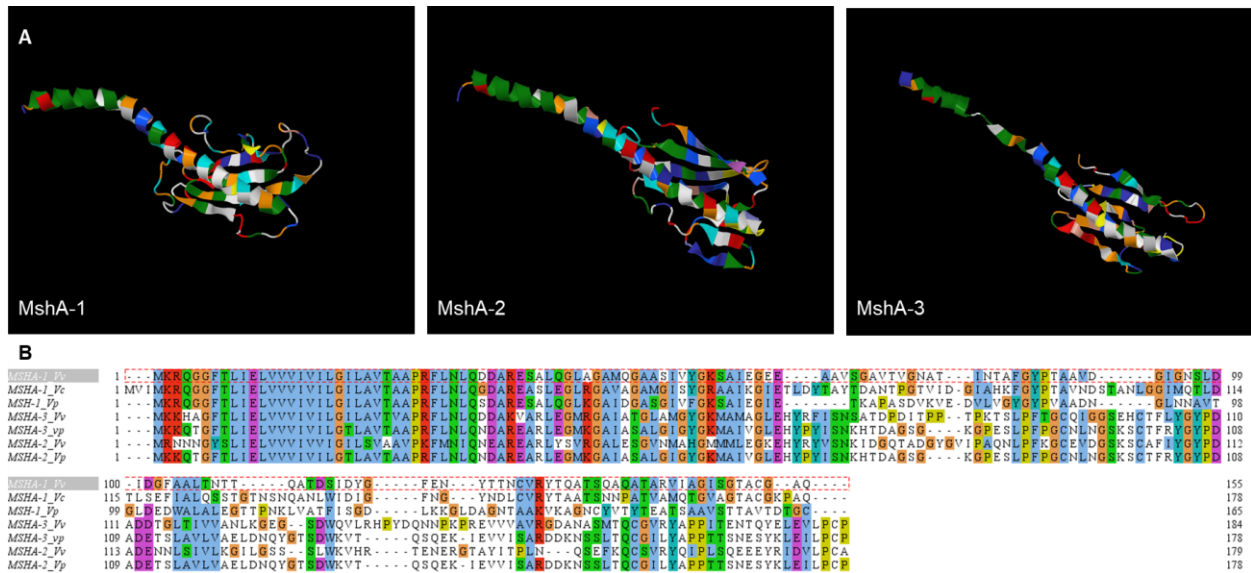


**Fig.3.** Structural modeling and alignment of the MSHA proteins from *V. vulnificus*. (A) 3D structures generated via Geneious 7.1.9® software. (B) Protein ClustalW alignment in Jalview 2.11.1.3® software.

We compared the expressions of all three *mshA* genes, in both the wild type and in the *mshA-1* mutant strain, in minimal media and iron restrictive conditions (**Figure 4**). There were no differences in gene expression between the wild type and the mutant strain regardless of the iron level in the medium, with the obvious exception of the mutated gene. This suggests that, neither *mshA-2* nor *mshA-3* increase their expression to complement the absence of the *mshA-1* gene. The results also showed that all three *mshA* genes, in case of the wild type strain, and the two genes, in case of the mutant, were expressed at similar levels in CM9. However, they were not similarly expressed under iron restriction, where the *mshA-2* gene was significantly less expressed than the rest (**Figure 4**). Finally, when the growth in iron-rich and iron-poor media was compared between each strain, it was clear that *mshA-1* and *mshA-3* were significantly upregulated under iron restriction (**Figure 4B**).

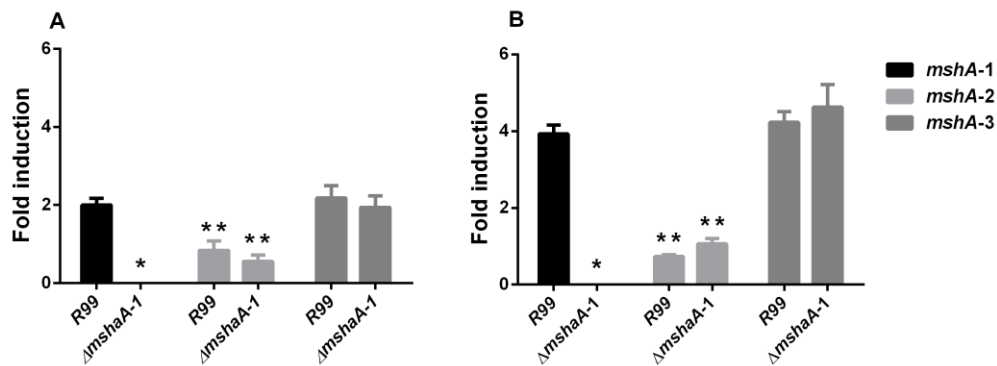


**Fig.4.** qPCR quantification of the *mshA* genes in CM9 (A) or CM9+Tf (B). Results are presented as the mean, and error bars represent the standard deviation. \*: significant differences between fold inductions of the same gene between strains. \*\*: Significant differences between fold inductions of different genes in the same strain. Significant differences ( $P < 0.05$ ) were determined by unpaired student T-test.

4.2.- Ex vivo and in vitro assays. Previous reports demonstrated the role of the *mshA-1* gene in the synthesis of the MSHA pilus and in biofilm formation (Watnick *et al.*, 1999; Chiavelli *et al.*, 2001; Zampini *et al.*, 2003). To our knowledge, there are no reports about the function of the two other *mshA* genes in biofilm formation. To investigate this, we created a battery of knock-out mutants in the *mshA* genes, obtaining single, double and triple in-frame deletion in all the possible combinations of these genes. Then we proceeded to quantify and compare their biofilm production between the wild type, the mutants, and the complemented strain. Remarkably, only  $\Delta mshA-1$  and the mutants presenting this deletion had a significant decrease in biofilm production ( $P < 0.05$ ), while complementation of  $\Delta mshA-1$  restored the biofilm to levels comparable to R99 (**Figure 5A**). The same biofilm assay was performed in iron-rich and iron-poor conditions. We found that biofilm formation by the wild type, and all the mutants strains that conserved the *mshA-1* gene, increased significantly under iron restrictive conditions (**Figure 5A and B**).

To further observe the biofilm formation by the wild type strain and the mutants, their biofilms 3D architecture was followed and analyzed by confocal microscopy (**Figure 6**). Again, only the *mshA-1* defective mutants showed a significant difference in their biofilms when compared to the wild type strain.



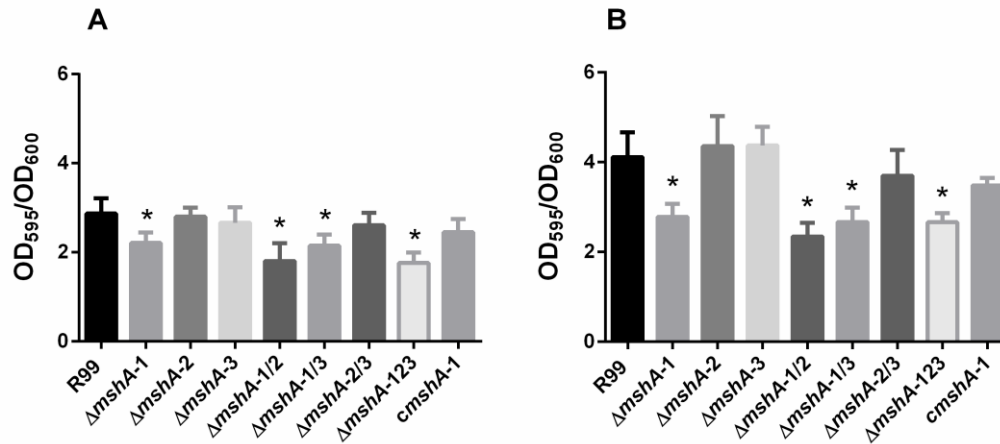


**Fig.5.** Biofilm production in CM9 (A) and CM9 + Tf (B) measured via crystal violet staining. Results are presented as the mean, and error bars represent the standard deviation. \*: significant differences between mutants and the wild type ( $P < 0.05$ ) were determined by one-way ANOVA.

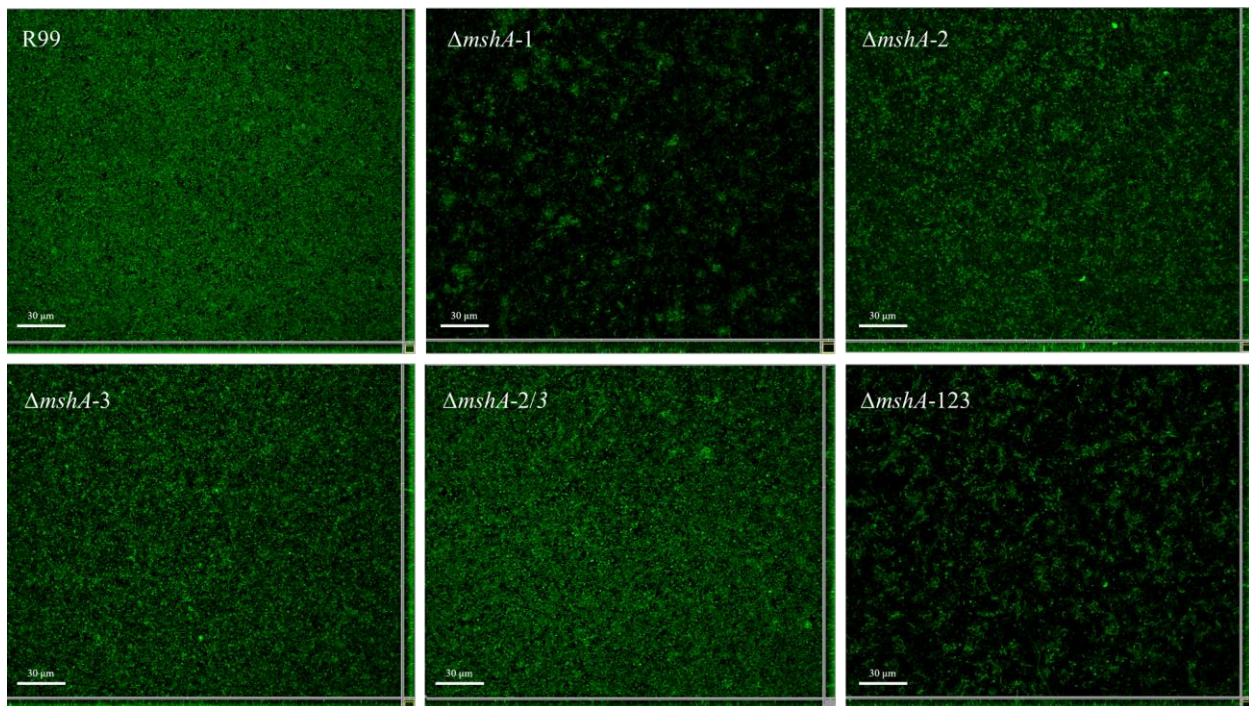


**Fig.6.** Fluorescent imaging of GFP labelled the zoonotic clonal-complex of *V. vulnificus* wild type and *mshA* simple and multiple mutant strains. Strains were grown overnight in static at 28°C in MSg + Km (150 μg/ml) in μ-dish® (Ibidi) plates. Images were captured using a confocal microscope and were analyzed using the Imaris viewer® (Bitplane) imaging software.

The *V. cholerae* O1 El Tor biotype and *V. cholerae* O139 serogroup strains produce MSHA pili, which is not present in the classical biotype. This pilus mediates a hemagglutination that is sensitive to mannose. Thus we determined and quantified the biofilm production in the presence of mannose of the zoonotic clonal-complex (**Table 4**). As expected, the wild type, the  $\Delta mshA-2$  and the  $\Delta mshA-3$  strains produced significantly less biofilm in presence of mannose. The amount of biofilm produced under these conditions was similar to the ones produced by mutations in the *mshA-1* gene (**Table 4 and Figure 7**).

**Table 4. Biofilm quantification of the R99 strain and its derivative mutants**

Strains	Biomass ( $\mu\text{m}^3/\mu\text{m}^2$ )		Thickness distribution ( $\mu\text{m}$ )		Roughness coefficient ( $R_a^*$ )	
	MSg	MSg + mannose	MSg	MSg + mannose	MSg	MSg + mannose
R99	2.26±0.54	1.56±0.35**	4.25±.023	3.61±.054**	1.05±.025	1.8±0.33**
$\Delta mshA-1$	1.42±0.48*	1.42±0.10	3.23±*.018	2.94±.063	2.24±0.57*	2.14±.061
$\Delta mshA-2$	1.99±0.13	1.59±0.54**	4.14±.045	2.87±.021**	1.13±.01	1.99±0.47**
$\Delta mshA-3$	2.11±0.33	1.39±0.36**	4.11±.026	3.02±.041**	1.11±.029	2.12±0.39**
$\Delta mshA-1/2$	1.50±0.5*	N/T	N/T	N/T	N/T	N/T
$\Delta mshA-1/3$	1.44±0.14*	N/T	N/T	N/T	N/T	N/T
$\Delta mshA-2/3$	1.97±0.12	N/T	N/T	N/T	N/T	N/T
$\Delta mshA-123$	1.52±0.15*	N/T	N/T	N/T	N/T	N/T
<i>cmshA-1</i>	1.92±0.16	1.35±0.21**	3.98±.012	2.97.028**	1.24±.02	2.23±0.16**

Biofilms total biomass, thickness distribution and roughness coefficient was measured and analyzed via Comstat 2.1® (Heydorn *et al.*, 2000) \*: significant differences in biomass between the wild type and the mutant strains was determined using ANOVA ( $P < 0.05$ ). \*\*: significant differences in biomass between the wild type and the derivative mutants grown with 4% D-mannose was determined using ANOVA ( $P < 0.05$ ).

The MSHA pili are necessary for the prevalence of the bacteria in the environment, as it plays a critical role in adhesion to both abiotic and biotic surfaces, which can include fish skin, ocean debris, exoskeletons of zooplankton, and many other shellfish carapaces (Marsh *et al.*, 1996; Chiavelli *et al.*, 2001). To determine the role of the *mshA* genes in adhesion to biotic surfaces, we incubated the bacteria in minimal media while adding crab shells as a biotic surface for adhesion and colonization. Only the strains lacking the *mshA-1* gene were significantly deficient in their capabilities of adhesion to crab shells (**Figure 8B**), the lack of adhesion was clearly noticeable after observing the shells under an optical microscope (**Figure 8A**). These results reinforce our previous data indicating that only the *mshA-1* gene is necessary for the correct functioning of the MSHA pili.

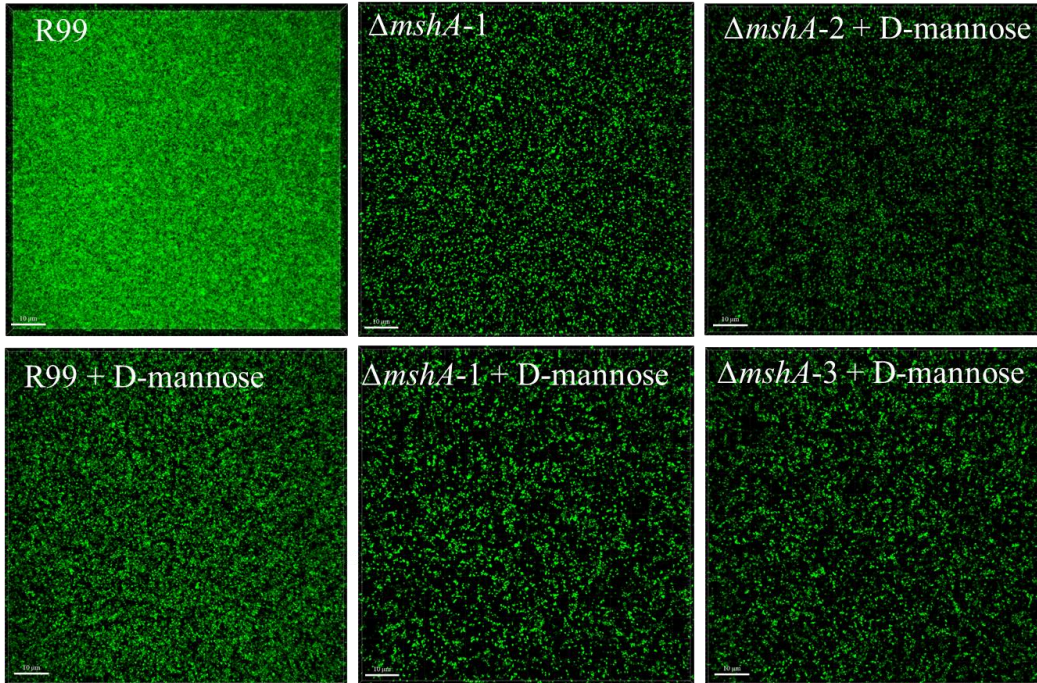


**Fig.7.** Fluorescent imaging of GFP labelled strains of the wild type and its derivative mutants. Strains were grown overnight in static at 28°C in M<sub>9</sub> + Km (150 µg/ml) with 4% D-mannose in µ-dish® (Ibidi) plates. R99 and *mshA-1* strains incubated without mannose were used as control. Images were captured using a confocal microscope and were analyzed using the Imaris viewer® (Bitplane) imaging software.

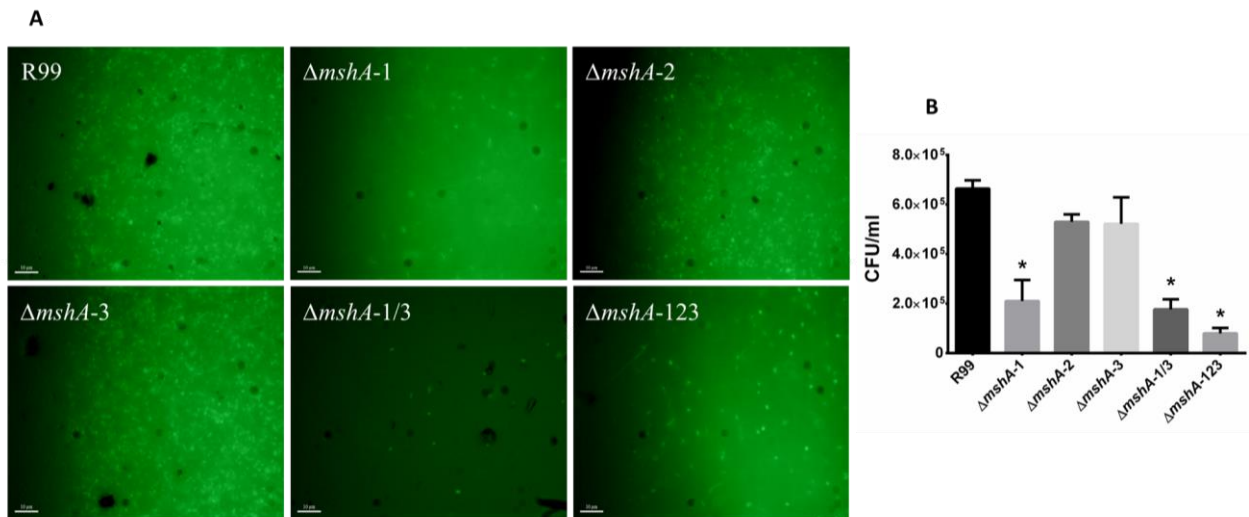


**Fig.8.** (A) *V. vulnificus* R99 and derivative mutant strains adhesion to crab shells. Shells were washed twice and mounted on a glass slide for microscope imaging. The images were taken with a Olympus fluorescent microscope. (B) Bacteria adhered to the crab shell after overnight incubation. \*: significant differences between mutants and the wild type ( $P < 0.05$ ) were determined by one-way ANOVA.



Since biofilm formation by *V. vulnificus* was inhibited by mannose, we performed a hemagglutination test with human red blood cells. The hemagglutination activity of the wild type,  $\Delta mshA-2$  and  $\Delta mshA-3$  was clearly visible after 1-3 minutes, while  $\Delta mshA-1$  showed no agglutination effect on the erythrocytes (**Figure 9**). When resuspended in 4% D-mannose and repeated the test, the wild type was unable to cause red cells agglutination.

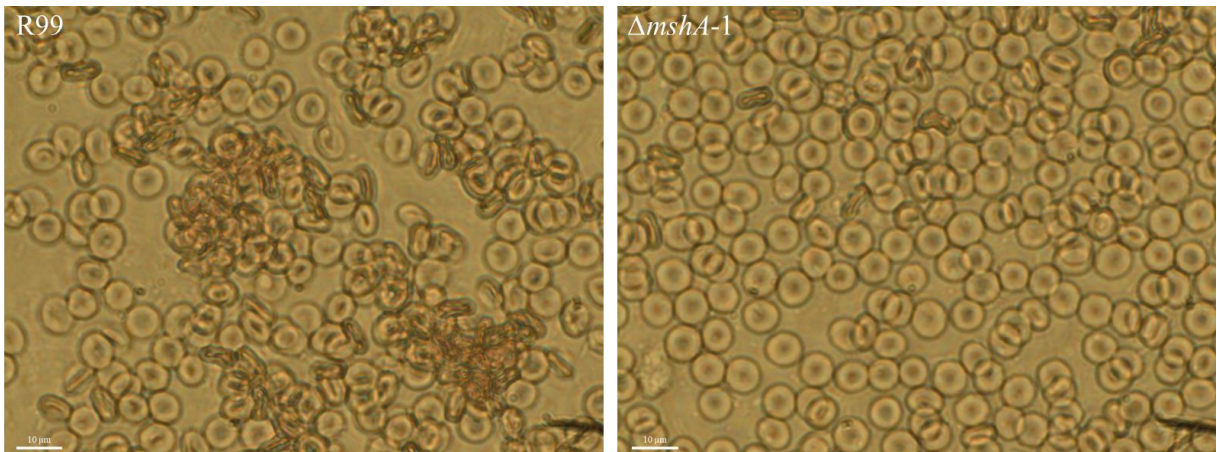


**Fig.9.** Hemagglutination activity of R99 and  $\Delta mshA-1$ . Bacterial and red blood cells were resuspended in PBS and gently mixed on a glass slide. Hemagglutination effect was visible on the R99 strain after 1-3 minutes, while it was completely absent in the *mshA-1* mutant.

4.3.- In vivo assays. The role of the three *mshA* genes in eel virulence was tested by determining the LD<sub>50</sub> of the mutants in comparison to the wild type strain in infection assays through both intraperitoneal injection (i.p.) and immersion challenge. The R99 + pTfoX strain was subjected to the same virulence tests as the wild type and its derivative mutants to rule out any variation in virulence influenced by the presence of the mutation plasmid. No change in virulence was induced by the pTfoX plasmid, and the *mshA-1* mutant remained as virulent as the wild type when administered through the intra-peritoneal injection, but was significantly less virulent than the wild type strain by immersion challenge (**Table 5**). In addition, neither  $\Delta mshA-2$  nor  $\Delta mshA-3$  were impaired in their virulence.

**Table 5. Virulence for eels and resistance of strain R99 and its derivative mutants to serum**

Strains	Virulence <sup>a</sup>		Resistance to <sup>b</sup>	
	intra-peritoneal	Immersion	Eel serum	Human serum
R99	1.5x10 <sup>2</sup>	1.4 x 10 <sup>6</sup>	+++	++
R99 + pTfoX	1.2x10 <sup>2</sup>	1.1x10 <sup>6</sup>	+++	++
$\Delta mshA-1$	1.1x10 <sup>2</sup>	> 10 <sup>7</sup> *	+++	++
$\Delta mshA-2$	1.2x10 <sup>2</sup>	1.2 x 10 <sup>6</sup>	+++	++
$\Delta mshA-3$	1.4x10 <sup>2</sup>	1.4x10 <sup>6</sup>	+++	++

a. Virulence was expressed as LD<sub>50</sub> in CFU/fish in case of intra-peritoneal injection and CFU/ml in case of bath infection (Amaro et al., 1995). Farmed eels (European eel *Anguilla anguilla*, were purchased from a local eel-farm that does not vaccinate against *V. vulnificus*).

b. Resistance to eel and human serum was measured as the ratio between bacterial counts at 0h and 4h of incubation. - <1; 1<+<10; 10<+++<25; +++>25.

\*: significant differences (P< 0.05) between R99 and the derivative mutant strains.

Then, we compared the colonization and invasion capability of the only mutant ( $\Delta mshA-1$ ) that showed a deficiency in virulence vs the wild type strain in a co-colonization assay, in which we infected eels by immersion with both strains in a 1:1 ratio. We found that the mutant strain was impaired in the early colonization of the eel, as significant lower numbers of  $\Delta mshA-1$  cells were recovered from all the sampled organs during the first 24 hours of infection. Interestingly, the differences in bacterial counts were specially significant during the first 12 hours post-infection (**Figure 10**). When sampled at 72 hours, the number of both strains were similar or slightly higher for the mutant (gills and spleen).

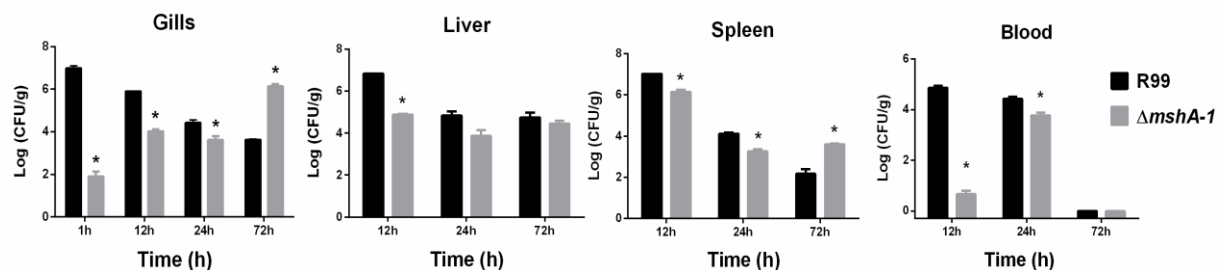


**Fig.10.** Co-colonization assay. Groups of 24 eels per strain were co-infected by immersion with a mixed (1:1) inoculum ( $2 \times 10^6$  CFU ml) of the R99 + Lac-Z and the mutant strain. Gills, blood, liver, head kidney and spleen were sampled at several times post-infection. Bacterial counts were performed in TSA-1 agar plates with X-gal for blue-white discrimination of R99. \*: significant differences between strains per organ and time point (P< 0.05) were determined by unpaired student's T-test.

## 5.- Prepilin peptidase virulence for eels.

Type IV pili of several gram negative bacteria need a dedicated prepilin peptidase required for both pilus biogenesis and extracellular secretion (Marsh and Taylor, 1998b). In *V. vulnificus*, the homologue to this prepilin peptidase, VvpD, enables the pathogen to express surface pili, adhere to epithelial cells, and is involved in extracellular secretion through the Type II secretion system (Paranjpye *et al.*, 1998). To determine whether these roles were conserved in the zoonotic clonal-complex, we subjected a *vvpD* mutant strain to the same tests as the MSHA pili mutants.

5.1.- *In vitro* assays. To find out whether  $\Delta vvpD$  was deficient in extracellular secretion of proteins, we tested the enzymatic activity (proteolysis and hemolysis) of  $\Delta vvpD$  and compared it with those of other *V. vulnificus* mutant strains (the *mshA-1* mutants, as the MSHA pilus is processed by VvpD), and the wild type strain (**Table 6**). The peptidase mutant was the only strain that showed a significant reduction in enzymatic activity, thus confirming previous results. Furthermore, the  $\Delta vvpD$  strain also had a significantly lower cell growth in comparison to R99 (**Figure 11A**).

**Table 6. Proteolytic and hemolytic activity of the ECP's of the R99 strain and its derivative mutants**

Strain	Proteolytic activity <sup>a</sup>	Hemolytic activity <sup>b</sup>
R99	128	64
$\Delta mshA-1$	128	64
$\Delta mshA-2$	128	64
$\Delta mshA-3$	128	64
$\Delta vvpD$	32*	8*

a. Proteolytic activity tested in LB-1 agar plates + casein, defined as the inverse of the ECP dilution that gave a positive result.

b. Hemolytic activity tested in LB-1 agar plates + eel blood (5% vol/vol), defined as the inverse of the ECP dilution that gave a positive result.

\*: significant differences ( $P < 0.05$ ) between R99 and the derivative mutant strains.

The peptidase mutant was also deficient in biofilm production, and had a higher roughness coefficient than the wild type strain (**Figure 11B and C**). Exactly the opposite of what happened with the FlgE mutant was observed (last section of results), as in this case, the mutant achieved lower growth rates and lower biomass (**Figure 11A, B**).

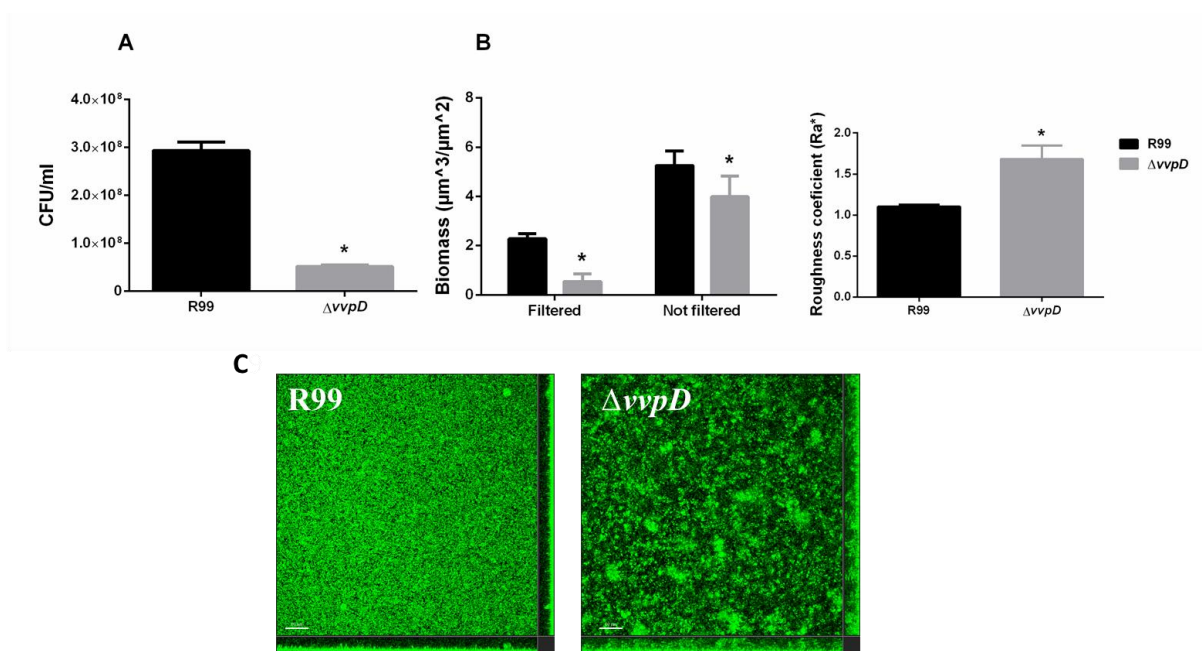


**Fig.11.** Growth and biofilm analysis of the prepilin peptidase VvpD mutant. Filtered: quantification of cells adhered to the substrate participating in biofilm formation. Not filtered: quantification of the total biomass present in the media (adhered and suspended cells). (A) Bacterial plate counts of the wild type and  $\Delta vvpD$  strains after an overnight incubation in minimal media CM9. (B) Biomass analysis of R99 and the mutant strain. (C) Confocal imaging of the GFP labelled strains. \*: significant differences between mutants and the wild type ( $P < 0.05$ ) were determined by unpaired student's T-test and one-way ANOVA.

5.2.- Ex vivo and in vivo experiments. The mutant showed a significant increase in LD<sub>50</sub> compared to R99 in both i.p. and immersion infection (**Table 7**), being completely avirulent as no mortality in the population was observed during the entire course of the experiments. These result suggests that the *vvpD* gene is essential for eel virulence, which could be explained by its role in both extracellular secretion of exoenzymes and EPS (Extracellular products) through the Type II secretion system (Marsh and Taylor, 1998b; Paranjpye *et al.*, 1998; Paranjpye and Strom, 2005). Furthermore, the peptidase mutant grew significantly less in eel serum than the wild type strain, however, both strains showed a similar resistance to human serum, as the cells remained static but alive (**Table 7**).

**Table 7. Virulence and resistance of strain R99 and its derivative mutants to eel and human serum**

Strains	Virulence <sup>a</sup>		Resistance to <sup>b</sup>	
	intra-peritoneal	Immersion	Eel serum	Human serum
R99	1 x 10 <sup>2</sup>	2 x 10 <sup>6</sup>	+++	+
<i>ΔvvpD</i>	>6 x 10 <sup>3*</sup>	>1 x 10 <sup>8*</sup>	+*	+

a. Virulence was expressed as LD<sub>50</sub> in CFU/fish in case of intra-peritoneal injection and CFU/ml in case of bath infection (Amaro *et al.*, 1995). Farmed eels (European eel *Anguilla anguilla*) were purchased from a local eel-farm that does not vaccinate against *V. vulnificus*.

b. Resistance to innate immunity in eel and human serum was measured as the ratio between bacterial counts at 0h and 4h of incubation in plasma serum. - <1; 1<+<10; 10<+<25; +++>25.

\*: significant differences in SI4h (P< 0.05) between R99 and the mutant strain.

## 6.- Tad pili in and eel virulence

Genetic studies have found out that several *tad* loci exist within bacterial genomes, in the *Vibrionaceae* family, several species harbor more than one *tad* locus, such as *V. vulnificus*, which has 3 different ones (Rosenfeld *et al.*, 2004; Pu *et al.*, 2018; Duong-Nu *et al.*, 2019). To investigate the role of the three distinct *tad* loci in the zoonotic clonal-complex of *V. vulnificus*, we obtained a battery of mutants in the *flp* pili genes of the three loci, including all combinations of double mutants, and a triple deletion. Then, we performed selected *in vivo*, *ex vivo* and *in vitro* tests to assess the effects of the impairment of each individual *tad* loci in biofilm production and virulence.

6.1.- *In vitro* assays. In order to understand the role of the *tad* loci in biofilm production in the zoonotic clonal-complex strain, we analyzed the biofilm production by using both crystal violet quantification assay and biomass analysis through confocal microscopy. As before, we also analyzed the strains in filtered and not filtered conditions to observe if there were any changes in their growth pattern. Our results suggest that neither biofilm production or total growth of the strains was affected with the loss of individual Tad pili, since no difference in biofilm production was observed in individual or double mutants. However, the triple *flp* mutant was significantly deficient in biofilm formation. Curiously, the biomass levels of the triple mutant were strikingly low (**Figure 12 and 13**).



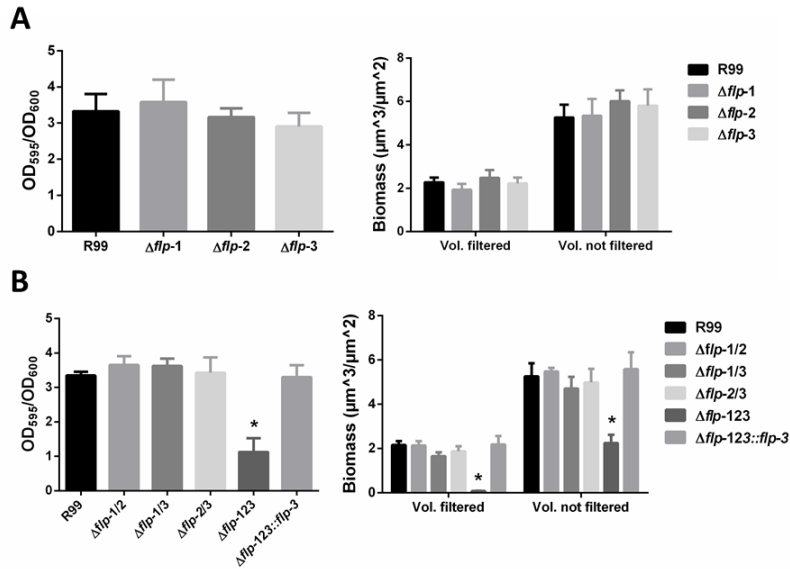


**Fig.12.** Biofilm analysis of the R99 and *tad* loci mutants. Filtered: quantification of cells adhered to the substrate participating in biofilm formation. Not filtered: quantification of the total biomass present in the media (adhered and suspended cells). Crystal violet staining and confocal microscopy were used to quantify the biofilm produced by the strains. \*:significant differences between mutants and the wild type ( $P < 0.05$ ) were determined by unpaired student's T-test and one-way ANOVA.

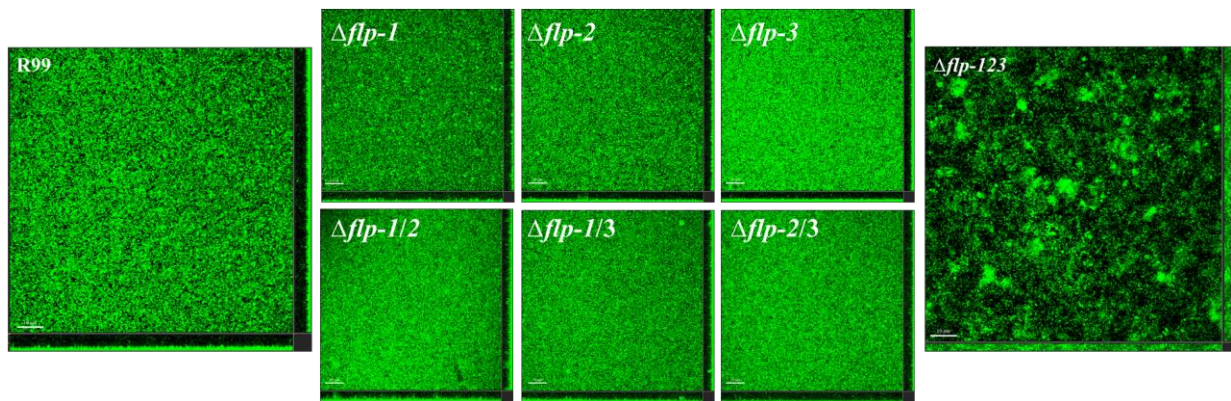


**Fig.13.** Confocal images of GFP labeled R99 and derivative *flp* mutant strains from all three *tad* loci, including a triple mutant.

Interestingly, the triple mutant produced considerably low quantities of biomass, which could indicate that the loss of the multiple pili is taxing on the bacteria. To deeply analyze the deficiency in biofilm production of the triple *flp* mutant, we compared the biofilms produced by this mutant with that produced by  $\Delta mshA-1$  in terms of biomass and 3D structures to that (**Figure 14**). Three parameters were measured; biomass (quantity of cells present), thickness

distribution (the average height reached by the population), and roughness coefficient (unevenness of surface), this last parameter was only measured in not filtered conditions, as it can only be applied to adhered cells. The  $\Delta flp-123$  strain produced a biofilm containing less biomass, thickness and roughness coefficient than that of  $\Delta mshA-1$ , although differences in thickness disappeared in the filtered condition, probably because non-adhered swimming cells were present in similar numbers. Therefore, the triple *flp* mutant showed a bigger deficiency in biofilm production than the  $\Delta mshA-1$ , although both presented an uneven biofilm structure (**Figure 14A**). By looking at the confocal microscopy images, these deficiencies in the 3D architecture of both mutants resulted quite evident (**Figure 14B**). In conclusion, an accumulative loss of three pili might be stressful enough for the cell to limit its growth and biofilm production.

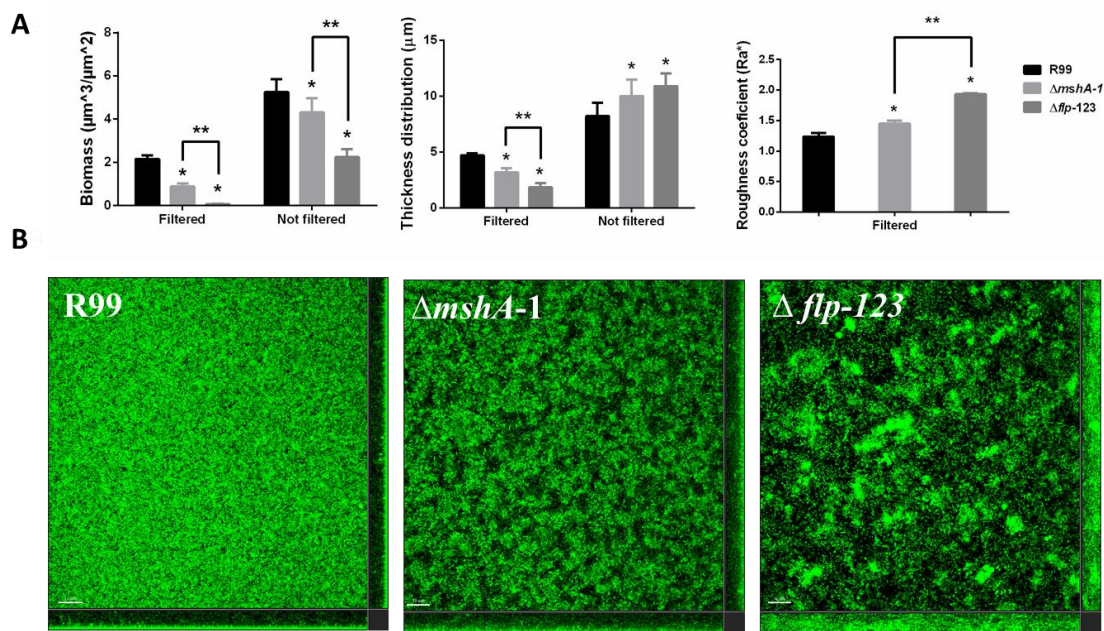


**Fig.14.** Biofilm analysis and comparison of R99 and the *mshA-1* and *flp-123* mutant strains. Filtered: Quantification of cells adhered to the substrate participating in biofilm formation. Not filtered: Quantification of the total biomass present in the media (adhered and suspended cells) (A) Biomass, thickness and roughness coefficient analysis of the wild type strains and its derivative mutants. (B) Confocal images of GFP labeled strains of the R99 and its derivative mutants.

6.2.- The Tad pili and their role in virulence. The role of the Tad pili in virulence in the zoonotic clonal-complex was tested by performing eel infections via i.p. injection and immersion challenge. Additional co-infections with several *flp* mutants were also performed. Finally, as serum provides important bactericidal activity and defense against pathogens like *V. vulnificus*, we also tested the susceptibility of the triple mutant against human and eel serum. None of the mutant strains showed any susceptibility to the bactericidal action of either sera, and virulence was not affected in the individual *flp* mutants from each *tad* loci in any of the infection assays. However, the triple mutant had a significantly higher LD<sub>50</sub> (around one log unit) than the wild type strain in the immersion challenge (**Table 8**). Interestingly, the LD<sub>50</sub> of the triple mutant remained the same than that of R99 after i.p. infection.

**Table 8. Virulence for eels and resistance of the R99 strain and its derivative mutants to serum**

Strains	Virulence <sup>a</sup>		Resistance to <sup>b</sup>	
	intra-peritoneal	Immersion	Eel serum	Human serum
R99	1 x 10 <sup>2</sup>	2 x 10 <sup>6</sup>	+++	++
$\Delta flp$ -1	2.2 x 10 <sup>2</sup>	1.6 x 10 <sup>6</sup>	+++	++
$\Delta flp$ -2	1.2 x 10 <sup>2</sup>	2.1 x 10 <sup>6</sup>	+++	++
$\Delta flp$ -3	1.5 x 10 <sup>2</sup>	1.9 x 10 <sup>6</sup>	+++	++
$\Delta flp$ -1/2	NT	NT	+++	++
$\Delta flp$ -1/3	NT	NT	+++	++
$\Delta flp$ -2/3	NT	NT	+++	++
$\Delta flp$ -123	1 x 10 <sup>2</sup>	>1 x 10 <sup>7</sup> *	+++	++

a. Virulence was expressed as LD<sub>50</sub> in CFU/fish in case of intra-peritoneal injection, and CFU/ml in case of bath infection. (Amaro *et al.*, 1995). Farmed eels (European eel *Anguilla anguilla*) were purchased from a local eel-farm that does not vaccinate against *V. vulnificus*).

b. Resistance to eel and human serum was measured as the ratio between bacterial counts at 0h and 4h of incubation - <1; 1<+<10; 10<+++<25; +++>25.

\*: significant differences (P< 0.05) between R99 and the derivative mutant strains.

To further investigate if the triple mutant was affected by other facets of the innate immune response, we monitored the phagocytic survival capacity of the bacterial cells in an infection assay in which human TPH-1 monocyte cells were infected with R99 and  $\Delta flp$ -123 (**Figure 15**). *E. coli* was used as control for the phagocytosis, and bacterial survival after phagocytosis was measured hourly by drop plate counting. There was no significant difference in survival between R99 and the triple mutant strains, however, both exhibited significantly higher survival rates than *E. coli* cells. In conclusion *tad* loci do not confer any type of protection against innate immunity and, consequently, they are not essential for eel virulence by i.p.

infection. However, the triple mutant was deficient in virulence by immersion challenge, which suggests a role of the loci in eel colonization.

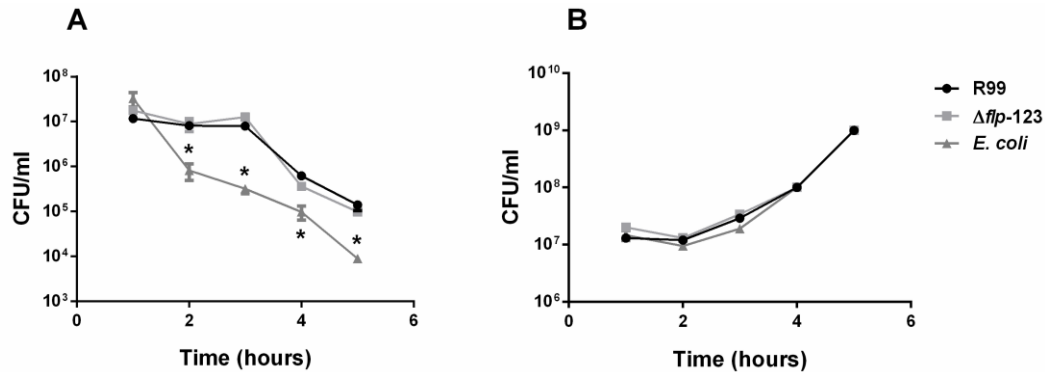


**Fig.15.** *V. vulnificus* zoonotic clonal-complex infection of human TPH-1 monocyte cells. Human monocytes were infected with the wild type and the triple *flp* mutant strains at a MOI of 10, survival of bacterial cells was quantified by drop plate \*: significant differences with R99 were determined by unpaired student's T-test ( $P < 0.05$ ).

Finally, we assessed the eel colonization capabilities performing several co-colonization assays (**Figure 16**). We demonstrated that, individually, the *tad* loci were not essential for colonization as, individual *flp* deletions did not affect the organ colonization and invasion. Interestingly, the triple *flp* mutant was deficient in gill colonization, but not in invasion to internal organs. These results suggest a minor role of each *tad* locus and a synergistic role of the three loci in gill colonization by the zoonotic clonal-complex.

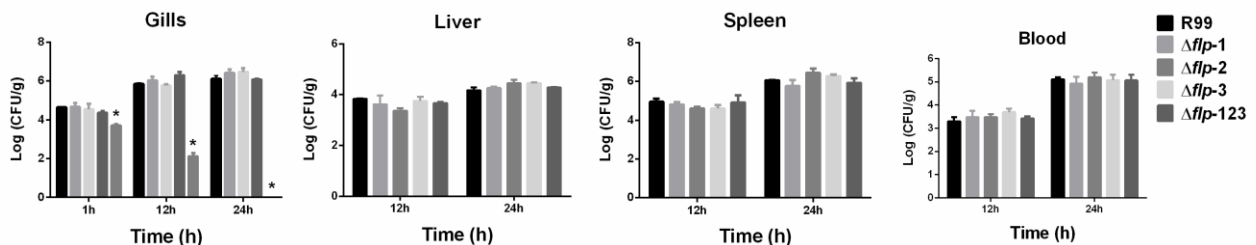


**Fig.16.** Role of the three *tad* loci in eel colonization. Co-colonization was performed by bath-infecting groups of 24 eels per each strain (3 animals per sampling point) with a dose of  $2 \times 10^6$  CFU/ml. Organs were sampled for bacterial counting on TSA-1 agar plates at 0, 12, 24 and 72h. \*: significant differences between strains per organ and time point were determined using unpaired Student t-test ( $P < 0.05$ ).

## 7.- Flagellum and virulence for eels

To study the implication of the flagellum in virulence for eels, we deleted the *flgE* gene coding for the hook protein that anchors the flagellar filament to the cell. Bacterial cells from the wild type and the mutant strains were negatively stained and observed with a transmission electron microscope (EMS): the wild type cells retained a polar flagellum (**Figure 17A**), while the mutant lost it completely (**Figure 17B, C**). To assess the loss of motility, the wild type and the mutant strains were inoculated in LB-1 soft agar (0.3%) and let to grow overnight at 28°C, and as expected, the mutant showed a complete loss of motility. The mutant grew as small and sharply delineated colony, whereas wild type strain showed a large diffuse halo (**Figure 18A**). When the bacteria were grown in liquid media, there was no observable aggregation (**Figure 18B**).

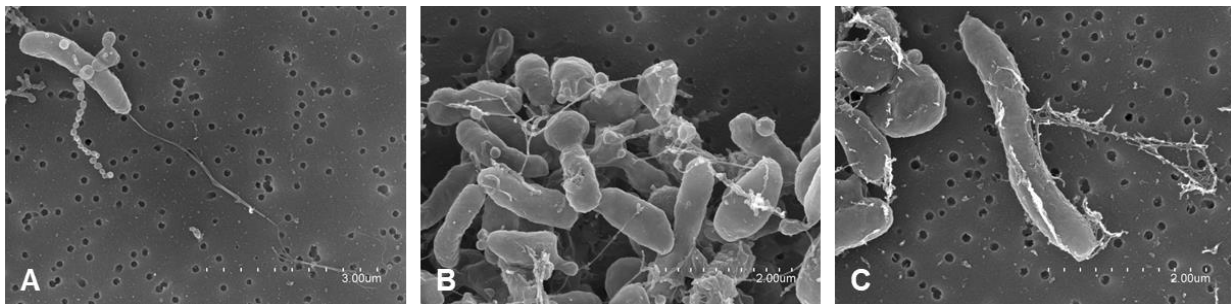


**Fig.17.** EMS images of the wild type (A) and the *flgE* mutant (B, C) strains. (A) Wild type strain presenting a polar flagella. (B) Cumulus of mutant bacteria and non-inserted flagellin filaments. (C) An isolated mutant cell without the polar flagellum.

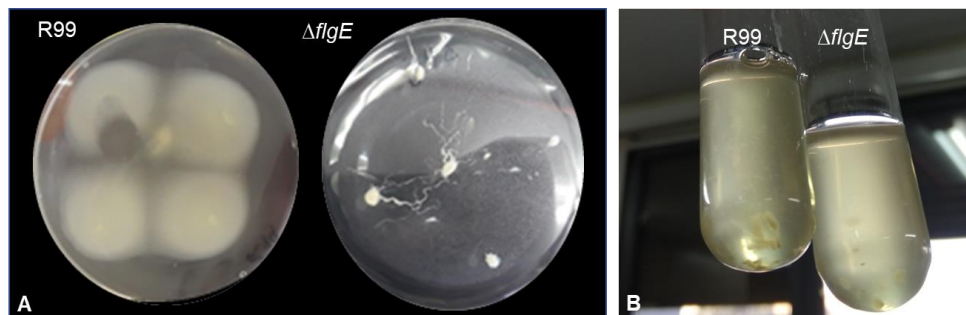


**Fig.18. Phenotype of the flagellar mutant  $\Delta flgE$ .** (A) The flagellar mutant shows a significant reduction in swimming motility in soft agar compared to the wild type. (B) The aflagellated mutants show no sedimentation or aggregation phenotype when grown in liquid media.



7.1.- In vitro assays. We noticed that the mutant strain seemed to grow to higher densities than the wild type at long term. To test this, we compared the growth of both strains by measuring absorbance at OD<sub>595</sub> in hourly intervals, and performed bacterial counts. The results showed that, in exponential growth there was no difference between the strains, however, the  $\Delta flgE$  strain achieved a higher absorbance and bacterial plate counts at 24 h of incubation (**Figure 19**). To assess the role of flagellum in biofilm production, we analyzed biofilm formation by confocal microscopy of strains grown in MSg. For this, we analyzed the biofilm production as we did with the *mshA* mutants through filtered and not filtered conditions (**Figure 20**).

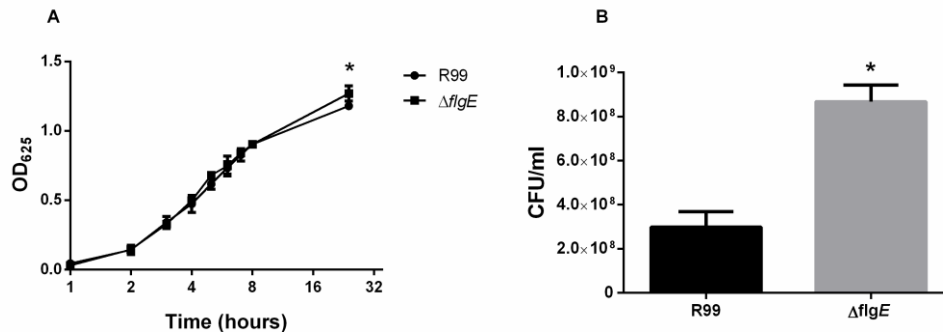


**Fig.19.** Differential growth between R99 and  $\Delta flgE$ . (A) Growth curves in CM9 media incubated at 28°C. (B) Bacterial counts for each strain after an overnight incubation at 28°C. \*: significant differences between strains ( $P < 0.05$ ) were determined by unpaired student's T-test.

Interestingly, although biofilm production was not affected by the loss of flagella, when measuring the unfiltered volume growth, total biomass production of the flagellar mutant was significantly higher than of the wild type (**Figure 20A**). In addition, the overall thickness of the biofilm when including the free-swimming cells was also higher than of R99. This implies that a great percentage of the mutant cells were suspended in the media, and were not actively forming part of the attached biofilm (**Figure 20B**). Moreover, a clear distinction between the cells attached to the substrate producing biofilm, and cells suspended in the media was clearly observed through the confocal microscope images (**Figure 21**).

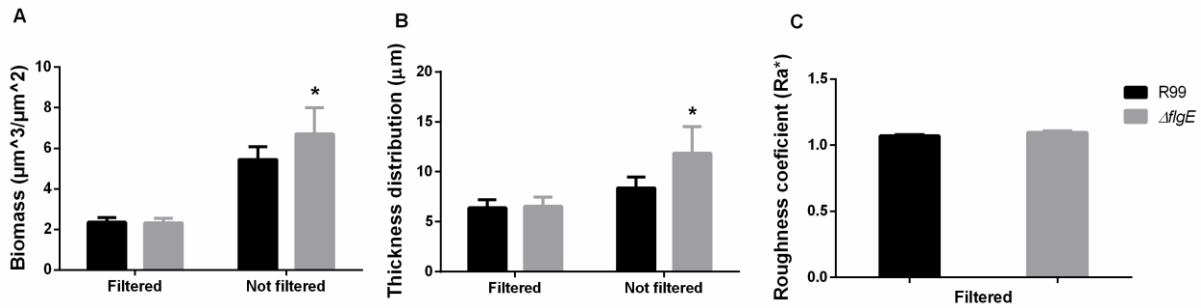


**Fig.20.** Biofilm analysis of the R99 and  $\Delta flgE$  strains. Filtered: Quantification of cells adhered to the substrate participating in biofilm formation. Not filtered: Quantification of the total biomass present in the media (adhered and suspended cells). (A) Total biomass. (C) Thickness distribution. (C) Roughness coefficient of adhered cells. \*: significant differences between strains per organ and time point ( $P < 0.05$ ) were determined by one-way ANOVA and unpaired student's T-test.

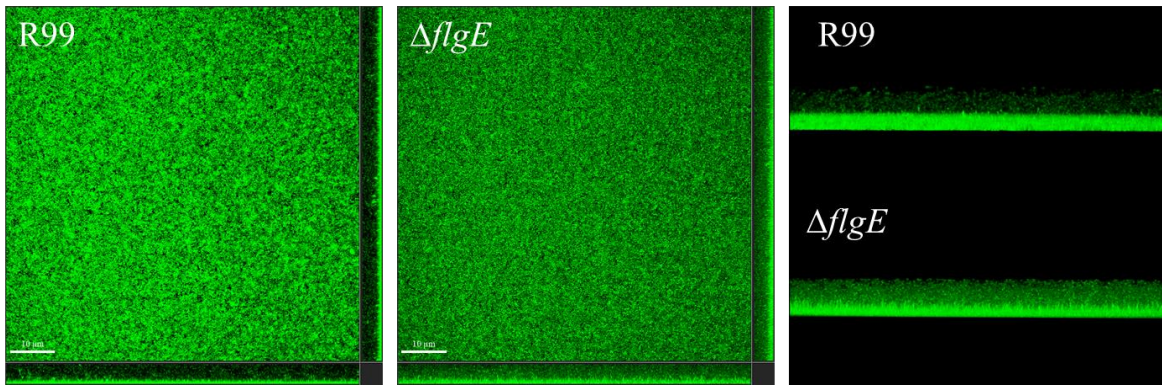


**Fig.21.** Fluorescent 3D imaging of GFP labelled *V. vulnificus* wild type and  $\Delta flgE$  strains. Strains were grown overnight in static at 28°C in MSg + Km (150  $\mu\text{g}/\text{ml}$ ) in  $\mu$ -dish® (Ibidi) plates by triplicate. Left images correspond to the total 3D structure rendering of all z-stacks of the biofilm. Right images correspond to the Y axis of the biofilm structure showing the distinction between cells allocated in the biofilm and the ones suspended in the media. Images were captured using a confocal microscope and analyzed using the Imaris viewer® (Bitplane) imaging software.

Since flagellar motility and the MSHA pili are intrinsically related to biofilm formation (Chiavelli *et al.*, 2001; Girón *et al.*, 2002; Liu *et al.*, 2008), we produced a *flgE/mshA-1* double mutant and tested it as the previous strains, and we included crystal violet staining as added reference for biofilm quantification (**Figure 22A**). As expected, both mutants deficient in *mshA-1* were impaired in their biofilm production, however, when taking into consideration the suspended cells, the flagellar mutant produced significantly more biomass when compared to R99 and  $\Delta flgE/mshA-1$  (**Figure 22B**). In addition, even though the double mutant showed less

growth than the wildtype, it still produced more biomass than  $\Delta mshA-1$ . This could mean that loss of flagella impacts the overall growth of the population independently of biofilm production.

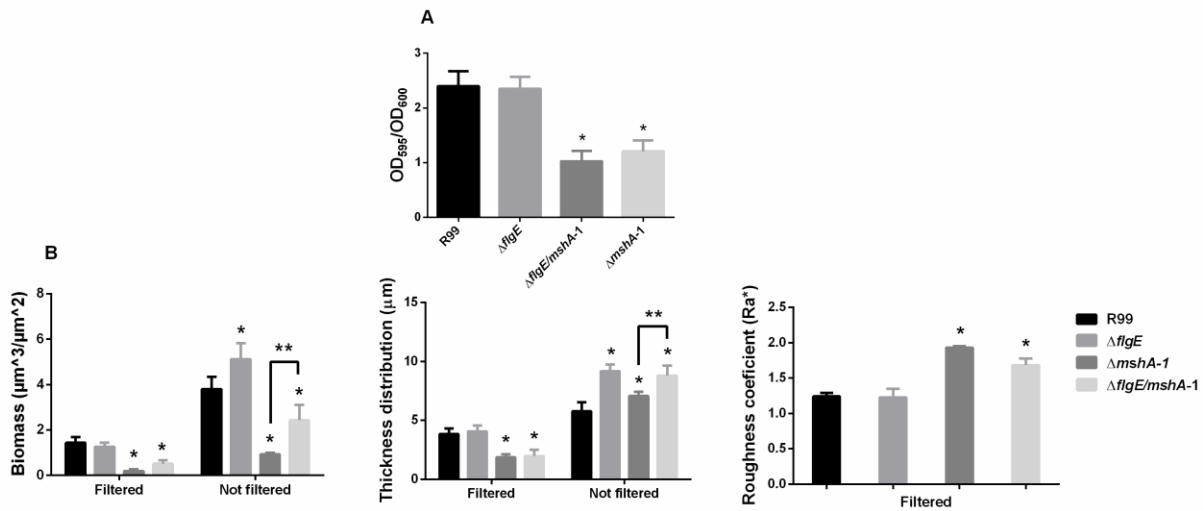


**Fig.22.** Biofilm analysis of the R99 strain and its derivative mutants. Filtered: Quantification of cells adhered to the substrate participating in biofilm formation. Not filtered: Quantification of the total biomass present in the media (adhered and suspended). (A) Crystal violet staining of R99 and its derivative stains. (B) Total biomass, thickness distribution and roughness coefficient analysis of the biofilms of R99 and its derivative mutants. \*: significant differences between strains ( $\Delta flgE$ ,  $\Delta mshA-1$  or  $\Delta flgE/mshA-1$  vs R99) ( $P < 0.05$ ); \*\*: significant differences between mutant strains ( $\Delta mshA-1$  vs  $\Delta flgE/mshA-1$ ) ( $P < 0.05$ ).

The disparity in the final growth of the strains was evident when comparing their 3D structures (**Figure 23**). In both flagella defective strains, there is an evident excess of swimming bacterial cells, independently of the biofilm production of the adhered cells in the substrate. Although the  $\Delta mshA-1$  biofilm architecture looks like it contained a great quantity of bacterial cells, this could be due to their inability to adhere to the substrate, thus most cells remain suspended and consequently there is a reduced formation of biofilm, however, this does not entails an increase in biomass like in the flagellar mutant.



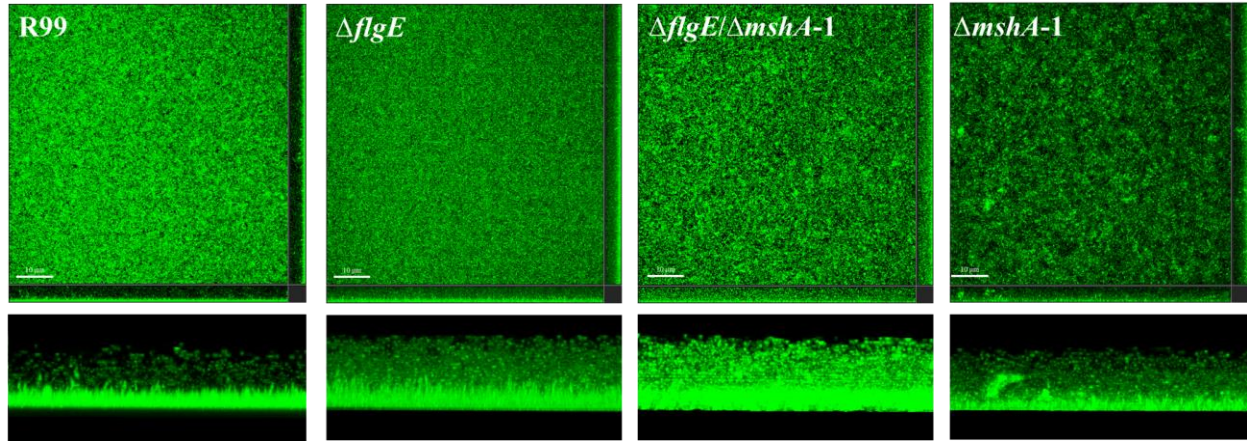


**Fig.23.** Representative images of the biofilms of the R99 and its derivative strains. GFP labelled strains were grown overnight in MSg at 28°C. These 3D images serve as a point of comparison between the differential architecture and cell arrangement found in the different R99 mutant strains. Aflagellated mutants showed an increase in bacterial population and non-adhered suspended bacterial cells.

7.2.- In vivo assays. We assessed the eel virulence of the  $\Delta flgE$  strain either by i.p. or immersion infection. Results showed that the flagellar mutant is significantly less virulent than R99 by immersion, but not by i.p. infection (**Table 9**). Thus, it seems that the zoonotic clonal-complex does not need the flagellum to cause disease when injected. Finally, the mutant strain did not show changes in resistance to eel or human sera (**Table 9**).

**Table 9. Virulence and resistance of strain R99 and its derivative mutants to eel and human serum**

Strains	Virulence <sup>a</sup>		Resistance to <sup>b</sup>	
	intra-peritoneal	Immersion	Eel serum	Human serum
R99	$9 \times 10^2$	$2 \times 10^6$	+++	++
$\Delta flgE$	$8.9 \times 10^2$	$2.3 \times 10^{8*}$	+++	++

a. Virulence was expressed as LD<sub>50</sub> in CFU/fish in case of intra-peritoneal injection and CFU/ml in case of bath infection (Amaro *et al.*, 1995). Farmed eels (European eel *Anguilla Anguilla*) were purchased from a local eel-farm that does not vaccinate against *V. vulnificus*).

b. Resistance to eel and human serum was measured as the ratio between bacterial counts at 0h and 4h of incubation - <1; 1<+<10; 10<+++<25; +++>25. \*: significant differences (P< 0.05) between R99 and the derivative mutant strains.

## 8.- References

1. Ballado, T., Camarena, L., González-Pedrajo, B., Silva-Herzog, E., and Dreyfus, G. (2001) The hook gene (*flgE*) is expressed from the *flgBCDEF* operon in *Rhodobacter sphaeroides*: Study of an *flgE* mutant. *J Bacteriol* **183**: 1680–1687.
2. Chiavelli, D.A., Marsh, J.W., and Taylor, R.K. (2001) The Mannose-Sensitive Hemagglutinin of *Vibrio cholerae* promotes adherence to zooplankton. *Appl Environ Microbiol* **67**: 3220–3225.
3. Duong-Nu, T.-M., Jeong, K., Hong, S.H., Puth, S., Kim, S.Y., Tan, W., et al. (2019) A stealth adhesion factor contributes to *Vibrio vulnificus* pathogenicity: Flp pili play roles in host invasion, survival in the blood stream and resistance to complement activation. *PLOS Pathog* **15**: 1–29.
4. Girón, J.A., Torres, A.G., Freer, E., Kaper, J.B., Rica, C., and Epec, H. (2002) The flagella of enteropathogenic *Escherichia coli* mediate adherence to epithelial cells. *Mol Microbiol* **44**: 361–379.
5. Heydorn, A., Nielsen, A.T., Hentzer, M., Sternberg, C., Givskov, M., Ersboll, B.K., and Molin, S. (2000) Quantification of biofilm structures by the novel computer program COMSTAT. *Microbiology* **146**: 2395–2407.
6. Lairson, L.L., Henrissat, B., Davies, G.J., and Withers, S.G. (2008) Glycosyl transferases: Structures, functions, and mechanisms. *Annu Rev Biochem* **77**: 521–555.
7. Lee, J.H., Rho, J.B., Park, K.J., Kim, C.B., Han, Y.S., Choi, S.H., et al. (2004) Role of flagellum and motility in pathogenesis of *Vibrio vulnificus*. *Infect Immun* **72**: 4905–4910.
8. Liu, Z., Miyashiro, T., Tsou, A., Hsiao, A., Goulian, M., and Zhu, J. (2008) Mucosal penetration primes *Vibrio cholerae* for host colonization by repressing *quorum sensing*. *PNAS* **105**: 9769–9774.
9. Marsh, J.W. and Taylor, R.K. (1998) Identification of the *Vibrio cholerae* type 4 prepilin peptidase required for cholera toxin secretion and pilus formation. *Mol Microbiol* **29**: 1481–1492.
10. Pajuelo, D., Hernández-Cabanyero, C., Sanjuan, E., Lee, C.-T., Silva-Hernández, F.X., Hor, L.-I., et al. (2016) Iron and fur in the life cycle of the zoonotic pathogen *Vibrio vulnificus*. *Environ Microbiol* **18**: 4005–4022.
11. Paranjpye, R.N., Lara, J.C., Pepe, J.C., Pepe, C.M., and Strom, M.S. (1998) The type IV leader peptidase/N-methyltransferase of *Vibrio vulnificus* controls factors required for adherence to HEp-2 cells and virulence in iron- overloaded mice. *Infect Immun* **66**: 5659–5668.
12. Paranjpye, R.N. and Strom, M.S. (2005) A *Vibrio vulnificus* type IV pilin contributes to biofilm formation, adherence to epithelial cells, and virulence. *Infect Immun* **73**: 1411–1422.

13. Pu, M., Duriez, P., Arazi, M., and Rowe-Magnus, D.A. (2018) A conserved tad pilus promotes *Vibrio vulnificus* oyster colonization. *Environ Microbiol* **20**: 828–841.
14. Pu, M. and Rowe-Magnus, D.A. (2018) A Tad pilus promotes the establishment and resistance of *Vibrio vulnificus* biofilms to mechanical clearance. *npj Biofilms Microbiomes* **4**:
15. Rosenfeld, J.A., Sarkar, I.N., Planet, P.J., Figurski, D.H., and DeSalle, R. (2004) ORFcurator: Molecular curation of genes and gene clusters in prokaryotic organisms. *Bioinformatics* **20**: 3462–3465.
16. Shao, C.P. and Hor, L.I. (2000) Metalloprotease is not essential for *Vibrio vulnificus* virulence in mice. *Infect Immun* **68**: 3569–3573.
17. Watnick, P.I., Fullner, K.J., and Kolter, R. (1999) A role for the mannose-sensitive hemagglutinin in biofilm formation by *Vibrio cholerae* El Tor. *J Bacteriol* **181**: 3606–3609.
18. Zampini, M., Canesi, L., Betti, M., Ciacci, C., Tarsi, R., Gallo, G., and Pruzzo, C. (2003) Role for mannose-sensitive hemagglutinin in promoting interactions between *Vibrio cholerae* El Tor and mussel hemolymph. *Appl Environ Microbiol* **69**: 5711–5715.





# DISCUSSION AND CONCLUSIONS

---



## 1.- Discussion

*V. vulnificus* is a zoonotic bacterial pathogen that inhabits tropical, subtropical and temperate brackish water environments around the globe (Horseman and Surani, 2011; Oliver, 2015). In temperate areas, the species is more abundant in the warmer months of the summer, which causes a spike in human infections by the consumption of contaminated seafood in the northern hemispheres (Oliver, 2013). Every year, due to climate change, the distribution of this zoonotic pathogen expands into colder environments, leading to an increased risk of infections for humans and fish (Oliver, 2013, 2015; Baker-Austin *et al.*, 2017). The various diseases caused by this pathogen in humans and fish are called vibriosis, and can be divided in two main types; primary septicemia and severe skin infections, the latter can lead to secondary septicemia (Jones and Oliver, 2009; Amaro *et al.*, 2015). Although cases of vibriosis in humans are rare, population at risk may contract the disease, and sometimes result in hospitalizations with a high mortality rate, and possibility of rapid death by fulminant septicemia (Bisharat *et al.*, 2013; T. Williams *et al.*, 2014; Oliver, 2015). *V. vulnificus* was formerly classified in three biotypes (Tison *et al.*, 1982; Bisharat *et al.*, 1999), however, a recent phylogenomic study proposed the subdivision of the species in 5 well-supported lineages, all of them potentially virulent for humans, and a pathovar with the specific ability to infect fish, due to a transferable virulence plasmid (Roig *et al.*, 2018). This pathovar is further subdivided into three different serovar-related subgroups, one of which, clusters all the known zoonotic strains and constitutes a clonal-complex with a worldwide distribution (Amaro and Biosca, 1996; Sanjuán *et al.*, 2011; Roig *et al.*, 2018). The present PhD thesis is precisely focused on this zoonotic clonal-complex.

First, we analyzed the differentially transcribed genes of R99 under iron-rich and iron-poor conditions, as iron is the main environmental signal that controls the life cycle of this pathogen (Hernández-Cabanyero and Amaro, 2020). We found that approximately 250 genes related to virulence and survival systems, like immune evasion, colonization, biofilm formation and motility belonged to an iron stimulon (Pajuelo *et al.*, 2016). Among these, several MSHA and Tad pili genes were upregulated under iron restriction, while several flagellum-related genes were downregulated. The Type IV pili are specialized appendages widespread among several genus of bacteria, that significantly contribute to motility, adherence, biofilm formation,

DNA uptake and virulence (Mattick, 2002; Shi and Sun, 2002). Since the role in virulence of these appendages has not been studied in the zoonotic clonal-complex, this was the main objective of the present PhD thesis.

To find out the function of a bacterial gene, one of the methodological approaches is to obtain in-frame deletion of the aforementioned gene, and compare its phenotypical characteristics to the ones of the parental (or wild type) strain. In *V. vulnificus*, several methods for obtaining knock-out mutants have been described, and some of them take advantage of the natural transformation mechanism that exists within the bacteria (Wu *et al.*, 2001; Meibom *et al.*, 2005; Sun *et al.*, 2013). However, this species is notoriously difficult to be artificially modified due to the presence of periplasmic nucleases that prevent the uptake of foreign DNA molecules (Wu *et al.*, 2001). Furthermore, transformation of this species is highly inefficient and large quantities of DNA are required, as well as linearized plasmids for their uptake by the cell (Jayakumar *et al.*, 2020).

We tested several mutation protocols described for strains of L1 (Shao and Hor, 2000; Baba *et al.*, 2006; Gulig *et al.*, 2009), but none of them yielded reproducible results in R99 strains. This strain is probably difficult to genetically modify because it contains the virulence plasmid, and various modification restriction systems that are not present in the genomes of strains from other lineages (unpublished results). In addition this particular strain is exceptionally sensitive to osmotic changes (Fouz and Amaro, 2003; Valiente and Amaro, 2006). So, we developed a two step novel mutagenesis protocol adapted to the zoonotic clonal-complex. The first step was to produce a mutation construct that could be efficiently taken up and incorporated by the R99 strain. To this end, we used an uncommon NotI restriction enzyme that only recognizes a large segment of DNA (7-8 bp). This enzyme exhibits a more restrictive nuclease activity, that will target a specific recognition site, and will not digest sequences normally found within the genome of the bacteria. This special site would be synthesized through Nested PCRs into the middle part of the mutation construct, so that it could incorporate an antibiotic cassette after being cut half and half by the NotI. This would also confer protection to the newly inserted cassette from the bacterial nucleases, after being ligated to a high copy number plasmid, and consequentially linearized through restriction



digestion at the exact opposite region where the construct is located (**Figure 3** from methodology).

The second step was to take advantage of *Vibrio*'s natural transformation system to effectively introduce the construct into the bacterium. This system has been well described in *V. cholerae* and it consists of an inducible system that is activated when the pathogen meets chitin (Meibom *et al.*, 2005). We first tried to obtain mutants using the NotI construct and natural transformation in the presence of crab shells based in protocols developed for L1 strains without success (Meibom *et al.*, 2005; Neiman *et al.*, 2011). Since the activation of the transformation machinery depends mainly on TfoX, an activator whose expression is precisely controlled by exogenous chitin (Lo Scudato and Blokesch, 2012), we introduced this gene through a plasmid designed for *V. cholerae* that would be under the control of arabinose when in the recipient strain. In this way we were able to induce the competence state in the zoonotic clonal-complex, and through a simpler nested PCR without the involvement of the NotI enzyme, we obtained the mutants studied in this work (**Table 1** general methodology ).

The MSHA pilus belongs to the Type IV pili family and is essential for biofilm formation and initial adhesion to biotic and abiotic surfaces (Marsh *et al.*, 1996; Chiavelli *et al.*, 2001). These pili are common among the *Vibrionaceae* family, and surprisingly, some of the species harbor more than one copy of the major pilin subunit (*mshA*) in their genomes (Barocchi and Telford, 2014). Interestingly, only some biotypes of *V. cholerae* (O1 El Tor and O139) express these pili (Watnick *et al.*, 1999; Chiavelli *et al.*, 2001), and therefore, the MSHA pilus has only been studied in the epidemic serogroups of this species (Thelin and Taylor, 1996; Watnick *et al.*, 1999; Zampini *et al.*, 2003). No apparent role in virulence was attributed to it in earlier studies (Thelin and Taylor, 1996; Watnick *et al.*, 1999; Chiavelli *et al.*, 2001; Utada *et al.*, 2014; Jones *et al.*, 2015; Sinha-Ray and Ali, 2017), however, this pilus has been related with colonization of mice intestine by this species (Hsiao *et al.*, 2006; Liu *et al.*, 2008). Once *V. cholerae* is inside the host, the MSHA pili must be repressed in order for the bacteria to escape recognition by immunoglobins, enabling colonization and induction of other virulence factors (Hsiao *et al.*, 2006). Nonetheless, not much has been described about the MSHA pili in *V. vulnificus*, and nothing has been studied about it in the zoonotic clonal-complex.

Our hypothesis was that this pilus should participate in both colonization of inert substrates, as demonstrated in L1 (Aagesen and Häse, 2012), and in the colonization of the eel. First, we found three different *mshA-1* genes in the genome of the R99 strain. We denominated them as *mshA-1*, *mshA-2* and *mshA-3*. Of the three, only *mshA-1* belonged to the MSHA locus. The three proteins coded by these genes presented the characteristic preserved N-terminal sequence, which includes the leader peptide and several ends with hydrophobic residues, which allows the formation of an extended  $\alpha$ -helix followed by the more heterogeneous C-terminal globular head (Berry and Pelicic, 2015) (**Figure 3**). In these proteins, the first hydrophobic residues are inserted into the previous filament assembly on the membrane, and are kept inside the mature filament as they are inserted in parallel to the axis in groups of three, akin to a wheat head .

All three genes were present in all *V. vulnificus* genomes belonging to L2 and in 40% of genomes belonging to L1, while none of them were present in L3 genomes. This could suggest that different clades/lineages of the species use different appendages to adhere to substrates in their natural environments or, alternatively, that they are adapted to different niches in nature, a hypothesis suggested by Giltner *et al.*, (2012). We also found *mshA-1* present in the genomes of the three main pathogenic species of *Vibrio*, while *mshA-3* was only present in *V. parahaemolyticus*, and *mshA-2* was exclusive to *V. vulnificus* (**Table 3**). We constructed a phylogenetic tree that encompassed the three *mshA* genes present in the three species, and compared them to unravel their evolutionary origin. Interestingly, this gene turned out to be highly variable, which could be related to the phenomenon of antigenic variability affecting genes coding for Type IV pili, which are exposed to the immune system, as described in *Neisseria gonorrhoeae* and *V. cholerae* (Merz and So, 2000; Hsiao *et al.*, 2006). On the other hand, the *mshA-3* of *V. vulnificus* was closer to the *mshA-3* of *V. parahaemolyticus* than to the rest of the *mshA* genes belonging to the same species, which relates this gene to horizontal gene transfer between both species. In addition, *mshA-2* and *mshA-3* are highly conserved within *V. vulnificus*, suggesting that they are not subject to the antigenic variability phenomena, and are under strong selective pressure.

The main role of the MSHA pili is to promote initial surface adhesion and biofilm formation (Jonson *et al.*, 1991; Watnick *et al.*, 1999; Zampini *et al.*, 2003), so we analyzed the biofilm production capabilities of all the strains by using both crystal violet staining and confocal imaging. Our results clearly showed that biofilm production by the zoonotic clonal-complex was influenced by *mshA-1*, since the elimination of this gene significantly reduced its production (**Table 4** and **Figure 5**). These results are in agreement with previous studies that related biofilm production to the MSHA pilus (Marsh and Taylor, 1998a; Watnick *et al.*, 1999; Utada *et al.*, 2014; Sinha-Ray and Ali, 2017). Furthermore, we obtained multiple evidences that neither *mshA-2* nor *mshA-3* played a role in the formation of biofilms under the tested conditions, and that they could not restore the formation of biofilms in the *mshA-1* mutants. Our results also confirmed, by analyzing the three-dimensional structure of the biofilms, that only the strains with *mshA-1* deletions produced a defective biofilm (**Figure 6**).

We then proved that the pilus produced by the zoonotic clonal-complex was sensitive to mannose, by performing the corresponding hemagglutination and biofilm formation tests in presence and absence of this molecule. This suggests that mannose residues recognize these pili. As expected, the two remaining *mshA* genes were not involved in inhibiting biofilm formation and hemagglutination in the presence of mannose (**Table 4, Figure 7 and 9**).

Our transcriptomic studies suggested that the MSHA pili production was under iron control, so we measured biofilm production under iron-rich and iron-poor conditions. Biofilm production by the wild type strain increased significantly under iron restriction (**Figure 5B**), which was compatible with the life cycle model proposed for this species by Pajuelo *et al.* According to this model and our results, iron restriction would trigger the formation of biofilms by activating MSHA pili production. Interestingly, *mshA-3* also increased its expression in iron restriction, while *mshA-2* was not iron-responsive. Although both genes were not involved in the formation of biofilms in the conditions tested, we could not rule out the possibility that both genes could be involved in the adhesion to other types of surfaces, therefore, we tested biofilm formation on chitin by using crab shells. Significant differences were observed only in the mutant deficient in the *mshA-1* gene, proving again that this gene is the only one required

for a functional pilus and biofilm formation on both hydrophobic (plastics) and hydrophilic (chitin) surfaces (**Figure 8**).

Previous studies have shown that MSHA pilus plays a role in the virulence of *V. cholerae* because it is involved in colonization of the intestines (Watnick *et al.*, 1999; Hsiao *et al.*, 2006). Therefore, we tested the virulence and colonization capabilities in eels by comparing the mutant against the wild type strain. Our results confirmed that the MSHA pilus of the zoonotic clonal-complex is involved in eel virulence, but only when eels are infected by the natural route of infection (water), as the mutant strain was significantly less virulent than the wild type during the immersion challenge. In fact, previous studies had shown that this bacterium colonizes the eel skin mucosa, forming biofilms directly in the gills (Marco-Noales Ester *et al.*, 2001). Our co-colonization trials supported the hypothesis that the MSHA pilus is involved in the virulence of eels by promoting early gill colonization through biofilm formation, as the colonization of eels by  $\Delta mshA-1$  was greatly impaired, most notably in the gill and in the first hours of infection (**Figure 10**). In addition, the MSHA pilus is not directly involved in the resistance of innate immunity, and needs to be repressed and degraded in order to not be recognized by immunoglobins and alert the immune system (Hsiao *et al.*, 2006; Liu *et al.*, 2008). Our results support this previous statements, as the MSHA pilus of the zoonotic clonal-complex was not involved in resistance to neither eel nor human serum. No statistical differences were detected when comparing the survival in serum between the mutant and the wild type strains. Probably the loss of the pilus by *V. vulnificus* does not affect its sensitivity to serum because the resistance to this innate immunity mechanisms relies exclusively in the capsule in the case of humans (Carda-Diéguez *et al.*, 2018), and in an outer membrane complex, in case of eels (Hernández-Cabanyero *et al.*, 2019).

Therefore, the MSHA pilus is needed for a successful early colonization of the gills, coincidentally, this is a critical step in the initiation of infection in eels by the zoonotic clonal-complex, as the gills serve as the main portal of entry for the pathogen into the bloodstream. (Amaro *et al.*, 1995; Amaro and Biosca, 1996; Marco-Noales Ester *et al.*, 2001). Our results showed a reduction in colonization of the gills during the first hours of infection, which could cause a reduced colonization of the internal organs: as there are less bacteria colonizing the gill,

a reduced bacterial load would be invading the bloodstream and internal organs, which in turn would be impacting the overall speed and severity of the infection.

The integral role of the MSHA pilus in virulence of *V. vulnificus* zoonotic clonal-complex could be to enable eel colonization by facilitating biofilm formation on the gills. These biofilms are produced in natural conditions as it was previously demonstrated by Marco-Noales *et al.*, (2001). In *V. cholerae* the expression of virulence and colonization determinants, including the repression of the MSHA pili early during infection, is performed through a transcriptional control mediated by ToxT (Hsiao *et al.*, 2006). Here we demonstrated that the transcription of MSHA pili is controlled by iron, which is the main external signal that governs the entire life cycle of this bacterium (Pajuelo *et al.*, 2016).

We propose that the reduction in virulence resulting by the elimination of functional MSHA pili is caused by a significant decrease in the quantity of bacterial cells adhering to the gills, which in turn, slows the entry of the pathogen into the organism. Immediately, a significantly smaller bacterial load enters the bloodstream and disperse the infection through other organs and tissue. Since the initial invasion of the host is being carried out by fewer cells, the odds of survival of the infected eel increases dramatically, as their immune system fends off significantly fewer bacterial cells than in a normal vibriosis infection. As previously stated, these pili are necessary for the initial adhesion to biotic surfaces, such as chitinous exoskeleton of zooplankton, and asymptomatic colonization of oysters and bivalves (Chiavelli *et al.*, 2001; Zampini *et al.*, 2003; Chodur *et al.*, 2018). However, as we demonstrate now, the MSHA pilus is also involved in the early steps of eel colonization and, therefore, in virulence for eels of the *V. vulnificus* zoonotic clonal-complex. This initial attachment allows this pathogen to colonize the main point of entry into the eel, ensuing an effective invasion of the bloodstream, consequential adhesion, and colonization of internal organs.

A prepilin peptidase is necessary to modify the MSHA pilus proteins in order for them to be functional (Fullner and Mekalanos, 1999). This peptidase was first described in 1991 in *P. aeruginosa* (Nunn and Lory, 1991), and since then, several homologues have been found in different genera of bacteria (Nunn *et al.*, 1990; Lory and Strom, 1997). In *V. cholerae*, the

homologous VcpD is a protein necessary for the secretion of the cholera toxin and a proper formation of the pilus (Marsh and Taylor, 1998b). This peptidase shares a high sequence homology to the VvpD protein of *V. vulnificus*. In this species, this peptidase is necessary for the correct biogenesis of the Type IV pili, and *vvpD* deletion in L1 strains caused defects in the pilus assembly and secretion of important degrading enzymes involved in cytotoxicity, adhesion, and virulence in mice. One of these enzymes is the hemolysin/cytolysin VvhA that is exported through a Type II secretion system pathway, which highlights the relation of the VvpD peptidase with this type of extracellular secretion (Paranjpye *et al.*, 1998).

In this study we analyzed the role of VvpD in biofilm formation and virulence for eels in the zoonotic clonal-complex. We found that the elimination of *vvpD* caused a dramatic reduction in biofilm formation, which could be related to a poor pilus biogenesis. We also observed that the mutant was deficient in exoenzymatic activity, growth in eel serum, and virulence for eels in both i.p. infection and immersion challenge. VvpD in *V. vulnificus* L1 is involved in the secretion of important virulence factors such as hemolysin VvhA and protease VvpE (Paranjpye *et al.*, 1998). Although no major role in human virulence has been yet attributed to either exoprotein (Jones and Oliver, 2009; Hor and Chen, 2013), both have been linked to eel pathogenicity, as mutants deficient in either gene were impaired in their virulence, especially by through water infection (Valiente, Lee, *et al.*, 2008). Thus, Valiente *et al.*, demonstrated that VvpE was involved in chemotaxis, eel colonization and virulence, and Cabanyero *et al.*, proved that VvhA is involved in growth in eel blood, as the VvhA mutants showed poor growth in fresh blood. In addition, our recent study that analyzed the essential genes needed for survival of *V. vulnificus* in human serum, linked the Type II secretion system to the capacity of growth in heat-inactivated sera and, therefore, to resistance to the nutritional restriction imposed by it (Carda-Diéguez *et al.*, 2018). All together, the impairment of our *vvpD* mutant in growth in eel serum and virulence for eels is clearly related to a deficiency in the Type II secretion system and in a reduction in secretion of VvhA and VvpE.

The Tight adherence pili or Tad pili, is a subfamily of the vastly diverse and multifunctional Type IV pili (Berry and Pelicic, 2015). These appendages set themselves aside from others by being remarkable small and having their own prepilin peptidase (FppA) that

process them into functional structures (Giltner *et al.*, 2012). Tad pili are not associated with cellular motility, but are inherently involved in pathogenic mechanisms such as colonization, biofilm formation and adhesion (Tomich *et al.*, 2007; Roux *et al.*, 2012; Duong-Nu *et al.*, 2019). A genomic study of several bacterial species revealed that, several Tad pili loci can be found within some bacterial genomes. In fact, *V. vulnificus* L1 strains possess up to three loci which are designated as *tad-1*, *tad-2* and *tad-3* (Rosenfeld *et al.*, 2004; Pu *et al.*, 2018). In *V. vulnificus* L1, evidence suggests the involvement of individual Tad pili in specific roles, such as production of biofilm, persistence in the environment and resistance to mechanical clearance (Alice *et al.*, 2008; T. C. Williams *et al.*, 2014; Pu and Rowe-Magnus, 2018; Pu *et al.*, 2018). Thus *tad-1* and *tad-2* loci are related to biofilm formation and *tad-3* to initial attachment and persistence in the environment. Finally, a recent study suggests that all three Tad pili need to be expressed in order to have an effect in virulence in mice (Duong-Nu *et al.*, 2019).

First we found that the *tad-1* locus was upregulated when the zoonotic strain was grown under iron-limited conditions (**Table 1**). This result was also found by Alice *et al.*, (2008) in L1 strains, and could be indicative of a role of the Tad-1 pilus in the life cycle of the bacterium. However, our results suggested that this *tad* locus had no role in virulence or in biofilm formation, as disruption of the *flp-1* gene did not affect biofilm levels or eel virulence (**Figure 12 and 13, Table 8**). This was also proved to be the case for the two other *flp* mutants, which showed no impairment in either virulence or biofilm production.

Subsequent tests addressed the effects of simultaneous disruptions of two or all three *tad* loci in biofilm production, serum resistance and virulence. The triple *flp* mutant showed significant differences when compared to the wild type (**Figure 13 and 14B, Table 8**), which support the previously stated results, that biofilm production is significantly affected only when all three *tad* loci are disrupted (Duong-Nu *et al.*, 2019). This suggests that anyone of the three genes can replace the one deleted in the processes of biofilm formation, colonization and eel virulence in the zoonotic clonal-complex. In addition, the deletion of the three *flp* genes sharply reduced the overall biomass of the mutant, suggesting that the impairment of all three Tad pili negatively impacts the bacteria causing a significant reduction in cellular growth. When compared to the  $\Delta mshA-1$  strain, the triple *flp* mutant showed a significantly less production of

biomass and biofilm, and a higher roughness coefficient, meaning that its biofilm structural integrity and composition were affected in a greater manner than in the MSHA pili mutant (**Figure 14**).

Interestingly, in our virulence assays, the triple *flp* mutant showed a significant reduction in virulence through the immersion challenge, but no difference was observed in the i.p injection assay. This contrasts directly with the results described by Duong-Nu *et al.*, (2019), where the triple *tad* loci deficient strain had a drastic reduction in lethality in mice, with a staggering 41-fold increase in the LD<sub>50</sub> of the mutant. Interestingly, the immersion challenge data from the  $\Delta flp$ -123 strain was similar to the water infection results of the MSHA pili mutant, as both mutants had a marked deficiency in water infection. This suggests that the reduction of lethality caused by the triple *flp* mutant, could be directly related to the attachment and colonization of the gills. As mentioned before, this should enable the pathogen to enter the host, (Marco-Noales Ester *et al.*, 2001), and initiate the course of the infection. Tad pili are widely known for their role in attachment and adhesion (Kachlany *et al.*, 2000; Tomich *et al.*, 2007), which supports the hypothesis that the role in virulence of the Tad pili is similar to that of the MSHA pili. Both mutants are deficient in attachment and adhesion to the principal point of entry to the host, which hinders the volume of bacterial cells promoting and kickstarting the infection. Thus the consequent impairment of the disease is not related to a reduction of cytotoxicity, but to a reduced number of infective cells. This is also supported by our i.p. infection results, where the virulence and lethality of both pili mutants was not affected (**Table 5 and 8**).

To prove if the triple *flp* mutant presented a defective adhesion to gills, and would further affect organ colonization in eels, as well as to compare its colonization capabilities to those of the MSHA pili mutant, we performed several co-colonization assays with the  $\Delta flp$ -1,  $\Delta flp$ -2,  $\Delta flp$ -3,  $\Delta flp$ -123 and R99 strains (**Figure 16**). In this tests, confirming our previous results, the triple mutant showed significant differences when colonizing the gills, however, unlike the MSHA mutant, the deficiency in colonization and consequent lower number of adhered bacterial cells was entirely localized in the gills. While the MSHA pili mutant was deficient in colonization of all organs, the Tad pili mutant strain showed no significant differences, when



compared to the wild type, in any of the organs in the remaining time points of the experiment (**Figure 16**). These results suggest that the MSHA pili exerts a greater effect during eel colonization than the *tad* loci, moreover, the bacterial counts in the blood of the triple mutant were similar to those of the wild type, even after 24 hours of infection. This contrasts with the results obtained by Duong-Nu *et al.*, (2019), where the triple *flp* mutant had a reduced viability in mice blood after intraperitoneal infection. In the same study, the authors suggested that the *tad* loci conferred protection to the bacteria against complement mediated bacteriolysis in human serum through the alternative pathway, stating that proteins in the complement were responsible for killing the *tad* loci mutant. Following the trend of previous results, the triple *flp* mutant was not affected by the bactericidal activities of eel serum, while the growth in human serum was halted, but cells remained alive (**Table 8**). The resistance of the Tad pili mutant to human and eel serum, suggests that the *tad* loci of the zoonotic clonal-complex do not play a role in the defense against serum bacteriolysis. Nonetheless the depletion of the complement in human serum would imply a greater survival and multiplication of bacterial cells, but the survival ratio of both the R99 and  $\Delta flp$ -123 were similar in unaltered human serum.

To further investigate the role of Tad pili against immune defense mechanisms, we decided to test if the Tad pili system conferred any kind of protection against phagocytosis. To this end we infected a human monocyte cell line with the triple mutant strain at a MOI of 10, while using the wild type and *E. coli* as phagocytosis controls (**Figure 15**). In the monocyte-absent media the strains grew uncontested, however, on the infection wells, the monocytes eliminated both R99 and  $\Delta flp$ -123 at the same constant rate, while *E. coli* was significantly more susceptible to phagocytosis after the first 2 hours. No significant differences were shown during the rest of the experiment in either of the *V. vulnificus* strains, this implies that the Tad pili does not confer any protection against phagocytosis, discarding another possible role of these pili in immune evasion. However, it is noteworthy to mention that, although belonging to the same species, the strains are bound to have several differences in their phenotype and genotype as observed amongst several other *Vibrio* species. Our strain belongs to the zoonotic clonal-complex of the *piscis* pathovar, which harbors the pVvbt2 plasmid, which enables it to

cause disease in fish, while the strain used by Duong-Nu and collaborators is a human clinical strain recovered from a vibriosis patient's blood.

Altogether, these polarizing results imply a marked divergence in the roles of Tad pili among different strains of *V. vulnificus*. Tad pili are ubiquitous complex machines found among various bacterial species, they are versatile filaments capable of perform a wide array of functions such as adhesion to many substrates, retract to enable motility and introduce exogenous DNA into the cell for nutrition or diversification of the genetic material (Wall and Kaiser, 1999; Berry and Pelicic, 2015). Thus, is possible to speculate that even the same pili systems can have different functions among different species, and even different strains. The heterogenicity between strains could lead to a diversification of bacterial mechanisms that help the bacteria adapt to their niche environments and, a prime example of this, could be the very versatile and complex Type IV pili nanomachines.

Flagella are remarkable structures that endow high speed motility and the ability to swim in liquid environments to many bacterial species, this allows them to respond and move to diverse stimuli in the environment (Aizawa, 2014). Normally the flagella are located outside the cell, protruding from the cell envelope and producing a structure that spans the entirety of this cellular structure. The flagellar apparatus shares a high homology to the virulence secretion systems of pathogenic species like Salmonella or Yersinia, which has been designated as the Type III secretion system (Lee, 1997; Macnab, 1999). The role of the flagellum in virulence of enteropathogenic bacteria was overlooked in the past, but flagella is actively involved in adherence, invasion and induction of the inflammatory response (Girón *et al.*, 2002; Aizawa, 2014). Moreover, through chemotaxis and motility, the pathogen is capable to reach its host, and consequentially invade and colonize the internal organs (Josenhans and Suerbaum, 2002).

In this study we analyzed the role of the flagellum in biofilm formation and virulence in the zoonotic clonal complex by obtaining an immobile mutant and analyzing its phenotype with respect to that of the wild-type strain. First, we demonstrated that several genes related to flagellum biogenesis and motility were overexpressed under iron-excess conditions, precisely as contrary to the ones promoting Type IV pili production (Pajuelo *et al.*, 2016). This result

suggests that, in the zoonotic clonal-complex, iron-restriction would promote biofilm formation, while iron-excess promotes motility and detachment from the biofilm ecosystem. Second, we found that the flagellum was essential for virulence through water, but not by injection. This result is similar to that obtained with different *mshA* and *flp* mutants. However, the differences in biofilm formation were not comparable to those of the pili mutants. So we concluded that the differences in virulence should be related to motility. In fact, flagellar-mediated motility is intimately connected to chemotaxis. In a previous work it has been described that *V. vulnificus* is chemoattracted towards all types of eel mucus, being the mucus from the gills the most chemoattractant for the bacteria, while the intestinal mucus the least (Valiente, Jiménez, *et al.*, 2008). In *V. cholerae* the flagellar machinery enable the cell to sense the mucin barrier of the intestine's epithelium, and proceeds to regulate diverse factors that aid in the colonization process, such as the MSHA pili. Later, the bacteria has to traverse the glycocalyx barrier of the mice intestine, where the it losses its flagella (Liu *et al.*, 2008). A similar process could be performed by *V. vulnificus* when colonizing the gills, where the pathogen arrives attracted by the mucus present in the organ.

While performing phenotypical tests, a remarkable trait was observed in the flagellar mutant. Even though the hook deficient strain showed no difference in biofilm, it had a significant increase in the total bacterial population growth, when compared to the wild type, after 24 hours of incubation (**Figure 19-21**). The difference in bacterial population was significantly higher than the wild type strain in both biofilm and normal media growth conditions. Moreover, when comparing the  $\Delta mshA-1$  to the  $\Delta flgE/\Delta mshA-1$  strain, the double mutant retained a significantly higher population growth than the MSHA pili mutant (**Figure 22 and 23**). This shows that, independently of biofilm production, aflagellated strains keep on producing a higher final population density and growth. In several  $\gamma$ -proteobacteria, loss of flagella during starvation is a common occurrence, although the molecular mechanisms involved are still unidentified, they may be part of a new signaling pathway (Zhu and Gao, 2020). Several species of bacteria eject the flagella when they sense a depletion of glucose in their environment, moreover the presence of flagella varies considerably across different growth phases (Ferreira *et al.*, 2019; Zhuang *et al.*, 2019). This suggests that, due to the great

energy expenditure that comes with the synthesis, maintenance and usage of the flagellar system, the bacteria chooses to lose the flagella in order to reroute all energy into survival of starvation. (Terashima *et al.*, 2008; Khan *et al.*, 2020). The increment in cell population observed in our flagellar mutant might be directly involved with a lower energy expenditure caused by the untethering of the flagella, which allows a spike in population growth by a more efficient use of the nutrients present in the media.

In summary, this thesis brings to light several novel roles of two important Type IV pili systems, and the flagellum, in the zoonotic clonal-complex of *V. vulnificus*. In addition, we have standardized a mutation protocol that allowed us to effectively and swiftly produce simple and compound mutants in a strain representative of this clonal-complex known for its reluctance for genetic manipulation. Through this, we had identified two extra copies of the *mshA* major pilin subunit gene located in the genome of *V. vulnificus* and demonstrated that they are not involved in the correct function of the MSHA pilus. At the same time, we proved for the first time the involvement of these pili in the virulence of *V. vulnificus* for eels, where these pili are responsible for initial attachment, adhesion and colonization of internal organs during the first hours of infection. Finally, we proved the need of three functional Tad pili systems for the initial attachment and virulence in eels, as well as their relative involvement in biofilm. However our results suggest that in the zoonotic clonal-complex the *tad* pili loci play no further role in virulence or resistance against the immune system. This contrasts with previous results stating that a synergistic activity of the three *tad* loci allowed the bacteria to “escape” the bactericidal effects of the complement. These interesting differences proven by our results, highlight a marked distinction between important functions of these two pili systems belonging to the same bacterial species. A statement should be made, pertinent to the results described in this work, to take caution when comparing the functions of important cellular mechanisms such as Type IV pili, which are involved in diverse virulence determinants. No generalizations among genes and protein roles should be taken as definite, given the fact that, as we prove in this work, same appendages and bacterial mechanisms showed significant differences in function between species of the same genus, and even between strains.

## 2.- Conclusions

After analyzing and discussing the results of this work, we have reached the following main conclusions:

- I. **We have developed a specific mutation protocol for the zoonotic clonal-complex of *V. vulnificus*.** The new protocol takes advantage of the natural transformation mechanism of the species by introducing a plasmid that encodes the main transformation activator, Tfox, under controlled transcription.
- II. ***V. vulnificus* produces three different types of MSHA protein, being the one coded by *mshA-2* exclusive to this species.** In addition, this gene is a highly conserved orphan gene that is mainly present in lineage 2 strains, and therefore in the zoonotic clonal-complex.
- III. **Of the three different *mshA* genes in the zoonotic clonal-complex, only *mshA-1* is involved in virulence for eels.** This gene belongs to the *mshA* locus and seems to have a common evolutionary origin with the *mshA-1* genes of *V. cholerae* and *V. parahaemolyticus*.
- IV. **The *mshA-1* gene is involved in the early stages of colonization of the eel by the zoonotic clonal-complex:** deletion of the gene causes the production of an uneven biofilm with a reduced biomass, resulting in fewer bacteria adhering to the gills and, consequently, in a reduction in the bacterial load that invades the bloodstream and reaches the internal organs.
- V. **The zoonotic clonal complex also produces three Tad pili, as the rest of the species, all being involved in biofilm formation, early eel colonization and virulence.** Unlike the MSHA pili, these pili are able to functionally complement each other, so only the triple mutant is deficient in biofilm formation, colonization and virulence.
- VI. **The prepilin peptidase of the zoonotic clonal-complex is involved** in the secretion of exoenzymes into the extracellular milieu, and, consequently, **in virulence and in resistance to the nutritional constraint in eel serum.**
- VII. **The flagellum is also a virulence gene in the zoonotic clonal-complex of *V. vulnificus*.** This appendage is necessary to cause death by septicemia as immotile mutants are deficient in biofilm formation, attachment to gills and subsequent colonization and invasion.
- VIII. Finally, we conclude that the process by which **the zoonotic clonal-complex of *V. vulnificus* causes illness and death in eels is a multifactorial process in which formation**

**of a compact biofilm during the first stages of the infection is highly relevant**, a process in which at least two types of pili and the flagellum are involved.

- IX. We demonstrated that these **two Type IV pili systems are influenced by iron concentrations**, thus acting as important regulation factor that can influence their roles in environmental and host survival.

### 3.- References

1. Aagesen, A.M. and Häse, C.C. (2012) Sequence analyses of Type IV Pili from *Vibrio cholerae*, *Vibrio parahaemolyticus*, and *Vibrio vulnificus*. *Microb Ecol* **64**: 509–524.
2. Aizawa, S.I. (2014) *Flagella*, Elsevier Ltd.
3. Alice, A.F., Naka, H., and Crosa, J.H. (2008) Global gene expression as a function of the iron status of the bacterial cell: Influence of differentially expressed genes in the virulence of the human pathogen *Vibrio vulnificus*. *Infect Immun* **76**: 4019–4037.
4. Amaro, C. and Biosca, E.G. (1996) *Vibrio vulnificus* biotype 2, pathogenic for eels, is also an opportunistic pathogen for humans. *Appl Environ Microbiol* **62**: 1454–1457.
5. Amaro, C., Biosca, E.G., Fouz, B., Alcaide, E., and Esteve, C. (1995) Evidence that water transmits *Vibrio vulnificus* biotype 2 infections to eels. *Appl Environ Microbiol* **61**: 1133–1137.
6. Amaro, C., Sanjuán, E., Fouz, B., Pajuelo, D., Lee, C.-T., Hor, L.-I., and Barrera, R. (2015) The Fish pathogen *Vibrio vulnificus* biotype 2: Epidemiology, phylogeny, and virulence factors involved in warm-water vibriosis. *Microbiol Spectr* **3**:
7. Baba, T., Ara, T., Hasegawa, M., Takai, Y., Okumura, Y., Baba, M., et al. (2006) Construction of *Escherichia coli* K-12 in-frame, single-gene knockout mutants: The Keio collection. *Mol Syst Biol* **2**:
8. Baker-Austin, C., Trinanes, J., Gonzalez-Escalona, N., and Martinez-Urtaza, J. (2017) Non-cholera *Vibrios*: The microbial barometer of climate change. *Trends Microbiol* **25**: 76–84.
9. Barocchi, Michèle A. and Telford, John L. (2014) Bacterial pili: structure, synthesis and role in disease, *Advances I.* (eds) Wallingford: CABI.
10. Berry, J.L. and Pelicic, V. (2015) Exceptionally widespread nanomachines composed of type IV pilins: The prokaryotic Swiss Army knives. *FEMS Microbiol Rev* **39**: 134–154.
11. Bisharat, N., Agmon, V., Finkelstein, R., Raz, R., Ben-Dror, G., Lerner, L., et al. (1999) Clinical, epidemiological, and microbiological features of *Vibrio vulnificus* biogroup 3 causing outbreaks of wound infection and bacteraemia in Israel. *Lancet* **354**: 1421–1424.
12. Bisharat, N., Bronstein, M., Korner, M., Schnitzer, T., and Koton, Y. (2013) Transcriptome profiling analysis of *Vibrio vulnificus* during human infection. *Microbiol (United Kingdom)* **159**: 1878–1887.
13. Carda-Diéguez, M., Silva-Hernández, F.X., Hubbard, T.P., Chao, M.C., Waldor, M.K., and Amaro, C. (2018) Comprehensive identification of *Vibrio vulnificus* genes required for growth in human serum. *Virulence* **9**: 981–993.
14. Chiavelli, D.A., Marsh, J.W., and Taylor, R.K. (2001) The Mannose-Sensitive Hemagglutinin of *Vibrio cholerae* promotes adherence to zooplankton. *Appl Environ*

*Microbiol* **67**: 3220–3225.

15. Chodur, D.M., Coulter, P., Isaacs, J., Pu, M., Fernandez, N., Waters, C.M., and Rowe-Magnus, D.A. (2018) Environmental calcium initiates a feed-forward signaling circuit that regulates biofilm formation and rugosity in *Vibrio vulnificus*. *Am Soc Microbiol* **9**: 1–14.
16. Duong-Nu, T.-M., Jeong, K., Hong, S.H., Puth, S., Kim, S.Y., Tan, W., et al. (2019) A stealth adhesion factor contributes to *Vibrio vulnificus* pathogenicity: Flp pili play roles in host invasion, survival in the blood stream and resistance to complement activation. *PLOS Pathog* **15**: 1–29.
17. Ferreira, J.L., Gao, F.Z., Rossmann, F.M., Nans, A., Brenzinger, S., Hosseini, R., et al. (2019)  $\gamma$ -proteobacteria eject their polar flagella under nutrient depletion, retaining flagellar motor relic structures. *Plos Biol* **17**: 1–25.
18. Fouz, B. and Amaro, C. (2003) Isolation of a new serovar of *Vibrio vulnificus* pathogenic for eels cultured in freshwater farms. *Aquaculture* **217**: 677–682.
19. Fullner, K.J. and Mekalanos, J.J. (1999) Genetic characterization of a new type IV-A pilus gene cluster found in both classical and El Tor biotypes of *Vibrio cholerae*. *Infect Immun* **67**: 1393–1404.
20. Giltner, C.L., Nguyen, Y., and Burrows, L.L. (2012) Type iv pilin proteins: versatile molecular modules. *Microbiol Mol Biol Rev* **76**: 740–772.
21. Girón, J.A., Torres, A.G., Freer, E., Kaper, J.B., Rica, C., and Epec, H. (2002) The flagella of enteropathogenic *Escherichia coli* mediate adherence to epithelial cells. *Mol Microbiol* **44**: 361–379.
22. Gulig, P.A., Tucker, M.S., Thiaville, P.C., Joseph, J.L., and Brown, R.N. (2009) USER friendly cloning coupled with chitin-based natural transformation enables rapid mutagenesis of *Vibrio vulnificus*. *Appl Environ Microbiol* **75**: 4936–4949.
23. Hernández-Cabanyero, C. and Amaro, C. (2020) Phylogeny and life cycle of the zoonotic pathogen *Vibrio vulnificus*. *Environ Microbiol*.
24. Hernández-Cabanyero, C., Lee, C. Te, Tolosa-Enguis, V., Sanjuán, E., Pajuelo, D., Reyes-López, F., et al. (2019) Adaptation to host in *Vibrio vulnificus*, a zoonotic pathogen that causes septicemia in fish and humans. *Environ Microbiol* **21**: 3118–3139.
25. Hor, L.I. and Chen, C.L. (2013) Cytotoxins of *Vibrio vulnificus*: Functions and roles in pathogenesis. *Biomed* **3**: 19–26.
26. Horseman, M.A. and Surani, S. (2011) A comprehensive review of *Vibrio vulnificus*: An important cause of severe sepsis and skin and soft-tissue infection. *Int J Infect Dis* **15**: e157–e166.
27. Hsiao, A., Liu, Z., Joelsson, A., and Zhu, J. (2006) *Vibrio cholerae* virulence regulator-coordinated evasion of host immunity. *PNAS* **103**: 14542–14547.



28. Jayakumar, J.M., Shapiro, O.H., and Almagro-Moreno, S. (2020) Improved Method for Transformation of *Vibrio vulnificus* by Electroporation. *Curr Protoc Microbiol* **58**: e106.
29. Jones, C.J., Utada, A., Davis, K.R., Thongsomboon, W., Zamorano Sanchez, D., Banakar, V., et al. (2015) C-di-GMP Regulates motile to sessile transition by modulating MshA pili biogenesis and near-surface motility behavior in *Vibrio cholerae*. *PLoS Pathog* **11**: 1–27.
30. Jones, M.K. and Oliver, J.D. (2009) *Vibrio vulnificus*: Disease and pathogenesis. *Infect Immun* **77**: 1723–1733.
31. Jonson, G., Holmgren, J., and Svennerholm, A.M. (1991) Identification of a mannose-binding pilus on *Vibrio cholerae* El Tor. *Microb Pathog* **11**: 433–441.
32. Josenhans, C. and Suerbaum, S. (2002) The role of motility as a virulence factor in bacteria. *Int J Med Microbiol* **291**: 605–614.
33. Kachlany, S.C., Planet, P.J., Bhattacharjee, M.K., Kollia, E., DeSalle, R., Fine, D.H., and Figurski, D.H. (2000) Nonspecific adherence by *Actinobacillus actinomycetemcomitans* requires genes widespread in Bacteria and Archaea. *J Bacteriol* **182**: 6169–6176.
34. Khan, F., Tabassum, N., Anand, R., and Kim, Y.M. (2020) Motility of *Vibrio* spp.: regulation and controlling strategies. *Appl Microbiol Biotechnol* **104**: 8187–8208.
35. Lee, C.A. (1997) Type III secretion systems: Machines to deliver bacterial proteins into eukaryotic cells? *Trends Microbiol* **5**: 148–156.
36. Liu, Z., Miyashiro, T., Tsou, A., Hsiao, A., Goulian, M., and Zhu, J. (2008) Mucosal penetration primes *Vibrio cholerae* for host colonization by repressing quorum sensing. *PNAS* **105**: 9769–9774.
37. Lory, S. and Strom, M.S. (1997) Structure-function relationship of type-IV prepilin peptidase of *Pseudomonas aeruginosa* - A review. *Gene* **192**: 117–121.
38. Macnab, R.M. (1999) The bacterial flagellum: Reversible rotary propellor and type III export apparatus. *J Bacteriol* **181**: 7149–7153.
39. Marco-Noales Ester, Milan, M., Fouz, B., Sanjuan, E., and Amaro, C. (2001) Transmission to Eels, Portals of Entry, and Putative Reservoirs of *Vibrio vulnificus* Serovar E ( Biotype 2 ). *Appl Environ Microbiol* **67**: 4717–4725.
40. Marsh, J.W., Sun, D., and Taylor, R.K. (1996) Physical linkage of the *Vibrio cholerae* mannose-sensitive hemagglutinin secretory and structural subunit gene loci: Identification of the mshG coding sequence. *Infect Immun* **64**: 460–465.
41. Marsh, J.W. and Taylor, R.K. (1998a) Genetic and transcriptional analyses of the *Vibrio cholerae* mannose-sensitive hemagglutinin type 4 pilus gene locus. *J Bacteriol* **181**: 1110–1117.
42. Marsh, J.W. and Taylor, R.K. (1998b) Identification of the *Vibrio cholerae* type 4 prepilin peptidase required for cholera toxin secretion and pilus formation. *Mol Microbiol* **29**:

1481–1492.

43. Mattick, J.S. (2002) Type IV Pili and Twitching Motility. *Annu Rev Microbiol* **56**: 289–314.
44. Meibom, K.L., Blokesch, M., Dolganov, N.A., Wu, C.Y., and Schoolnik, G.K. (2005) Chitin induces natural competence in *Vibrio cholerae*. *Science* (80- ) **310**: 1824–1827.
45. Merz, A.J. and So, M. (2000) Interactions of pathogenic *Neisseriae* with epithelial cell membranes. *Annu Rev Cell Dev Biol* **16**: 423–457.
46. Neiman, J., Guo, Y., and Rowe-Magnus, D.A. (2011) Chitin-Induced carbotype conversion in *Vibrio vulnificus*. *Infect Immun* **79**: 3195–3203.
47. Nunn, D., Bergman, S., and Lory, S. (1990) Products of three accessory genes, pilB, pilC, and pilD, are required for biogenesis of *Pseudomonas aeruginosa* pili. *J Bacteriol* **172**: 2911–2919.
48. Nunn, D.N. and Lory, S. (1991) Product of the *Pseudomonas aeruginosa* gene *pilD* is a prepilin leader peptidase. *Proc Natl Acad Sci U S A* **88**: 3281–3285.
49. Oliver, J.D. (2015) The Biology of *Vibrio vulnificus*. *Microbiol Spectr* **3**: 1–10.
50. Oliver, J.D. (2013) *Vibrio vulnificus*: Death on the half shell. A Personal journey with the pathogen and its ecology. *Microb Ecol* **65**: 793–799.
51. Pajuelo, D., Hernández-Cabanyero, C., Sanjuan, E., Lee, C.-T., Silva-Hernández, F.X., Hor, L.-I., et al. (2016) Iron and fur in the life cycle of the zoonotic pathogen *Vibrio vulnificus*. *Environ Microbiol* **18**: 4005–4022.
52. Paranjpye, R.N., Lara, J.C., Pepe, J.C., Pepe, C.M., and Strom, M.S. (1998) The type IV leader peptidase/N-methyltransferase of *Vibrio vulnificus* controls factors required for adherence to HEp-2 cells and virulence in iron-overloaded mice. *Infect Immun* **66**: 5659–5668.
53. Pu, M., Duriez, P., Arazi, M., and Rowe-Magnus, D.A. (2018) A conserved *tad* pilus promotes *Vibrio vulnificus* oyster colonization. *Environ Microbiol* **20**: 828–841.
54. Pu, M. and Rowe-Magnus, D.A. (2018) A Tad pilus promotes the establishment and resistance of *Vibrio vulnificus* biofilms to mechanical clearance. *npj Biofilms Microbiomes* **4**.
55. Roig, F.J., González-Candelas, F., Sanjuán, E., Fouz, B., Feil, E.J., Llorens, C., et al. (2018) Phylogeny of *Vibrio vulnificus* from the analysis of the core-genome: Implications for intra-species taxonomy. *Front Microbiol* **8**: 1–13.
56. Rosenfeld, J.A., Sarkar, I.N., Planet, P.J., Figurski, D.H., and DeSalle, R. (2004) ORFcurator: Molecular curation of genes and gene clusters in prokaryotic organisms. *Bioinformatics* **20**: 3462–3465.
57. Roux, N., Spagnolo, J., and De Bentzmann, S. (2012) Neglected but amazingly diverse type IVb pili. *Res Microbiol* **163**: 659–673.

58. Sanjuán, E., González-Candelas, F., and Amaro, C. (2011) Polyphyletic origin of *Vibrio vulnificus* biotype 2 as revealed by sequence-based analysis. *Appl Environ Microbiol* **77**: 688–695.
59. Lo Scrudato, M. and Blokesch, M. (2012) The regulatory network of natural competence and transformation of *Vibrio cholerae*. *PLoS Genet* **8**:
60. Shao, C.P. and Hor, L.I. (2000) Metalloprotease is not essential for *Vibrio vulnificus* virulence in mice. *Infect Immun* **68**: 3569–3573.
61. Shi, W. and Sun, H. (2002) Type IV pilus-dependent motility and its possible role in bacterial pathogenesis. *Infect Immun* **70**: 1–4.
62. Sinha-Ray, S. and Ali, A. (2017) Mutation in *flrA* and *mshA* genes of *Vibrio cholerae* inversely involved in vps-independent biofilm driving bacterium toward nutrients in lake water. *Front Microbiol* **8**: 1–13.
63. Sun, Y., Bernardy, E.E., Hammer, B.K., and Miyashiro, T. (2013) Competence and natural transformation in vibrios. *Mol Microbiol* **89**: 583–595.
64. Terashima, H., Kojima, S., and Homma, M. (2008) Flagellar motility in bacteria: structure and function of flagellar motor. In, Terashima, H., Kojima, S., and Homma, M. (eds), *International Review of Cell and Molecular Biology*. Elsevier Inc., pp. 39–85.
65. Thelin, K.H. and Taylor, R.K. (1996) Toxin-coregulated pilus, but not mannose-sensitive hemagglutinin, is required for colonization by *Vibrio cholerae* O1 El Tor biotype and O139 strains. *Infect Immun* **64**: 2853–2856.
66. Tison, D.L., Nishibuchi, M., Greenwood, J.D., and Seidler, R.J. (1982) *Vibrio vulnificus* biogroup 2: new biogroup pathogenic for eels. *Appl Environ Microbiol* **44**: 640–6.
67. Tomich, M., Planet, P.J., and Figurski, D.H. (2007) The *tad* locus: Postcards from the widespread colonization island. *Nat Rev Microbiol* **5**: 363–375.
68. Utada, A.S., Bennett, R.R., Fong, J.C.N., Gibiansky, M.L., Yildiz, F.H., Golestanian, R., and Wong, G.C.L. (2014) *Vibrio cholerae* use pili and flagella synergistically to effect motility switching and conditional surface attachment. *Nat Commun* **5**: 4913.
69. Valiente, E. and Amaro, C. (2006) A method to diagnose the carrier state of *Vibrio vulnificus* serovar E in eels: Development and field studies. *Aquaculture* **258**: 173–179.
70. Valiente, Esmeralda, Jiménez, N., Merino, S., Tomas, J.M., and Amaro, C. (2008) *Vibrio vulnificus* biotype 2 serovar E *gne* but not *galE* is essential for lipopolysaccharide biosynthesis and virulence. *Infect Immun* **76**: 1628–1638.
71. Valiente, Esmeralda, Lee, C.-T., Lamas, J., Hor, L.-I., and Amaro, C. (2008) Role of the virulence plasmid pR99 and the metalloprotease VvpE in resistance of *Vibrio vulnificus* serovar E to eel innate immunity. *Fish Shellfish Immunol* **24**: 134–141.
72. Wall, D. and Kaiser, D. (1999) Type IV pili and cell motility. *Mol Microbiol* **32**: 01–10.

73. Watnick, P.I., Fullner, K.J., and Kolter, R. (1999) A role for the mannose-sensitive hemagglutinin in biofilm formation by *Vibrio cholerae* El Tor. *J Bacteriol* **181**: 3606–3609.
74. Williams, T., Ayrapetyan, M., Ryan, H., and Oliver, J. (2014) Serum survival of *Vibrio vulnificus*: Role of genotype, capsule, complement, clinical origin, and *in situ* Incubation. *Pathogens* **3**: 822–832.
75. Williams, T.C., Blackman, E.R., Morrison, S.S., Gibas, C.J., and Oliver, J.D. (2014) Transcriptome sequencing reveals the virulence and environmental genetic programs of *Vibrio vulnificus* exposed to host and estuarine conditions. *PLoS One* **9**: e114376.
76. Wu, S.I., Lo, S.K., Shao, C.P., Tsai, H.W., and Hor, L.I. (2001) Cloning and characterization of a periplasmic nuclease of *Vibrio vulnificus* and its role in preventing uptake of foreign DNA. *Appl Environ Microbiol* **67**: 82–88.
77. Zampini, M., Canesi, L., Betti, M., Ciacci, C., Tarsi, R., Gallo, G., and Pruzzo, C. (2003) Role for mannose-sensitive hemagglutinin in promoting interactions between *Vibrio cholerae* El Tor and mussel hemolymph. *Appl Environ Microbiol* **69**: 5711–5715.
78. Zhu, S. and Gao, B. (2020) Bacterial Flagella Loss under Starvation, Elsevier Ltd.
79. Zhuang, X., Guo, S., Li, Z., Zhao, Z., and Kojima, S. (2019) Dynamic production and loss of flagellar filaments during the bacterial life cycle.



# APPENDIX

---

# Role of the MSHA pilus in host invasion and colonization in the zoonotic pathogen *Vibrio vulnificus*

Silva-Hernández FX<sup>1</sup>, Hernández-Cabanyero C<sup>1</sup>, Dean-Rowe M<sup>2</sup>, Sanjuan E<sup>1</sup>, Amaro C<sup>1\*</sup>

<sup>1</sup>ERI-Biotecmed, University of Valencia, Valencia, Spain, <sup>2</sup>Department of Biology, Indiana University Bloomington, Bloomington, Indiana, USA

## Summary

*V. vulnificus* is a highly heterogeneous species that includes a zoonotic clonal-complex distributed worldwide that can cause vibriosis in humans and fish. In our previous transcriptomic study we found that several genes related to virulence and survival were differentially expressed under iron deficient conditions in the zoonotic clonal-complex. Among them, there were several genes belonging to the MSHA pili. In this work we analyzed the three distinct major pilin subunit genes of MSHA pili harbored in its genome, and found out that only the *mshA-1* gene is necessary for biofilm formation, adhesion to biotic and abiotic surfaces, and virulence for eels. This gene plays a critical role in the initial steps of gills colonization, while on the other hand, *mshA-2* and *mshA-3* do not have any apparent role in these functions or virulence. This work gives the first description of the two extra *mshA* genes harbored in the genome of *V. vulnificus*, and the first documented role of the MSHA pili in virulence for eels, which is essential for forming biofilms in the gills and initial colonization that leads to a successful infection of the host.

## Introduction

*Vibrio vulnificus* is a halophilic gram negative bacteria that inhabits tropical and subtropical waters around the globe, and can be found either as free-living planktonic bacteria or sessile cells forming biofilm in biotic or abiotic surfaces (Horseman and Surani, 2011; III *et al.*, 2015; Oliver, 2015). This species is more prevalent in the water column during warmer months, this leads to a spike in human infections by the consumption of contaminated seafood (Oliver, 2013). Every year, due to climate change, the distribution of this zoonotic pathogen expands into colder environments, leading to a higher risk of vibrio infections for humans and fish (Oliver, 2013, 2015; Baker-Austin *et al.*, 2017). *V. vulnificus* is capable of causing disease in humans and fish, commonly denominated as vibriosis, in humans, vibriosis can either cause gastroenteritis and primary septicemia, or wound infections that can evolve into secondary septicemia (Jones and Oliver, 2009; Amaro *et al.*, 2015). Although cases of vibriosis in humans are rare, population at risk may contract the disease by contact with diseased fish or contaminated water, resulting in hospitalizations with high mortality rates and a higher risk of death by fulminant septicemia (Bisharat *et al.*, 2013; Williams *et al.*, 2014; Oliver, 2015). Fish vibriosis commonly occurs in waters over 25°C and presents similar clinical signs as humans, as it can also result in septicemia with a high probability of death by sepsis (Amaro *et al.*, 1995, 2015).

*V. vulnificus* was formerly classified in different biotypes (Tison *et al.*, 1982; Bisharat *et al.*, 1999), however, a recent phylogenomic study involving the analysis of 80 genomes, grouped the species in five supported lineages (L1-5) (Roig *et al.*, 2018). The study showed that 75% of the genes involved in virulence for humans were readily present in the core genome of the species, suggesting that all strains are possibly

pathogenic for humans. In addition, the authors proposed that a specific group of strains known previously as biotype 2 (Tison *et al.*, 1982; Lee *et al.*, 2008), which contain a plasmid (pVvBT2) that confers virulence to fish, to be denominated as a pathovar (*pv. piscis*), and be further divided into different serovars. One of them, serovar E (Ser E), is a zoonotic clonal-complex with a worldwide distribution and is known to cause severe wound infections and septicemia, via contact and handling of diseased eels (Amaro and Biosca, 1996; Sanjuán *et al.*, 2011; Roig *et al.*, 2018). The representative strain of this group is the CECT 4999 strain, which was first isolated in 1999 from European eels (Roig *et al.*, 2018).

Our previous transcriptomic study analyzed the general response of the zoonotic clonal-complex to iron stimulation, and the results showed that approximately 250 putative genes were differentially regulated. Several of these genes were related to virulence and survival systems, such as immune evasion, colonization, biofilm formation and motility (Pajuelo *et al.*, 2016). Among these, components of the mannose-sensitive hemagglutinin (MSHA) locus were present. This Type IV pili was first classified in *V. cholerae* (Jonson *et al.*, 1991) and is present in all El tor biotype strains, this pilus is essential for biofilm formation in biotic and abiotic surfaces, as well as motility and environmental persistence (Marsh and Taylor, 1998a; Watnick *et al.*, 1999; Chiavelli *et al.*, 2001). Knockout mutants of the MSHA pilus exhibit impaired biofilm production and deficient initial attachment, furthermore, impairment of these pili increases roaming movement due to unrepressed flagellar activity, which prevents pili interactions with potential surfaces for irreversible adhesion (Utada *et al.*, 2014; Jones *et al.*, 2015; Sinha-Ray and Ali, 2017; Pu *et al.*, 2018). Although the MSHA pilus plays an instrumental role for the bacteria in environmental niches, no involvement in organ colonization,

or any other type of virulence was attributed to it (Thelin and Taylor, 1996; Watnick *et al.*, 1999; Zampini *et al.*, 2003; Pruzzo *et al.*, 2008). However, recent studies in *V. cholerae* showed that the MSHA pilus expression must be repressed by ToxT, a transcriptional regulator, in order to avoid recognition by immunoglobins and successfully colonize mice intestines (Hsiao *et al.*, 2006). Moreover, the MSHA pilus is lysed by a dedicated peptidase which is also regulated by ToxT, further masking the bacteria's presence and recognition by the immune system (Liu *et al.*, 2008).

We suspect an involvement of the MSHA pilus in virulence given the differential expression of some of its locus components by the iron stimulation, so we assessed the involvement of this pilus in biofilm production, virulence and colonization in the eel model (*Anguilla anguilla*). Interestingly, *V. vulnificus* possesses three distinct MSHA genes, *mshA-1*, *mshA-2* and *mshA-3* as we have denominated them, but only *mshA-1* is encoded within a locus. The two extra genes have no physiological roles yet attributed to them, thus we sought to find the function, if any, of the two extra genes. To this end, we obtained simple and compound mutants in the three *mshA* genes which code for a major pilin subunit of the MSHA pilus, and tested their role in virulence and colonization via a series of *in vitro*, *ex vivo* and *in vivo* experiments. Our main objective was to determine the involvement of each individual gene in adhesion and biofilm formation, and if this pilus was involved in pathogenesis in the zoonotic clonal-complex of *V. vulnificus*.

## Results

### The zoonotic clonal-complex of *V. vulnificus* harbors three distinct copies of the MSHA major pilin subunit gene

Our transcriptomic analysis revealed that several genes of the representative strain of the zoonotic clonal-complex were differentially expressed under iron-excess and iron-poor conditions (Pajueto *et al.*, 2016). Among these, there were multiple genes belonging to the MSHA locus, and 2 “orphan” *mshA* genes (**Table 1**). Interestingly, most of the genes of the MSHA locus were upregulated in iron restrictive conditions, except for the major pilin subunit *mshA* gene, which is the core structural protein of the pilus. The genome of the representative strain of the zoonotic clonal-complex contains three distinct *mshA* genes, all of which encode proteins with the characteristic conserved N-terminal region of the MSHA major pilin subunit. We have designated these proteins as *mshA-1* (vvect4999\_RS02145), *mshA-2* (vvect4999\_RS12730) and *mshA-3* (vvect4999\_RS20940). The *mshA-1* gene is the only one that belongs to a MSHA locus, which is located in the chromosome I, while *mshA-2* and *mshA-3* are “orphan” genes located in the chromosome I and II respectively (**Figure 1**).

The microarray analysis of the three genes was validated by quantifying the transcription level of the three genes by RT-qPCR (**Table 2**). In general, the results obtained with both techniques were consistent, but we observed some differences among the expressions of the three *mshA* pilins. The most remarkable result was the downregulation of the *mshA-3* expression in the microarray, whereas it seemed to be slightly

upregulated when quantitative PCR was used. From the three, *mshA-1* and *mshA-2* were not iron-responsive, while *mshA-3* was downregulated under iron starvation, in addition a second *mshQ* (involved in the biogenesis of the pilus) was also upregulated in iron restriction conditions (**Table 1**). Thus, given the presence of multiple *mshA* genes which are differentially regulated, we decided to generate mutants in these genes, and study their role in virulence and biofilm formation. To this end, we produced simple, double and triple in-frame deletion mutants, and tested them through several *in vivo*, *ex vivo* and *in vitro* assays. Finally, we decided to include in the study a *vvpD* deficient mutant, this gene codes for a prepilin peptidase in charge of processing Type IVa pilin precursors which are pilin-like Type II secretion system proteins, such as MSHA pilin proteins. In addition, this enzyme is necessary for the important virulence factors like the expression of surface pili, secretion of cytolysin, metalloprotease and chitinase, and in *V. cholerae*, for the correct assembly of the MSHA pilus (Lory and Strom, 1997; Paranjpye and Strom, 2005; De Bentzmann *et al.*, 2006). We also analyzed the presence and homology of *mshA* genes in a selection of genomes of other pathogenic *Vibrio* species, as well as genomes belonging to representative strains of the main *V. vulnificus* lineages (**Table 3**). All *V. vulnificus* strains of L2 contained all three *mshA* genes (*mshA<sub>Vv</sub>* in this analysis), while most L1 strains (60%) showed only *mshA<sub>Vv</sub>-1* and *mshA<sub>Vv</sub>-3*, and all L3 strains lacked all *mshA* genes or homologues of these. All *V. cholerae* strains presented only the *mshA-1* gene, while all *V. parahaemolyticus* showed *mshA-1* and *mshA-3* genes (**Table 3**). Therefore, *mshA<sub>Vv</sub>-2* appears to be exclusive to *V. vulnificus* and is mostly present in L2 strains. Finally, *mshA<sub>Vv</sub>-1* showed the highest genetic variability, while *mshA<sub>Vv</sub>-2* and *mshA<sub>Vv</sub>-3* were more conserved.

To further compare the sequence similarities of the three *mshA* genes, we constructed a phylogenetic tree from all the analyzed sequences (**Figure 2**). The three genes clustered in three different groups within *V. vulnificus*, and did not correspond with the aggrupation suggested by the lineage classification. Furthermore, *mshA-2* and *mshA-3* of *V. vulnificus* were closer to the *mshA-3* of *V. parahaemolyticus*, this probably due to an event of horizontal gene transfer and subsequent divergence. The analysis also confirmed the high homology of the *mshA-2* and *mshA-3* genes of all the species, except for the *mshA-2* of the *V. vulnificus* FORC 017 strain. Interestingly, all the *mshA-1* genes of *V. vulnificus* not only showed the highest variability among the different isolates, but were also grouped in one cluster together with the *mshA-1* of *V. parahaemolyticus* and *V. cholerae*. This could suggest a common origin for this gene in these three species. PHYRE 2 was used for the prediction of the 3D structures of the three MSHA<sub>Vv</sub> proteins (**Figure 3A**). Even though the DNA sequences of the proteins showed some differences, their 3D model structures are strikingly similar and they show high homology to proteins of fimbriae, pilin subunits, and other prepilin-like proteins. Furthermore, we performed a clustalW alignment of the aminoacidic sequences of the *mshA* genes of *V. vulnificus* R99 (Vv), *V. cholera* O1 El Tor FJ147 (Vc) and *V. parahaemolyticus* RIMD 2210633 (Vp) strains. After the analysis, we observed that the conserved N-terminal sequence

(pilus core) of the prepilin was similar in all of the sequences analyzed (**Figure 3B**).

Finally, we compared the expressions of all three *mshA* genes in both the wild type, and in the *mshA-1* mutant strain, in iron restrictive conditions (**Figure 4**). There were no significant differences in gene expression between the wild type and the mutant strain regardless of the iron levels in the medium, with the obvious exception of the mutated gene. This suggests that, neither *mshA-2* nor *mshA-3* increase their expression to complement the absence of the *mshA-1* gene. The results also showed that all three *mshA* genes, in case of the wild type strain, and the two genes in case of the mutant, were expressed at similar levels in CM9. However, they were not similarly expressed under iron restriction conditions, where the *mshA-2* gene was significantly less expressed than the rest (**Figure 4**). When the growth in iron-rich and iron-poor media was compared between each strain, it was clear that *mshA-1* and *mshA-3* were significantly upregulated under iron restriction (**Figure 4B**).

### **Only *mshA-1* is involved in biofilm and adhesion in the zoonotic clonal-complex of *V. vulnificus***

Previous reports demonstrated the role of the *mshA-1* gene in biofilm formation (Watnick *et al.*, 1999; Chiavelli *et al.*, 2001; Zampini *et al.*, 2003), however, there are no reports about the function of the two other *mshA* genes in biofilm formation or any other role. Remarkably, our results showed that only  $\Delta mshA-1$ , and the mutants presenting this deletion, had a significant decrease in biofilm production ( $P < 0.05$ ), while complementation of this gene restored the biofilm to levels comparable to R99 (**Figure 5A**). The same biofilm assay was performed in iron-rich and iron-poor conditions, where we found that biofilm formation by the wild type, and all the mutant strains that conserved the *mshA-1* gene, increased significantly under iron restrictive conditions (**Figure 5A and B**). In addition, to further observe the biofilm formation by the wild type and mutant strains, their biofilms 3D architecture was followed and analyzed through confocal microscopy (**Figure 6**). Again, only the *mshA-1* defective mutants showed a significant difference in the structure of their biofilms when compared to the wild type strain.

The *V. cholerae* O1 El Tor biotype and the *V. cholerae* O139 serogroup strains are bacterial vectors of cholera disease that produce MSHA pili, interestingly, these pili are not present in the classical biotype. This pilus mediates a hemagglutination that is sensitive to mannose, which is an important immune response against the pathogen, and is involved in virulence. Thus we decided to observe the effect of the MSHA pilus of the zoonotic clonal-complex in the presence of blood, by performing a hemagglutination test with human red blood cells. The hemagglutination activity of the wild type,  $\Delta mshA-2$  and  $\Delta mshA-3$  was clearly visible after 1-3 minutes, while  $\Delta mshA-1$  showed no agglutination effect on the erythrocytes (**Figure 7**). When resuspended in 4% D-mannose and repeated the test, all the strains (excluding  $\Delta mshA-1$ ) were unable to cause red cells agglutination. Since hemagglutination was inhibited by mannose, we tested its influence in biofilm production (**Table 4**). As expected, the wild type, the  $\Delta mshA-2$  and the  $\Delta mshA-3$  strains produced significantly less biofilm

in presence of mannose, and the amount of biofilm produced under these conditions was similar to the ones produced by the *mshA-1* mutant (**Table 4 and Figure 8**).

The MSHA pili are necessary for the prevalence of the bacteria in the environment (Marsh *et al.*, 1996; Chiavelli *et al.*, 2001), so to determine the role of the *mshA* genes in adhesion to biotic surfaces, we incubated the bacteria in minimal media while adding crab shells as a biotic substrate for adhesion and colonization. Only the strains lacking the *mshA-1* gene were significantly deficient in adhesion to crab shells (**Figure 9B**), this was clearly noticeable after observing the shells under an optical microscope (**Figure 9A**). These results reinforce our previous data indicating that only the *mshA-1* gene is necessary for the correct functioning of the MSHA pili.

### **The MSHA pilus of the zoonotic clonal-complex plays a role in virulence and colonization for eels**

The role of the three *mshA* genes in eel virulence was tested by determining and comparing the LD<sub>50</sub> of the mutants and the wild type strain in infection assays through both intraperitoneal injection (i.p.) and immersion challenge. The R99 + pTfoX strain was subjected to the same virulence tests as the wild type and its derivative mutants to rule out any variation in virulence influenced that could be influenced by the presence of the mutation plasmid. No change in virulence was induced by the pTfoX plasmid, and the *mshA-1* mutant remained as virulent as the wild type when administered through the intra-peritoneal injection. However, it was significantly less virulent than the wild type by immersion challenge (**Table 5**), in addition, neither  $\Delta mshA-2$  nor  $\Delta mshA-3$  were impaired in their virulence. Then, we compared the colonization and invasion capability of  $\Delta mshA-1$ , as it was the only mutant that showed a deficiency in virulence, vs the wild type strain in a co-colonization assay, in which we infected eels by immersion with both strains in a 1:1 ratio. The mutant strain was impaired in the early colonization of the eel, significant lower numbers of  $\Delta mshA-1$  cells were recovered from all the sampled organs during the first 24 hours of infection. Interestingly, the differences in bacterial counts were specially significant during the first 12 hours post-infection (**Figure 10**). When sampled at 72 hours, the number of both strains were similar, or slightly higher for the mutant (gills and spleen).

## **Discussion**

In the present work we sought to discover the role of the MSHA pilus in the virulence of the zoonotic clonal-complex of *V. vulnificus*, and to discover the role, if any, of the two extra *mshA* genes located in its genome that had been previously neglected. For this, we selected several genes from our previous transcriptomic analysis where we analyzed the differentially transcribed genes of R99 under iron-rich and iron-poor conditions (Pajuelo *et al.*, 2016), as iron is the main environmental signal that controls the life cycle of this pathogen (Hernández-Cabanyero and Amaro, 2020). From approximately 250 genes related to virulence and survival



systems, several genes belonging to the MSHA pilus biosynthesis were upregulated under iron restriction.

The MSHA pilus belongs to the Type IV pili family and is essential for biofilm formation and initial adhesion to biotic and abiotic surfaces (Marsh *et al.*, 1996; Chiavelli *et al.*, 2001). These pili are common among the *Vibrionaceae* family, and surprisingly, some of the species harbor more than one copy of the major pilin subunit (*mshA*) in their genomes (Barocchi and Telford, 2014). Interestingly, only some biotypes of *V. cholerae* (O1 El Tor and O139) express these pili (Watnick *et al.*, 1999; Chiavelli *et al.*, 2001), and therefore, the MSHA pilus has only been studied in the epidemic serogroups of this species (Thelin and Taylor, 1996; Watnick *et al.*, 1999; Zampini *et al.*, 2003). No apparent role in virulence was attributed to it in earlier studies (Thelin and Taylor, 1996; Watnick *et al.*, 1999; Chiavelli *et al.*, 2001; Utada *et al.*, 2014; Jones *et al.*, 2015; Sinha-Ray and Ali, 2017), however, this pilus has been related with colonization of mice intestine by this species (Hsiao *et al.*, 2006; Liu *et al.*, 2008). Once *V. cholerae* is inside the mice host, the MSHA pili must be repressed in order for the bacteria to escape recognition by immunoglobins, enabling colonization and induction of other virulence factors (Hsiao *et al.*, 2006). Nonetheless, not much has been described about the MSHA pili in *V. vulnificus*, and nothing has been studied about it in the zoonotic clonal-complex until now.

First, we found three different *mshA-1* genes in the genome of the R99 strain and denominated them as *mshA-1*, *mshA-2* and *mshA-3*. Of the three, only *mshA-1* belonged to the MSHA locus. The three proteins coded by these genes presented the characteristic preserved N-terminal sequence, which includes the leader peptide and several ends with hydrophobic residues, which allows the formation of an extended  $\alpha$ -helix (pilus core) followed by the more heterogeneous C-terminal globular head (Berry and Pelicic, 2015) (**Figure 3**). All three genes were present in all *V. vulnificus* genomes belonging to L2 and in 40% of genomes belonging to L1, while none of them were present in L3 genomes. This could suggest that different clades/lineages of the species use different appendages to adhere to substrates in their natural environments, or alternatively, that they are adapted to different niches in nature, a hypothesis suggested by Giltner *et al.*, (2012). We also found *mshA-1* present in the genomes of the three main pathogenic *Vibrio* species, while *mshA-3* was only present in *V. parahaemolyticus*, and *mshA-2* was exclusive to *V. vulnificus* (**Table 3**). We constructed a phylogenetic tree that encompassed the three *mshA* genes present in the three species, and compared them to unravel their evolutionary origin. Interestingly, this gene turned out to be highly variable, which could be related to the phenomenon of antigenic variability affecting genes coding for Type IV pili, which are exposed to the immune system, as described in *Neisseria gonorrhoeae* and *V. cholerae* (Merz and So, 2000; Hsiao *et al.*, 2006). On the other hand, the *mshA-3* of *V. vulnificus* was closer to the *mshA-3* of *V. parahaemolyticus* than to the rest of the *mshA* genes belonging to the same species, which relates this gene to horizontal gene transfer between both species. In addition, *mshA-2* and *mshA-3* are highly conserved within *V. vulnificus*, suggesting that they are not subject to the antigenic variability phenomena, and are under strong selective pressure.

The main role of the MSHA pili is to promote initial surface adhesion and biofilm formation (Jonson *et al.*, 1991; Watnick *et al.*, 1999; Zampini *et al.*, 2003), so we analyzed the biofilm production capabilities of all the strains by using both crystal violet staining and confocal imaging. Our results clearly showed that biofilm production by the zoonotic clonal-complex was influenced by *mshA-1*, since the elimination of this gene significantly reduced its production (**Table 4 and Figure 5**), which has been described extensively in previous works (Marsh and Taylor, 1998a; Watnick *et al.*, 1999; Utada *et al.*, 2014; Sinha-Ray and Ali, 2017). Furthermore, we obtained multiple evidences that neither *mshA-2* nor *mshA-3* played a role in the formation of biofilms, and that they could not restore the formation of biofilms in the *mshA-1* mutants. Our results also confirmed, by analyzing the three-dimensional structure of the biofilms, that only the strains with *mshA-1* deletions produced a defective biofilm (**Figure 6**). We then proved that the pilus produced by the zoonotic clonal-complex was sensitive to mannose, by performing hemagglutination and biofilm formation tests in presence and absence of this molecule. This suggests that mannose residues can recognize these pili, and as expected, the two remaining *mshA* genes were not involved in the inhibition of biofilm formation and hemagglutination in the presence of mannose (**Table 4, Figure 7 and 8**).

We also measured biofilm production under iron-rich and iron-poor conditions, and observed that biofilm production of the wild type strain increased significantly under iron restriction (**Figure 5B**), which was compatible with the life cycle model proposed for this species by Pajuelo *et al.* According to this model and our results, iron restriction would trigger the formation of biofilms by activating MSHA pili production, interestingly, *mshA-3* also increased its expression in iron restriction, while *mshA-2* was not iron-responsive. Although both genes were not involved in the formation of biofilms, we could not rule out the possibility of their involvement in adhesion to other types of surfaces, therefore, we tested biofilm formation on chitin by using crab shells. Significant differences were observed only in the *mshA-1* mutant strain, proving again that this gene is the only one required for a functional pilus and biofilm formation on both hydrophobic (plastics) and hydrophilic (chitin) surfaces (**Figure 9**).

The MSHA pilus plays is involved in the virulence of *V. cholerae* in the colonization of the intestines (Watnick *et al.*, 1999; Hsiao *et al.*, 2006). So we tested the virulence and colonization capabilities of the MSHA mutants of the zoonotic clonal-complex in eels by comparing them to the wild type strain. Our results showed that the MSHA pilus is involved in eel virulence only through the natural route of infection (water), as the mutant strain was significantly less virulent than the wild type only during the immersion challenge. Previous studies had shown that this bacterium colonizes the eel skin mucosa, forming biofilms directly in the gills (Marco-Noales Ester *et al.*, 2001). This statements are supported by our co-colonization trials, where the colonization of eels by  $\Delta$ *mshA-1* was greatly impaired, most notably in the gills and in the first hours of infection (**Figure 10**). Therefore, the MSHA pilus is needed for a successful early colonization of the gills which, in the zoonotic clonal-complex, is a critical step in the initiation of infection in the eels, as these organs serve as the

main portal of entry for the pathogen into the host and the bloodstream. (Amaro *et al.*, 1995; Amaro and Biosca, 1996; Marco-Noales Ester *et al.*, 2001). Other studies in *V. cholerae* had shown that the MSHA pilus is not directly involved in the resistance to innate immunity, as it needs to be repressed and degraded in order to not be recognized by immunoglobins and alert the immune system, however, it does not confer any additional protection (Hsiao *et al.*, 2006; Liu *et al.*, 2008). Our results support this statements, as the MSHA pilus of the zoonotic clonal-complex was not involved in resistance to neither eel nor human serum, and no statistical differences were detected when comparing the survival in serum between the mutant and the wild type strain. Probably the loss of the pilus by *V. vulnificus* does not affect its resistance to this innate immunity mechanism, as this is exclusively mediated by the capsule in the case of humans (Carda-Diéguez *et al.*, 2018), and by an outer membrane complex in the case of eels (Hernández-Cabanyero *et al.*, 2019).

## Conclusions

In summary, Our results showed that from all the three *mshA* genes located in the genome of the zoonotic clonal-complex of *V. vulnificus*, only *mshA-1* is functional and involved in adhesion, biofilm formation and virulence. The deletion of this gene causes a reduction in colonization of the gills during the first hours of infection, which could cause a reduced colonization of the internal organs: as there are less bacteria colonizing the gill, a reduced bacterial load would be invading the bloodstream and internal organs, and in turn would be impacting the overall speed and severity of the infection. We propose that the reduction in virulence resulting by the elimination of functional MSHA pili is caused by a significant decrease in the quantity of bacterial cells adhering to the gills, this slows the entry of the pathogen into the organism. Immediately, a significantly smaller bacterial load enters the bloodstream and disperse the infection through other organs and tissue. Since the initial invasion of the host is being carried out by fewer cells, the odds of survival of the infected eel increases dramatically, as their immune system fend off significantly fewer bacterial cells than in a normal vibriosis infection. As previously stated, these pili are necessary for the initial adhesion to biotic surfaces, such as chitinous exoskeleton of zooplankton, and asymptomatic colonization of oysters and bivalves. However, as we demonstrate now, the MSHA pilus is also involved in the early steps of eel colonization and, therefore, in virulence for eels of the *V. vulnificus* zoonotic clonal-complex. This initial attachment allows the pathogen to colonize the main point of entry into the eel, ensuing an effective invasion of the bloodstream, consequential adhesion, and colonization of internal organs.

## Experimental procedures

### Strains and general culture conditions

All strains (Supporting Information **Table S1**) were actively grown in Luria-Betani broth (LB+0.5% NaCl), TSA-1 (TSA [tryptone soy agar], 1% NaCl), CM9 (M9 broth/agar (Miller, 1972) supplemented with 0.2% casamino acids), Minimal salts

medium with glycerol (MS+10% glycerol [MSg]) and LB-agar (LBA) at 28°C. For the genetic manipulations of the strains, the following antibiotic concentrations were used: chloramphenicol (Cnf), 20 µg/ml (*Escherichia coli*) or 2 µg/ml (*V. vulnificus*); kanamycin (Km), 40 µg/ml (*E. coli*) or 150 µg/ml (*V. vulnificus*); and trimethoprim (Tp), 25 µg/ml (*V. vulnificus*). To analyze the effect of exogenous iron on growth, the following culture media were used: CM9 + Fe (media supplemented with 100 µM FeCl<sub>3</sub>) and CM9 + Tf (media supplemented with 10 µM of the iron chelator human apo-transferrin [Sigma- Aldrich]). In case of liquid cultures, 5 ml of medium were inoculated with overnight bacteria at a ratio 1:100 (v/v), and incubated with shaking (60 rpm, New Brunswick Scientific Agitator). For bacterial counting, the drop plate method on TSA-1 was used (Hoben and Somasegaran, 1982). All strains were stored at -80 °C in LB-1 supplemented with 20% (v/v) glycerol.

### Maintenance of animals and serum/blood cells obtention

Non vaccinated farmed eels (*Anguilla anguilla*) were purchased from a local eel farm, and were maintained and handled by authorized personal in the facilities of the Central Service for Experimental Research (SCSIE) of the University of Valencia (Spain) following the ethic statement. Eel blood and serum were obtained as previously described (Biosca *et al.*, 1993; Lee *et al.*, 2013). Briefly, eel sera was aseptically obtained from healthy fish. The fish were bled by caudal fin puncture, and blood was allowed to clot. The separated sera was used immediately. Human serum was purchased from a commercial house (Sigma-Aldrich)

### Transcriptomic analysis and RT-qPCR

We analyzed the global response to iron in the zoonotic clonal-complex of *V. vulnificus* by using a previously generated mutant in the regulator of iron uptake (Fur) in the selected strain CECT 4999, and a previously designed microarray (Pajuelo *et al.*, 2016). The CECT4999-specific microarray contained 4553 probes of 60 nucleotides in length, corresponding to the three replicons of the strain (ChrI, ChrII and pVvbt2), with 3 probes per target (GEO repository; accession number GPL19040). The bacterium and its derivative mutants were grown in CM9, CM9 + Fe and CM9 + Tf up to the mid-log phase of growth. Then, RNA was extracted by centrifuging 1ml of the cultures at 13000 rpm for 5 min, discarding the supernatant and resuspending the pellet in 500 µl of NucleoZOL® (Macherey-Nagel). After 15 min of room temperature incubation, 400ul of RNAase-free water per 1ml of NucleoZOL® was added to the lysate. Samples were centrifuged for 15 min at 14,000 rpm and the supernatant was transferred to a fresh tube where 1 ml of isopropanol was added to precipitate de RNA. The mixture was incubated for 10 min at room temperature and centrifuged at maximum potency for another 10 min. The resulting supernatant was discarded and the pellet was washed twice with 75% of ethanol, finally the ethanol was removed and the RNA was treated with Turbo DNAase kit (Invitrogen) to remove the possible DNA contamination, and cleaned using the GeneJET® RNA Cleanup and Concentration Micro Kit (Thermo Fisher) following the manufacturer's instructions. RNA was quantified with a Nanodrop ND-2000 and only

samples with  $A_{260}/A_{280} > 1.8$  and  $A_{260}/A_{230} > 2$  were used.

### **Microarray data analysis**

The data was analyzed with Genespring 14.5 GX software (Agilent technologies) using the 75% percentile normalization for the comparisons of iron overloaded CM9 vs iron deficient CM9. Student's t-test ( $P < 0.05$ ) was applied to observe transcriptomic profile differences between the conditions. The same RNA samples used for the microarray analysis were analyzed by RT-qPCR to calculate the expression of the selected genes (primers listed in supporting information **Table S2**). To this end, cDNA was produced from 1  $\mu\text{g}$  of RNA using Maxima Reverse Transcriptase (Thermo Scientific) as described by the manufacturer. The qPCRs were carried out using Power SYBR® Green PCR Master Mix (Applied Biosystems) and the StepOne® Plus RT-PCR System (Applied Biosystems). Reactions were carried out in a final volume of 10  $\mu\text{l}$  (5  $\mu\text{l}$  2x Master Mix, 2  $\mu\text{l}$  DEPC H<sub>2</sub>O, 1  $\mu\text{l}$  cDNA, 1  $\mu\text{l}$  forward primer, 1  $\mu\text{l}$  reverse primer, both at a concentration of 100nM) and the settings consisted of 10 min of denaturalization at 95°C followed by 40 cycles of 15 seconds of denaturalization at 95°C and 1 min of annealing and extension at 62°C. The *recA* gene was used as standard and the fold induction ( $2^{-\Delta\Delta\text{Ct}}$ ) for each gene was calculated according to Livak and Schmittgen (2001).

### **Deletion mutants and complementation**

The mutation protocol was modified from a previous work where it was used to generate mutants from the clinical strain CMPC6 of *V. vulnificus* (Chodur *et al.*, 2018). A nested PCR was performed utilizing specially designed primers (Supporting information **Table S2**) to amplify 1-1.5 KB upstream and downstream of the target gene, as well as the desired antibiotic resistance cassette (Tp, Km or Cm). The resulting products were stitched together to generate the mutation construct by a second PCR. The conjugated wild type strain was incubated overnight at 28°C in LB-1 + ampicillin with .5M IPTG (Isopropyl  $\beta$ -D-1-thiogalactopyranoside) to induce natural transformation. Then, 500  $\mu\text{l}$  of Sea salt mix (Instant ocean™) (20 ppt) was mixed with 10  $\mu\text{l}$  of the overnight culture and 50  $\mu\text{l}$  of the nested PCR product. The mixture was incubated overnight at 28°C, 1 ml of LB-1 was then added and incubated for 6 hours in agitation before plating in LBA plates with the appropriate antibiotic. Complementation was performed by amplifying a linearized version of the pMMB207 vector as a backbone for ligating the target gene sequence via complementary 5' and 3' ends (primers listed in **Table S2**). Both PCR products were ligated using the In-fusion® HD Cloning kit (Takara), the resulting product was transformed into *E. coli* SM17-1 $\lambda$ pir by electroporation (R. Simon, 1983). Transformed cells were conjugated with the corresponding knock-out mutant using the same protocol as before, transformants were confirmed by PCR.

### **Analysis and alignment of the *mshA* genes and proteins**

In the published genome of *V. vulnificus* R99 three different *mshA* genes are annotated. Homology search for the three protein were carried out with BLAST (Altschul *et al.*, 1990). The gene sequences obtained were used to carry out the

phylogenetic analysis using the MEGA X program. The evolutionary history was inferred by using the Maximum Likelihood method based on the Tamura 3-parameter model. CLUSTAL W alignment of MshA protein sequences of *V. vulnificus* R99, *V. cholerae* El Tor FJ147 and *V. parahaemolyticus* RIMD 2210633 were performed and visualized in the Jalview 2.11.1.3© software. The prediction of the 3D structures of the MSHA proteins was performed with PHYRE 2 software. This tool develops template-based modeling in which the proteins are aligned to another of known structure based on patterns of evolutionary variation (Kelley *et al.*, 2015).

### **Biofilm formation and quantification**

The process of biofilm formation on plastic devices was tested by using confocal microscopy analysis and crystal violet staining. For confocal microscopy analysis, GFP (green fluorescent protein) tagged strains were used (**Table S1**). An overnight culture in CM9 + Km was used to inoculate (1:50) 3 ml of MSg with and without 4% D-mannose (wt/vol) on a 35 mm  $\mu$ -Dish® (Ibidi) plate. Strains were grown overnight at 28°C in static and the biofilm was visualized in a confocal microscope FV1000 (Olympus FluoView®). Each biofilm was scanned at three randomly selected positions on three biological replicates, and the Z stacks were generated by optical sectioning at each of these positions. Images of the biofilms were analyzed with the Imaris viewer® (Bitplane) software. The biofilm biovolume (total amount of space/biomass occupied by a biofilm, average thickness (thickness of each biofilm extending from the bottom to the top of the growth/viewing channel surface), and roughness coefficient (a measure of heterogeneity in biofilm architecture) were determined with COMSTAT 2.1® biofilm analysis software (Heydorn *et al.*, 2000). When needed, biofilms were analyzed in two conditions: Filtered (quantification of the cells adhered to the substrate forming biofilm) and not filtered (quantification of total biomass present in the media). For quantification via crystal violet staining, the biofilm was quantified by a modified crystal violet staining method (Guo and Rowe-Magnus, 2010). Briefly, overnight CM9, and CM9 + Fe or + Tf cultures were used to inoculate fresh media to an OD<sub>600</sub> of 0.5. Then, the cultures were placed into a 96-well microtiter plate (6 wells per strain) and left overnight for static growth at 30°C. After incubation, bacterial growth was measured at A<sub>600</sub> before carefully removing the media by aspiration and staining the biofilm of the plate walls with 150  $\mu\text{l}$  of 0.1% crystal violet for 30 min. Wells were rinsed with PBS (180  $\mu\text{l}$ ) three times and the violet stain was solubilized with 150  $\mu\text{l}$  of 96% ethanol. The OD<sub>595</sub> of the solubilized biofilm was measured and the OD<sub>595</sub>/OD<sub>600</sub> ratio was calculated to determine the relative biofilm production.

### **Resistance and growth in serum**

Overnight culture were adjusted to  $1 \times 10^3$  CFU/ml in PBS, mixed at a 1:1 ratio with eel or human serum (Sigma-Aldrich), and incubated at 28°C (eel) or 37°C (human) for 4 hours. The survival ratio was determined after 4h of incubation as previously described by Lee *et al.*, (2013).

## Hemagglutination test

The hemagglutination capacity of the R99 and *mshA* mutant strains was tested by mixing with fresh human erythrocytes (small quantities of human blood were donated by Valencian La Fe clinical hospital) with a bacterial suspension. Briefly, 500  $\mu$ l of fresh human blood was centrifuged at 3000 rpm for 5 min at 4°C, then 6  $\mu$ l of the red blood cells precipitant was carefully resuspended in 194  $\mu$ l of PBS 1x. Bacterial cells from a 5ml tube of an overnight culture were pelleted and washed twice and resuspended in 1 ml of PBS. Volumes of 20  $\mu$ l of both suspensions were mixed on a glass-slide and bacteria and red blood cells were mixed by gentle agitation for 1 min. Visible agglutination before 3 min was recorded as a positive result. Negative controls were bacteria or red blood cells mixed with PBS.

## Adhesion to crab shells as biotic surfaces

The capacity of adhesion to biotic surfaces was assessed by inoculating a 1:1000 dilution of a mid-exponential CM9 culture of R99 and derivative mutants into a 48-well tissue culture test plate (3 wells per strain) containing 1 ml of CM9 and a piece of sterile crab shell with an area of approximately 1 cm<sup>2</sup>. The strains were incubated for 5 hours at 28°C in static, then the supernatant was removed, and the shells were carefully washed three times with 1 ml of fresh PBS. Finally, the crab shells were transferred into a tube containing 1ml of fresh PBS, the tubes were vortexed vigorously for 20 seconds and the resultant supernatant was 10-fold diluted and plated for bacterial counts (CFU/ml). The same experiment was performed with GFP tagged strains to observe the bacteria adhered to the shells with a Olympus TH4-200 fluorescence inverted optical microscope at 600x magnification.

## Virulence and co-colonization assays

Virulence of the strains was determined as LD<sub>50</sub> (Reed and Muench, 1938) by intra-peritoneal injection (i.p.) and immersion challenge, both performed by infecting the animals with the LD<sub>50</sub> dose of R99 pertinent to each way of infection (Amaro *et al.*, 1995; Hernández-Cabanyero *et al.*, 2019). Briefly, groups of 6 eels (20 grs) were infected with the LD<sub>50</sub> of R99 (1x10<sup>2</sup> for IP and 1x10<sup>6</sup> for Immersion) and doses above and below this threshold of the selected Type IV mutant. For the immersion challenge, each group of eels were incubated one hour in infective baths containing the bacterial load. Mortalities were validated by recovering the bacteria from internal organs of diseased eels, and the LD<sub>50</sub> of the mutants was determined through serial bacterial 10-fold dilutions in PBS (Amaro *et al.*, 1995).

The co-colonization and invasion assays were performed by immersion of groups of 24 eels (40 g) in a mixed infective bath containing a R99 harboring a *lacZ* gene for white-blue colony and the selected *mshA* mutant. Three live eels per group were randomly sacrificed at 1, 12, 24 and 72h, and samples of gills, liver, kidney and blood were pooled and plated for bacterial counts (CFU/organ). TSA-1 + X-gal plates were used for the bacterial count, in these plates, the blue colonies corresponding to the R99 (*lacZ* +) and the white ones to the mutant (*lacZ* -) strain were easily distinguished.

## Statistical analysis

All the experiments were performed by triplicate, the results are presented as means  $\pm$  SE (standard error), significance of differences ( $P < 0.05$ ) between the means was tested by unpaired student t-test. When comparison of two or more conditions was necessary, analysis of variance (ANOVA) was utilized. All analyses were performed using GraphPad Prism® version 6.04 for Windows.

## Ethic statement

All assays involving animals were approved by the Institutional Animal Care and Use Committee and the local authority (Generalitat Valenciana), following European Directive 2010/63/EU and the Spanish law 'Real Decreto' 53/2013 and were performed in the SCSIE facilities by using the protocol 2019/VSC/PEA/0063 (colonization and invasion in eels). We also have a permission from Generalitat Valenciana to use eels for scientific research purposes.

## References

- Altschul, S.F., Gish, W., Miller, W., Myers, E.W., and Lipman, D.J. (1990) Basic local alignment search tool. *J Mol Biol* **215**: 403–410.
- Amaro, C. and Biosca, E.G. (1996) *Vibrio vulnificus* biotype 2, pathogenic for eels, is also an opportunistic pathogen for humans. *Appl Environ Microbiol* **62**: 1454–1457.
- Amaro, C., Biosca, E.G., Fouz, B., Alcaide, E., and Esteve, C. (1995) Evidence that water transmits *Vibrio vulnificus* biotype 2 infections to eels. *Appl Environ Microbiol* **61**: 1133–1137.
- Amaro, C., Sanjuán, E., Fouz, B., Pajuelo, D., Lee, C.-T., Hor, L.-I., and Barrera, R. (2015) The fish pathogen *Vibrio vulnificus* Biotype 2: Epidemiology, phylogeny, and virulence factors involved in warm-water vibriosis. *Microbiol Spectr* **3**.
- Baker-Austin, C., Trinanes, J., Gonzalez-Escalona, N., and Martinez-Urtaza, J. (2017) Non-cholera Vibrios: The microbial barometer of climate change. *Trends Microbiol* **25**: 76–84.
- Barocchi, Michèle A. and Telford, John L. (2014) Bacterial pili: structure, synthesis and role in disease, *Advances in Bacteriology*. Barocchi, M. A. and Telford, J. L. (eds) Wallingford: CABI.
- De Bentzmann, S., Aurouze, M., Ball, G., and Filloux, A. (2006) FppA, a novel *Pseudomonas aeruginosa* prepilin peptidase involved in assembly of type IVb pili. *J Bacteriol* **188**: 4851–4860.
- Berry, J.L. and Pelicic, V. (2015) Exceptionally widespread nanomachines composed of type IV pilins: The prokaryotic Swiss Army knives. *FEMS Microbiol Rev* **39**: 134–154.
- Biosca, E.G., Llorens, H., Garay, E., and Amaro, C. (1993) Presence of a capsule in *Vibrio vulnificus* biotype 2 and its relationship to virulence for eels. *Infect Immun* **61**: 1611–1618.
- Bisharat, N., Agmon, V., Finkelstein, R., Raz, R., Ben-Dror,

- G., Lerner, L., et al. (1999) Clinical, epidemiological, and microbiological features of *Vibrio vulnificus* biogroup 3 causing outbreaks of wound infection and bacteraemia in Israel. *Lancet* **354**: 1421–1424.
- Bisharat, N., Bronstein, M., Korner, M., Schnitzer, T., and Koton, Y. (2013) Transcriptome profiling analysis of *Vibrio vulnificus* during human infection. *Microbiol (United Kingdom)* **159**: 1878–1887.
- Carda-Diéguez, M., Silva-Hernández, F.X., Hubbard, T.P., Chao, M.C., Waldor, M.K., and Amaro, C. (2018) Comprehensive identification of *Vibrio vulnificus* genes required for growth in human serum. *Virulence* **9**: 981–993.
- Chiavelli, D.A., Marsh, J.W., and Taylor, R.K. (2001) The Mannose-Sensitive Hemagglutinin of *Vibrio cholerae* promotes adherence to zooplankton. *Appl Environ Microbiol* **67**: 3220–3225.
- Chodur, D.M., Coulter, P., Isaacs, J., Pu, M., Fernandez, N., Waters, C.M., and Rowe-Magnus, D.A. (2018) Environmental calcium initiates a feed-forward signaling circuit that regulates biofilm formation and rugosity in *Vibrio vulnificus*. *Am Soc Microbiol* **9**: 1–14.
- Giltner, C.L., Nguyen, Y., and Burrows, L.L. (2012) Type IV Pilin Proteins: Versatile Molecular Modules. *Microbiol Mol Biol Rev* **76**: 740–772.
- Guo, Y. and Rowe-Magnus, D.A. (2010) Identification of a c-di-GMP-regulated polysaccharide locus governing stress resistance and biofilm and rugose colony formation in *Vibrio vulnificus*. *Infect Immun* **78**: 1390–1402.
- Hernández-Cabanyero, C. and Amaro, C. (2020) Phylogeny and life cycle of the zoonotic pathogen *Vibrio vulnificus*. *Environ Microbiol*.
- Hernández-Cabanyero, C., Lee, C. Te, Tolosa-Enguis, V., Sanjuán, E., Pajuelo, D., Reyes-López, F., et al. (2019) Adaptation to host in *Vibrio vulnificus*, a zoonotic pathogen that causes septicemia in fish and humans. *Environ Microbiol* **21**: 3118–3139.
- Heydorn, A., Nielsen, A.T., Hentzer, M., Sternberg, C., Givskov, M., Ersboll, B.K., and Molin, S. (2000) Quantification of biofilm structures by the novel computer program COMSTAT. *Microbiology* **146**: 2395–2407.
- Hoben, H.J. and Somasegaran, P. (1982) Comparison of the pour, spread, and drop plate methods for enumeration of *Rhizobium spp.* in inoculants made from presterilized peat. *Appl Environ Microbiol* **44**: 1246–1247.
- Horseman, M.A. and Surani, S. (2011) A comprehensive review of *Vibrio vulnificus*: An important cause of severe sepsis and skin and soft-tissue infection. *Int J Infect Dis* **15**: e157–e166.
- Hsiao, A., Liu, Z., Joelsson, A., and Zhu, J. (2006) *Vibrio cholerae* virulence regulator-coordinated evasion of host immunity. *PNAS* **103**: 14542–14547.
- III, J.J.F., Brenner, F.W., Cameron, D.N., Birkhead, K.M., Control, D., and Janda, J.M. (2015) *Vibrio*, Bergey's M. John Wiley & Sons, Inc.
- Jones, C.J., Utada, A., Davis, K.R., Thongsomboon, W., Zamorano Sanchez, D., Banakar, V., et al. (2015) C-di-GMP regulates motile to sessile transition by modulating MSHA pili biogenesis and near-surface motility behavior in *Vibrio cholerae*. *PLoS Pathog* **11**: 1–27.
- Jones, M.K. and Oliver, J.D. (2009) *Vibrio vulnificus*: Disease and pathogenesis. *Infect Immun* **77**: 1723–1733.
- Jonson, G., Holmgren, J., and Svennerholm, A.M. (1991) Identification of a mannose-binding pilus on *Vibrio cholerae* El Tor. *Microb Pathog* **11**: 433–441.
- Kelley, L.A., Mezulis, S., Yates, C.M., Wass, M.N., and Sternberg, M.J.E. (2015) The PHYRE2 web portal for protein modeling, prediction and analysis. *Nat Protoc* **10**: 845–858.
- Lee, C. Te, Amaro, C., Wu, K.M., Valiente, E., Chang, Y.F., Tsai, S.F., et al. (2008) A common virulence plasmid in biotype 2 *Vibrio vulnificus* and its dissemination aided by a conjugal plasmid. *J Bacteriol* **190**: 1638–1648.
- Lee, C. Te, Pajuelo, D., Llorens, A., Chen, Y.H., Leiro, J.M., Padrós, F., et al. (2013) MARTX of *Vibrio vulnificus* biotype 2 is a virulence and survival factor. *Environ Microbiol* **15**: 419–432.
- Liu, Z., Miyashiro, T., Tsou, A., Hsiao, A., Goulian, M., and Zhu, J. (2008) Mucosal penetration primes *Vibrio cholerae* for host colonization by repressing *quorum sensing*. *PNAS* **105**: 9769–9774.
- Lory, S. and Strom, M.S. (1997) Structure-function relationship of type-IV prepilin peptidase of *Pseudomonas aeruginosa* - A review. *Gene* **192**: 117–121.
- Marco-Noales Ester, Milan, M., Fouz, B., Sanjuan, E., and Amaro, C. (2001) Transmission to Eels, Portals of Entry, and Putative Reservoirs of *Vibrio vulnificus* Serovar E ( Biotype 2 ). *Appl Environ Microbiol* **67**: 4717–4725.
- Marsh, J.W., Sun, D., and Taylor, R.K. (1996) Physical linkage of the *Vibrio cholerae* mannose-sensitive hemagglutinin secretory and structural subunit gene loci: Identification of the *mshG* coding sequence. *Infect Immun* **64**: 460–465.
- Marsh, J.W. and Taylor, R.K. (1998a) Genetic and transcriptional analyses of the *Vibrio cholerae* mannose-sensitive hemagglutinin type 4 pilus gene locus. *J Bacteriol* **181**: 1110–1117.
- Merz, A.J. and So, M. (2000) Interactions of pathogenic *Neisseriae* with epithelial cell membranes. *Annu Rev Cell Dev Biol* **16**: 423–457.
- Miller, J.H. (1972) Experiments in molecular genetics. In, *Experiments in molecular genetics*. Cold Spring Harbor, N.Y.: Cold Spring Harbor Laboratory, p. 466.
- Oliver, J.D. (2015) The biology of *Vibrio vulnificus*. *Microbiol Spectr* **3**: 1–10.
- Oliver, J.D. (2013) *Vibrio vulnificus*: Death on the half shell. A personal journey with the pathogen and its ecology. *Microb*



*Ecol* **65**: 793–799.

Pajuelo, D., Hernández-Cabanyero, C., Sanjuan, E., Lee, C.-T., Silva-Hernández, F.X., Hor, L.-I., et al. (2016) Iron and fur in the life cycle of the zoonotic pathogen *Vibrio vulnificus*. *Environ Microbiol* **18**: 4005–4022.

Paranjpye, R.N. and Strom, M.S. (2005) A *Vibrio vulnificus* type IV pilin contributes to biofilm formation, adherence to epithelial cells, and virulence. *Infect Immun* **73**: 1411–1422.

Pruzzo, C., Vezzulli, L., and Colwell, R.R. (2008) Global impact of *Vibrio cholerae* interactions with chitin. *Environ Microbiol* **10**: 1400–1410.

Pu, M., Duriez, P., Arazi, M., and Rowe-Magnus, D.A. (2018) A conserved tad pilus promotes *Vibrio vulnificus* oyster colonization. *Environ Microbiol* **20**: 828–841.

R. Simon, U.P. and A.P. (1983) A broad host range mobilization system for *in vivo* genetic engineering: Transposon mutagenesis in gram negative bacteria. *Nat Biotechnol* **1**: 784–791.

Reed, L.J. and Muench, H. (1938) A simple method of estimating fifty percent endpoints. *Am J Epidemiol* **27**: 493–497.

Roig, F.J., González-Candelas, F., Sanjuán, E., Fouz, B., Feil, E.J., Llorens, C., et al. (2018) Phylogeny of *Vibrio vulnificus* from the analysis of the core-genome: Implications for intra-species taxonomy. *Front Microbiol* **8**: 1–13.

Sanjuán, E., González-Candelas, F., and Amaro, C. (2011) Polyphyletic origin of *Vibrio vulnificus* biotype 2 as revealed by sequence-based analysis. *Appl Environ Microbiol* **77**: 688–695.

Sinha-Ray, S. and Ali, A. (2017) Mutation in *flrA* and *mshA* genes of *Vibrio cholerae* inversely involved in *vps*-independent biofilm driving bacterium toward nutrients in lake water. *Front Microbiol* **8**: 1–13.

Theelin, K.H. and Taylor, R.K. (1996) Toxin-coregulated pilus, but not mannose-sensitive hemagglutinin, is required for colonization by *Vibrio cholerae* O1 El Tor biotype and O139 strains. *Infect Immun* **64**: 2853–2856.

Tison, D.L., Nishibuchi, M., Greenwood, J.D., and Seidler, R.J. (1982) *Vibrio vulnificus* biogroup 2: new biogroup pathogenic for eels. *Appl Environ Microbiol* **44**: 640–6.

Utada, A.S., Bennett, R.R., Fong, J.C.N., Gibiansky, M.L., Yildiz, F.H., Golestani, R., and Wong, G.C.L. (2014) *Vibrio cholerae* use pili and flagella synergistically to effect motility switching and conditional surface attachment. *Nat Commun* **5**: 4913.

Watnick, P.I., Fullner, K.J., and Kolter, R. (1999) A role for the mannose-sensitive hemagglutinin in biofilm formation by *Vibrio cholerae* El Tor. *J Bacteriol* **181**: 3606–3609.

Williams, T., Ayrapetyan, M., Ryan, H., and Oliver, J. (2014) Serum survival of *Vibrio vulnificus*: Role of genotype, capsule, complement, clinical origin, and *in situ* incubation. *Pathogens* **3**: 822–832.

Zampini, M., Canesi, L., Betti, M., Ciacci, C., Tarsi, R., Gallo, G., and Pruzzo, C. (2003) Role for mannose-sensitive hemagglutinin in promoting interactions between *Vibrio cholerae* El Tor and mussel hemolymph. *Appl Environ Microbiol* **69**: 5711–5715.

## Figures and tables

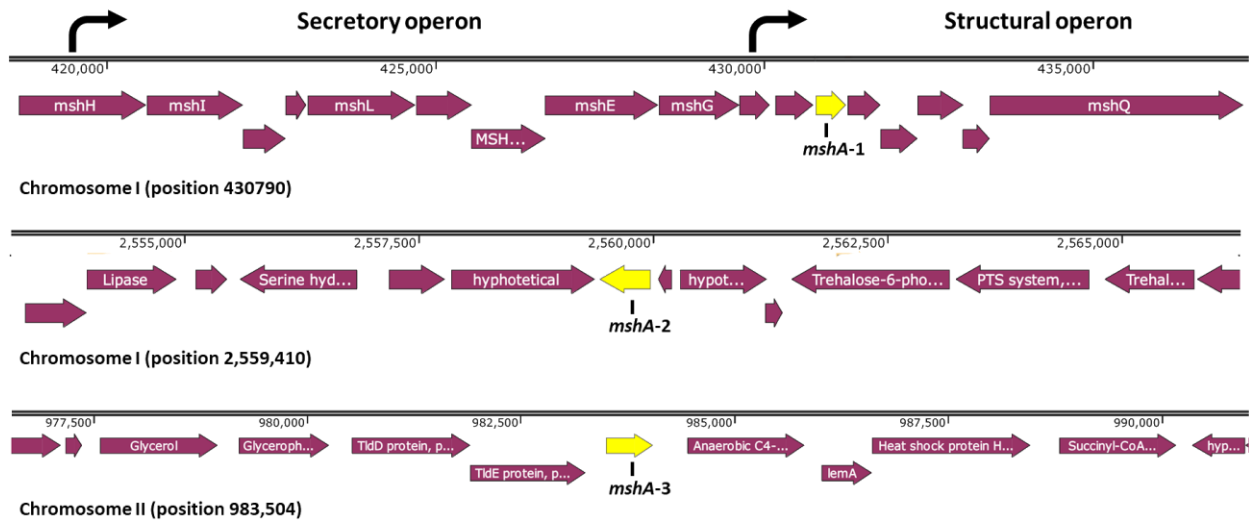


**Fig.1.** Schematic representation of the MSHA genes located in the genome of *Vibrio vulnificus*. The major MSHA pilin subunit gene (*mshA-1*) is located in a locus spanning 16.7 kb with 16 contiguous open reading frames. The promoters required for the expression of the pilus are indicated by arrows. The other two genes do not belong to any loci. ORFs were drawn to scale using SnapGene® software.

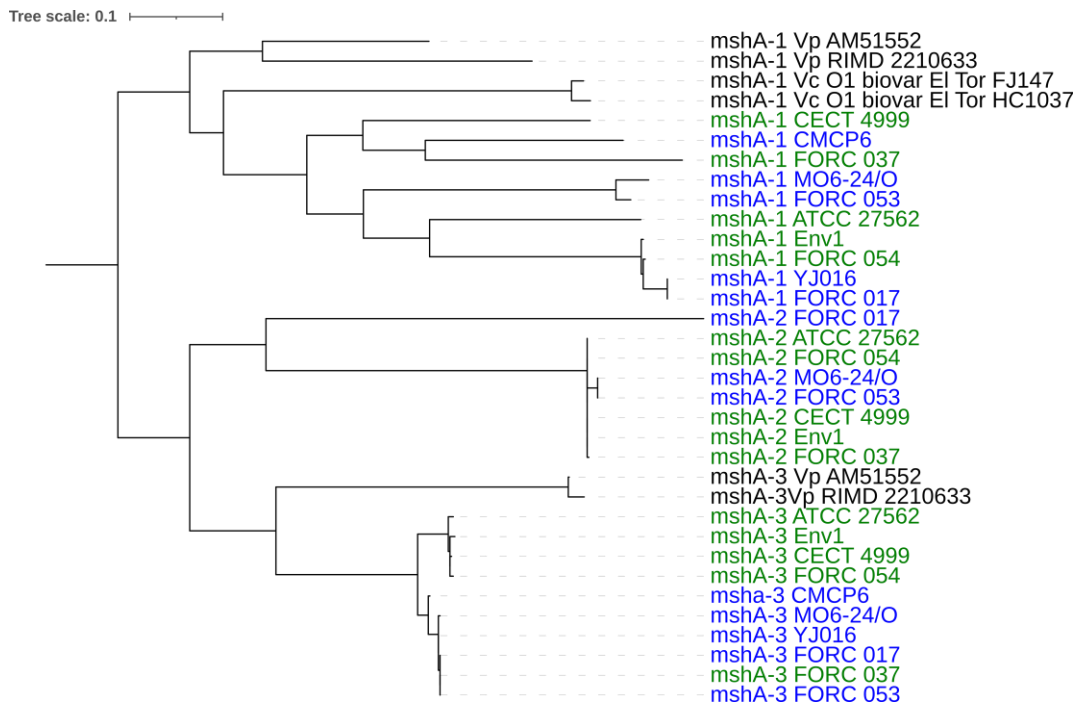


**Fig.2.** Phylogenetic tree of *mshA* genes. Maximum-likelihood tree derived from the sequence of the three genes in human pathogen vibrios. Bootstrap support values higher than 80% are indicated in the corresponding nodes. Non *V. vulnificus* strains marked in black, strains belonging to L2 are marked in green, and strains from L3 are marked in blue.

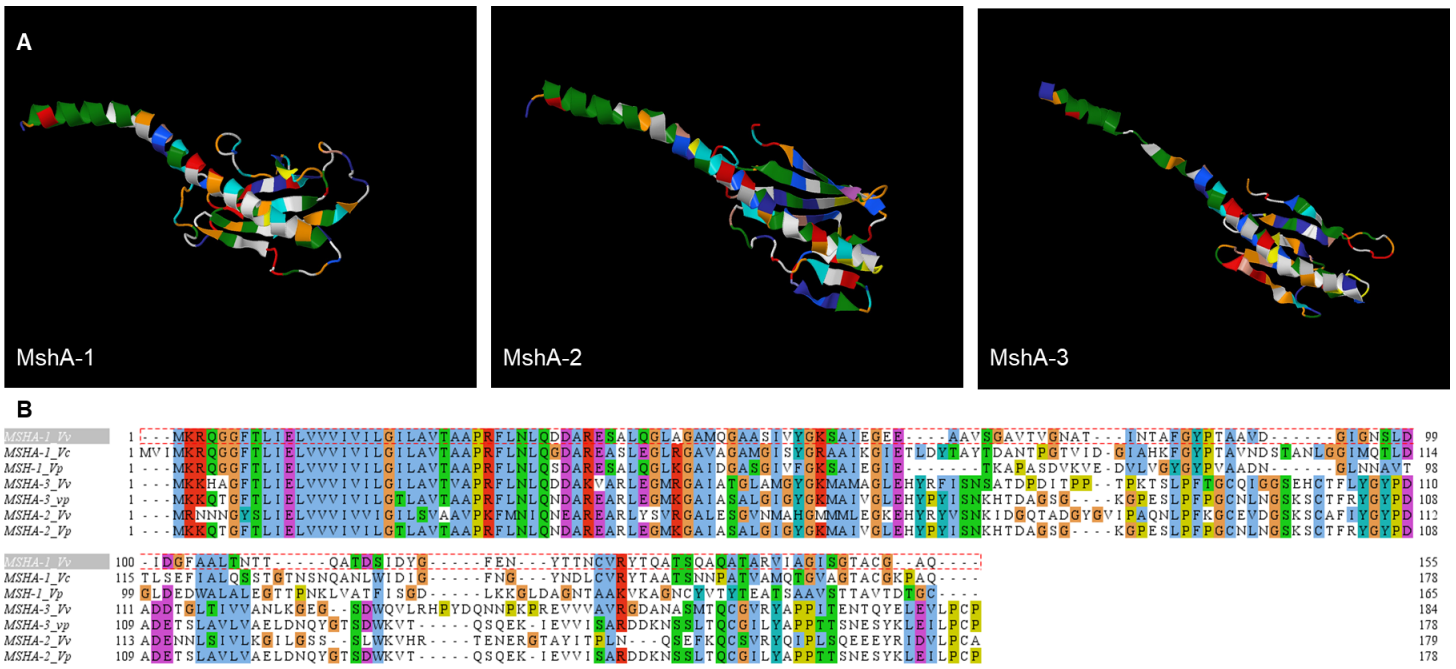


**Fig.3.** Structural modeling and alignment of the MSHA proteins from *V. vulnificus*. (A) 3D structures generated via Geneious 7.1.9® software. (B) Protein ClustalW alignment in Jalview 2.11.1.3® software. Reference sequence of the *mshA-1* gene of the zoonotic clonal-complex is highlighted in gray and boxed in red on

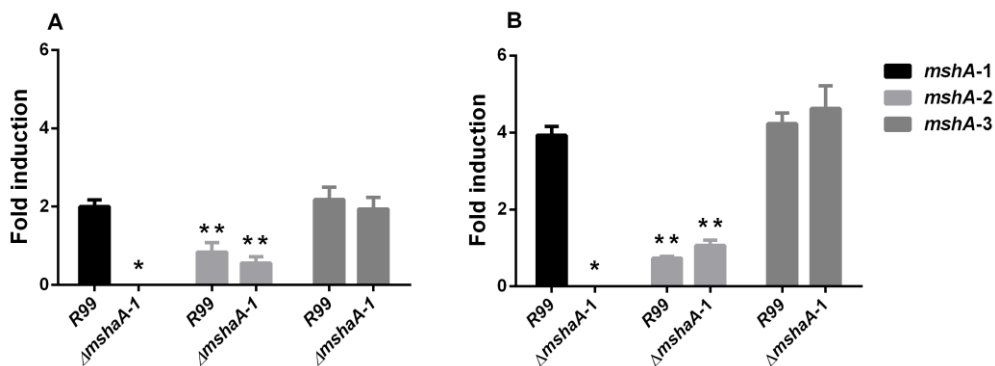


**Fig.4.** qPCR quantification of the *mshA* genes in CM9 (A) or CM9+Tf (B). Results are presented as the mean, and error bars represent the standard deviation. \*: significant differences between fold inductions of the same gene between strains. \*\*: Significant differences between fold inductions of different genes in the same strain. Significant differences ( $P < 0.05$ ) were determined by unpaired students T-test.



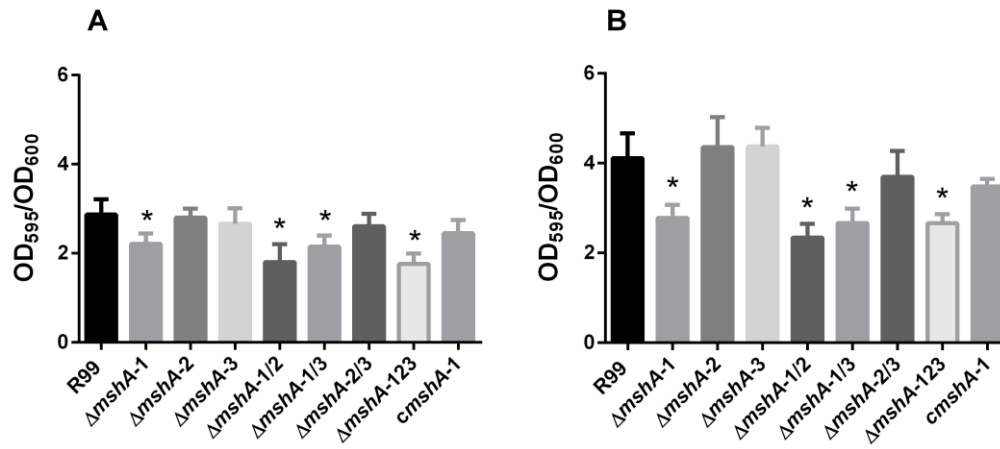


**Fig.5.** Biofilm production in CM9 (A) and CM9-Tf (B) measured via crystal violet staining. Results are presented as the mean, and error bars represent the standard deviation. \*: significant differences between mutants and the wild type ( $P < 0.05$ ) were determined by one-way ANOVA.

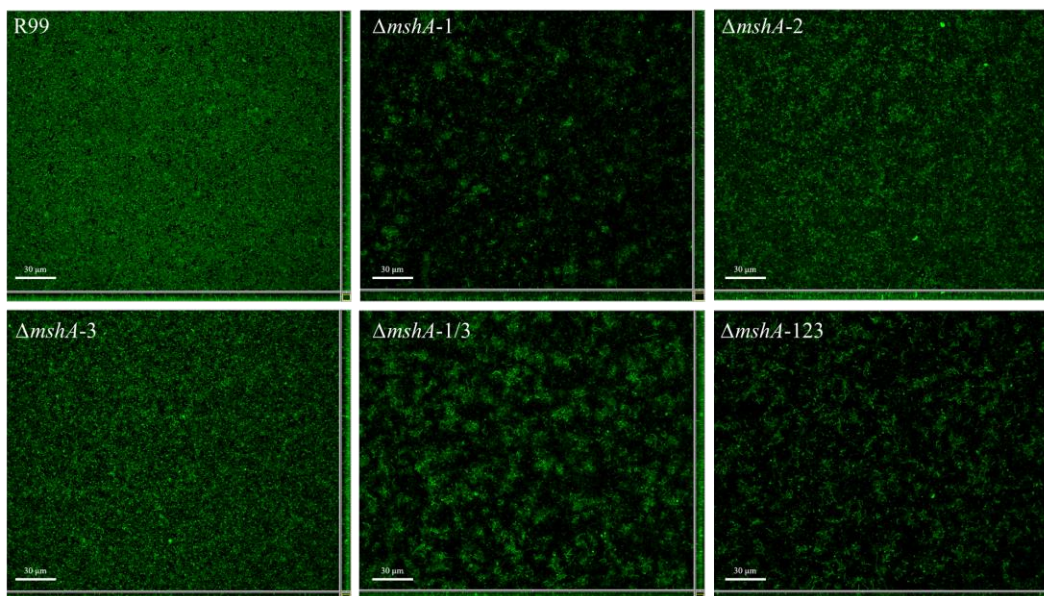


**Fig.6.** Fluorescent imaging of GFP labelled the zoonotic clonal-complex of *V. vulnificus* wild type and *mshA* simple and multiple mutant strains. Strains were grown overnight in static at 28°C in MSg + Km (150 μg/ml) in μ-dish® (Ibidi) plates. Images were captured using a confocal microscope and were analyzed using the Imaris viewer® (Bitplane) imaging software.

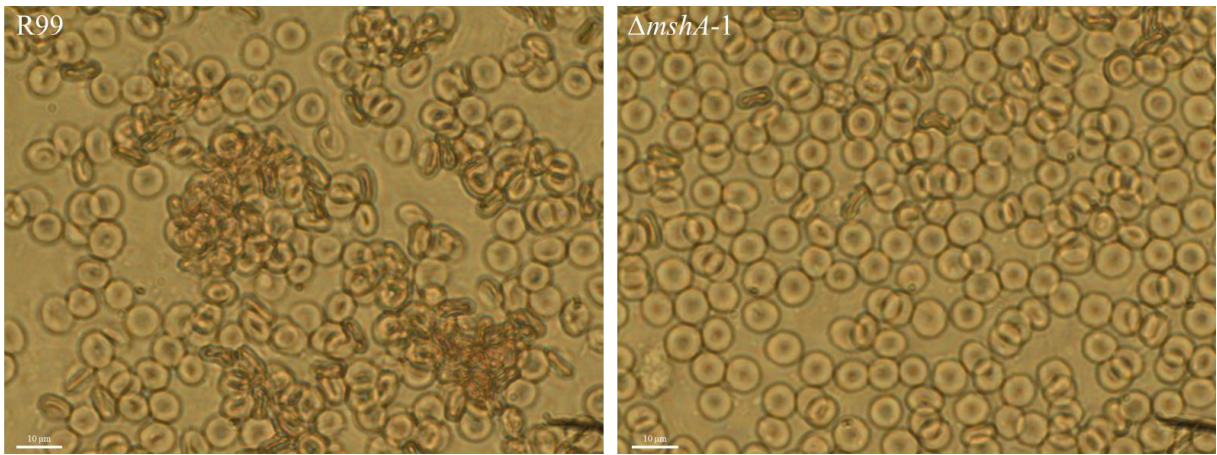


**Fig.7.** Hemagglutination activity of R99 and  $\Delta mshA-1$ . Bacterial and red blood cells were resuspended in PBS 1X and mixed on a glass slide by a cross-like motion. Hemagglutination effect was visible on the R99 strain after 1-3 minutes, while it was completely absent in the *mshA-1* mutant.

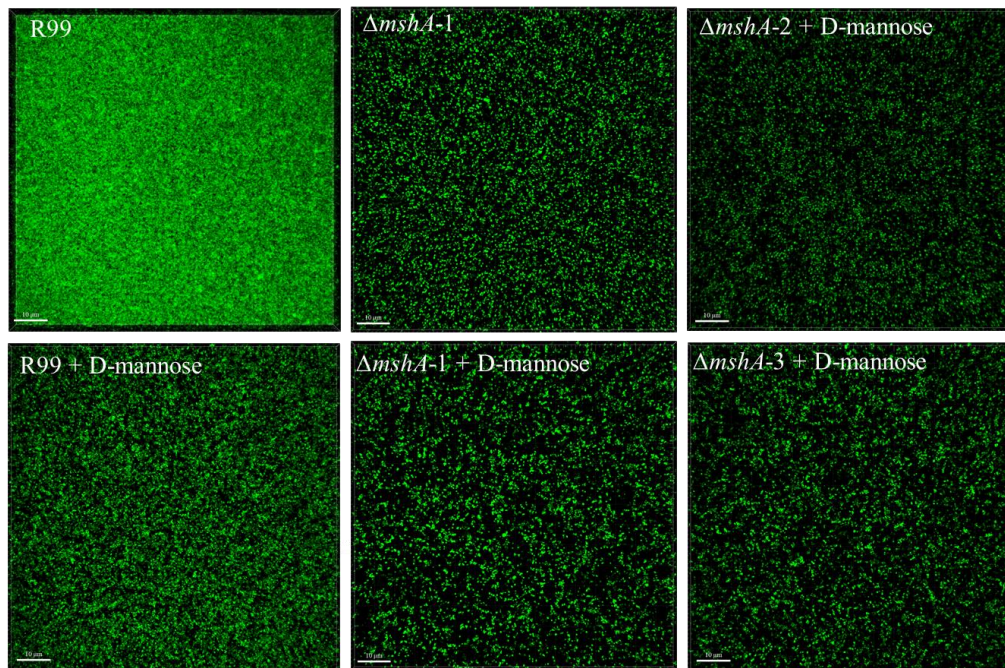


**Fig.8.** Fluorescent imaging of GFP-labelled of the zoonotic clonal-complex of *V. vulnificus* wild type and *mshA* simple and compound mutant strains. Strains were grown overnight in static at 28°C in M<sub>5</sub>g + Km (150 μg/ml) with 4% D-mannose in μ-dish® (Ibidi) plates. R99 and *mshA-1* strains incubated without mannose were used as control, only the wild type strain is shown as reference. Images were captured using a confocal microscope and were analyzed using the Imaris viewer® (Bitplane) imaging software.



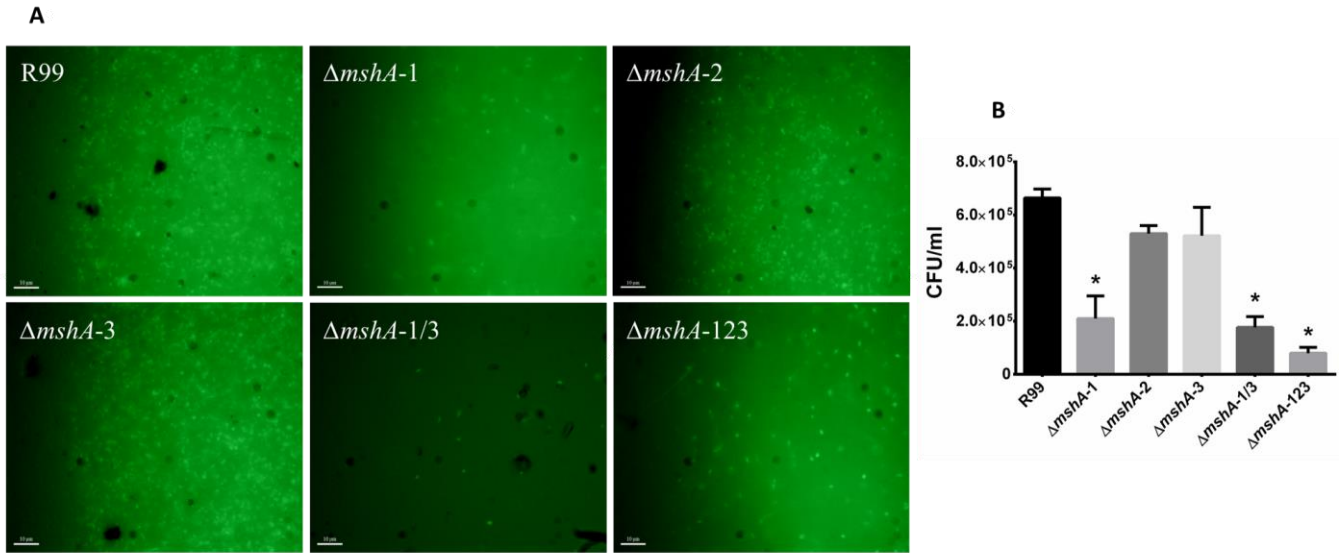


**Fig.9.** (A) *V. vulnificus* R99 and derivative mutant strains adhesion to crab shells. Shells were washed twice and mounted on a glass slide for microscope imaging. The images were taken with an Olympus fluorescent microscope. (B) Bacteria adhered to the crab shell after overnight incubation. \*: significant differences between mutants and the wild type ( $P < 0.05$ ) were determined by one-way ANOVA.

**Table 1. Genes of interest related to biofilm and virulence selected from the transcriptomic analysis.**

Name	Function	Location in the genome	Iron restriction stimulon (FC <sup>1</sup> )
<b>Chromosome I (3,394,464 bp)</b>			
<i>mshL</i>	Type II secretin	423,063	+2.47
<i>mshM</i>	ATPase	424,717	+31.93
<i>mshQ</i>	MSHA biogenesis protein	433,440	+18.68
<i>mshA-1</i>	MSHA major pilin subunit	430,790	0
<i>mshA-2*</i>	MSHA major pilin subunit	2,559,410	0
<b>Chromosome II (1,700,225 bp)</b>			
<i>mshQ</i>	MSHA biogenesis protein	944,651	+32.92
<i>mshA-3*</i>	MSHA major pilin subunit	983,504	-7.67

\*Orphan major pilin subunit genes not located within the MSHA locus.

<sup>1</sup> FC: fold change value or range of fold change values for each individual gene.

**Table 2. Comparison of fold change values between the array and RT-qPCR in the selected genes. For the RT-qPCR, *recA* was used as the reference gene and the fold induction ( $2^{-\Delta\Delta Ct}$ ) for each gene was calculated.**

Gene	FC <sup>1</sup>	
	Array	RT-qPCR
<i>mshA-1</i>	--	3.3 (+)
<i>mshA-2</i>	--	-5.5 (-)
<i>mshA-3</i>	-7.6 (-)	4.3 (+)

<sup>1</sup>FC: fold change values qualitative classification: -,  $-2 < X < -10$ ; --,  $-10 \leq X < -25$ ; =,  $-2 < X < 2$ ; +,  $2 \leq X < 10$ ; ++,  $10 \leq X < 35$

**Table 3. Sequence analysis and alignment to R99 of the three distinct *mshA* genes among different strains and species**

Species	Strains (Lineage) <sup>a</sup>	Genes					
		Length (bp)			Identity to R99 <sup>b</sup> (%)		
		<i>mshA-1</i>	<i>mshA-2</i>	<i>mshA-3</i>	<i>mshA-1</i>	<i>mshA-2</i>	<i>mshA-3</i>
<i>Vibrio vulnificus</i>	R99 (L2)	468	540	555	100	100	100
	ATCC 27562 (L2)	447	540	555	63.3	100	99.1
	CMCP6 (L1)	456	-	555	65.6	-	95.1
	ENV1 (L2)	471	540	555	66.6	100	99.3
	FORC_017 (L1)	471	537	549	67.1	54.7	94.1
	FORC_037 (L2)	492	540	555	63.9	99.8	94.1
	FORC_053 (L1)	510	540	555	66.7	98.9	94.1
	FORC_054 (L2)	471	540	555	66.4	100	99.5
	MO6-24/O (L1)	510	540	555	66.7	98.9	94.1
	YJ016 (L1)	471	-	555	67.1	-	94.2
	Vvyb1 (L3)	-	-	-	-	-	-
	12 (L3)	-	-	-	-	-	-
	11028 (L3)	-	-	-	-	-	-
	32 (L3)	-	-	-	-	-	-
162 (L3)	-	-	-	-	-	-	
<i>Vibrio cholerae</i>	El Tor FJ147	528	-	-	61.2	-	-
	HC1037	537	-	-	60.2	-	-
	N16961	537	-	-	60.2	-	-
<i>Vibrio parahaemolyticus</i>	FORC_004	468	-	528	66.3	-	62.1
	RIMD 2210633	498	-	537	60.4	-	61.9
	VPD14	498	-	537	60.4	-	61.9
<i>Shewanella ioihica</i>	ATCC 51908	492	-	-	55.1	-	-
<i>Shewanella woodyi</i>	PV-4	501	-	-	56.4	-	-

a. Phylogenetic Lineage of *V. vulnificus* according to Roig *et al.* (2018) and unpublished results.

b. Pairwise alignment was performed with the Geneious 7.1.9™ software using the Needleman–Wunsch algorithm.

**Table 4. Biofilm quantification of the R99 strain and its derivative mutants**

Strains	Biomass ( $\mu\text{m}^3/\mu\text{m}^2$ )		Thickness distribution ( $\mu\text{m}$ )		Roughness coefficient (Ra*)	
	MSg	MSg + mannose	MSg	MSg + mannose	MSg	MSg + mannose
R99	2.26±0.54	1.56±0.35**	4.25	3.61**	1.05	1.8**
$\Delta mshA-1$	1.42±0.48*	1.42±0.10	3.23*	2.94	2.24*	2.14
$\Delta mshA-2$	1.99±0.13	1.59±0.54**	4.14	2.87**	1.13	1.99**
$\Delta mshA-3$	2.11±0.33	1.39±0.36**	4.11	3.02**	1.11	2.12**
$\Delta mshA-1/2$	1.50±0.5*	N/T	N/T	N/T	N/T	N/T
$\Delta mshA-1/3$	1.44±0.14*	N/T	N/T	N/T	N/T	N/T
$\Delta mshA-2/3$	1.97±0.12	N/T	N/T	N/T	N/T	N/T
$\Delta mshA-123$	1.52±0.15*	N/T	N/T	N/T	N/T	N/T
<i>cmshA-1</i>	1.92±0.16	1.35±0.21**	3.98	2.97**	1.24	2.23**

Biofilms total biomass, thickness distribution and roughness coefficient was measured and analyzed via Comstat 2.1® (Heydorn *et al.*, 2000) \*: significant differences in biomass between the wild type and the mutant strains was determined using ANOVA ( $P < 0.05$ ). \*\*: significant differences in biomass between the wild type and the derivative mutants grown with 4% D-mannose was determined using ANOVA ( $P < 0.05$ ).

**Table.5 Virulence for eels and resistance of strain R99 and its derivative mutants to serum**

Strains	Virulence <sup>a</sup>		Resistance to <sup>b</sup>	
	intra-peritoneal	Immersion	Eel serum	Human serum
R99	1.5x10 <sup>2</sup>	1.4 x 10 <sup>6</sup>	+++	++
R99 + pTfoX	1.2x10 <sup>2</sup>	1.1x10 <sup>6</sup>	+++	++
$\Delta mshA-1$	1.1x10 <sup>2</sup>	> 10 <sup>7</sup> *	+++	++
$\Delta mshA-2$	1.2x10 <sup>2</sup>	1.2 x 10 <sup>6</sup>	+++	++
$\Delta mshA-3$	1.4x10 <sup>2</sup>	NT	+++	++

a. Virulence was expressed as LD<sub>50</sub> in CFU/fish in case of intra-peritoneal injection and CFU/ml in case of bath infection (Amaro et al., 1995). Farmed eels (European eel *Anguilla anguilla*, were purchased from a local eel-farm that does not vaccinate against *V. vulnificus*).

b. Resistance to eel and human serum was measured as the ratio between bacterial counts at 0h and 4h of incubation.

- <1; 1<+<10; 10<+<25; +++>25.

\*: significant differences (P< 0.05) between R99 and the derivative mutant strains.

**Table S1. Species, strains and plasmids used in the study**

Species, strain, plasmid	Characteristics	Source
R99	<i>V. vulnificus</i> zoonotic clonal-complex representative strain CECT4999, (Roig <i>et al.</i> , 2018)	Diseased eel
R99 + pTfoX	CECT4999 + pTfoX	This study
R99 + <i>LacZ</i>	CECT4999 + pVSV103	Lab Collection
$\Delta mshA-1$	CECT4999 <i>mshA-1</i> defective mutant	This study
$\Delta mshA-2$	CECT4999 <i>mshA-2</i> defective mutant	This study
$\Delta mshA-3$	CECT4999 <i>mshA-3</i> defective mutant	This study
$\Delta mshA-1/2$	CECT4999 <i>mshA-1/mshA-2</i> defective mutant	This study
$\Delta mshA-1/3$	CECT4999 <i>mshA-1/mshA-3</i> defective mutant	This study
$\Delta mshA-2/3$	CECT4999 <i>mshA-2/mshA-3</i> defective mutant	This study
$\Delta mshA-123$	CECT4999 <i>mshA-1/mshA-2/mshA-3</i> defective mutant	This study
<i>cmshA-1</i>	$\Delta mshA-1$ + pMMB207 carrying the <i>mshA-1</i> gene	This study
$\Delta mshA-1$ + GFP	$\Delta mshA-1$ + pVSV102	This study
$\Delta mshA-2$ + GFP	$\Delta mshA-2$ + pVSV102	This study
$\Delta mshA-3$ + GFP	$\Delta mshA-3$ + pVSV102	This study
$\Delta mshA-1/2$ + GFP	$\Delta mshA-1/2$ + pVSV102	This study
$\Delta mshA-1/3$ + GFP	$\Delta mshA-1/3$ + pVSV102	This study
$\Delta mshA-2/3$ + GFP	$\Delta mshA-2/3$ + pVSV102	This study
$\Delta mshA-123$ + GFP	$\Delta mshA-123$ + pVSV102	This study
SM17 $\lambda$ pir	<i>E. coli</i> cloning strain and transposon donor, <i>pir</i> <sup>+</sup> <i>tra</i> <sup>+</sup> , Sm <sup>R</sup> , Tmp <sup>R</sup>	(R. Simon, 1983)
SM17 $\lambda$ pir + GFP	SM17 $\lambda$ pir + pVSV102	This study
Plasmids	Characteristics	Source
pMMB207	Complementation vector	Addgene
pTfoX	pMMB207 vector with inducible <i>tfoX</i> gene, Amp <sup>R</sup>	(Dalia <i>et al.</i> , 2014)
pVSV102	Vector with inducible green fluorescent protein (GFP) gene, km <sup>R</sup>	(Dunn <i>et al.</i> , 2006)
pVSV103	Vector with inducible <i>lacZ</i> gene, km <sup>R</sup>	(Dunn <i>et al.</i> , 2006)

Amp: Ampicillin  
Sm: Streptomycin  
Tmp: Trimethoprim  
Km: Kanamycin

**Table S2. Primers used for mutation and complementation**

Product	Primer	Sequence	Size (bp)	Utilization
<i>ΔmshA-1</i>	MshA-1	CCTGTATAAGCAGGAATGGC	1200±	Upstream construct
	MshATmp-2	GTCGACGGATCCCCGGAATCATAGTGTCTCTCTCTA		
	MshACnf-2	AACCTCTTACGTGCCGATCACATAGTGTCTCTCTATG		Downstream construct
	MshATmp-3	GAAGCAGCTCCAGCCTACATAGAAAAGTTAAGTGCCTT		
	MshACnf-3	AGTGGCAGGGCGGGCGTAGAAAAGTTAAGTGCCTTA		
	MshA-4	TCACTGCCGTCCATGTTGC		
<i>ΔmshA-2</i>	MshA2-1	CCAAATGAGAGAGCTTCTCT	1200±	Upstream construct
	MshA2Tmp-2	GAAGCAGCTCCAGCCTACATAATCATAGACACTAGATAAGT		
	MshA2Km-2	GATGCTCGATGAGTTTTTCTAATAATCATAGACACTAGAT		Downstream construct
	MshA2Tmp-3	GTCGACGGATCCCCGGAATCATTATTCTCTCTATTTTTAT		
	MshA2Km-3	GTAGAAAAGATCAAAGGATCTTCCATTATTCTCTCTATTT		
	MshA2-4	CTCAAGAAATTTGCCATTTTCTA		
<i>ΔmshA-3</i>	MshA3-1	TATGGCGGGGGCGATGAG	1200±	Upstream construct
	MshA3Tmp-2	GTCGACGGATCCCCGGAATCATCCGTACTCCACTACTCA		
	MshA3Tmp-3	GAAGCAGCTCCAGCCTACATAGAACATTGACTCACCAACAA		Downstream construct
	MshA3-4	CATAACAATAATGGCGCAAATAG		
<i>cmshA-1</i>	MshA-Fx	AACAGAATTCGAGCTCGGTACATGAAAAGACAAGGCGGTTTC	468	Complementation
	MshA-Rx	TGATTTAATCTGTATCAGGCTGCTATTGCGCGCCGCAAGC		
pMMB207	pMMB207-F	TTGGCGGATGAGAGAAGATT	9000±	Complementation
	pMMB207-R	GTACCGAGCTCGAATTCTGTT		
Trimethoprim	Tp-F	ATCCGGGATCCGTCGAC	692	Antibiotic cassette
	Tp-R	TGTAGGCTGGAGCTGCTTC		
Chloramphenicol	Cf-F	TGATCGGCACGTAAGAGGTT	760	Antibiotic cassette
	Cf-R	CGCCCCGCCCTGCCACT		
Kanamycin	Km-F	GAAGATCCTTTGATCTTTTCTAC	937	Antibiotic cassette
	Km-R	TTAGAAAAACTCATCGAGCATC		
<i>mshA-1</i>	qPCRM1-F	ACAAGGCGGTTTACCCTG	105	qRT-PCR
	qPCRM1-R	CGCGCATCATCTGCAGAT		
<i>mshA-2</i>	qPCRM2-F	AGCATCGGATAGCCATAAAT	115	qRT-PCR
	qPCRM2-R	TTATGGTGTCAATCTGCACA		
<i>mshA-3</i>	qPCRM3-F	GAAGTAGTGTCGTCATCGTC	105	qRT-PCR
	qPCRM3-R	TTCTAGCCGTGCCACTTTG		

RESEARCH ARTICLE



## Comprehensive identification of *Vibrio vulnificus* genes required for growth in human serum

M. Carda-Diéguez<sup>a,b</sup>, F. X. Silva-Hernández <sup>a</sup>, T. P. Hubbard<sup>c,e</sup>, M. C. Chao <sup>c,d,e</sup>, M. K. Waldor <sup>c,d,e</sup> and C. Amaro <sup>a,b</sup>

<sup>a</sup>Department of Microbiology and Ecology, University of Valencia. Dr. Moliner 50, Burjassot, Spain; <sup>b</sup>ERI BIOTECMED, Universitat de València. Dr Moliner 50, Burjassot, Spain; <sup>c</sup>Division of Infectious Disease, Brigham and Women's Hospital, Boston, Massachusetts, United States of America; <sup>d</sup>Howard Hughes Medical Institute, Boston, Massachusetts, United States of America; <sup>e</sup>Department of Microbiology and Immunobiology, Harvard Medical School, Boston, Massachusetts, United States of America

### ABSTRACT

*Vibrio vulnificus* can be a highly invasive pathogen capable of spreading from an infection site to the bloodstream, causing sepsis and death. To survive and proliferate in blood, the pathogen requires mechanisms to overcome the innate immune defenses and metabolic limitations of this host niche. We created a high-density transposon mutant library in YJ016, a strain representative of the most virulent *V. vulnificus* lineage (or phylogroup) and used transposon insertion sequencing (TIS) screens to identify loci that enable the pathogen to survive and proliferate in human serum. Initially, genes underrepresented for insertions were used to estimate the *V. vulnificus* essential gene set; comparisons of these genes with similar TIS-based classification of underrepresented genes in other vibrios enabled the compilation of a common *Vibrio* essential gene set. Analysis of the relative abundance of insertion mutants in the library after exposure to serum suggested that genes involved in capsule biogenesis are critical for YJ016 complement resistance. Notably, homologues of two genes required for YJ016 serum-resistance and capsule biogenesis were not previously linked to capsule biogenesis and are largely absent from other *V. vulnificus* strains. The relative abundance of mutants after exposure to heat inactivated serum was compared with the findings from the serum screen. These comparisons suggest that in both conditions the pathogen relies on its Na<sup>+</sup> transporting NADH-ubiquinone reductase (NQR) complex and type II secretion system to survive/proliferate within the metabolic constraints of serum. Collectively, our findings reveal the potency of comparative TIS screens to provide knowledge of how a pathogen overcomes the diverse limitations to growth imposed by serum.

### ARTICLE HISTORY

Received 6 November 2017  
Accepted 16 March 2018

### KEYWORDS



capsule; resistance to human complement; septicemia; transposon insertion sequencing (TIS); *Vibrio vulnificus*



## Introduction

*Vibrio vulnificus* is an aquatic, gram-negative bacterium capable of causing a range of pathologies upon infecting fish or human hosts [1,2]. *V. vulnificus* infection of fish occurs principally in aquaculture, when outbreaks of hemorrhagic septicemia are perpetuated by *V. vulnificus* transmission through water or direct contact among animals. In humans, two distinct types of disease –severe skin lesions and septicemia– commonly result from *V. vulnificus* infection. Skin lesions develop following exposure of wounds to seawater or marine animals colonized by *V. vulnificus*, whereas septicemia results from ingestion of seafood contaminated by the pathogen [1]. Wound infections can also result in septicemia, particularly in immunocompromised individuals and those with high blood iron levels associated with chronic liver

diseases, who exhibit 80-fold higher risk of *V. vulnificus* septicemia than healthy individuals [1,3].

The different contexts of *V. vulnificus* infection, in addition to the geographic range and pathogenicity of this organism, are used to classify *V. vulnificus* into three biotypes (Bt) [4,5]. In general, Bt1 causes sporadic cases of human skin infections and gastroenteritis and it is considered the most dangerous one [1], Bt2 causes both zoonotic cases of human skin infections and outbreaks of infection in fish [2,6], and Bt3 causes human skin infections associated with the handling of healthy tilapia (a spiny fish) [5,7]. In susceptible hosts, all three biotypes are thought to be able to spread from the skin or intestinal epithelium to the bloodstream, where they replicate rapidly and cause severe disease [8]. A recent phylogenomic analysis from the core genome of 80 *V. vulnificus*

**CONTACT** C. Amaro  [carmen.amaro@uv.es](mailto:carmen.amaro@uv.es)  ERI BioTecMed, Department of Microbiology and Ecology, Faculty of Biology, University of Valencia, Campus de Burjassot, Valencia 46100, Spain.

 Supplemental data for this article can be accessed at  [publisher's website](#).

© 2018 The Author(s). Published by Informa UK Limited, trading as Taylor & Francis Group. This is an Open Access article distributed under the terms of the Creative Commons Attribution License (<http://creativecommons.org/licenses/by/4.0/>), which permits unrestricted use, distribution, and reproduction in any medium, provided the original work is properly cited.

strains belonging to the three Bts demonstrates that this species is subdivided in five well-supported phylogenetic groups or lineages that do not correspond to Bts [9]. Lineage 1 comprises a mixture of clinical and environmental Bt1 strains, most of them involved in human clinical cases related to raw seafood ingestion. Lineage 2 accounts for a mixture of Bt1 and Bt2 strains from various sources related to aquaculture industry. Lineage 3 comprises exclusively all Bt3 strains, and Lineages 4 and 5 comprise a few Bt1 strains associated with specific geographical areas. This study also proposes a new updated classification of the species based on phylogenetic lineages as well as the inclusion of all Bt2 strains in a unique pathovar with the particular ability to cause fish vibriosis due to a transferable virulence plasmid (pathovar or *pv. piscis*) [10].

An eel (*Anguilla anguilla*) model of infection enabled study of mechanisms underlying the growth and pathogenesis of *pv. piscis* strains *in vivo* [2]. By using this model, it was demonstrated that *V. vulnificus* must overcome multiple host processes that constrain bacterial growth by using a series of virulence factors that promote survival within an aquatic host: i.e. the chromosomally-encoded O-antigen confers resistance to fish complement and a plasmid-borne gene encodes an outer membrane protein receptor for fish transferrin that contributes to growth in serum [11–13]. The *V. vulnificus* genes and processes related to human diseases are less well understood, due both to the greater genetic variability among *V. vulnificus* strains that induce pathology in humans and to variation in disease severity associated with patient immune status and blood-iron content [1]. Nevertheless, several *V. vulnificus* factors have been reported to play a role in human septicemia such as a potassium pump [14], a capsular polysaccharide (CPS) [15–18], a surface lipoprotein [19], the siderophore vulnibactin [16], the flagellum [20,21], the RtxA (or MARTX) toxin [22,23], and surface modifications by sialic acid moieties [24], all of which either contribute to growth in serum (potassium pump, siderophore...) or inflammation (CPS, lipoprotein, RtxA...) or immune evasion (RtxA, CPS...) or invasion (flagellum..).

To identify bacterial processes that enable *V. vulnificus* growth in human serum (HS) we undertook a forward genetic screen. Using an isolate of *V. vulnificus* capable of robust growth in HS, we first generated a nearly saturated transposon-insertion library and performed transposon-insertion sequencing to identify genes that are likely necessary for the *in vitro* growth of *V. vulnificus*. Comparative analyses that integrated these data with previously published results from transposon studies in other *Vibrio* species enabled us to define a set of core genes that multiple vibrios require for growth *in*

*vitro*. Additionally, library sequencing following passage of the *V. vulnificus* mutant library in HS allowed us to identify genes that contribute to growth in this selective condition. To distinguish *V. vulnificus* genes that enable resistance to heat-labile antimicrobial factors from genes required to overcome the nutritional limitations, we developed an approach to integrate the results of parallel screens conducted in HS and heat inactivated HS. Our findings provide a comprehensive assessment of the bacterial factors required for *V. vulnificus* growth in HS and uncovered new genes required for CPS production in this human pathogen.

## Results

### *V. vulnificus* transposon library: generation and analysis

We selected a *V. vulnificus* strain able to multiply in HS by assaying the viability in serum of a selection of isolates representative of the different phylogenetic lineages [9] (Table S1). The selected strain was YJ016 (Fig. 1), a blood isolate from a septicemic patient who ingested raw oysters in Taiwan [25]. Then, we implemented Transposon-Insertion Sequencing (TIS) [26] in YJ016 by adapting an established mutagenesis protocol [27]. We used conjugation to deliver the Mariner-based Himar1 transposon, which randomly inserts into TA dinucleotide sequences

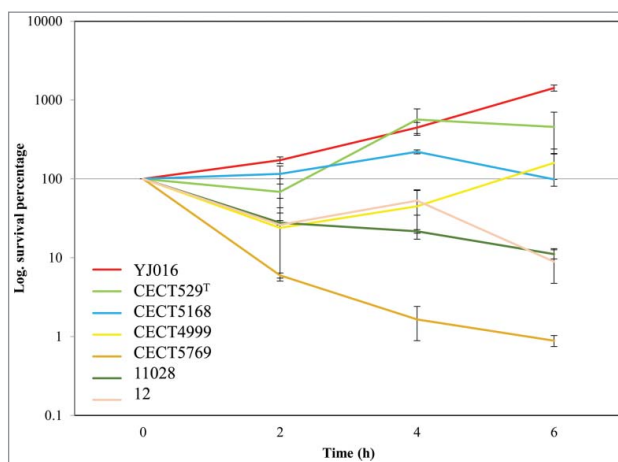


**Figure 1.** Resistance of *V. vulnificus* to HS. The initial bacterial population of the different *V. vulnificus* strains was considered “100” and survival at each time was calculated as a percentage. Bars indicate the standard deviation for three replicates. CECT, Spanish Type Culture Collection. Subspecific classification of the strains according to<sup>9</sup>: YJ016 and CECT5168 (or CDC-7184), formerly classified as Bt1, belong to Lineage 1, CECT529<sup>T</sup> (or ATCC27562, type strain of the species), formerly classified as Bt1, belongs to Lineage 2; CECT4999 and CECT5769, formerly classified as Bt2 belongs to Lineage 2 and *pv. piscis*; 11028 and 12, formerly classified as Bt3, belongs to Lineage 3.



[28,29]. Our analysis revealed that the *V. vulnificus* mutant library contained at least 159,709 unique insertion mutants, corresponding to disruption of 75.9% of potential insertion sites. Genes were binned according to the proportion of TA sites disrupted per gene and these data were plotted for *V. vulnificus*' two chromosomes (Fig. 2AB). For both chromosomes, insertions were detected in >50% of potential insertion sites within most genes, with a modal insertion frequency of 70–80%, suggesting that 70–80% of non-essential insertion sites have sustained one or more insertion.

Approximately 300 genes encoded on *V. vulnificus*' large chromosome were disrupted in fewer than 10% of potential insertion sites, giving rise to a secondary peak within the distribution curve showing gene disruption frequency (Fig. 2A). This minor peak was absent from the small chromosome's distribution curve (Fig. 2B). Both observations are consistent with TIS-based studies of other *Vibrio* species, which report that the large chromosome harbours a disproportionately large number of essential genes relative to the small chromosome [27].

To identify the genes required for optimal *V. vulnificus* growth *in vitro*, we implemented the EL-ART-IST pipeline, which systematically identifies insertion mutants that are underrepresented among the pool of viable mutants that constitutes the transposon library. When all or most of the TA sites in a gene are

infrequently disrupted, the gene is classified as “underrepresented” (U, in Fig. 2A,2B), and these genes are likely essential for *V. vulnificus* viability. When only a portion of a TA sites in a gene are infrequently disrupted, the gene is classified as “regional” (R, in Fig. 2A,2B), suggesting that part of the gene is essential for *V. vulnificus* viability. Finally, when few or none of the TA sites within a gene are infrequently disrupted, the gene is classified as “neutral” (N, in Fig. 2A,2B), and these genes are presumed to be dispensable for *V. vulnificus* viability. EL-ART-IST classified 455 chromosomal *V. vulnificus* genes as underrepresented and 195 genes as regional (9% and 4%, respectively) while the other 4259 chromosomal genes were classified as neutral (see Table S2, where these data are presented in full). Most of the non-neutral genes were encoded on the large chromosome; however, 59 were encoded on the small chromosome and 4 were encoded on a conjugative plasmid, pYJ016, which is dispensable for bacterial growth (Lien-I Hor, personal communication) (Fig. 2 and Table S2). Similar TIS data studies have shown that factors such as binding of the histone-like nucleoid structuring protein H-NS can lead to a low frequency of transposon-insertion in some non-essential genes [31]; consequently, the underrepresented and regional categories provide a comprehensive overestimate of the genes essential for the organism's growth *in vitro*

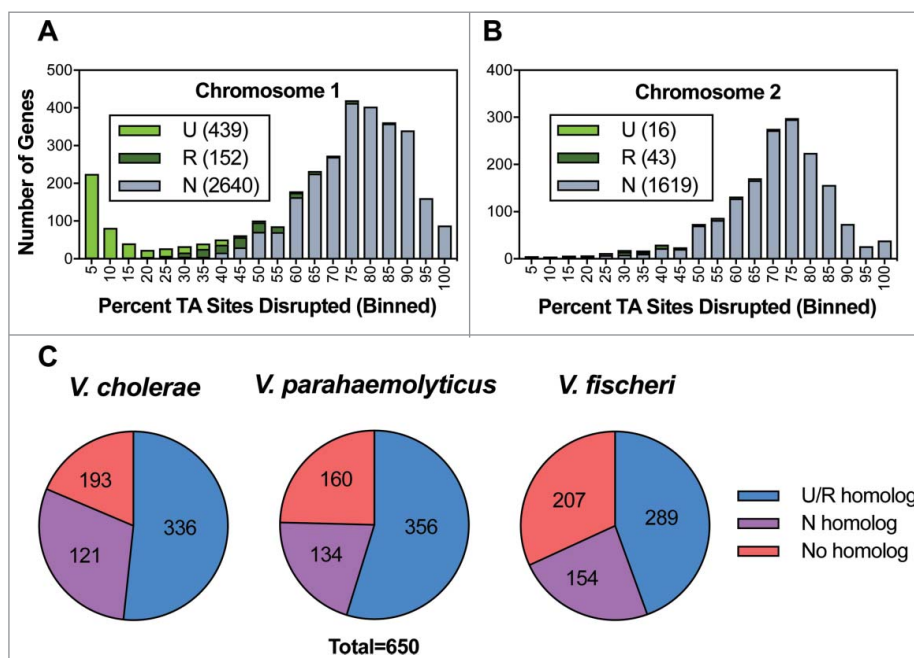


**Figure 2.** Characterization of the *V. vulnificus* transposon insertion library. Distribution of the percentage of TA sites disrupted per gene encoded on the large chromosome (A) and the small chromosome (B). Genes classified as underrepresented (U), regional (R), or neutral (N) are represented within each bin for each chromosome. (C) Status of genes homologous to a non-neutral *V. vulnificus* gene in *V. cholerae*, *V. parahaemolyticus*, and *V. fischeri*. U/R indicates underrepresented, regional, or comparably classified, homolog and N indicates neutral or comparably classified homolog.

[32]. This should be taken into account especially in case of the plasmid as extrachromosomal elements are the main targets for H-NS proteins [33].

To better understand the bacterial processes required for the growth of *V. vulnificus* relative to other *Vibrio* species, we compared the non-neutral *V. vulnificus* genes with similar TIS-based gene classifications from *V. cholerae*, *V. parahaemolyticus*, and *V. fischeri* [27,32,34]. The 650 chromosomally-encoded non-neutral *V. vulnificus* genes showed greatest concordance (i.e., non-neutral classification in both data sets) with *V. parahaemolyticus* (356), followed by *V. cholerae* (336) and *V. fischeri* (289) (Fig. 2C). However, these comparisons should be interpreted with caution because of methodological biases that could reflect evolutionary relatedness (e.g., *V. vulnificus* and *V. parahaemolyticus* encode more genes than *V. cholerae* and *V. fischeri*). Organism-specific gene duplications and speciation events that yielded functionally redundant genes lacking sequence homology may also account for species-specific results.

Despite such potential confounding factors, 253 genes were concordantly classified as non-neutral across the 4 species, and therefore represent a TIS-defined set of *Vibrio* ‘essential’ genes. The list of concordant genes, along with their functional categorization (based on ‘Gene Ontology’ obtained via Uniprot [35] and discrepancies identified from individual comparisons of each species against *V. vulnificus*, are reported in the supplemental materials (Table S3 and S4).

Since the plasmid pYJ016 is not found in *V. parahaemolyticus*, *V. cholerae* or *V. fischeri*, the classification of 4 plasmid-encoded genes as non-neutral in *V. vulnificus* was somewhat unexpected. Two of these genes, *VVP32* and *VVP66*, encode putative addiction module antitoxins, and thus are likely involved in plasmid maintenance. A low frequency of transposon insertion attributable to H-NS binding could explain why the other two non-neutral plasmid genes, *VVP39*, a putative PilT protein, and *VVP67*, a hypothetical protein, were classified as underrepresented.

We also compared the *V. vulnificus* gene classifications and the 253 non-neutral genes observed across all 4 *Vibrio* species to the set of essential genes from *E. coli* K-12, in order to identify genetic requirements for bacterial growth that differ between vibrios and other genera. *V. vulnificus* homologs of 31 essential *E. coli* genes were classified as neutral in our analysis. Of these, 20 were found to be duplicated in the *V. vulnificus* genome, which likely accounts for the dispensability of individual homologs for the strain’s *in vitro* growth. The remaining 11 genes (Table S5) were identified as discordant in previously published comparisons of the essential *E. coli* genes to *V. cholerae* and *V. parahaemolyticus* genes

classified as neutral [27,32], suggesting that these genes’ lack of essentiality is a common feature that distinguishes vibrios from *E. coli*. These genes include riboflavin biosynthesis and chromosome compaction genes, some of which Chao *et al.* confirmed are dispensable for the viability of *V. cholerae* [27]. Future studies can investigate how such processes differentially contribute to the viability of *E. coli* and vibrios and how their cellular roles have diverged among these gamma-proteobacteria.

### Identification of *V. vulnificus* genes required for survival/growth in HS

We used TIS to identify genes involved in resistance to the multiple heat sensitive (i.e. complement proteins) and heat stable (nutritional constraint) anti-bacterial factors present in HS [36]. First, we optimized screening conditions by generating a mutant unable to synthesize capsular polysaccharides by in-frame deletion. The selected gene was *wza*, a gene encoding an outer membrane protein involved in the CPS translocation [37,38]. As expected, the mutant  $\Delta VV0337/\Delta wza$  exhibited phenotypes indicative of capsule deficiency (translucent colonies on agar plates and sedimentation/aggregation in the bottom of culture tubes) (Fig. S1). The mutant was incubated in HS and we found that no cfu were recovered after 2h incubation (Fig. 3C). Consequently, we determined that 2 h incubation would be sufficient to select against mutants unable to survive/grow within HS.

Then, we compared the relative abundance of insertion mutants in the transposon library when this was incubated in HS vs. LB (Fig. 2 and 3). We binned genes from both chromosomes according to the proportion of TA sites disrupted per gene and plotted these data for the LB and serum populations (Fig. 3A). Comparison of the LB and HS distributions revealed that the large population of genes with insertions in a high proportion of TA sites in the LB library underwent a substantial left-shift in the HS-selected library. This trend is consistent with a genotype-independent population constriction (i.e., an experimental bottleneck) that occurred during exposure to HS. We implemented a modified version of the Con-ARTIST pipeline, which performs simulation-based normalization to model and compensate for the stochastic effects of an experimental bottleneck [30], to compare the abundance of individual mutants in the LB and HS-selected libraries (Table S6). Importantly, our modified analysis integrates data from independent insertions across the length of each gene in an additional effort to minimize the impacts of experimental noise. Thus, our analysis was restricted to the 4243 genes with 5+ independent insertions; 687 did not meet this criterion and are classified as “insufficient data”, (ID) in

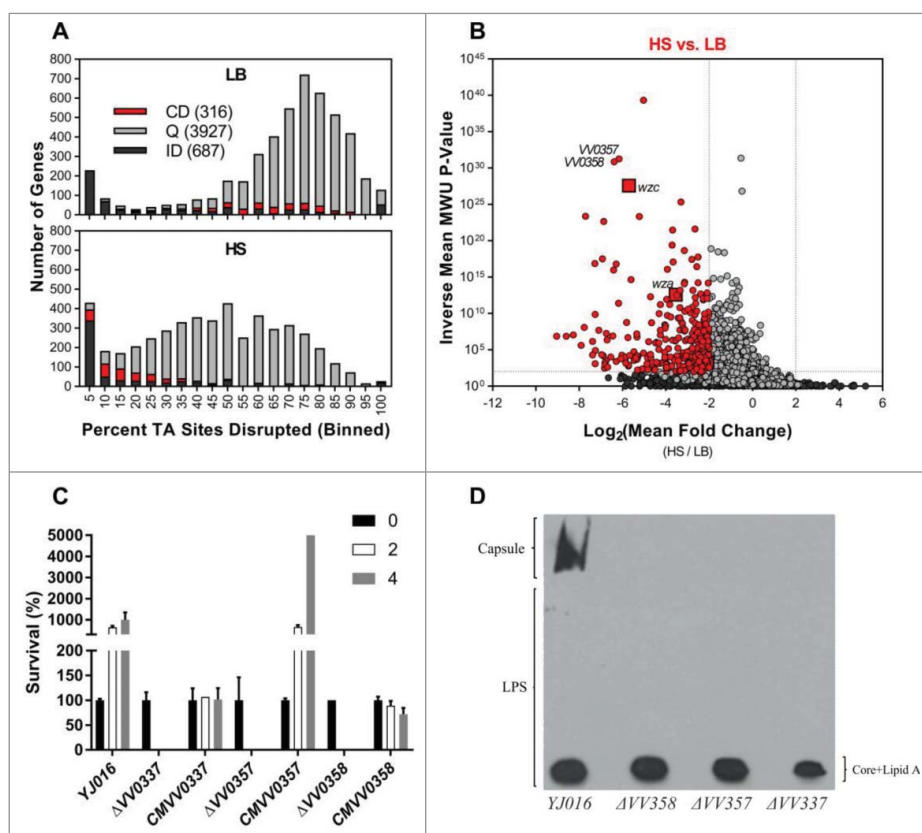


**Figure 3.** Identification of genes conditionally depleted in human serum (A and B) and characterization of mutants in selected genes (C and D). (A) Distribution of the percentage of TA sites disrupted per gene in the LB or HS-selected libraries. Genes classified as conditionally depleted (CD), queried (Q), or insufficient data (ID) are indicated in each bin. (B) Results of Con-ARTIST analysis. x-axis indicates change in relative abundance of insertion mutants per gene between LB and HS, and the y-axis indicates the concordance of independent insertion mutants within each gene. Genes exhibiting a greater than 4-fold change ( $\text{Log}_2(\text{mean fold change}) < -2$  or  $> 2$ ) across multiple mutants (mean inverse P-value  $> 10^2$ ) are considered conditionally depleted and are shown in red. Large red squares indicate *wza* and *wzc*, which are known to be attenuated in HS. (C) Survival percentage of YJ016, the deletion mutants and its complemented strains after 2 and 4 h incubated in human serum. (D) CPS detection by immunostaining. Bacteria were grown in LB (1% NaCl), associated-cell polysaccharides were extracted, separated by SDS-PAGE, transferred to NC-sheets and immunostained with specific antibodies against YJ016.

**Fig 3A.** 316 genes met criteria used to define the loci required to survive/grow in HS ( $\text{Log}_2(\text{mean fold change}) < -2$ , inverse mean MWU P-value  $> 100$ ; **Fig. 3B**, genes shown in red); these genes were classified as conditionally depleted (CD).

As expected, these genes included the control gene *wza* (VV0337) together with *wzb* (VV0339) and *wzc* (VV0340) (**Fig. 3B**, large squares), whose homologs also encode proteins involved in the translocation of CPS type 1 polysaccharides (CPS-1) in *E. coli* and *V. vulnificus* (PMC403799) [37,39–41], as well as numerous (23) additional genes that likely mediate lipopolysaccharide (LPS) and CPS biosynthesis and transport. Identification of genes previously linked to capsule biogenesis and sensitivity to HS in other strains [37–42] provides confidence that our screening approach and analysis is sufficient to identify genes required for survival/growth in HS. Genes outside of the CPS locus that were found to be required for growth in HS include loci predicted to

encode ABC transporters, mediators of succinate metabolism, Clp protease, genes for nucleotide biosynthesis, the virulence  $\text{K}^+$  related transporter (*trkA*), the membrane protein OmpH, the TolBARQ membrane system, the type 2 secretion system (T2SS) and the  $\text{Na}^+$  transporting NADH-ubiquinone reductase (NQR) complex.

To validate the results of our screen, we selected 2 genes – VV0357 and VV0358 – for further study. Both genes were classified as conditionally depleted following exposure to HS (**Fig. 3B**), but neither were previously associated with survival in HS. We generated in-frame deletions of each gene and assessed the survival/growth of these single-gene deletion mutants in HS relative to wild type *V. vulnificus* and the  $\Delta$ VV0337 mutant (**Fig. 3C**). Both the  $\Delta$ VV0357 and  $\Delta$ VV0358 mutants were as sensitive as the  $\Delta$ VV0337 mutant to HS; no colonies were recovered after 2 h incubation in HS (**Fig. 3C**). In addition to serum-sensitivity, the  $\Delta$ VV0357 and  $\Delta$ VV0358 strains exhibited phenotypes consistent with

**Table 1.** Virulence assays on iron-overloaded BALB/C mice.

Strain	LD <sub>50</sub> (cfu/mouse)*
YJ016	1 ± 0.5 × 10 <sup>2</sup>
ΔVV337	>10 <sup>7</sup>
CMVV337	2.5 ± 5 × 10 <sup>2</sup>
ΔVV357	>10 <sup>7</sup>
CMVV357	3 ± 2 × 10 <sup>3</sup>
ΔVV358	>10 <sup>7</sup>
CMVV358	7 ± 2 × 10 <sup>3</sup>

\*average and standard deviation from three different experiments.

capsule-deficient mutants, including agglutination in culture tubes and translucent colony morphology (Fig. S1). Given the importance of the capsule for *V. vulnificus* growth *in vivo*, we tested the virulence of the mutant strains for mice (iron-overloaded model) and found that all three mutants were avirulent (Table 1). Complementation with plasmid-based expression of the deleted genes was sufficient to restore wild type phenotypes to the mutant strains (Fig. S1 and Table 1), although the complemented strains survived in HS without multiplication (Fig. 3C). Therefore, we hypothesized that VV0357 and VV0358, like *wza* homologue VV0337, are involved in capsule biosynthesis. The absence of capsule production in the VV0357 and VV0358 mutants was confirmed via immunoblotting: no CPS was observed in the surface polysaccharide fractions from ΔVV0357 and ΔVV0358 (Fig. 3D). Collectively, these results indicate that VV0357 and VV0358 encode proteins that are necessary for capsule formation, HS-resistance, and virulence in mice.

VV0357 and VV0358 are annotated as a “zinc-binding dehydrogenase” and a “hypothetical protein” respectively, and both genes are located in relative proximity to the annotated CPS gene cluster (Fig. S2). However, homology searches revealed VV0358 and VV0357 are not widespread among *V. vulnificus* and only the strain CG64, an environmental isolate recovered in geographic and temporal proximity to the YJ016 [43], encodes a VV0358 homolog, raising the possibility that this gene was acquired by horizontal transmission (Fig. S2). Phyre2-based structural homology analyses suggest that VV0357 encodes a protein with two transmembrane helices potentially implicated in protein translocation and that VV0358 encodes a protein with strong structural homology to a heparinase III protein (Fig. S3). BLASTP queries also identified a putative heparinase II/III-like domain (pfam07940) in VV0358.

### Comparison of the genes required for growth in HS and hiHS

We analysed the relative abundance of insertion mutants in the *V. vulnificus* transposon library when

this was incubated in heat inactivated HS (hiHS) to discriminate between genetic factors that protect against heat sensitive vs. heat labile constraints. Again, we binned genes from both chromosomes according to the proportion of TA sites disrupted per gene (Fig. 4A) and compared these data for the LB and hiHS populations. The left-shift in the large population of genes disrupted in a high proportion of TA sites was minimal compared to that observed in the HS-selected library, indicating that the experimental bottleneck was less severe in the hiHS screen. Using Con-ARTIST, we compared the abundance of individual mutants in the LB and hiHS-selected libraries (Table S7), with analysis restricted to the 4268 chromosomal genes with 5+ independent mutations, and 662 genes classified as “insufficient data”. 223 genes met criteria used to define the genes required to survive/grow in hiHS ( $\text{Log}_2(\text{mean fold change}) < -2$ , inverse mean MWU *P*-value > 100) (blue genes in Fig. 4B). Thus, fewer genes are classified as conditionally depleted following exposure to hiHS than HS. Notably, none of the *wza-wzb-wzc* genes found to be conditionally depleted in HS were conditionally depleted in hiHS, which indicates, as expected, that the components of serum (such as complement) that prevent the survival/growth of capsule deficient mutants are heat sensitive. Several genes that encode or are predicted to encode ABC transporters, Clp protease, succinate metabolism, TolBARQ, TrkA K<sup>+</sup> transporter, OmpH membrane protein, T2SS, and the NQR system were found to be conditionally depleted in hiHS as well as in HS. Thus, we speculate that these genes contribute to processes required for growth in HS independently of the heat-labile antimicrobial properties of HS.

To integrate the results of our parallel screens in HS and hiHS, we compared each gene’s  $\text{Log}_2(\text{MFC})$  values (vs. LB, as shown in Figs. 3B and 4B), which are a reflection of fitness in the selective condition, for the parallel screens. To minimize the effects of noise, we restricted this comparison to the 4224 genes with 5+ independent mutations in both the HS and hiHS analyses (706 genes did not meet this criterion and are classified as “insufficient data”) (Fig. 4C). Most genes showed minimal difference between the two screens ( $-3 < \Delta\text{Log}_2\text{MFC} < 3$ ), however 83 genes showed a > 8-fold discrepancy between the two screens and were classified as “divergent” (the 2 tails in Fig 4C) (Table S8-S9). To highlight the source of disparity between the HS and hiHS screens, we plotted the  $\text{Log}_2\text{MFC}$  values observed in HS and hiHS on the x- and y-axes, respectively (Fig. 4D). Genes in the lower right of the graph exhibited more severe



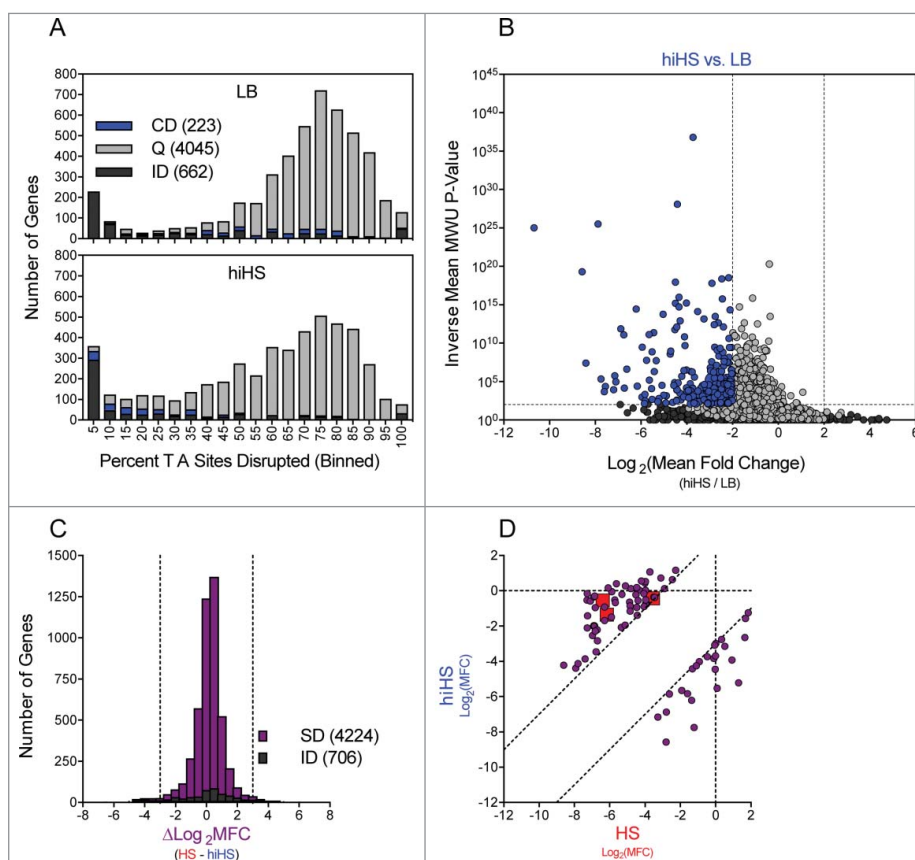


**Figure 4.** Identification of genes conditionally depleted in heat inactivated human serum. (A) Distribution of the percentage of TA sites disrupted per gene in the LB or hiHS-selected libraries. Genes classified as conditionally depleted (CD), queried (Q), or insufficient data (ID) are indicated in each bin. (B) Results of Con-ARTIST analysis. x-axis indicates change in relative abundance of insertion mutants per gene between LB and HS, and the y-axis indicates the concordance of independent insertion mutants within each gene. Genes exhibiting a greater than 4-fold change ( $\text{Log}_2(\text{mean fold change}) < -2$  or  $> 2$ ) across multiple mutants (mean inverse P-value  $> 10^2$ ) are considered conditionally depleted. (C) The difference in  $\text{Log}_2(\text{Mean Fold Change})$  (HS – hiHS) was plotted for SD (sufficient data:  $< 5$  informative sites in one or more comparisons) genes. (D)  $\text{Log}_2(\text{Mean Fold Change Values})$  from the HS and hiHS samples are plotted on the x- and y-axes, respectively, for genes with  $> 8$ -fold difference between the two selections. Large red squares indicate *wza*, *VV0357*, and *VV0358*, which were conditionally depleted in HS but not in hiHS.

attenuation in hiHS than in HS, while genes in the upper left of the graph, including *VV0337*, *VV0357*, *VV0358*, and other components of the CPS locus, exhibited more severe attenuation in HS than in hiHS. Apart from the CPS locus, a number of additional genes, including 32 predicted to encode hypothetical proteins (Table S8), without clear associations with CPS biosynthesis, were also found to be more severely attenuated in HS than in hiHS. Further studies are necessary to determine whether these genes encode previously undescribed mediators of CPS biosynthesis or factors that contribute to additional processes that fortify bacterial growth in the presence of heat-labile antimicrobial factors.

While many heat-labile components of HS are directly bactericidal, the nutrient content of HS also imposes a restriction on bacterial growth [36]. We hypothesized that many of the mutants found to be similarly

attenuated in the HS and hiHS screens had a reduced capacity to overcome the nutritional constraints of HS (Table S9). 110 genes were found to be conditionally depleted in both screens to a comparable degree ( $-3 < \Delta\text{Log}_2\text{MFC} < 3$ ), including all 6 components of the  $\text{Na}^+$  transporting NADH-Ubiquinone reductase (NQR) complex (Fig. S4). The NQR complex is a membrane pump that creates an electrochemical gradient to drive uptake of diverse substrates (including several amino acids, citrate, and inorganic phosphate), and efflux of antibiotics in *V. cholerae* [44]. In addition to the NQR complex, mutants in 7/12 components of the type II secretion system (Fig. S4) were comparably attenuated in both conditions. *V. vulnificus* utilizes the T2SS to secrete a number of proteins, including VvpE, a protease that degrades haemoglobin, and VvhA, a hemolysin [45] and these secreted products may facilitate nutrient acquisition. Moreover, both Clp protease subunits, the potassium

transporter TrkA, 10 dehydrogenases, a TolBARQ system and a series of genes involved in nucleotide metabolism (VV0625, VV0752, VV0775, VV0776 and VV0843) were also attenuated when YJ016 was grown either in HS or hiHS.

## Discussion

Here we report the first application of saturating transposon mutagenesis to study the opportunistic pathogen, *V. vulnificus*. Using TIS, we identified genes that likely enable the growth of *V. vulnificus* in rich media, in addition to those that allow this organism to overcome impediments to bacterial growth intrinsic to HS. By integrating our analysis of these *in vitro* data sets with previously reported transposon studies conducted in related vibrios and with an additional screen conducted in parallel, we offer a strategy to: 1) identify genes required for the growth of multiple *Vibrio* species, and 2) distinguish genes that are required to resist the heat-labile antimicrobial activity of HS, mediated by complement and other protein factors, from genes that enable *V. vulnificus* growth or survival in HS even in the absence of heat-labile antimicrobial activities.

Integrating our observations gleaned from analyses of the *V. vulnificus* transposon-insertion library grown in rich medium with the findings from 3 previous similar studies conducted in related *Vibrio* species revealed that 253 genes are likely required for the *in vitro* growth of all 4 *Vibrio* species. While further studies are necessary to validate and curate this list, these 253 genes represent the best available estimation of the *in vitro* essential gene set of members of the *Vibrio* genus. The majority of core *Vibrio* “essential” genes are essential for the *in vitro* growth of *E. coli* K-12 as well, yet we also identified a number of discordantly classified genes. Many of these discrepancies are apparently attributable to gene duplication events; however others (e.g., riboflavin biosynthesis) constitute verifiable differences in the genes necessary for the growth of vibrios relative to *E. coli*. Thus, our approach, which highlights differentially required growth processes, could facilitate future studies of the genetic divergence of these gamma proteobacteria.

Through our screens of *V. vulnificus* growth in HS, we identified VV0357 and VV0358, which are 1) genetically linked to the capsular polysaccharide biosynthesis gene cluster specifically in *V. vulnificus* YJ016, 2) dispensable for growth in rich medium, and 3) required for growth in HS, but not in hiHS. Additional studies, utilizing in-frame deletions of the VV0357 and VV0358 genes, validated our screen and revealed that VV0357 and VV0358 are necessary for production of the *V. vulnificus* capsule. These findings were further supported by observations

that VV0357 and VV0358 display phenotypes consistent with capsule-deficient mutants, including translucent colony morphology, serum sensitivity and avirulence for mice. Although the role of capsule in resistance to serum has been previously reported in *V. vulnificus*, most of this research was performed with spontaneous translucent variants [16–18]. Regarding the role of both genes in capsule biosynthesis, *in silico* analyses suggest that VV0357 and VV0358 may act as a membrane dehydrogenase and a heparinase II/III-like protein, respectively. Heparinases II and III cleave at the linkages between hexosamine and uronic (or derivatives) acid residues in heparan sulfate, yielding mainly disaccharides. Considering that bacteria with related-CPS can use lyases to degrade molecules aberrantly released to the periplasm [46,47], we propose that CPS of *V. vulnificus* YJ016 may be a heparosan/alginate-like polysaccharide. Nevertheless, this would be a rare event in the species since only one genome (from strain CG64) among the total ones analysed contained a homologous gene. This genome corresponds to a *V. vulnificus* strain isolated from the environment in the same geographical area than YJ016 [43]. This isolate was further analysed and resulted to belong to the same lineage than YJ016 (Roig et al., unpublished). In addition, this isolate was positive for all the genetic markers for human virulence described in *V. vulnificus* [48]. The existence of a specific group of Taiwanese clones presenting a heparosan/alginate-like polysaccharides on their surfaces should be confirmed by chemical analysis of the CPS.

The comparison of the relative abundance of insertion mutants in the HS and hiHS libraries allowed us to discover the genes that the bacterium would use to overcome nutritional constrain in HS. We found evidence that *V. vulnificus* YJ016 could respond to the restriction in purines and pyrimidines in serum supporting Samant et al study [49], by producing its own biosynthetic enzymes, as well as to the absence of simple carbon and nitrogen sources by using T2SS to secrete exoenzymes that would degrade complex macromolecules, such as proteins, present in serum. The genes encoding the NQR system, which maintains the Na<sup>+</sup>/proton gradient in certain natural environments [50], were also found to be required for growth in both HS and hiHS. We speculate that the NQR system could help to maintain the electrostatic equilibrium in a stressing medium such as HS. This conclusion is further supported by reports that the NQR system maintains the proton-motive force when bacterial membranes are altered [44], and by our finding that genes necessary either for resistance to bactericidal peptides (e.g., *ompH*) [51] or for LPS modifications that also promote resistance to these peptides [52], were required for growth/survival in HS and hiHS. Similarly,

the peripheral membrane protein TrkA, an essential member of the potassium transporter was described as essential for YJ016 to grow in HS and hiHS [14]. Finally, and in contrast to previous reports [24], the sialic acid genes were not found relevant for serum growth in the present study.

In summary, our TIS-based studies yielded many observations worthy of future investigation and illustrate the potency of TIS-based analyses to dissect complex phenotypes like pathogen growth in HS. When applying this technique to *V. vulnificus*, a dangerous septicaemic pathogen, we have been able to describe new genes involved in protection against human complement from new CPS biosynthetic genes to genes for hypothetical proteins as well as genes with a putative role in overcoming heat-resistant constraints in serum such as genes for OMPs (OmpH and others), biosynthetic/modifying LPS enzymes, a NQR system, a T2SS, and biosynthetic nucleotide enzymes, all of them supposedly essential to grow in serum and to allow the pathogen to proliferate in blood and cause death by septicemia.

## Material and methods

### Strains, plasmids and general culture conditions

Strains and plasmids are listed in S1 Table. All the strains were routinely grown in Luria-Bertani broth (LB+0.5% NaCl) with shaking (200 rpm) or on LB-agar (LBA) at 37 °C for 18–24 h. A spontaneous streptomycin resistant mutant (YJSm<sup>r</sup>) was selected after growing the strain YJ016 on LBA-Sm (streptomycin, 500 µg/ml) and checking that the mutant and the wild-type's growth curves in LB were statistically similar. YJSm<sup>r</sup> was used as the recipient strain in conjugation experiments with the Tn-donor strain and is the parental strain for all knockout mutants in the genes selected after TIS assays. Antibiotic concentrations used in the experiments for genetic modification were: Sm, 500 µg/ml; chloramphenicol (Cm), 20 µg/ml (*E.coli*) or 2 µg/ml (*V. vulnificus*); and kanamycin (Km), 150 µg/ml. *E. coli* SM10 *lambda pir* carrying the Himar1 suicide Tn vector pYB742 (CmR) was used for Tn mutagenesis [53]. All strains were kept in LB+ 20% glycerol at -80 °C.

### Resistance and growth in HS

Cells in exponential phase of growth in LB were washed twice in PBS and were inoculated in HS (commercial HS, Sigma, H4522) or heat-inactivated HS (56 °C, 30 min) at 10<sup>4–5</sup> cfu/ml by triplicate. Tubes were incubated at 37°C with shaking (170 rpm) and bacterial growth was monitored by plating on LBA plates at 0, 2, 4 and

6 h post inoculation. (Human complement starts to inactivate spontaneously after 6–8 h of incubation at 37°C; unpublished result). Serial ten-fold dilutions in PBS (phosphate buffered saline, pH 7) were spotted (10 µl) on LBA plates (drop plate count). Plate counting was performed by triplicate.

### Tn library construction

The Mariner-based Himar1 Tn (which inserts into TA sites) and a previously published protocol [26,30] were used to construct two independent libraries for each condition assayed. Few changes were made in order to optimize the saturation of our transposon mutant library. An initial Tn-library was created in LBA by mixing washed bacteria from 1 ml of an overnight culture of Tn donor and receptor (Table S1) in a final volume of 500 µl of fresh LB at a ratio of 1:1. Then, 50 µl-aliqouts were spotted onto 0.45 µm-filters (Millipore, HAWP04700) placed on LBA plates that were incubated for 6 h. After conjugation, the filters were recovered and grown bacteria were spread onto LBA+Sm+Km plates of 24.5 × 24.5cm [2] (Corning) that were incubated at 37°C for 24 h.

Bacteria grown on the plates (approx. 1.5 million) were scrapped with 12 ml of fresh LB and 3 ml were used to obtain genomic DNA exactly as Chao *et al.* described [26,27] and the rest (around 20 ml) was kept with 20% glycerol at -80 °C. DNA from this library was used for determination of genes required for *V. vulnificus* growth in vitro

### Library selection

The obtained Tn-library was again inoculated in LB (control) and, in parallel, in HS (tested condition 1) and inactivated-HS (tested condition 2) at a ratio 1:30 vol/vol (approximately 10<sup>8</sup> cfu/ml) and incubated at 37°C for 2 h. Cells were recovered by centrifugation, resuspended in 3 ml of LB and immediately spread on LBA+Sm+Km plates (24.5 × 24.5cm [2, Corning) that were incubated at 37°C overnight. Bacteria were recovered and DNA genomic was obtained as explained before. A volume of around 20 ml of bacterial suspension was separately kept with 20% glycerol at -80 °C.

### Mapping and analysis of transposon insertion sites

5–10 µg of genomic DNA was fragmented into pieces of ≈350 bp by sonication (M220 focused ultrasonicator, Covaris, Woburn, MA), then DNA ends were repaired with the Quick Blunting™ Kit (NEB, E1201L), the Tn junctions were amplified, adaptor sequences were

attached and each Tn-library sequenced on a MiSeq (Illumina, San Diego, CA) [26,27].

Reads of more than 15 nucleotides were mapped to the *V. vulnificus* YJ016 genome, which is composed of two chromosomes (chromosome 1, NC\_005139.1; and 2, NC\_005140.1) and one plasmid (pYJ016, NC\_005128.1) [25]. We discarded reads that did not align to any TA site in the genome, and we randomly distributed the reads mapping to multiple TA sites. The number of reads at each TA site was tallied, datasets were normalized for origin proximity, and Tn-insertion profiles were depicted using Artemis software [54]. Then, EL-ARTIST software [30] was used to analyze the two chromosomes and the plasmid pYJ016, independently. ARTIST uses simulation-based normalization to model and compensate for experimental noise, and thereby enhances the statistical power in conditional TIS analyses. The statistical models and analysis to provide robust significance of the results are detailed in [30]. Chromosome 1 classifications were obtained using hidden Markov model analysis following usual values for sliding window (SW) training (10 TA sites;  $P < 0.005$ ) while chromosome 2 classifications were obtained using 15 TA sites. For chromosome 1 and plasmid, genetic loci with fewer than 10 TA sites were retroactively excluded from classification. In chromosome 2, at least 15 TA sites were used.

Because of the differences in TA % disrupted between Tn-libraries, we used Mann-Whitney test in order to compare the TA abundances. Minimum 90% Mann-Whitney U (MWU) test values,  $p$ -value  $< 0.00001$  and fold change (FC) bigger than 5 were considered for the analysis. The FC represents the number of times a gene is more represented in one Tn-library vs. other. Considering the TA positions that could have been disrupted and the TA positions covered in our Tn-library, we classified genomic loci as “under-represented”/“regional” when the number of sequenced transposons in the loci was significantly low, or “neutral”, when reads were mapped in practically the total sequence of the gene. Further, we differentiated two categories within essential genes on the basis of the location of reads, “under-represented” and “regional” when the reads were located in the full sequence or in a part of the gene, respectively.

### Bioinformatic analyses

Genes listed as under-represented for survival/growth in HS were subject to additional bioinformatic analyses; in particular, genes annotated as hypothetical proteins were re-annotated using HHPred or BLASTP against Genbank. Moreover, domains were analysed

using the Conserved Domain Database (CDD) on the NCBI website. The Protein homology/analogy recognition engine V 2.0 (Phyre [2]) pipeline was used for analysis of the predicted VV0358 amino acid sequence [55]. Primers were designed manually using basic sequence edition programs, mainly ApE (A plasmid Editor v2.0.47; <http://biologylabs.utah.edu/jorgensen/wayned/ap/>).

The BLASTP tool was used to check for the presence of a genes found to be under-represented in *V. vulnificus* YJ016 in *V. cholerae* N16961, *V. parahaemolyticus* RIMD 2210633, *V. fischeri* ES114, *Moraxella catarrhalis* BBH18, *E. coli* ST131 and *E. coli* K12. In these comparisons, we only considered hits that had at least 50% of identity, covered 85% of the predicted polypeptide sequence and had a  $p$ -value was smaller than  $10^{-5}$ . Genes of interest were functionally classified using UniProt [35].

### Deletion mutants and complementation

Mutants (Table S10) were obtained using allelic exchange [56]. Mutants were constructed by ligating  $\approx 500$  bp PCR-products, generated from the primers in Table S10, to the suicide vector, pDM4, using Gibson assembly [57]. Allele exchange vectors were transferred from *E. coli* SM10 to YJSm<sup>r</sup> by conjugation.

To carry out the conjugation, 40  $\mu$ l of washed overnight cultures of each bacterium were mixed and spotted on 0.45  $\mu$ m-filter (Millipore, HAWP04700). After 4h of incubation, cells were recovered in LB and spread on LBA+Cm+Sm. Finally, sucrose-based counter-selection was performed as described by Donnenberg and Kaper [56]. Briefly, 3 random Cm+Sm resistant colonies were grown overnight, the culture was diluted 1:100 in LB +10% saccharose (wt/vol) and was incubated again until it reached a value of  $Abs_{600} = 0.5$ . Then, 100  $\mu$ l of each one of a serial ten-fold dilutions of the culture were spread on LBA plates. Colonies were checked by PCR and DNA sequencing to confirm the deletion was in frame, and the mutants were kept in LB+ 20% glycerol at  $-80^{\circ}\text{C}$ .

Complementation of the mutants was done using derivatives of pMMB207 (Cm<sup>r</sup>). The selected genes were amplified by PCR (S10 Table). PCR purified products and the pMMB207 were digested with two different FastDigest enzymes (Thermo Scientific). Plasmid was treated with FastAP Thermosensitive Alkaline Phosphatase (Thermo Scientific, EF0652) and ligated to the gene with T4 ligase (Thermo Scientific). Transformed *E. coli* SM10 cells (same protocol as deletion mutants) were conjugated with the corresponding deletion mutant using the same protocol described before. Colonies were checked to confirm the



gene was inserted in frame, and the complemented mutants were kept in LB+ 20% glycerol at -80 °C until used.

### Phenotypic characterization of the mutants

#### a) Animal model of sepsis: mean lethal dose determination ( $LD_{50}$ )

The bacterial virulence for mice of the wild-type and each one of the selected mutants was determined in 6- to 8-week old female (mice BALB/c, Charles River, France) by using the iron-overloaded model of infection according to [58]. This model consists in pre-inoculating mice with 2  $\mu$ g of iron per g of body weight as hemin 2 h prior to the infection, and then, intraperitoneally injecting animals with ten-fold serially diluted bacterial suspensions in PBS. The  $LD_{50}$  was calculated as described [59].

#### b) Growth in serum

The growth of the mutants with regard to the wild-type strain was tested in the following media: HS, HIS, Inoculated media ( $10^5$  cfu/ml) were incubated for 6 h at 37°C, samples were taken at 0, 2 and 6 h post-incubation for bacterial counting on LBA plates by drop plate [60].

#### c) Surface antigen analysis

Crude fractions of cell-associated polysaccharides were obtained from overnight cultures in LB essentially as described by Hitchcock and Brown [61] and Valiente [12]. Polysaccharides were separated by SDS-PAGE [62] in discontinuous gels (4% stacking gel, 10% separating gel), transferred to a PVDF membrane (Bio-Rad) [63] and subjected to immunoblot analysis. The membranes were stained with a rabbit anti-inactivated YJ016 cells serum especially enriched in antibodies against capsular antigens (anti-capsular serum) [64]. The serum was diluted 1:3000 and membranes were developed following incubation with anti-rabbit IgG HRP-conjugated secondary antibody diluted 1:10000 (Sigma), using Immobilon Western Chemiluminescent HRP Substrate (Millipore).

### Disclosure of potential conflicts of interest

No potential conflicts of interest were disclosed.

### Statistical analysis

All the experiments were performed by triplicate. Statistical analysis was performed using SPSS 17.0 for windows. The results are presented as means  $\pm$  SE (standard error of the means). The significance of the differences between means was tested by using the unpaired Student's t-test with a  $P < 0.05$ . When the effects of more than two independent variables were


taken into account, the results were analyzed by variance analysis ANOVA followed by Tukey's test.


### Funding


Secretaría de Estado de Investigación, Desarrollo e Innovación (BES-2012-052361), Secretaría de Estado de Investigación, Desarrollo e Innovación plus FEDER funds (Programa Consolider-Ingenio 2010 CSD2009-00006; AGL2014-58933-P; and AGL2017-87723-P) and National Institutes of Health (NIH F31 AI-120665). Hubbard TP has been financed by NIH F31 AI-120665.

### ORCID

F. X. Silva-Hernández  <http://orcid.org/0000-0002-4294-9295>

M. C. Chao  <http://orcid.org/0000-0002-6046-585X>

M. K. Waldor  <http://orcid.org/0000-0003-1843-7000>

C. Amaro  <http://orcid.org/0000-0003-1323-6330>

### References

- [1] Oliver JD. The Biology of *Vibrio vulnificus*. *Microbiol Spectr.* 2015;3(3):VE-0001-2014. doi:10.1128/microbiolspec.VE-0001-2014.
- [2] Amaro C, Sanjuán E, Fouz B, et al. The fish pathogen *Vibrio vulnificus* biotype 2: epidemiology, phylogeny, and virulence factors involved in warm-water vibriosis. *Microbiol Spectr.* 2015;3(3):VE-0005-2014. doi:10.1128/microbiolspec.VE-0005-2014.
- [3] Crim SM, Griffin PM, Tauxe R, et al. Preliminary incidence and trends of infection with pathogens transmitted commonly through food — Foodborne Diseases Active Surveillance Network, 10 U.S. Sites, 2006–2014. *MMWR Morb Mortal Wkly Rep.* 2015;64(18):495–9. Atlanta.
- [4] Tison DL, Nishibuchi M, Greenwood JD, et al. *Vibrio vulnificus* biogroup 2: new biogroup pathogenic for eels. *Appl Environ Microbiol.* 1982;44:640–6.
- [5] Bisharat N, Agmon V, Finkelstein R, et al. Clinical, epidemiological, and microbiological features of *Vibrio vulnificus* biogroup 3 causing outbreaks of wound infection and bacteraemia in Israel. *Israel Vibrio Study Group. Lancet.* 1999;354:1421–4.
- [6] Amaro C, Biosca EG. *Vibrio vulnificus* biotype 2, pathogenic for eels, is also an opportunistic pathogen for humans. *Appl Environ Microbiol.* 1996;62:1454–7.
- [7] Paz S, Bisharat N, Paz E, et al. Climate change and the emergence of *Vibrio vulnificus* disease in Israel. *Environ Res.* 2007;103:390–6.
- [8] Jones MK, Oliver JD. *Vibrio vulnificus*: disease and pathogenesis. *Infect Immun.* 2009;77:1723–33.
- [9] Roig FJ, González-Candelas F, Sanjuán E, et al. Phylogeny of *Vibrio vulnificus* from the analysis of the core-genome: implications for intra-species taxonomy. *Front Microbiol.* 2018;8:2613.
- [10] Lee C-T, Amaro C, Wu K-M, et al. A common virulence plasmid in biotype 2 *Vibrio vulnificus* and its dissemination aided by a conjugal plasmid. *J Bacteriol.* 2008;190:1638–48.

- [11] Pajuelo D, Lee C-T, Roig FJ, et al. Novel host-specific iron acquisition system in the zoonotic pathogen *Vibrio vulnificus*. *Environ Microbiol.* **2015**;17:2076–89.
- [12] Valiente E, Lee CT, Lamas J, et al. Role of the virulence plasmid pR99 and the metalloprotease Vvp in resistance of *Vibrio vulnificus* serovar E to eel innate immunity. *Fish Shellfish Immunol.* **2008**;24:134–41.
- [13] Valiente E, Jiménez N, Merino S, et al. *Vibrio vulnificus* biotype 2 serovar E *gne* but not *galE* is essential for lipopolysaccharide biosynthesis and virulence. *Infect Immun.* **2008**;76:1628–38.
- [14] Chen Y-C, Chuang Y-C, Chang C-C, et al. A K<sup>+</sup> uptake protein, TrkA, is required for serum, protamine, and polymyxin B resistance in *Vibrio vulnificus*. *Infect Immun.* **2004**;72:629–36.
- [15] Yoshida S, Ogawa M, Mizuguchi Y. Relation of capsular materials and colony opacity to virulence of *Vibrio vulnificus*. *Infect Immun.* **1985**;47:446–51.
- [16] Bogard R, Oliver JD. Role of iron in human serum resistance of the clinical and environmental *Vibrio vulnificus* genotypes. *Appl Environ Microbiol.* **2007**;73:7501–7505.
- [17] Williams T C, Blackman E R, Morrison SS, et al. Transcriptome sequencing reveals the virulence and environmental genetic programs of *Vibrio vulnificus* exposed to host and estuarine conditions. *PLoS One.* **2014**;9(12):e114376.
- [18] Williams T, Ayrapetyan M, Ryan H, et al. Serum survival of *Vibrio vulnificus*: role of genotype, capsule, complement, clinical origin, and in situ incubation. *Pathogens.* **2014**;3:822–32.
- [19] Goo SY, Han YS, Kim WH, et al. *Vibrio vulnificus* IlpA-induced cytokine production is mediated by Toll-like receptor 2. *J Biol Chem.* **2007**;282:27647–58.
- [20] Lee JH, Rho JB, Park KJ, et al. Role of flagellum and motility in pathogenesis of *Vibrio vulnificus*. *Infect Immun.* **2004**;72(8):4905–10.
- [21] Kim SY, Thanh XT, Jeong K, et al. Contribution of six flagellin genes to the flagellum biogenesis of *Vibrio vulnificus* and in vivo invasion. *Infect Immun.* **2014**;82(1):29–42.
- [22] Lo H-R, Lin J-H, Chen Y-H, et al. RTX Toxin Enhances the survival of *Vibrio vulnificus* during infection by protecting the organism from phagocytosis. *J Infect Dis.* **2011**;203:1866–74.
- [23] Murciano C, Lee CT, Fernández-Bravo A, et al. MARTX toxin in the zoonotic serovar of *Vibrio vulnificus* triggers an early cytokine storm in mice. *Front Cell Infect Microbiol.* **2017**;7:332.
- [24] Lubin J-B, Lewis WG, Gilbert NM, et al. Host-like carbohydrates promote bloodstream survival of *Vibrio vulnificus* in vivo. *Infect Immun.* **2015**;83:3126–36.
- [25] Chen C-Y. Comparative Genome Analysis of *Vibrio vulnificus*, a marine pathogen. *Genome Res.* **2003**;13:2577–87.
- [26] Chao MC, Abel S, Davis BM, et al. The design and analysis of transposon insertion sequencing experiments. *Nat Rev Microbiol.* **2016**;14:119–28.
- [27] Chao MC, Pritchard JR, Zhang YJ, et al. High-resolution definition of the *Vibrio cholerae* essential gene set with hidden Markov model-based analyses of transposon-insertion sequencing data. *Nucleic Acids Res.* **2013**;41:9033–48.
- [28] Rubin EJ, Akerley BJ, Novik VN, et al. In vivo transposition of mariner-based elements in enteric bacteria and mycobacteria. *Proc Natl Acad Sci U S A.* **1999**;96:1645–50.
- [29] Lampe DJ, Grant TE, Robertson HM. Factors affecting transposition of the Himar1 mariner transposon in vitro. *Genetics.* **1998**;149:179–87.
- [30] Pritchard JR, Chao MC, Abel S, et al. ARTIST: High-Resolution Genome-Wide Assessment of fitness using transposon-insertion sequencing. *PLoS Genet.* **2014**;10:e1004782.
- [31] Kimura S, Hubbard TP, Davis BM, et al. The nucleoid binding protein H-NS biases genome-wide transposon insertion landscapes. *MBio.* **2016**;7:e01351–16. Available from: <http://mbio.asm.org/lookup/doi/10.1128/mBio.01351-16>
- [32] Hubbard TP, Chao MC, Abel S, et al. Genetic analysis of *Vibrio parahaemolyticus* intestinal colonization. *Proc Natl Acad Sci.* **2016**;113:6283–8.
- [33] Hüttener M, Paytubi S, Juárez A. Success in incorporating horizontally transferred genes: the H-NS protein. *Trends Microbiol.* **2015**;23:67–9.
- [34] Brooks JF, Gyllborg MC, Cronin DC, et al. Global discovery of colonization determinants in the squid symbiont *Vibrio fischeri*. *Proc Natl Acad Sci.* **2014**;111:17284–9.
- [35] Consortium TU. Activities at the Universal Protein Resource (UniProt). *Nucleic Acids Res.* **2014**;42:D191–8.
- [36] Bullen J, Griffiths E, Rogers H, et al. Sepsis: the critical role of iron. *Microbes Infect.* **2000**;2(4):409–15.
- [37] Wright AC, Powell JL, Kaper JB, et al. Identification of a group 1-like capsular polysaccharide operon for *Vibrio vulnificus*. *Infect Immun.* **2001**;69:6893–901.
- [38] Dong C, Beis K, Nesper J, et al. Wza the translocon for *E. coli* capsular polysaccharides defines a new class of membrane protein. *Nature.* **2006**;444:226–9.
- [39] Chatzidaki-livanis M, Jones MK, Anita C, et al. Genetic variation in the *Vibrio vulnificus* group 1 capsular polysaccharide operon. *J Bacteriol.* **2006**;188:1987–98.
- [40] Beis K, Collins RF, Ford RC, et al. Three-dimensional structure of Wza, the protein required for translocation of group 1 capsular polysaccharide across the outer membrane of *Escherichia coli*. *J Biol Chem.* **2004**;279:28227–32.
- [41] Drummelsmith J, Whitfield C. Translocation of group 1 capsular polysaccharide to the surface of *Escherichia coli* requires a multimeric complex in the outer membrane. *EMBO J.* **2000**;19:57–66.
- [42] Garrett SB, Garrison-Schilling KL, Cooke JT, et al. Capsular polysaccharide production and serum survival of *Vibrio vulnificus* are dependent on antitermination control by RfaH. *FEBS Lett.* **2016**;590(24):4564–4572.
- [43] Hor L-I, Gao C-T, Wan L. Isolation and Characterization of *Vibrio vulnificus* Inhabiting the marine environment of the Southwestern area of Taiwan. *J Biomed Sci.* **1995**;2:384–9.
- [44] Steuber J, Vohl G, Casutt MS, et al. Structure of the *V. cholerae* Na<sup>+</sup>-pumping NADH:quinone oxidoreductase. *Nature.* **2014**;516:62–7.
- [45] Hwang W, Lee NY, Kim J, et al. Functional characterization of EpsC, a component of the type II secretion system, in the pathogenicity of *Vibrio vulnificus*. *Infect Immun.* **2011**;79:4068–80.
- [46] Wong TY, Preston LA, Schiller NL. ALGINATE LYASE: review of major sources and enzyme characteristics, structure-function analysis, biological roles, and applications. *Annu Rev Microbiol.* **2000**;54:289–340.

- [47] Badur AH, Jagtap SS, Yalamanchili G, et al. Alginate lyases from alginate-degrading *Vibrio splendidus* 12B01 are endolytic. *Appl Environ Microbiol.* 2015;81:1865–73.
- [48] Kim H-J, Cho J-C. Genotypic diversity and population structure of *Vibrio vulnificus* strains isolated in Taiwan and Korea as determined by multilocus sequence typing. *PLoS One.* 2015;10:e0142657.
- [49] Samant S, Lee H, Ghassemi M, et al. Nucleotide biosynthesis is critical for growth of bacteria in human blood. *PLoS Pathog.* 2008;4:e37.
- [50] Häse CC, Barquera B. Role of sodium bioenergetics in *Vibrio cholerae*. *Biochim Biophys Acta.* 2001;1505:169–78.
- [51] Alice AF, Naka H, Crosa JH. Global gene expression as a function of the iron status of the bacterial cell: influence of differentially expressed genes in the virulence of the human pathogen *Vibrio vulnificus*. *Infect Immun.* 2008;76(9):4019–37.
- [52] Rosenfeld Y, Shai Y. Lipopolysaccharide (Endotoxin)-host defense antibacterial peptides interactions: Role in bacterial resistance and prevention of sepsis. *Biochim Biophys Acta – Biomembr.* 2006;1758:1513–22.
- [53] Yamaichi Y, Chao MC, Sasabe J, et al. High-resolution genetic analysis of the requirements for horizontal transmission of the ESBL plasmid from *Escherichia coli* O104:H4. *Nucleic Acids Res.* 2015;43:348–60.
- [54] Carver TJ, Rutherford KM, Berriman M, et al. ACT: the Artemis comparison tool. *Bioinformatics.* 2005;21:3422–3.
- [55] Kelley LA, Mezulis S, Yates CM, et al. The Phyre2 web portal for protein modeling, prediction and analysis. *Nat Protoc.* 2015;10:845–58.
- [56] Donnenberg MS, Kaper JB. Construction of an *eae* deletion mutant of enteropathogenic *Escherichia coli* by using a positive-selection suicide vector. *Infect Immun.* 1991;59(12):4310–7.
- [57] Gibson DG, Young L, Chuang R-Y, et al. Enzymatic assembly of DNA molecules up to several hundred kilobases. *Nat Meth.* 2009;6:343–5.
- [58] Amaro C, Biosca EG, Fouz B, et al. Role of iron, capsule, and toxins in the pathogenicity of *Vibrio vulnificus* biotype 2 for mice. *Infect Immun.* 1994;62(2):759–63.
- [59] Reed LJ, Muench H. A simple method of estimating fifty percent endpoints. *Am J Epidemiol.* 1938;27:493–7.
- [60] Hoben HJ, Somasegaran P. Comparison of the pour, spread, and drop plate methods for enumeration of *Rhizobium* spp. in inoculants made from presterilized peat. *Appl Environ Microbiol.* 1982;44:1246–7.
- [61] Hitchcock PJ, Brown TM. Morphological heterogeneity among *Salmonella* lipopolysaccharide chemotypes in silver-stained polyacrylamide gels. *J Bacteriol.* 1983;154:269–77.
- [62] Laemmli UK. Cleavage of structural proteins during the assembly of the head of bacteriophage T4. *Nature.* 1970;227:680–5.
- [63] Towbin H, Staehelin T, Gordon J. Electrophoretic transfer of proteins from polyacrylamide gels to nitrocellulose sheets: procedure and some applications. *Proc Natl Acad Sci U S A.* 1979;76:4350–4.
- [64] Amaro C, Biosca EG, Fouz B, et al. Electrophoretic analysis of heterogeneous lipopolysaccharides from various strains of *Vibrio vulnificus* biotypes 1 and 2 by silver staining and immunoblotting. *Curr Microbiol.* 1992;25:99–104.

# Iron and Fur in the life cycle of the zoonotic pathogen *Vibrio vulnificus*

David Pajuelo,<sup>1</sup> Carla Hernández-Cabanyero,<sup>1</sup>  
Eva Sanjuan,<sup>1</sup> Chung-Te Lee,<sup>2</sup>  
Francisco Xavier Silva-Hernández,<sup>1</sup> Lien-I Hor,<sup>2,3</sup>  
Simon MacKenzie<sup>4</sup> and Carmen Amaro<sup>1\*</sup>

<sup>1</sup>Estructura de Recerca Interdisciplinaria en Biotecnologia i Biomedicina (ERI BIOTECMED), University of Valencia, Dr. Moliner, 50, Valencia 46100, Spain.

<sup>2</sup>Department of Microbiology and Immunology, Institute of Basic Medical Sciences, Tainan, Taiwan, Republic of China.

<sup>3</sup>College of Medicine, National Cheng Kung University, Tainan 701, Taiwan, Republic of China.

<sup>4</sup>Institute of Aquaculture, University of Stirling, Stirling, UK.

## Summary

In this study, we aimed to analyze the global response to iron in the broad-range host pathogen *Vibrio vulnificus* under the hypothesis that iron is one of the main signals triggering survival mechanisms both inside and outside its hosts. To this end, we selected a strain from the main zoonotic clonal-complex, obtained a mutant in the ferric-uptake-regulator (Fur), and analyzed their transcriptomic profiles in both iron-excess and iron-poor conditions by using a strain-specific microarray platform. Among the genes differentially expressed, we identified around 250 as putatively involved in virulence and survival-related mechanisms. Then, we designed and performed a series of *in vivo* and *in vitro* tests to find out if the processes highlighted by the microarray experiments were in fact under iron and/or Fur control. Our results support the hypothesis that iron acts as a niche marker, not always through Fur, for *V. vulnificus* controlling its entire life cycle. This ranges from survival in the marine environment, including motility and chemotaxis, to survival in the blood of their hosts, including host-specific mechanisms of resistance to innate immunity. These mechanisms allow the bacterium to multiply and persist inside and between their hosts.

Received 13 June, 2016; accepted 17 June, 2016. \*For correspondence. E-mail carmen.amaro@uv.es; Tel. (+34) 96 354 31 04; Fax (+34) 96 354 31 87.

## Introduction

*Vibrio vulnificus* is an emerging zoonotic pathogen that inhabits aquatic ecosystems from temperate, tropical and subtropical climates, in which it survives as planktonic form or associated with the mucosal surfaces of aquatic animals (Oliver, 2015). The species is subdivided in three biotypes (Bt) that differ in phenotypic traits and host range (Tison *et al.*, 1982; Bisharat *et al.*, 1999). The three Bts are considered opportunistic human pathogens while only Bt2 is also able to infect fishes (Tison *et al.*, 1982; Amaro and Biosca, 1996). This ability relies on a transferable virulence plasmid (called pVvbt2) that confers resistance to the fish innate immune response (Lee *et al.*, 2008; Valiente *et al.*, 2008). Among the Bt2-clones, the most dangerous for public health is the worldwide distributed clonal-complex formed by SerE strains (Sanjuán *et al.*, 2011). Human infection cases of known etiology related with this clonal-complex correspond to severe wound infections or secondary septicemia after diseased-eel handling (Amaro and Biosca, 1996; Sanjuán *et al.*, 2011; Haenen *et al.*, 2014).

Iron is an essential nutrient for *V. vulnificus*. In fact, the severity of the disease in humans is strongly related to iron levels in blood, being septicemic when these levels are abnormally high due to hemochromatosis or other disorders characterized by elevated iron levels (Horseman and Surani, 2011). Free-iron is presumably available to *V. vulnificus* in the nutrient-enriched environment characteristic of intensive fish-farming industry but it is unavailable inside the hosts due to nutritional immunity, an ancestral mechanism of defense common to fish and mammals (Weinberg, 2009). Thus, iron is present in host tissues either complexed to heme, forming part of the hemic proteins such as hemoglobin, or sequestered by transferrin in blood or lactoferrin in secretions, with all of these proteins binding Fe<sup>3+</sup> with an exceptionally high affinity (Hood and Skaar, 2012). *V. vulnificus* Bt2-SerE senses the lack of free-iron in blood and produces vulnibactin (a siderophore or iron-chelator) that competes with transferrin for iron together with its receptor VuuA, as well as a receptor for hemin. Both of these systems are required for virulence in humans and fish (Pajuelo *et al.*, 2014). However, Bt2-SerE can also produce a third iron-uptake system encoded by pVvbt2 that is eel-specific. This system relies on an outer membrane receptor for eel transferrin (Ftbp, fish transferrin binding



protein), which optimizes the growth of the pathogen in blood and makes it a highly virulent eel-pathogen (LD<sub>50</sub> for eels around 10–200 CFU per animal) (Amaro *et al.*, 1995; Pajuelo *et al.*, 2015).

The main iron-responsive transcriptional factor is Fur (ferric uptake regulator), most of the time acting as a negative regulator that uses iron as a cofactor (holo-repression) to control the transcription of iron acquisition-related genes (Hantke, 2001). However, recent studies suggest that Fur could also control other bacterial processes such as acid shock response, chemotaxis, metabolic pathways, bioluminescence, and production of toxins and other virulence factors, and, in some cases, through a positive regulation (Troxell and Hassan, 2013). In the case of *V. vulnificus*, it has been demonstrated that Fur controls its own transcription as well as that of a few virulence genes (including those for iron-uptake) and two master-regulator genes, *smcR* and *rpoS* (Lee *et al.*, 2003; Alice *et al.*, 2008; Kim *et al.*, 2013).

In this study, we aimed to analyze the global response of *V. vulnificus* to changes in iron levels by simulating the infection of a fish from tank water (bacteria “would sense” a decrease in iron concentration) and the infection of a “susceptible” human (high iron levels in blood) from a diseased-fish (bacteria “would sense” an increase in iron concentration) under the hypothesis that iron is a global signal for both virulence and survival gene switching. To this end, we selected a strain belonging to the zoonotic clonal-complex, whose genome has been sequenced and annotated, and obtained a *fur* deletion mutant ( $\Delta fur$ ) and the corresponding complemented strain (*cfur*). Then, we analyzed the transcriptomic profiles of the wild-type and the mutant strains growing in presence and absence of free-iron, and performed a series of confirmatory phenotypic *in vivo* and *in vitro* experiments also using the complemented strain. For the transcriptomic analysis we developed a custom microarray platform containing probes for all the predicted ORFs in the genome of the strain used in this study, the Bt2-SerE isolate CECT4999.

## Results

### Virulence in mice and eels

The role of iron and Fur in virulence was tested by comparing the virulence for normal and iron-overloaded animals of the wild-type (CECT4999), the mutant ( $\Delta fur$ ) and the complemented (*cfur*) strains. Iron-pretreatment increased by more than 2 log units the susceptibility to vibriosis of intraperitoneal (i.p.)-infected mice, regardless of the inoculated strain, whereas it did not affect virulence in eels (Table 1) (iron-overloaded eels were not i.p. infected due to the high virulence of the pathogen when using this route). In addition, *fur* deletion slightly reduced virulence for both mice and eels, regardless of the infection route (Table 1), and delayed internal organ colonization (Fig. 1).

### Differentially expressed genes

A total of 1229 genes (25.78% of the total genes measured) were differentially expressed by CECT4999 grown in iron-poor versus iron-rich media while 1712 genes (35.91% of the total genes) were differentially expressed by  $\Delta fur$  versus wild-type strain (Supporting Information Tables S1 and S2). Among the genes that showed the highest change in expression level in iron limitation, we found a strong induction of those related with iron acquisition (siderophores and ferrous iron), cold shock, plasmid genes (*vep06*, *vep23* or transthyretin and *vep71*), and DNA sulfur modification (*dndE*), whereas genes belonging to the flagellar operon, chemotaxis or drug resistance were remarkably repressed (Supporting Information Table S1). Interestingly the pattern of the genes most strongly regulated by Fur was similar to that of iron restriction, including upregulated genes in the *fur* mutant for iron acquisition (siderophores, ferrous iron and heme) and chemotaxis, and downregulated genes such as those related to flagellum biosynthesis (Supporting Information Tables S1 and S2). It is worth highlighting that most genes encoding response to stress, outer membrane proteins, uptake of different nutrients and metabolic pathways were found to

**Table 1.** Effect of *fur* in cursive deletion and iron concentration on virulence for eels and mice in *V. vulnificus*.

Strains	Virulence for <sup>a</sup>				
	Mice		Eels		
	Normal	Iron-overloaded	Normal (i.p.)	Normal (immersion)	Iron-overloaded (immersion)
CECT4999	$2.6 \times 10^4$	$<5 \times 10^1$	$1 \times 10^2$	$1.2 \times 10^6$	$7.6 \times 10^5$
$\Delta fur$	$9 \times 10^4$	$1 \times 10^2$	$3 \times 10^3$	$7.2 \times 10^6$	$1 \times 10^6$
<i>cfur</i>	$2.0 \times 10^4$	ND	$1.25 \times 10^2$	$7.1 \times 10^6$	ND

<sup>a</sup>Virulence was determined as the lethal mean dosis (LD<sub>50</sub>) for both normal and iron-overloaded animals and was expressed as colony forming units (CFU) per g (intraperitoneally infected [i.p.] animals) or ml (immersion infected eels [Amaro *et al.*, 1995]) according to Reed and Muench (1938). Each value represents the average of two independent experiments.

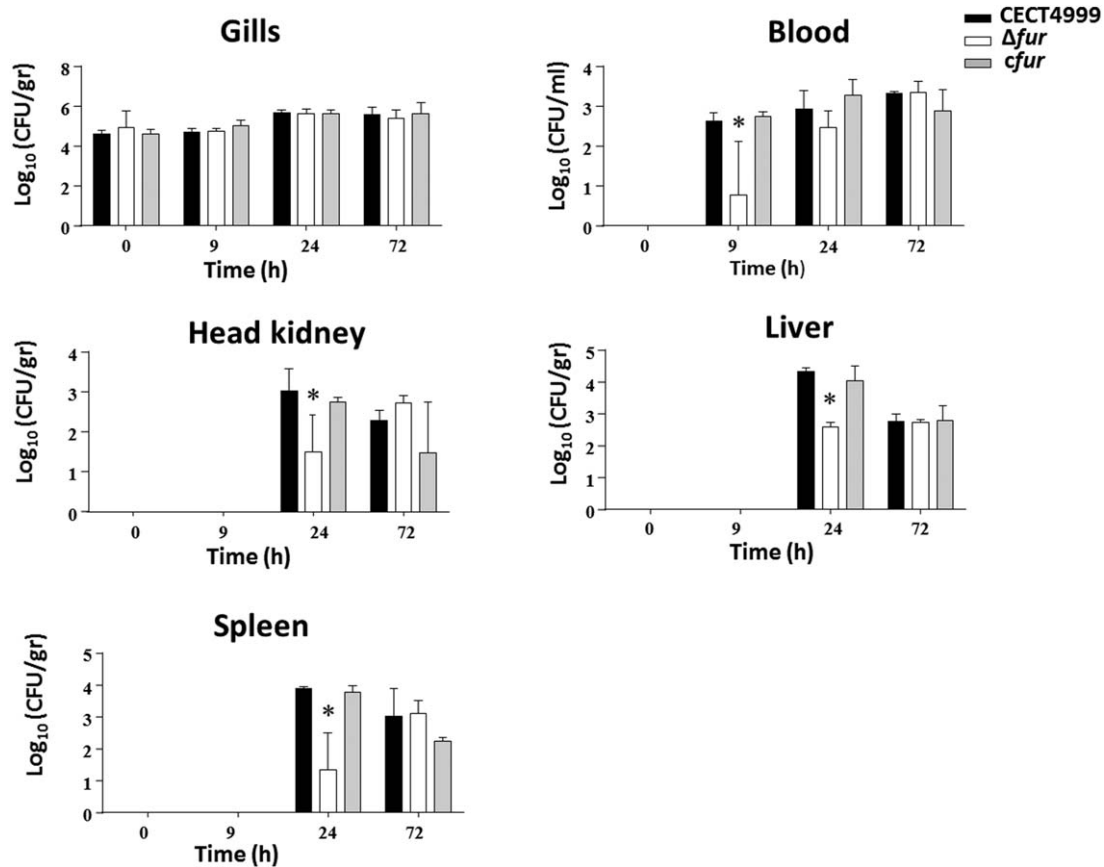


**Fig. 1.** Fur and *in vivo* colonization by *V. vulnificus* CECT4999. Eels were bath-infected with the wild-type strain (CECT4999),  $\Delta fur$  and *cfur* at a dose of  $10^6$  CFU/ml for 1 h. Then, bacterial colonization of external (gills) and internal (blood, liver, head kidney and spleen) organs was measured as bacterial counts (colony forming units or CFU) per g or ml at 0, 9, 24, and 72 h post-challenge and the bacterial counts per sampling point were statistically compared. Asterisks indicate significant differences in bacterial counts per sampling point (Student's *t*-test;  $P < 0.05$ ).

be under putative control by Fur and iron (Supporting Information Tables S1 and S2). We found an acceptable correlation between microarray and qRT-PCR data corresponding to the 12 genes selected for validation (Supporting Information Table S3). Figures 2A and 3A show the distribution of the three regulation categories (up-, down- and nonregulation) per chromosome (Chr) and plasmid for putative iron- and Fur-controlled genes, respectively, and Supporting Information Fig. S1A the distribution of the eight mixed categories. Around 250 virulence- and survival-related genes were identified as putatively controlled by iron and/or Fur (Figs 2B and 3B, Supporting Information Tables S1 and S2), among them, genes encoding global transcriptional regulators (SmcR, the cAMP-mediated regulator, ToxR) and multiple genes that contain GGDEF and/or EAL domains (related with intracellular signaling) (Supporting Information Tables S1 and S2). The Fur protein was positively auto-regulated as previously published (Lee *et al.*, 2007). Using the sequences of Fur boxes already described for *V. vulnificus*

(Ahmad *et al.*, 2009), we identified the putative Fur boxes for the virulence- and survival-related genes (Supporting Information Table S5). A consensus *V. vulnificus* Fur box motif built from putative Fur boxes founded is shown in Supporting Information Fig. S1B.

#### *Iron and Fur in the life-cycle of V. vulnificus*

A series of phenotypic experiments were designed and performed to ascertain if the virulence- and survival-related processes identified by the transcriptomic study responded to exogenous iron levels and/or could be directly or indirectly controlled by Fur.

**Viable but non-culturable (VBNC) state.** *V. vulnificus* enters into the viable but non culturable (VBNC) state in seawater in cold months especially when temperatures are below 10°C (Whitesides and Oliver, 1997). To test whether entry into the VBNC state could be under iron and/or Fur control we analyzed the culturability of the three strains at 4°C under iron-excess or iron-poor conditions. Importantly,

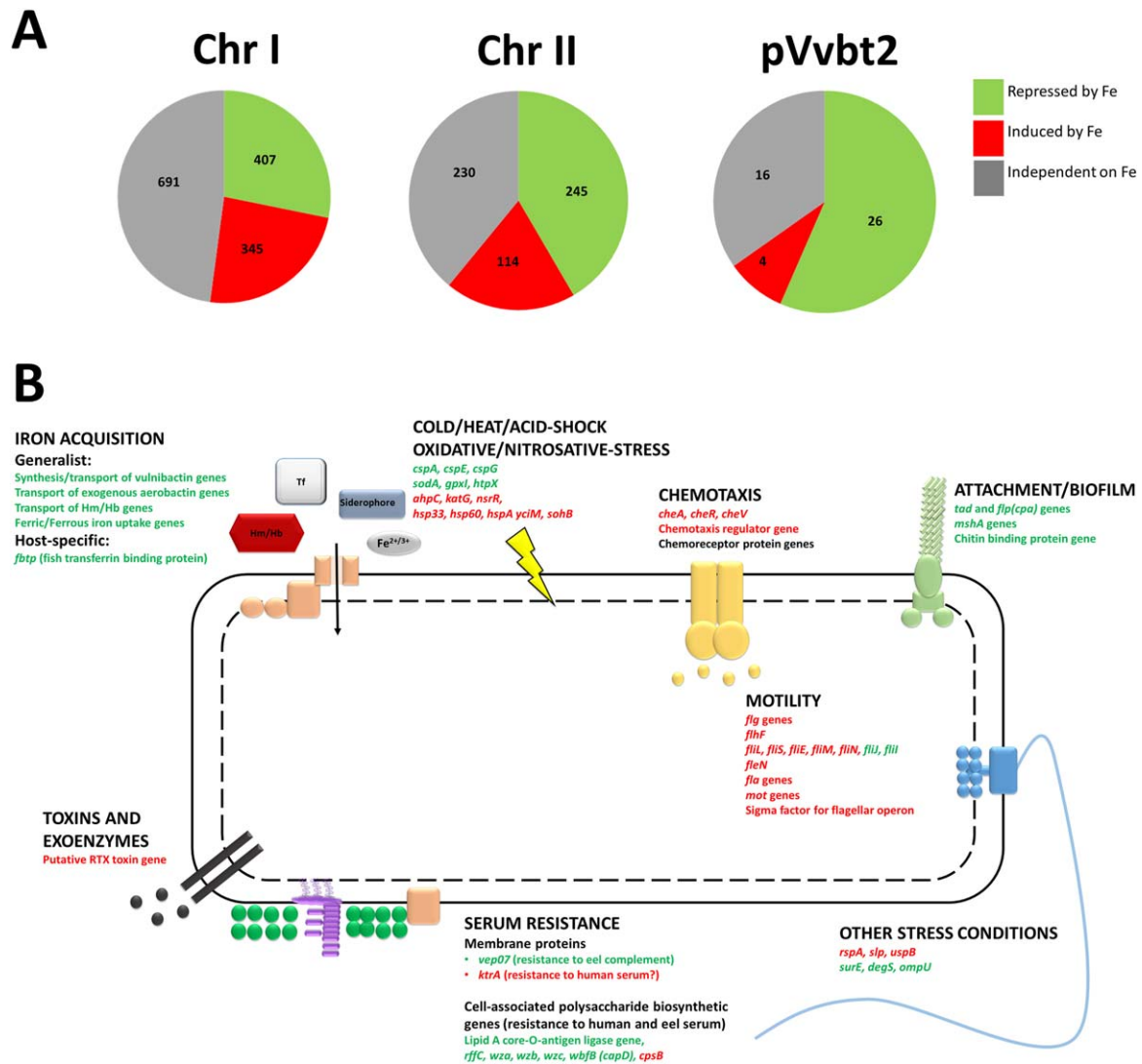


**Fig. 2.** Differentially expressed genes (DEGs) by *V. vulnificus* in response to iron (starvation versus excess). (A) Distribution of DEGs per regulation category and replicon (two chromosomes and one plasmid). The categories are represented in a color's code. (B) Main virulence- and survival-related processes that are putatively under control of iron. Red color: upregulated genes; Green color; downregulated genes; Black color: a group of related genes, some up- and other downregulated.

bacterial viability gradually decreased and the entrance into the VBNC state of  $\Delta fur$  was accelerated (15 day before CECT4999), especially under iron-excess conditions (d10 in artificial seawater (ASW) (Mården *et al.*, 1988) with iron (ASW + Fe) versus d 21 in ASW without iron (ASW – Fe) (Fig. 4A). In contrast, the iron content of the medium did not affect the entry into the VBNC state of the wild-type strain (Fig. 4A). No differences were observed among the strains and conditions in resuscitation kinetics from the VBNC state (Fig. 4A). These results are compatible with the hypothesis that the entrance into the VBNC state in *V. vulnificus* would be directly or indirectly controlled by Fur in an iron-independent manner. Entry into the VBNC state in

some vibrios has previously been suggested to be due to cold-induced loss of the antioxidative activity of catalase (KatG) and/or alkyl hydroperoxide reductase protein C (AhpC) (Oliver, 2010; Wang *et al.*, 2013; Rao *et al.*, 2014). Gene transcripts for both enzymes were significantly upregulated by iron (fold change values of 27.75 and 8.90 for *katG* and *ahpC*, respectively) and Fur (fold change values of 5.33 and 3.23 for *katG* and *ahpC* respectively). Our experimental assays confirmed that both genes were also upregulated in the wild-type strain after 3, 7, and 16 days post-inoculation at 4°C and that only *ahpC* expression was significantly less in the mutant in comparison to the wild-type strain (Fig. 4B). Interestingly, only *ahpC* has a putative

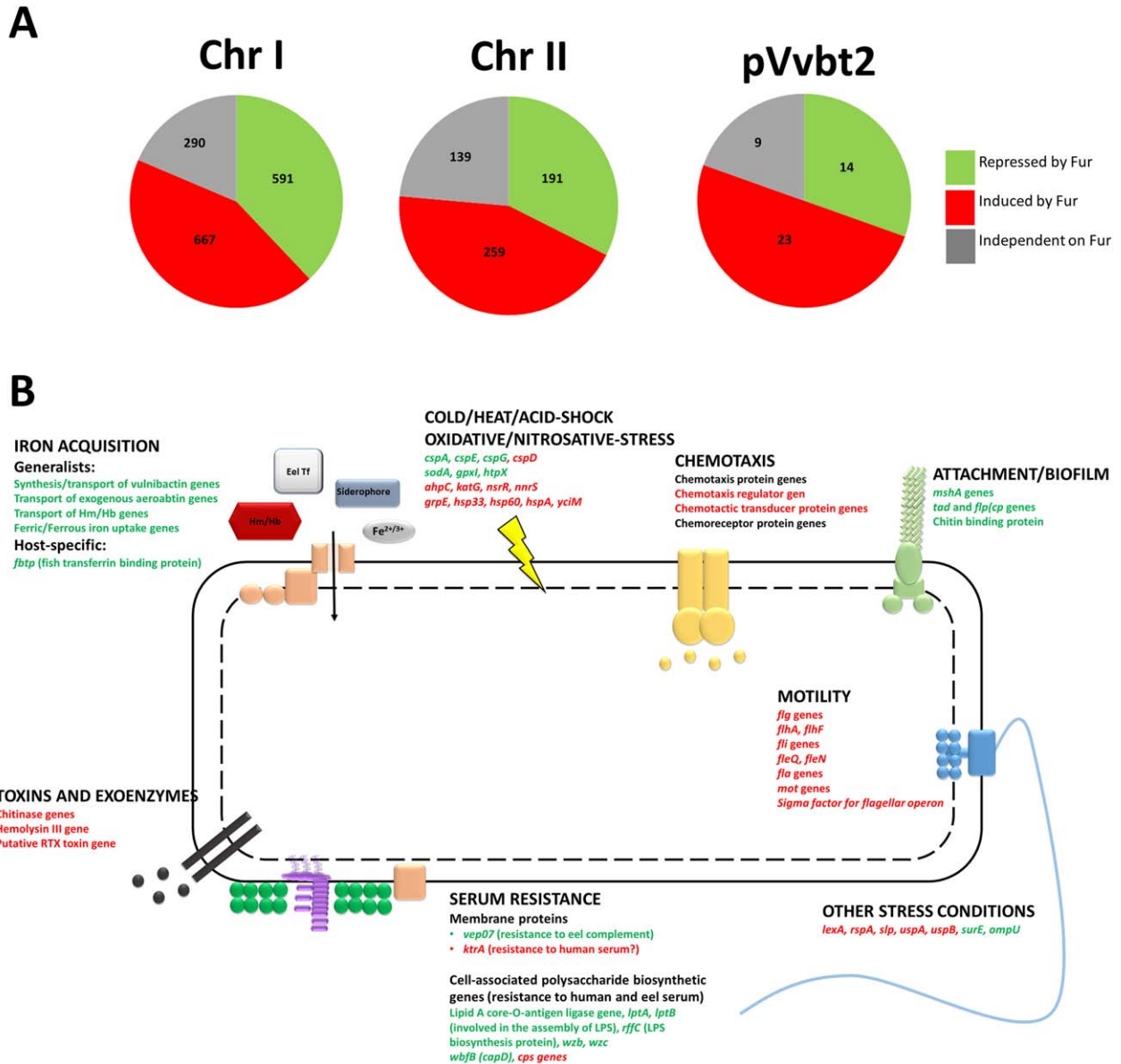


**Fig. 3.** Differentially expressed genes (DEGs) by *V. vulnificus*  $\Delta fur$  versus wild-type. (A) Distribution of DEGs per regulation category and replicon (two chromosomes and one plasmid). The categories are represented in a color's code. (B) Main virulence- and survival-related processes directly or indirectly controlled by Fur. Red color: upregulated genes; Green color; downregulated genes; Black color: a group of related genes, some up- and other downregulated.

Fur box (Supporting Information Table S5) therefore being a candidate gene to be directly activated by Fur. Finally, the faster entrance into the VBNC state of  $\Delta fur$  under iron-excess conditions could be explained by the formation of highly reactive hydroxyl radicals that have been reported to be produced under iron-excess conditions (Becker and Skaar, 2014) together with the increased sensitivity of the mutant to oxidative stress.

*Chemotaxis and motility.* Flagella and motility are known *V. vulnificus* virulence factors in mice (Lee *et al.*, 2004).

The microarray results revealed that both iron and Fur could positively and negatively impact the transcription of genes involved in motility and chemotaxis (Figs 2B and 3B; Supporting Information Tables S1 and S2). In case of motility, almost all of the genes involved in flagellum biosynthesis together with different regulators and a specific sigma factor were revealed to be putatively upregulated by Fur and iron (Figs 2B and 3B; Supporting Information Tables S1 and S2). We then designed and performed a test confirming that motility corresponding to CECT4999 was significantly higher than that of  $\Delta fur$  in all tested



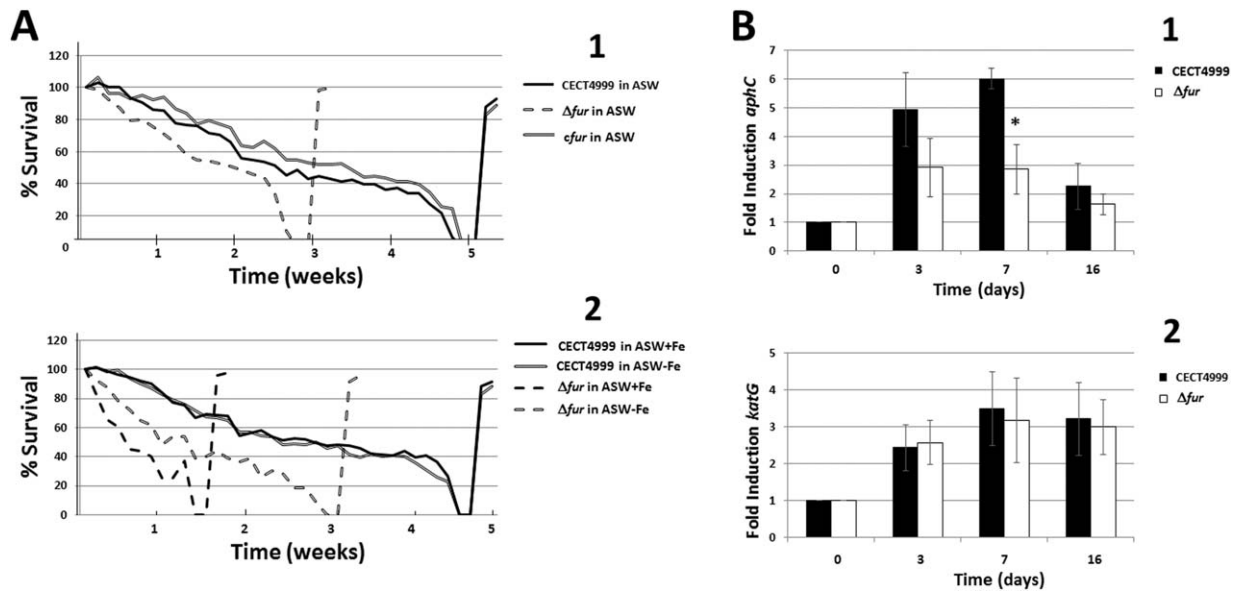


**Fig. 4.** Induction of VBNC state and resuscitation in *V. vulnificus* and transcription levels of *aphC* and *katG* during the induction of the VBNC state. (A) Cells from overnight cultures in MSWYE were transferred to ASW (1), ASW + Fe (2) or ASW-Fe<sub>(D)</sub> (2) and were maintained at 4°C with shaking (60 r.p.m.) till no bacteria was recovered on CM9A plates (VBNC state) and then the VBNC-cultures were placed at 22°C with shaking (60 r.p.m.) and resuscitation was monitored by plate counting on CM9A plates. Percent (%) survival refers to percentage of culturable bacteria (CFU/ml on CM9A) with respect to time 0 (100%). All values of % survival for  $\Delta fur$  were significantly lower than those corresponding to CECT4999/*cfur* ( $P < 0.05$ ) from day 2 till the induction of the VBNC state. (B) Transcription levels of *aphC* (1) and *katG* (2) determined as fold induction by qRT-PCR at 0, 3, 7 and 10 days of bacteria incubation in ASW at 4°C. \*Significant differences ( $P < 0.05$ ).

conditions. Furthermore motility of all of the strains, except that of the mutant, was enhanced significantly when iron was added (Fig. 5A). Unexpectedly, the motility of the mutant decreased significantly, as was the case for the rest of strains, when iron was removed from the growth medium (Fig. 5A). This indicates that other regulators, distinct from Fur could be involved in the motile response to variable iron conditions. The microarray results revealed that iron and Fur could also control the transcription of chemotaxis-related genes (Figs 2B and 3B; Supporting Information Tables S1 and S2). Since motile *Vibrio* cells are positively chemo-attracted by blood liberated by eel skin wounds (Valiente *et al.*, 2008), the chemotaxis toward eel and human plasma were tested under iron-excess and iron-poor conditions (Fig. 5B). Plasma and hemolytic plasma positively attracted CECT4999, and this attraction was significantly enhanced by iron while *fur* deletion significantly decreased chemo-attraction across all plasma types (Fig. 5B). Interestingly,  $\Delta fur$  was repelled by human plasma, which suggests a higher sensitivity to the bactericidal action of human serum. The flagellum- and chemotaxis-related genes with putative Fur boxes are indicated in Supporting Information Table S5. In conclusion, both chemotaxis toward blood and motility in *V. vulnificus* would be controlled directly or

indirectly by Fur in an iron-dependent manner, although motility also seems to involve other iron-responsive regulator or regulators.

**Attachment and biofilm formation on abiotic surfaces.** *V. vulnificus* is able to adhere and form biofilm on biotic and abiotic surfaces (Paranjpye and Strom, 2005). Among the attachment genes putatively regulated by Fur and/or iron we identified some of those encoding a putative Tad (tight adherence) system (the machinery required for the assembly of an adhesive Flp [fimbrial low-molecular-weight protein] pilus) together with the *flp* (*cpa*) genes as well as those putatively encoding a MSHA pilus (Supporting Information Tables S1 and S2). Interestingly, *tad*, *flp* (*cpa*), and *msha* genes were mostly downregulated by iron and Fur (Figs 2B and 3B; Supporting Information Tables S1 and S2) however none of these genes contains a putative Fur box. Biofilm production on a hydrophobic surface (polystyrene) was then analyzed and we found that this was time- and iron-dependent. Biofilms increased gradually, achieving a maximum at 1 week, and were decreased with increased iron concentration (Fig. 5C). These results suggest that biofilm formation and/or its dispersal is an iron-dependent process in which Fur does not play an essential role.

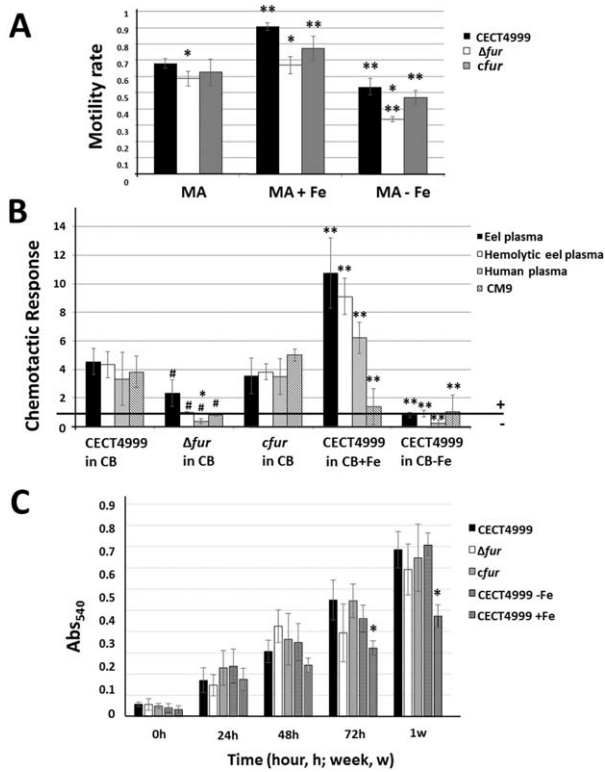


**Fig. 5.** Motility, chemotaxis and biofilm formation in *V. vulnificus*. (A) Motility on Motility agar (MA) measured as Motility rate (Mr) ("colony" surface in cm<sup>2</sup>/log of "colony" bacterial number in CFU). \*Significant differences in Mr between strains ( $\Delta fur$  or *cfur* versus CECT4999) ( $P < 0.05$ ); \*\*significant differences between conditions (with iron [MA + Fe] or without iron [MA - Fe<sub>(D)</sub>] versus MA) for the same strain ( $P < 0.05$ ). (B) Chemotaxis toward eel plasma (EP), hemolytic eel plasma (HEP), human plasma (HP), and CM9 was measured as Chemotactic response (Cr) (ratio bacterial numbers in EP-HEP-, HP-, or CM9-capillaries versus control-capillaries [containing Chemotaxis buffer (CB)]). Horizontal line marks the borderline between positive and negative chemotaxis. \*Significant differences in Cr toward EP, HEP, or HP versus CM9 per strain ( $P < 0.05$ ); #, significant differences between strains ( $\Delta fur$  or *cfur* versus CECT4999) per tested attractant (EP, HEP, HP, CM9) ( $P < 0.05$ ); \*\*significant differences in function of iron content in the chemotaxis buffer (CB + Fe or CB - Fe versus CB) per tested medium for the strain CECT4999 ( $P < 0.05$ ). (C) Biofilm quantification: bacteria were grown in polystyrene wells, planktonic bacteria were eliminated and biofilm was quantified after staining with crystal violet by measuring absorbance at 540 nm at 0, 24, 48, 72 h and 1 week post-incubation. \*Significant differences between conditions (+Fe versus -Fe) for strain CECT4999 ( $P < 0.05$ ).

**Toxins and exoenzymes.** A few genes for toxins (putative hemolysins) and proteases were identified as likely to be under iron and/or Fur control (Supporting Information Tables S1 and S2). None of them corresponded to the major toxins (Multifunctional Autoprocessive Repeat in Toxin, RtxA1 and the hemolysin VvhA) and exoenzymes (protease VvpE) of *V. vulnificus* (Shao and Hor, 2000; Lee

*et al.*, 2004; 2013). We did not find significant differences in either cell-associated- or extracellular-hemolytic/proteolytic activities among strains and conditions (iron excess versus iron deficiency) (Supporting Information Fig. S2 and data not shown).

**Resistance to stress conditions.** A series of genes related to resistance to various stressors from the innate immune response were identified to be putatively controlled by iron and/or Fur (Figs 2B and 3B; Supporting Information Tables S1 and S2). Firstly, we tested resistance to the antimicrobial compounds polymyxin B, lysozyme, and deoxycholate (a bile salt) and found that the MIC (minimal inhibitory concentration) values did not change with either iron concentration or *fur*-deletion (MICs: polymyxin B, 500 U/ml; lysozyme, 500  $\mu\text{g}/\mu\text{l}$ ; human apotransferrin, 50  $\mu\text{M}$ ). Bacterial survival for all experimental strains was determined under acidic or oxidative conditions, as well as the effect of nitric oxide (NO) on growth in both strains (Fig. 6). Survival decreased significantly in all strains when the pH of the medium was adjusted to 5 instead of 7 (Fig. 6A). Univariate analysis of the variance showed that all single variables, strain ( $\Delta fur$  versus CECT4999), iron (MSWYE [Marine Seawater Yeast Extract [Biosca and Amaro, 1996] + Fe versus MSWYE - Fe<sub>(TF)</sub>) and pH (acid versus neutral) were highly significant at 4 and 6 h post incubation (Supporting Information Table S4). At these times all interactions with the exception of strain\*pH were also highly significant (Supporting Information Table S4). When the effect of the pH\*iron on the growth of each single strain was analyzed separately we uncovered a strongly significant effect only for the mutant ( $P < 0.0001$ ) (data not shown). These results support the observation that the mutant's survival at pH 5 was strongly dependent on iron where it was not recoverable after 4 h of incubation in MSWYE + Fe. In contrast the mutant survived significantly more than the wild-type strain in MSWYE-Fe<sub>(TF)</sub> (supplemented with human apotransferrin) (Fig. 6A; times 2 and 4 h). The deleterious effect of acid pH on the mutant in presence of an iron excess could be due to the spontaneous production of radical peroxide ions previously reported to be induced under these conditions (Teranishi *et al.*, 2016). In fact, the mutant was significantly more sensitive than the wild-type strain to H<sub>2</sub>O<sub>2</sub> (Fig. 6B) where the observed sensitivity was independent on iron levels at pH 7 (Fig. 6B) and strongly dependent at pH 5 (no cultivable cell was recovered on agar plates) (data not shown). In the case of NO, the mutant was significantly more resistant than the wild-type strain both under iron-excess (time 4 h) and iron-starvation conditions (times 4 and 7) (Fig. 6C). Univariate analysis highlighted that all single variables, strain ( $\Delta fur$  versus CECT4999), iron (MSWYE + Fe versus MSWYE - Fe<sub>(TF)</sub>) and NO (with versus without) were highly significant (Supporting Information Table S4; times 4 and

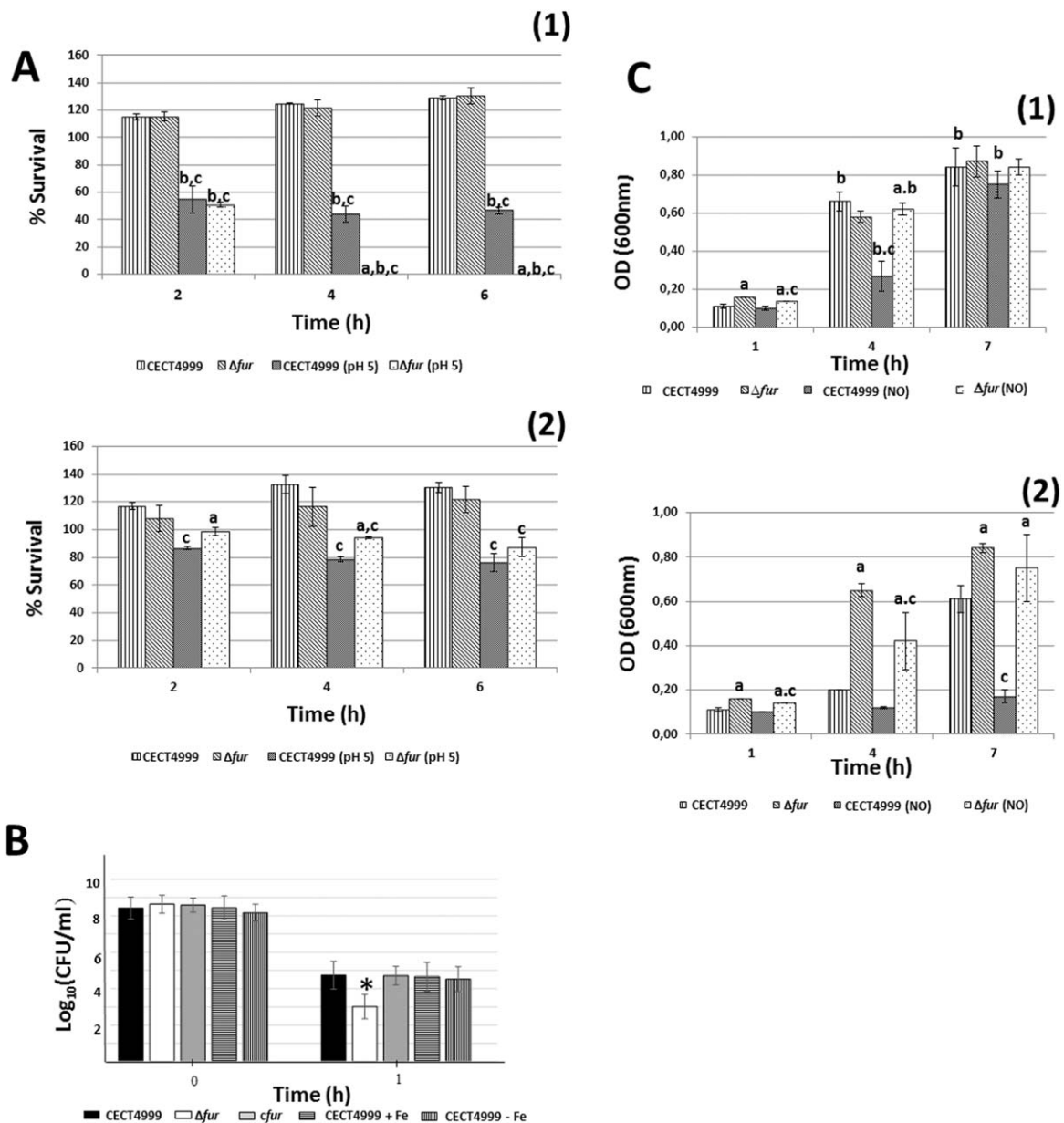


**Fig. 6.** Sensitivity to acid-, oxidative- and nitrosative-stress in *V. vulnificus*. Resistance to acid stress (A) was tested by incubating bacteria in MSWYE + Fe (A1) or MSWYE-Fe<sub>(TT)</sub> (A2) adjusted to neutral (7) or acid pH (5), and counting survivors (% survival) on agar plates at different 2-h intervals for 8 h. a, significant differences between strains ( $\Delta fur$  versus CECT4999) for the same culture medium and pH condition (normal or acid medium); b, significant differences between culture media (MSWYE + Fe versus MSWYE - Fe<sub>(TT)</sub>) for the same strain and pH condition; c, significant differences between pH conditions (acid versus neutral medium) for the same strain and culture medium ( $P < 0.05$ ). Resistance to H<sub>2</sub>O<sub>2</sub> (B) was tested by incubating bacteria in PBS-H<sub>2</sub>O<sub>2</sub> (0.1%), respectively, and counting survivors (CFU/ml) on agar plates at different time intervals. \*Significant differences between strains ( $\Delta fur$  or  $cfur$  versus wild-type) ( $P < 0.05$ ). Resistance to nitrosative stress (C) was tested by following growth in CM9 + Fe (C1) or CM9 - Fe<sub>(TT)</sub> (C2) with and without nitric oxide (NO) 400  $\mu\text{M}$  (NO was added as dipropylentriamine NONOate [DPTA NONOate is a NO donor from Cayman chemicals] by measuring absorbance at 600 nm at 1-h intervals for 7 h. a, significant differences between strains ( $\Delta fur$  versus CECT4999) for the same culture medium and NO condition (with or without NO); b, significant differences between culture media (CM9 + Fe versus CM9 - Fe) for the same strain and NO condition; c, significant differences between NO conditions (with NO versus without NO) for the same strain and culture medium ( $P < 0.05$ ).

7 h post incubation). However only the interaction strain\*iron was highly significant at both sampling times (Supporting Information Table S4). When the effect of the three variables on the growth of each single strain was

separately analyzed it was revealed that the interaction iron\*NO was strongly significant only for the wild-type strain ( $P < 0.0001$ ). These results support the finding that the wild-type strain's resistance to NO was strongly

dependent on iron (Fig. 6C). The main mechanism by which NO inhibits bacterial growth is by binding iron and forming dinitrosyl iron complexes bound to iron-sulfur bacterial proteins, inhibiting their functions (Toledo *et al.*, 2008). In a medium such as CM9 (M9 minimal medium broth supplemented with casaminoacids 0.2%, wt/vol [Miller, 1972]) with transferrin CM9 – Fe<sub>(TF)</sub> with practically no free-iron, all NO would bind to bacterial proteins and the bactericidal effect would be stronger than in an iron-rich medium thus explaining the higher sensitivity to NO of the wild-type strain. All these measures provide a functional validation of the data obtained from the microarray analysis where *sodA* that encodes an enzyme involved in resistance to acid-stress in *V. vulnificus* (Kim *et al.*, 2005), *nsrR*, encoding a repressor specifically dedicated to sensing nitric oxide (Bodenmiller and Spiro, 2006), and *ahpC/katG* (related to entry into the VBNC state) were up-, down- and downregulated, respectively, in the mutant. As previously mentioned for *ahpC*, *sodA* genes also contain a Fur box (Supporting Information Table S5), while no Fur box was detected in *nsrR*. In conclusion, resistance to oxidative-stress could be directly controlled by Fur in an iron-independent manner; resistance to acid-stress also by Fur but in an iron-dependent way and, finally, resistance to nitrosative stress should be a process indirectly depending on Fur.

**Growth under iron-restriction.** As expected, genes involved in iron acquisition were putatively downregulated by Fur and iron with very few exceptions (Figs 2B and 3B, and Supporting Information Tables S1 and S2). Amongst them, the plasmid gene *vep20* encoding a recently described eel-transferrin receptor, Ftbp, is worth highlighting due to its key role in eel virulence (Pajuelo *et al.*, 2015). The genes containing putative Fur boxes are indicated in Supporting Information Table S5. When all the strains were grown with hemin or holotransferrin as the sole iron source  $\Delta fur$  grew faster achieving significantly higher absorbance values than the wild-type and the complemented strains during the log phase of growth (Fig. 7). These data again validate the results obtained using the microarray therefore highlighted the validity and value of this approach.

**Resistance to serum.** A series of genes related to resistance to the bactericidal action of fresh serum were identified. The plasmid gene, *vep07*, involved in resistance to eel serum (Lee and Hor, 2010) and *trkH*, a gene related to a potassium-uptake system involved in human serum resistance (Chen *et al.*, 2004), were found to be differentially expressed depending upon the medium iron content and/or *fur* deletion (Supporting Information Tables S1 and S2). *vep07* was upregulated both under iron restriction and in the mutant while *trkH* was upregulated in the mutant, independently of iron, and showed a putative Fur box (Figs 2B and 3B, Supporting Information Tables S1, S2, and S4). Interestingly, a second potassium uptake pump

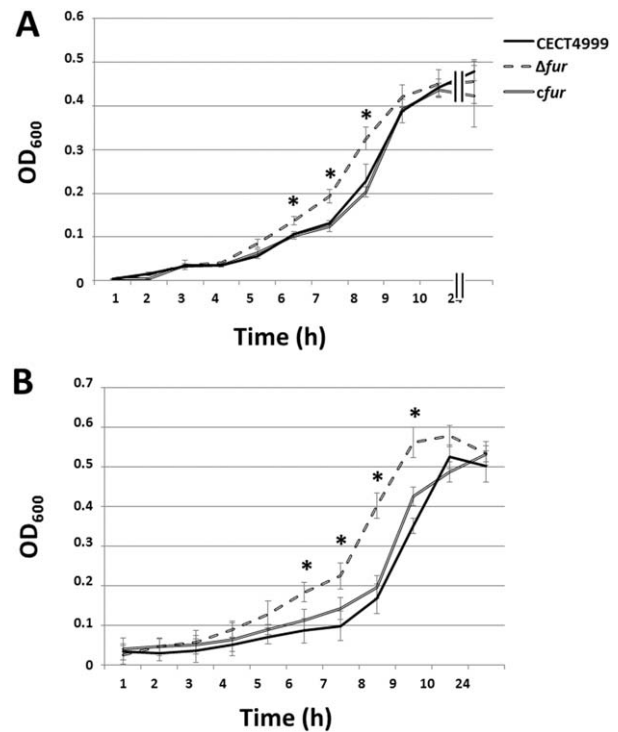


**Fig. 7.** Bacterial growth in presence of hemin and transferrin as the sole iron sources. The three strains of *V. vulnificus* were inoculated in CM9-Hm (A) and CM9 – Fe<sub>(TF)</sub> (B) and growth was followed by measuring the OD<sub>600</sub> at regular time intervals. \*Significant differences in values of OD<sub>600</sub> between the  $\Delta fur$  versus wild-type/*cfur* strains ( $P < 0.05$ ).

(depending on *ktrAB* locus), found in *V. vulnificus* by Chen *et al.* (2004), but still uncharacterized, was found to be upregulated by iron, independently of Fur (Figs 2B and 3B, and Supporting Information Tables S1 and S2). This finding is compatible with the hypothesis that the second system would be inducible in iron-overloaded human serum. We also found genes involved in Lipid A-core, O-antigen, capsular polysaccharide and EPS (extracellular polysaccharide) biosynthesis as differentially expressed under the assayed conditions (Figs 2A and 3A and Supporting Information Tables S1 and S2). Capsular polysaccharides have been previously shown to provide resistance to the bactericidal effect of human serum but not with resistance to eel serum (Wright *et al.*, 1990; Biosca *et al.*, 1993). Most of the genes involved in core-lipid A and antigen O biosynthesis were putatively repressed by Fur, with or without iron dependence, whereas those involved in capsule/EPS biosynthesis were mostly upregulated by Fur in an iron-dependent manner (Supporting Information Tables S1 and S2). In agreement, we found evidence of outer-membrane alterations between the wild-type and the mutant revealed by differences in saponin sensitivity, a non-ionic surfactant of vegetal origin (Fig. 8A). From all DEGs related to polysaccharide



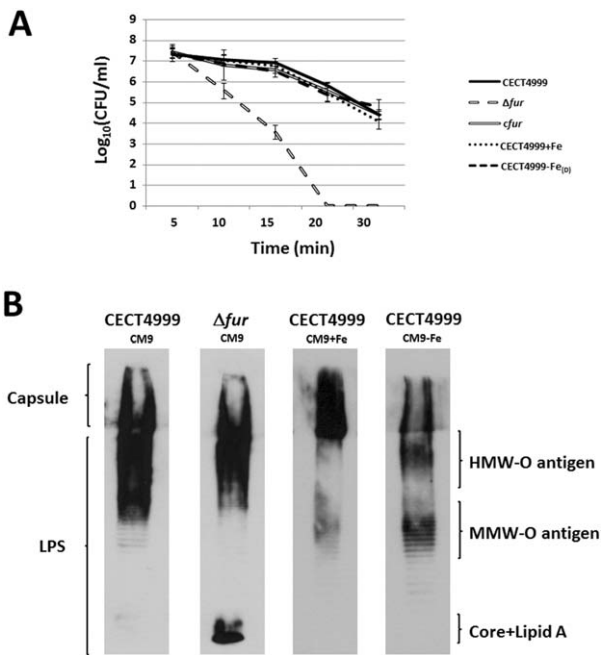


**Fig. 8.** Cell-associated polysaccharides of *V. vulnificus*. (A) The sensitivity to detergents was tested by incubating bacteria in PBS-saponin (100  $\mu\text{g/ml}$ ) for 30 min at 28°C and drop-plate counting at specific sampling points. (B) Cell-associated polysaccharides (LPS + capsule) were extracted with the method of Hitchcock and Brown (1983), separated by SDS-PAGE and immunostained with rabbit primary antibody anti-CECT4999 and secondary anti-rabbit HRP-conjugated. Lane A, LPS + capsule from wild-type strain grown in CM9; Lane B, LPS + capsule from  $\Delta fur$  grown in CM9; Lane C, LPS + capsule from wild-type strain grown in CM9 + Fe; Lane D LPS + capsule from wild-type strain grown in CM9-Fe<sub>(10)</sub>. HMW, high molecular weight; MMW, medium molecular weight.

biosynthesis, only three genes involved in core-lipid A biosynthesis contain a putative Fur box (Supporting Information Table S5). The cell-associated polysaccharides from the wild-type, the mutant and the complemented strains, grown in presence or absence of iron, were extracted and the polysaccharides quantified and analyzed. As predicted by microarray analyses of nascent bacterial transcripts, the quantity of polysaccharides ( $\mu\text{g}$  per  $10^8$  cells) significantly increased with iron concentration in the wild-type ( $P < 0.05$ ), significantly decreased in  $\Delta fur$  with respect to the wild-type/complemented strain

( $P < 0.05$ ) and did not significantly change in the *fur* mutant with iron ( $P > 0.05$ ) (Table 2). Finally, the cell-associated polysaccharide pattern varied among strains and conditions: i.e. the core-lipid A increased with *fur* deletion while the capsule increased concomitantly with a decrease in O-antigen when the wild-type strain was incubated under iron-excess conditions (Fig. 8B).

## Discussion

The results obtained in this study support the hypothesis that iron has a key role in controlling virulence and survival in the aquatic environment of the pathogen *V. vulnificus*. The custom-built microarray platform generated from all predicted ORFs in the Bt2-SerE isolate CECT4999 highlighted that iron stimulon involves 25% of the genes present in the genome. This perhaps is not surprising given that *V. vulnificus* is a septicemic microorganism that has the ability to grow and survive in the blood, a medium where free-iron is bound by transferrin. In a similar manner ~20% of the gonococcal genome is regulated in response to growth under iron-replete versus -depleted conditions both dependently and independently of Fur (Ducey *et al.*, 2005; Jackson *et al.*, 2010). Furthermore most of the genes in the plasmid, pVvbt2, were repressed by iron which would ensure its expression in eel blood. This plasmid encodes a host-specific resistance system to the bacteriolytic and bacteriostatic effect of eel serum that is essential for virulence (Lee *et al.*, 2008). We also uncovered evidence that Fur could repress as well as activate genes both independently and dependently of iron. These results suggest that the Fur protein in *V. vulnificus* would be as versatile as Fur in *V. cholerae* (Mey *et al.*, 2005). Several mechanisms have been suggested to explain how Fur acts as an activator, with the “antirepressor” model as the major mechanism for Fur-dependent activation (Troxe and Hassan, 2013). In this study we found that Fur directly or indirectly represses the transcription of *smcR*, *crp*, and *toxR*, thus directly affecting processes controlled by these global regulators. Thus, the repression of *smcR* by Fur could for example “activate” the transcription of genes repressed by this global regulator. Although the repression of *smcR* by Fur has already been demonstrated (Kim *et al.* 2013) this is the first time to our knowledge that the effect

**Table 2.** Effect of iron concentration and *fur* deletion on the quantity of cellular-associated polysaccharides.

	CECT4999			$\Delta fur$		
	CM9 – Fe	CM9	CM9 + Fe	CM9 – Fe	CM9	CM9 + Fe
$\mu\text{g}/10^8$ cells	219.84 $\pm$ 9.7 $\neq$	235.2 $\pm$ 6.8**	298.84 $\pm$ 18.3	178.6 $\pm$ 22*	187.1 $\pm$ 3.6*	196.9 $\pm$ 10.8*

\*Significant differences between strains ( $\Delta fur$  versus CECT4999) for the same condition ( $P < 0.05$ ).

\*\*Significant differences between conditions (CM9 versus CM9 + Fe) for the same strain ( $P < 0.05$ ).

$\neq$ Significant differences between conditions (CM9 – Fe versus CM9 + Fe) for the same strain ( $P < 0.05$ ).

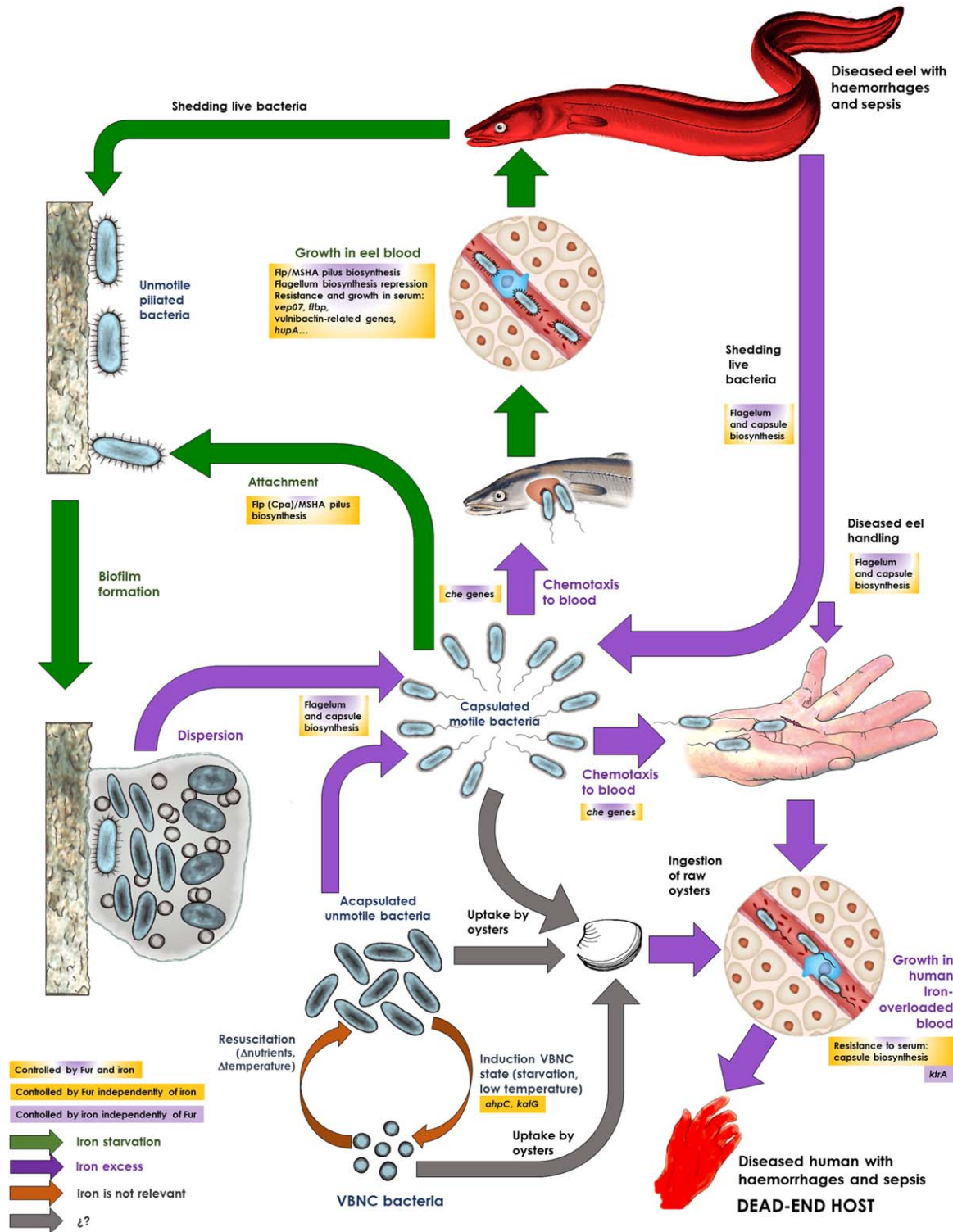
of Fur on ToxR and Crp expression has been reported in *Vibrio*.

Figure 9 represents a hypothetical life cycle for *V. vulnificus* based on the main results obtained in the present study. *V. vulnificus* is a marine pathogen from warm brackish-water ecosystems that can infect fish and humans causing septicemia (Jones and Oliver, 2009). Previous studies performed in artificial and natural seawater microcosms demonstrated that *V. vulnificus* can survive under nutrient starvation in seawater for years maintaining its pathogenic potential for fish and humans by entering into the VBNC state (Marco-Noales *et al.*, 1999). This state can be induced in the laboratory by incubating the pathogen at 4°C (Wolf and Oliver, 1992; Biosca *et al.*, 1996; Whitesides and Oliver, 1997). Our results clearly show that Fur is involved in the entrance into the VBNC state as the Fur mutant becomes non-culturable much earlier than the wild-type strain. We also found experimental evidence relating this process to a reduction in oxidative stress resistance (experiments of survival in H<sub>2</sub>O<sub>2</sub>) concomitantly with a downregulation of *aphC* expression, a gene that possesses a Fur box (Fig. 9). Collectively these results support the hypothesis of Li *et al.* (2014) about the role of resistance to oxidative stress in the entrance into the VBNC state.

*V. vulnificus* resuscitates from the VBNC state with an increase in temperature in the presence of nutrients (Marco-Noales *et al.*, 1999). Our study suggests that neither iron nor Fur have a clear role in the resuscitation from the VBNC state, at least under our experimental conditions (Fig. 9). Although nutrients are scarce in the open sea, they are more abundant in the coast regions, especially in estuarine waters, a habitat common for both *V. vulnificus* (Oliver, 2015) and the eel (Aarestrup *et al.*, 2009). We have found clear evidence that, once resuscitated, *V. vulnificus* could be attracted by blood liberated from a human's or an eel's wound; attraction and bacterial motility being favored in an iron-rich environment (Fig. 9). Furthermore it is likely that both motility and chemotaxis to blood are probably activated by Fur and here we highlight possible candidate genes that may be directly involved. Previous studies have demonstrated that flagellum biosynthesis in *V. vulnificus* is controlled by direct binding of *smcR* to the promoter of *flhF*, a gene driving activation of flagellum biosynthesis (Kim *et al.*, 2012). In this study *smcR* was upregulated in the *fur* mutant, suggesting an additional indirect activation of flagellum biosynthetic genes by Fur. The regulatory role of Fur in flagellum biosynthesis remains to be investigated in further studies. On the other hand, the genes for Flp (Cpa) and MSHA pili biosynthesis were mostly upregulated under iron-restriction and in the *fur* mutant, although in this case we did not find related Fur boxes. Thus, the bacterium would express the flagellum being motile in iron-excess and could express a Flp (Cpa)/MSHA pilus remaining sessile under iron-restriction (Fig. 9). In any case, to our

knowledge this is the first time that Flp (Cpa)/MSHA pilus and flagellum biosynthesis have been linked with iron and Fur in *Vibrio*. Flp (Cpa) and MSHA pili have a role in attachment to surfaces in *Pseudomonas* and *V. cholerae* (Tomich *et al.*, 2007; Utada *et al.*, 2014). Thus we analyzed biofilm formation in iron-excess and iron-starvation by the wild-type and mutant strains. Our results suggest that iron starvation could directly or indirectly activate biofilm formation in *V. vulnificus* as biofilm production by the wild-type strain was decreased in iron-excess (Fig. 9). In parallel, under iron-restriction capsule production decreased in direct agreement with the reported inverse correlation between capsule production and biofilm production in *V. vulnificus* (Joseph and Wright, 2004). Iron is presumably sequestered by eel lactoferrin thus biofilm formation on the external and internal mucous surfaces of the eel would be favored. Our hypothesis is that all *V. vulnificus* Bts are able to colonize eel or fish surfaces by forming biofilms.

*V. vulnificus* either as free living form or associated with particulate material could be accumulated by oysters, the main reservoir for this pathogen and, then cause human infection after ingestion (Oliver, 2015). After colonizing a fish/human wound after contact, or human intestine after ingestion, *V. vulnificus* could invade bloodstream where it would sense a reduction in iron concentration due to iron being bound to transferrin (Fig. 9). The pathogen is then able to sequester iron from hemin/hemoglobin (main receptor HupA), vulnibactin, (receptor VuuA) and eel transferrin, (receptor Ftbp) (Pajuelo *et al.*, 2014; 2015). In this study, we found that virtually all genes involved in the three iron-acquisition systems were repressed by iron and Fur, which would ensure that the bacterium, once in blood, would activate the transcription of genes involved in iron uptake to multiply (Fig. 9). However, the bacterium also needs to resist the bactericidal action of complement to achieve efficient multiplication in this environment. The capsule of *V. vulnificus* is the only virulence factor unequivocally involved in resistance to human serum (Wright *et al.*, 1990). As previously mentioned we found both phenotypic and transcriptomic evidence that iron restriction through Fur would produce a decrease in the amount of capsular polysaccharide (Fig. 9). The fact that the capsule could be repressed in normal human blood could explain why most of *V. vulnificus* strains preferentially cause sepsis in patients with high iron-levels in blood, regardless of the infection route (oral or contact) (Oliver, 2015). On the contrary, the ability to resist eel complement is attributable to the plasmid gene *vep07* but not to the capsule (Amaro *et al.*, 2015; Biosca *et al.*, 1993). The gene, *vep07* containing a putative Fur box, was strongly activated under iron restriction (Fig. 9). The mechanism of action of Vep07 is unknown, but the deletion of the gene results in sensitivity to eel complement but not to human complement (Lee *et al.*, 2008). We also found evidence that Fur directly or



**Fig. 9.** Iron and Fur and the life cycle of the zoonotic pathogen *V. vulnificus*. This figure summarizes the role of iron and Fur in the life cycle of *V. vulnificus*. Only the strains that possess the virulence plasmid pVvbt2 (Bt2) could invade successfully the eel blood and cause death by septicemia. The rest of the strains or Bts would colonize mucosal surfaces of the eel or other fish species without invading them.

indirectly represses genes for lipid A-core biosynthesis. Thus, the mutant presented an altered OM pattern together with a notable increase in sensitivity to detergents such as saponin, in both cases without a clear relationship to the iron concentration. Furthermore we identified a Fur box in three of the genes involved in core-lipid A biosynthesis, which would be candidates to be directly regulated by Fur. This would be the first report in which a link between iron, capsule-LPS biosynthesis and Fur in *Vibrio* is suggested. Our results also suggest that Fur may play a role in resistance to more general stressors related to innate immunity (NO, oxidative stress, acid pH...) in an iron-independent way. Thus, Fur would activate resistance to oxidative stress and would repress resistance to acid and nitrosative stress, in both cases directly or indirectly.

The virulence assays performed in eels and mice revealed that the *fur* mutant showed a slight increase in LD<sub>50</sub> for both species together with a delayed colonization of internal organs, which contrasts with the reduction in virulence of more than 2 log units reported for other pathogens in different animal models including fishes (Porcheron and Dozois, 2015). Remarkably, the effect of iron in virulence was much more evident because virulence for mice and eels increased in more than 2 log. units with iron-pretreatment, which is in accordance with previous reports for *V. vulnificus* (Amaro *et al.*, 1994). Thus, the minor variation in virulence of the *fur* mutant would be the result of the sum of different processes: the faster growth in iron-restricted conditions together with the higher resistance to acid and nitrosative stresses contrasts with the detrimental changes to the OM and a higher sensitivity to oxidative stress.

Human vibriosis differs from fish vibriosis in that the most severe form of the disease in humans (sepsis) is mostly produced when iron levels in blood are high while this condition is not necessary in the eel. In the present study we have found evidence that iron concentration in

the animal's blood determines the outcome of human and animal disease. Thus, the higher virulence toward eels would be partially due to the two plasmid-encoded proteins that confer specific resistance to the bactericidal (Vep07) and bacteriostatic effect (Ftbp) of eel blood. Both targets are repressed by Fur and iron therefore are expressed in eel blood under normal circumstances. In contrast, this pathogen only possesses generalist systems to overcome the bacteriostatic and bactericidal action of human serum, the first ones those depending upon HupR and VuuA are repressed by Fur and iron, and would be expressed in normal human serum but the second ones those depending upon capsule biosynthesis would only be optimally expressed in iron-overloaded serum, thus explaining why human sepsis is correlated to iron-overloading.

In summary our results support the hypothesis that iron, not always through Fur, is one of the main signals acting as niche marker for *V. vulnificus*. Iron impacts the entire life cycle of the pathogen from its survival in the marine environment, including motility and chemotaxis, to its survival in the blood of their hosts. In blood, iron concentration would be the key signal for this septicemic bacterium, triggering the expression of genes involved in survival and resistance to the innate immune response (the plasmid genes *vep07* and *ftbp* in eel's blood and the chromosomal genes involved in capsule biosynthesis in iron-overloaded human blood) allowing the bacterium to multiply and persist inside their hosts.

## Experimental procedures

### Bacterial strains, growth media and conditions

The bacterial strains used in the study are listed in Table 3. The bacteria were routinely grown in LB-1/LBA-1 (Luria-Bertani broth/agar, 1% NaCl) or CM9/CM9A. If necessary, ampicillin (100 µg/ml), chloramphenicol (20 µg/ml for *Escherichia coli* and 2 µg/ml for *V. vulnificus*) or polymyxin B (50 U/ml) were added to the media. To analyze the effect of different

**Table 3.** Strains and plasmids used in this study.

Designation	Description	Isolation source/reference
<i>V. vulnificus</i>		
CECT4999	Biotype 2 Serovar E	Diseased eel (Spain)
$\Delta fur$	CECT4999 <i>fur</i> -defective mutant	This study
<i>cfur</i>	$\Delta fur$ complemented strain	This study
<i>E. coli</i>		
DH5 $\alpha$	Cloning strain	Invitrogen
s17- $\lambda_{pir}$	Strain containing the pCVD442 plasmid. <i>thi pro hsdR hsdM+ recA::RP4-2-Tc::Mu <math>\lambda_{pir}</math> Km<sup>r</sup> Nal<sup>r</sup></i>	Simon <i>et al.</i> (1983)
Plasmids		
pGemT-easy	T/A Cloning vector, Amp <sup>r</sup>	Promega
pIT009	Derivative of pJRD215 with the Sm <sup>r</sup> gene between two <i>XmnI</i> sites replaced by the multiple-cloning-site-containing <i>lacZ</i> gene cloned from pUC19	Lee <i>et al.</i> (2008)
p $\Delta fur$	pGemT-easy with $\Delta fur$ in the MCS	This study
pIT $fur$	pIT009 with <i>fur</i> gene and promoter in MCS	This study



iron sources on growth, bacteria were grown in CM9 – Fe<sub>(D)</sub> (CM9 plus 50 μM 4,4 – Dipyridyl [Sigma-Aldrich, Madrid, Spain] ), CM9-Hm (CM9 – Fe<sub>(D)</sub> plus 0.1 μM bovine hemin [Sigma-Aldrich]), CM9 + Fe (CM9 plus 100 μM FeCl<sub>3</sub>) and CM9 – Fe<sub>(TF)</sub> (CM9 plus 40 μM of unsaturated human transferrin or apotransferrin, [Sigma-Aldrich]). *V. vulnificus* strains were incubated at 28°C and *E. coli* strains at 37°C for 18–24 h. All the strains were stored in LB-1 plus glycerol (17%) at –80°C.

#### DNA purification, PCR and generation of mutant and complemented strains

The genomic DNA was extracted as described by Ausubel *et al.* (1999). DNA amplification by PCR was performed as described by Pajuelo *et al.* (2014) and primers were designed from the genome of *V. vulnificus* CECT4999 (NCBI Accession No. CP01436 for chromosome I, CP01437 for chromosome II and CP01438) and the virulence plasmid pR99 (AM293858). To obtain a Fur-deficient strain, *fur* deletion mutant was obtained by chitin-based natural transformation (Gulig *et al.*, 2009) with slight modifications. Briefly, the regions of the chromosome corresponding to up-(1382 nt) and downstream (1329 nt) of *fur* gene were amplified using primer sets (Fur-1/Fur-2 and Fur-3/Fur-4) (Supporting Information Table S5) and cloned into the pGEMT-easy. Chloramphenicol resistance marker was inserted at *Xba*I site of the cloned construction thus obtaining plasmid pΔ*fur*. Plasmid was linearized by *Xmn*I digestion and introduced into *V. vulnificus* CECT4999 by natural transformation as previously described (Meibom *et al.*, 2005). Transformants were selected using LB plates supplemented with chloramphenicol. To generate the complemented strain, *cfur*, the entire *fur* gene and its promoter region were amplified from *V. vulnificus* CECT4999 with primers Fur-5/Fur-6 with a *Bam*HI restriction site added, and cloned into the *Bam*HI site of a recombinant plasmid, pIT009 (Lee *et al.*, 2008). The resultant plasmid (pIT*fur*) was introduced into Δ*fur* strain by conjugation.

#### Microarray analysis

**Microarray design.** The CECT4999-specific gene expression microarray (8 × 15 K) slides were custom designed with eArray software (Agilent technologies), following MIAME guidelines for array design (Brazma *et al.*, 2001), taking as reference the predicted annotated ORF's of CECT4999 strain genome for the probes design. The arrays contained in total 4553 probes of 60-oligonucleotide length. These probes were distributed in 3 probes per target (13659) with an e-value of 0.0 and the rest were filled with internal control probes of Agilent. The platform was submitted to the GEO repository with the accession number GPL19040.

**Sample preparation, labeling and hybridization.** Total RNA from mid-log phase cultures was extracted with TRI reagent (Sigma). RNA was subjected to a DNase treatment with the TURBO™ DNase (Ambion, Madrid, Spain) and cleaned with the RNeasy® MinEute® Cleanup Kit (Qiagen, Barcelona, Spain) as described by the manufacturers. RNA concentration and integrity were measured by 2100 Bioanalyzer (Agilent, Madrid, Spain). General procedures to obtain

labeled cRNA were performed as described in protocols of the kit “One-Color Microarray-Based Gene Expression Analysis: Low Input Quick Amp Labeling” (Agilent). To obtain cDNA, 200 μg of total RNA (template) were mixed with 200 ng of T7N9 primers, a random nonamers that amplify all the RNA (Moreno-Paz and Parro, 2006). Resultant cDNA was subjected to a transcription reaction to finally obtain cRNA labeled with cyanine 3 dye (Cy3), was dispensed onto the gasket well on the slides and were placed in a hybridization oven with rotation at 10 r.p.m. at 65°C for 17 h. After washing steps of the slides, scanning was performed with an Axon Scanner 4000B.

**Microarray validation by qRT-PCR.** The same samples used for the microarray analysis were analyzed by qRT-PCR (Pajuelo *et al.*, 2014) to calculate the expression of 12 selected genes (primers listed in Supporting Information Table S3). The *recA* gene was used as standard and the fold induction ( $2^{-\Delta\Delta Ct}$ ) for each gene was calculated according to Livak and Schmittgen (2001). The tested genes were classified as induced (fold change  $\geq 2$ ), repressed (fold change  $\leq -2$ ) and equally expressed ( $2 > \text{fold change} > -2$ ) genes comparing their expression in Δ*fur* versus wild-type or in iron-restriction versus iron-excess.

#### In silico analysis of putative Fur boxes

The sequences of already described *V. vulnificus* Fur boxes (Ahmad *et al.*, 2009) were used to scan the CECT4999 genome for potential Fur boxes with a maximum 30% of mismatches by using Ugene (Okonechnikov *et al.*, 2012). We used subsystem annotation tools implemented in the SEED genomic platform (<http://theseed.uchicago.edu/FIG/index.cgi>) (Overbeek *et al.*, 2005) to search for genes implicated in virulence and survival and manually extract the putative Fur boxes. WebLogo (Crooks *et al.*, 2004) was used to build a consensus sequence logo, in which the height of individual letters within a stack of letters represents the relative frequency of that letter at a given position, and the overall height of the stack represents the degree of conservation at that position.

#### In vivo assays

**Animal maintenance.** Three populations of farmed European eel (*Anguilla anguilla*) of 10 g, 20 g and 100 g were used for virulence assays, colonization assays and blood extraction respectively. The eels were purchased from a local eel-farm that does not vaccinate against *V. vulnificus*. Fishes were placed in quarantine in 170 L-tanks (6 fish of 100 g, 12 of 20 g, or 20 of 10 g per tank, respectively) containing brackish water (1.5% NaCl, pH 7.6) with aeration, filtration and feeding systems at 25°C for a week. Six to 8-week-old BALB/c mice were purchased from Harlan Laboratory Models S.L. and maintained for 48 h in 100 l plastic cages with water and feed supplied by the Animal housing facilities of the University of Valencia (UV).

**Virulence.** Virulence for eels (10 g of body weight) was determined after immersion (normal or iron-overloaded eels [pre-injected with 9 μg/g of FeCl<sub>3</sub>] or i.p. injection according to Amaro *et al.* (1995). Virulence for mice was tested by i.p.

injection of normal and iron-overloaded (pre-injected with  $\text{FeCl}_3$  [9  $\mu\text{g/g}$  of mouse] 2 h before challenge) mice (BALBc, 20 g of body weight) according to Amaro *et al.* (1994). For both eels and mice, a total of six animals were used per control, strain and dose and were maintained in independent cages or tanks. Animal mortality was recorded for one week and was only considered if the inoculated bacterium was re-isolated in pure-culture from the moribund animal. Virulence (Lethal Dose 50% or  $\text{LD}_{50}$ ) was calculated according to Reed and Muench (1938) and was expressed as CFU/g (i.p. injection) or ml of infective bath (immersion challenge).

**Colonization.** A total of 24 eels per strain were infected by immersion with the  $\text{LD}_{50}$  of the wild-type strain and additional six eels were immersed in a control bath (PBS-1) for 1 h. Then eels were captured and placed in independent tanks per strain for 1 week. A total of 12 live eels were randomly sampled at 0, 9, 24, and 72 h post-infection, at a ratio of 3 per sampling point (Pajuelo *et al.*, 2014). The rest of the eels were monitored for 1 week to check that the mortality was around 50%. Samples for determination of bacterial numbers on TSA-1 were taken from blood, head kidney, liver, spleen and gills, according to (Pajuelo *et al.*, 2014) and bacterial counts were expressed as CFU/ml (blood) or CFU/g.

All the protocols were reviewed and approved by the Animal Ethics Committee of the University of Valencia.

#### In vitro assays

**Induction of the VBNC state and resuscitation.** Cells from overnight cultures in MSWYE were transferred to ASW, ASW + Fe or ASW –  $\text{Fe}_{(\text{D})}$  (28°C, 160 r.p.m.) and were incubated at 4°C with shaking (60 r.p.m.) until no bacteria were detectable by drop plating on CM9A (induction of VBNC state). Then, cultures were incubated at 22°C with shaking (160 r.p.m.) and the resuscitation was monitored again by drop plating on CM9A. Selected genes from the microarray results were quantified by qRT-PCR during the induction of the VBNC state. The genes and the primers are indicated in Supporting Information Table S5.

**Motility and chemotaxis toward blood components.** Motility was assayed on Motility agar (CM9 agar [CM9A] 0.3% agar wt/vol) plus 100  $\mu\text{M}$   $\text{FeCl}_3$  (MA + Fe) or plus 20  $\mu\text{M}$  of D (MA –  $\text{Fe}_{(\text{D})}$ ) by inoculating 5  $\mu\text{l}$  from an exponential phase culture (6 h). Plates were incubated at 28°C for 24 h and the surface of the bacterial mass on the plate ("colony") in  $\text{cm}^2$  (SC) as well as the number of bacteria forming the "colony" in CFU (NB) were determined. Then, the parameter *motility rate* (Mr) was calculated as  $\text{SC}/\log \text{NB}$ . In parallel, microscopic observations of bacterial suspensions were made in a Nikon Phase-Contrast Microscope.

Human-, eel- and hemolytic-eel-plasma (HP, EP and HEP) were obtained as described previously (Pajuelo *et al.*, 2014). The chemotactic response (Cr) toward plasma was determined by using the capillary assay as described by Larsen *et al.* (2001). To this end, bacteria were recovered from cultures grown 6 h in CM9, washed twice in PBS and diluted in chemotaxis buffer (PBS, 0.01 mM EDTA) at  $10^7$  CFU per ml (Larsen *et al.*, 2001). Then, volumes of 0.5 ml of bacterial suspension were dispensed in 1.5 ml tubes that were put into contact with HP, EP, HEP or chemotaxis buffer (control)

contained in capillary tubes (5- $\mu\text{l}$  pre-calibrated pipettes; Vitrex) for 35 min. The number of bacteria inside the capillaries was determined on CM9A plates and the chemotaxis toward HP, EP or HEP was expressed as the ratio between bacterial numbers in the corresponding capillaries versus control capillaries.

**Biofilm formation.** Bacteria were grown in 96-well plates (NUNC) containing 200  $\mu\text{l}$  of LB-1, supplemented or not with either  $\text{FeCl}_3$  100  $\mu\text{M}$  or 20  $\mu\text{M}$  of D and biofilm production was quantified by staining with crystal violet (Jones *et al.*, 2008) at specific time intervals.

**Growth in iron-restriction and in presence of hemin and Tf as the sole iron-sources.** Growth in CM9-Hm and CM9 –  $\text{Fe}_{(\text{Tf})}$  was monitored as previously described (Pajuelo *et al.*, 2014).

**Minimal inhibitory concentration (MIC) of iron chelators, microcide peptides, and saponin.** MICs for polymyxin B sulfate (Sigma), lysozyme (Sigma) and sodium deoxycholate (SDC) (Sigma) were determined in CM9A, CM9A + Fe and CM9A –  $\text{Fe}_{(\text{D})}$  plates. Plates were inoculated with exponential phase cultures (6 h) in CM9, CM9 + Fe or CM9 –  $\text{Fe}_{(\text{D})}$  and sterile disks impregnated with different concentrations of polymyxin B sulfate (1– $10^3$   $\mu\text{g/ml}$ ), lysozyme (1– $10^3$   $\mu\text{g/ml}$ ), or SDC ( $10^3$ – $10^6$   $\mu\text{g/ml}$ ) were added. The MIC was defined as the lowest substrate concentration at which there was not growth. In the case of saponin (Sigma), 96-well plates (NUNC) containing 200  $\mu\text{l}$  of PBS + saponin (100  $\mu\text{g/ml}$ ), were inoculated with overnight cultures in CM9 in a ratio 1:100 (v/v), were incubated at 28°C with shaking (160 r.p.m.) and viable bacterial count on CM9A was performed at 5, 10, 15, 20, and 30 min post-incubation by the drop-plate method (Hoben and Somasegaran, 1982).

**Resistance to acid, oxidative, and nitrosative stresses.** Washed bacteria from overnight cultures in CM9 or CM9 –  $\text{Fe}_{(\text{D})}$  at 28°C were inoculated in tubes containing 5 ml of MSWYE (control), MSWYE-pH5 (acid-stress) or PBS- $\text{H}_2\text{O}_2$  (0.1% vol/vol) (oxidative stress), supplemented or not with 20  $\mu\text{M}$  Dipyrindyl, at a ratio of  $10^5$  CFU/ml. Tubes were incubated at 28°C with shaking (60 r.p.m.) for 180 min. Viable bacterial counts were estimated by drop plating on CM9A at intervals of 30 min. To test resistance to nitrosative stress, bacteria from overnight cultures in CM9, CM9 + Fe or CM9 –  $\text{Fe}_{(\text{Tf})}$  at 28°C were washed in PBS and inoculated in the respective fresh medium supplemented or not with 400  $\mu\text{M}$  DPTA NONOate (NO donor, Cayman Chemical, Michigan, USA). DPTA NONOate was decay for 3 h in the medium in order to achieve a constant NO release (Henares *et al.*, 2012). Growth was followed by measuring absorbance at 600 nm on a spectrophotometer (Thermo scientific) at 1-h intervals for 8 h.

**Proteolytic and hemolytic activity.** The extracellular products (ECP) from the three strains were obtained as previously described (Biosca and Amaro, 1996) from overnight cultures on CM9A – Fe or CM9A –  $\text{Fe}_{(\text{D})}$  and the maximal dilution of ECP with positive activity on agarose-erythrocytes (bovine erythrocytes from Sigma) or agarose-casein was determined. In parallel, the hemolytic activity of live cells at short term was determined according to Shinoda *et al.* (1985).

**Cell-associated polysaccharides.** Crude fractions of cell-associated polysaccharides (LPS plus capsule) were obtained from overnight cultures of the three strains in CM9 + Fe or CM9 – Fe<sub>(TF)</sub> as described by Hitchcock and Brown (1983). The polysaccharide concentration was determined with Total Carbohydrate Assay Kit (BioVision) as described by the manufacturers and samples were adjusted to 0.2 µg/µl of polysaccharide. LPS and capsule antigens were separated by SDS-PAGE (Laemmli, 1970) in discontinuous gels (4% stacking gel, 10% separating gel), transferred to a PVDF membrane (Bio-Rad, Madrid, Spain) (Towbin *et al.*, 1979) and subjected to immunoblot analysis. The membranes were probed with serovar E-specific sera (Amaro *et al.*, 1992) diluted 1:3000 and were developed following incubation with anti-rabbit IgG HRP-conjugated secondary antibody diluted 1:10 000 (Sigma), using Immobilon Western Chemiluminescent HRP Substrate (Millipore, Madrid, Spain).

**Statistical analysis.** All the experiments, except the virulence assays, were performed by triplicate. Statistical analysis was performed using the SPSS 17.0 for windows. The results are presented as means ± SE (standard error of the means). The significance of the differences between means was tested by using the unpaired Student's t-test with a  $P < 0.05$ . When the effects of more than two independent variables were taken into account, a GLM (general linear modeling) univariate analysis was performed. This analysis allows to highlight not only the significance of the single variables but also that of their interactions.

- A. Effect of strain (wild-type vs mutant), iron (with vs without) and pH (neutral vs acid) on bacterial growth at 2, 4 and 6 h post-incubation
- B. Effect of strain (wild-type vs mutant), iron (with vs without) and NO (with vs without) on bacterial growth at 1 4 and 7 h post-incubation

## Acknowledgements

This work has been financed by grants AGL2014-58933-P and Programa Consolider-Ingenio 2010 CSD2009-00006 from MICINN (Spain) and with grant NSC 97-2320-B-006-009-MY3 from National Science Council (Taiwan).

## References

Aarestrup, K., Okland, F., Hansen, M.M., Righton, D., Gargan, P., Castonguay, M., *et al.* (2009) Oceanic spawning migration of the European eel (*Anguilla anguilla*). *Science* **325**: 1660.

Ahmad, R., Hjerde, E., Hansen, G.A., Haugen, P., and Willassen, N.P. (2009) Prediction and experimental testing of ferric uptake regulator regulons in *Vibrios*. *J Mol Microbiol Biotechnol* **16**: 159–168.

Alice, A.F., Naka, H., and Crosa, J.H. (2008) Global gene expression as a function of the iron status of the bacterial cell: influence of differentially expressed genes in the virulence of the human pathogen *Vibrio vulnificus*. *Infect Immun* **76**: 4019–4037.

Amaro, C., and Biosca, E.G. (1996) *Vibrio vulnificus* biotype 2, pathogenic for eels, is also an opportunistic pathogen for humans. *Appl Environ Microbiol* **62**: 1454–1457.

Amaro, C., Biosca, E.G., Fouz, B., Alcaide, E., and Esteve, C. (1995) Evidence that water transmits *Vibrio vulnificus* biotype 2 infections to eels. *Appl Environ Microbiol* **61**: 1133–1137.

Amaro, C., Biosca, E.G., Fouz, B., and Garay, E. (1992) Electrophoretic analysis of heterogeneous lipopolysaccharides from various strains of *Vibrio vulnificus* biotypes 1 and 2 by silver staining and immunoblotting. *Curr Microbiol* **25**: 99–104.

Amaro, C., Biosca, E.G., Fouz, B., Toranzo, A.E., and Garay, E. (1994) Role of iron, capsule, and toxins in the pathogenicity of *Vibrio vulnificus* biotype 2 for mice. *Infect Immun* **62**: 759–763.

Amaro, C., Sanjuán, E., Fouz, B., Pajuelo, D., Lee, C.T., Hor, L.I., and Barrera, R. (2015). The fish pathogen *Vibrio vulnificus* biotype 2: epidemiology, phylogeny, and virulence factors involved in warm-water vibriosis. *Microbiol Spectr.* **3**. doi: 10.1128/microbiolspec.VE-0005-2014.

Ausubel, F.M., Brent, R., Kingston, R.E., and Moore, D.D. (1999) *Short Protocols in Molecular Biology* 4th ed. Ausubel, F.M., Brent, R., Kingston, R.E., and Moore, D.D. (eds.) New York: John Wiley & Sons, Inc.

Bailey, T.L., Boden, M., Buske, F.A., Frith, M., Grant, C.E., Clementi, L., *et al.* (2009) MEME SUITE: tools for motif discovery and searching. *Nucleic Acids Res* **37**: W202–W208.

Becker, K.W., and Skaar, E.P. (2014) Metal limitation and toxicity at the interface between host and pathogen. *FEMS Microbiol Rev* **38**: 1235–1249.

Biosca, E.G., and Amaro, C. (1996) Toxic and enzymatic activities of *Vibrio vulnificus* biotype 2 with respect to host specificity. *Appl Environ Microbiol* **62**: 2331–2337.

Biosca, E.G., Amaro, C., Marco-Noales, E., and Oliver, J.D. (1996) Effect of low temperature on starvation-survival of the eel pathogen *Vibrio vulnificus* biotype 2. *Appl Environ Microbiol* **62**: 450–455.

Biosca, E.G., Llorens, H., Garay, E., and Amaro, C. (1993) Presence of a capsule in *Vibrio vulnificus* biotype 2 and its relationship to virulence for eels. *Infect Immun* **61**: 1611–1618.

Bisharat, N., Agmon, V., Finkelstein, R., Raz, R., Ben-Dror, G., Lerner, L., *et al.* (1999) Clinical, epidemiological, and microbiological features of *Vibrio vulnificus* biogroup 3 causing outbreaks of wound infection and bacteraemia in Israel. *Lancet* **354**: 1421–1424.

Bodenmiller, D.M., and Spiro, S. (2006) The *yjeB* (*nsrR*) gene of *Escherichia coli* encodes a nitric oxide-sensitive transcriptional regulator. *J Bacteriol* **188**: 874–881.

Brazma, A., Hingamp, P., Quackenbush, J., Sherlock, G., Spellman, P., Stoeckert, C., *et al.* (2001) Minimum information about a microarray experiment (MIAME)-toward standards for microarray data. *Nat Genet* **29**: 365–371.

Chen, Y.C., Chuang, Y.C., Chang, C.C., Jeang, C.L., and Chang, M.C. (2004) A K<sup>+</sup> uptake protein, TrkA, is required for serum, protamine, and polymyxin B resistance in *Vibrio vulnificus*. *Infect Immun* **72**: 629–636.

Crooks, G.E., Hon, G., Chandonia, J.M., and Brenner, S.E. (2004) WebLogo: a sequence logo generator. *Genome Res* **14**: 1188–1190.



- Ducey, T.F., Carson, M.B., Orvis, J., Stintzi, A.P., and Dyer, D.W. (2005) Identification of the iron-responsive genes of *Neisseria gonorrhoeae* by microarray analysis in defined medium. *J Bacteriol* **187**: 4865–4874.
- Gulig, P.A., Tucker, M.S., Thiaville, P.C., Joseph, J.L., and Brown, R.N. (2009) USER friendly cloning coupled with chitin-based natural transformation enables rapid mutagenesis of *Vibrio vulnificus*. *Appl Environ Microbiol* **75**: 4936–4949.
- Haenen, O.L.M., van Zanten, E., Jansen, R., Roozenburg, I., Engelsma, M.Y., Dijkstra, A., *et al.* (2014) *Vibrio vulnificus* outbreaks in Dutch eel farms since 1996: strain diversity and impact. *Dis Aquat Organ* **108**: 201–209.
- Hantke, K. (2001) Iron and metal regulation in bacteria. *Curr Opin Microbiol* **4**: 172–177.
- Henares, B.M., Higgins, K.E., and Boon, E.M. (2012) Discovery of a nitric oxide responsive quorum sensing circuit in *Vibrio harveyi*. *ACS Chem Biol* **7**: 1331–1336.
- Hitchcock, P.J., and Brown, T.M. (1983) Morphological heterogeneity among *Salmonella* lipopolysaccharide chemotypes in silver-stained polyacrylamide gels. *J Bacteriol* **154**: 269–277.
- Hoben, H.J., and Somasegaran, P. (1982) Comparison of the pour, spread, and drop plate methods for enumeration of *Rhizobium* spp. in inoculants made from presterilized peat. *Appl Environ Microbiol* **44**: 1246–1247.
- Hood, M.I., and Skaar, E.P. (2012) Nutritional immunity: transition metals at the pathogen–host interface. *Nat Rev Microbiol* **10**: 525–537.
- Horseman, M.A., and Surani, S. (2011) A comprehensive review of *Vibrio vulnificus*: an important cause of severe sepsis and skin and soft-tissue infection. *Int J Infect Dis* **15**: e157–e166.
- Jackson, L.A., Ducey, T.F., Day, M.W., Zaitshik, J.B., Orvis, J., and Dyer, D.W. (2010) Transcriptional and functional analysis of the *Neisseria gonorrhoeae* Fur regulon. *J Bacteriol* **192**: 77–85.
- Jones, M.K., and Oliver, J.D. (2009) *Vibrio vulnificus*: disease and pathogenesis. *Infect Immun* **77**: 1723–1733.
- Jones, M.K., Warner, E.B., and Oliver, J.D. (2008) *csrA* inhibits the formation of biofilms by *Vibrio vulnificus*. *Appl Environ Microbiol* **74**: 7064–7066.
- Joseph, L.A., and Wright, A.C. (2004) Expression of *Vibrio vulnificus* capsular polysaccharide inhibits biofilm formation. *J Bacteriol* **186**: 889–893.
- Kim, I.H., Wen, Y., Son, J.S., Lee, K.H., and Kim, K.S. (2013) The Fur–iron complex modulates expression of the quorum-sensing master regulator, SmcR, to control expression of virulence factors in *Vibrio vulnificus*. *Infect Immun* **81**: 2888–2898.
- Kim, J.S., Sung, M.H., Kho, D.H., and Lee, J.K. (2005) Induction of manganese-containing superoxide dismutase is required for acid tolerance in *Vibrio vulnificus*. *J Bacteriol* **187**: 5984–5995.
- Kim, S.M., Lee, D.H., and Choi, S.H. (2012) Evidence that the *Vibrio vulnificus* flagellar regulator FlhF is regulated by a quorum sensing master regulator SmcR. *Microbiology (United Kingdom)* **158**: 2017–2025.
- Laemmli, U.K. (1970) Cleavage of structural proteins during the assembly of the head of bacteriophage T4. *Nature* **227**: 680–685.
- Larsen, M.H., Larsen, J.L., and Olsen, J.E. (2001) Chemotaxis of *Vibrio anguillarum* to fish mucus: role of the origin of the fish mucus, the fish species and the serogroup of the pathogen. *FEMS Microbiol Ecol* **38**: 77–80.
- Lee, C.T., Amaro, C., Wu, K.M., Valiente, E., Chang, Y.F., Tsai, S.F., *et al.* (2008) A common virulence plasmid in biotype 2 *Vibrio vulnificus* and its dissemination aided by a conjugal plasmid. *J Bacteriol* **190**: 1638–1648.
- Lee, C.T., Pajuelo, D., Llorens, A., Chen, Y.H., Leiro, J.M., Padrós, F., *et al.* (2013) MARTX of *Vibrio vulnificus* biotype 2 is a virulence and survival factor. *Environ Microbiol* **15**: 419–432.
- Lee, H.J., Bang, S.H., Lee, K.H., and Park, S.J. (2007) Positive regulation of *fur* gene expression via direct interaction of Fur in a pathogenic bacterium, *Vibrio vulnificus*. *J Bacteriol* **189**: 2629–2636.
- Lee, H.J., Park, K.J., Lee, A.Y., Park, S.G., Park, B.C., Lee, K.H., and Park, S.J. (2003) Regulation of *fur* expression by RpoS and Fur in *Vibrio vulnificus*. *J Bacteriol* **185**: 5891–5896.
- Lee, J.H.H., Rho, J.B., Park, K.J.J., Kim, C.B., Han, Y.S.S., Choi, S.H., *et al.* (2004) Role of flagellum and motility in pathogenesis of *Vibrio vulnificus*. *Infect Immun* **72**: 4905–4910.
- Li, L., Mendis, N., Trigui, H., Oliver, J.D., and Faucher, S.P. (2014) The importance of the viable but non-culturable state in human bacterial pathogens. *Front Microbiol* **5**: 1–20.
- Livak, K.J., and Schmittgen, T.D. (2001) Analysis of relative gene expression data using real-time quantitative PCR and the 2<sup>-ΔΔC(T)</sup> method. *Methods* **25**: 402–408.
- Marco-Noales, E., Biosca, E.G., and Amaro, C. (1999) Effects of salinity and temperature on long-term survival of the eel pathogen *Vibrio vulnificus* biotype 2 (serovar E). *Appl Environ Microbiol* **65**: 1117–1126.
- Mården, P., Hermansson, M., and Kjelleberg, S. (1988) Incorporation of tritiated thymidine by marine bacterial isolates when undergoing a starvation survival response. *Arch Microbiol* **149**: 427–432.
- Meibom, K.L., Blokesch, M., Dolganov, N.A., Wu, C.Y., and Schoolnik, G.K. (2005) Chitin induces natural competence in *Vibrio cholerae*. *Science* **310**: 1824–1827.
- Mey, A.R., Wyckoff, E.E., Kanukurthy, V., Fisher, C.R., and Payne, S.M. (2005) Iron and Fur regulation in *Vibrio cholerae* and the role of Fur in virulence. *Infect Immun* **73**: 8167–8178.
- Miller, J.H. (1972) *Experiments in Molecular Genetics*. Cold Spring Harbor, NY: Cold Spring Harbor Laboratory Press.
- Moreno-Paz, M., and Parro, V. (2006) Amplification of low quantity bacterial RNA for microarray studies: time-course analysis of *Leptospirillum ferrooxidans* under nitrogen-fixing conditions. *Environ Microbiol* **8**: 1064–1073.
- Okonechnikov, K., Golosova, O., and Fursov, M. (2012) UniPro UGENE: a unified bioinformatics toolkit. *Bioinformatics* **28**: 1166–1167.
- Oliver, J.D. (2010) Recent findings on the viable but nonculturable state in pathogenic bacteria. *FEMS Microbiol Rev* **34**: 415–425.
- Oliver, J.D. (2015) The biology of *Vibrio vulnificus*. *Microbiol Spectr* **3**: VE-0001–2014.
- Overbeek, R., Begley, T., Butler, R.M., Choudhuri, J.V., Chuang, H.Y., Cohoon, M., *et al.* (2005) The subsystems

- approach to genome annotation and its use in the project to annotate 1000 genomes. *Nucleic Acids Res* **33**: 5691–5702.
- Pajuelo, D., Lee, C.T., Roig, F.J., Hor, L.I., and Amaro, C. (2015) Novel host-specific iron acquisition system in the zoonotic pathogen *Vibrio vulnificus*. *Environ Microbiol* **17**: 2076–2089.
- Pajuelo, D., Lee, C.T., Roig, F.J., Lemos, M.L., Hor, L.I., and Amaro, C. (2014) Host-nonspecific iron acquisition systems and virulence in the zoonotic serovar of *Vibrio vulnificus*. *Infect Immun* **82**: 731–744.
- Paranjpye, R.N., and Strom, M.S. (2005) A *Vibrio vulnificus* type IV pilin contributes to biofilm formation, adherence to epithelial cells, and virulence. *Infect Immun* **73**: 1411–1422.
- Porcheron, G., and Dozois, C.M. (2015) Interplay between iron homeostasis and virulence: Fur and RyhB as major regulators of bacterial pathogenicity. *Vet Microbiol* **179**: 2–14.
- Rao, N.V., Shashidhar, R., and Bandekar, J.R. (2014) Induction, resuscitation and quantitative real-time polymerase chain reaction analyses of viable but nonculturable *Vibrio vulnificus* in artificial sea water. *World J Microbiol Biotechnol* **30**: 2205–2212.
- Reed, L.J., and Muench, H. (1938) A simple method of estimating fifty percent endpoints. *Am J Hyg* **27**: 493–497.
- Sanjuán, E., González-Candelas, F., and Amaro, C. (2011) Polyphyletic origin of *Vibrio vulnificus* biotype 2 as revealed by sequence-based analysis. *Appl Environ Microbiol* **77**: 688–695.
- Shao, C.P., and Hor, L.I. (2000) Metalloprotease is not essential for *Vibrio vulnificus* virulence in mice. *Infect Immun* **68**: 3569–3573.
- Shinoda, S., Miyoshi, S., Yamanaka, H., and Miyoshi-Nakahara, N. (1985) Some properties of *Vibrio vulnificus* hemolysin. *Microbiol Immunol* **29**: 583–590.
- Simon, R., Priefer, U., and Pühler, A. (1983) A broad host range mobilization system for *in vivo* genetic engineering: transposon mutagenesis in gram negative bacteria. *Nat Biotechnol* **1**: 784–791.
- Teranishi, M., Naya, S., and Tada, H. (2016) Temperature- and pH-dependence of hydrogen peroxide formation from molecular oxygen by gold nanoparticle-loaded titanium(IV) oxide photocatalyst. *J Phys Chem C* **120**: 1083–1088.
- Tison, D.L., Nishibuchi, M., Greenwood, J.D., and Seidler, R.J. (1982) *Vibrio vulnificus* biogroup 2: new biogroup pathogenic for eels. *Appl Environ Microbiol* **44**: 640–646.
- Toledo, J.C., Bosworth, C.A., Hennon, S.W., Mahtani, H.A., Bergonia, H.A., and Lancaster, J.R. (2008) Nitric oxide-induced conversion of cellular chelatable iron into macromolecule-bound paramagnetic dinitrosyliron complexes. *J Biol Chem* **283**: 28926–28933.
- Tomich, M., Planet, P.J., and Figurski, D.H. (2007) The *tad* locus: postcards from the widespread colonization island. *Nat Rev Microbiol* **5**: 363–375.
- Towbin, H., Staehelin, T., and Gordon, J. (1979) Electrophoretic transfer of proteins from polyacrylamide gels to nitrocellulose sheets: procedure and some applications. *Proc Natl Acad Sci U S A* **76**: 4350–4354.
- Troxell, B., and Hassan, H.M. (2013) Transcriptional regulation by ferric uptake regulator (Fur) in pathogenic bacteria. *Front Cell Infect Microbiol* **3**: 13.
- Utada, A.S., Bennett, R.R., Fong, J.C.N., Gibiansky, M.L., Yildiz, F.H., Golestanian, R., and Wong, G.C.L. (2014) *Vibrio cholerae* use pili and flagella synergistically to effect motility switching and conditional surface attachment. *Nat Commun* **5**: 1–8.
- Valiente, E., Lee, C.T., Hor, L.I., Fouz, B., and Amaro, C. (2008) Role of the metalloprotease Vvp and the virulence plasmid pR99 of *Vibrio vulnificus* serovar E in surface colonization and fish virulence. *Environ Microbiol* **10**: 328–338.
- Valiente, E., Lee, C.T., Lamas, J., Hor, L., and Amaro, C. (2008) Role of the virulence plasmid pR99 and the metalloprotease Vvp in resistance of *Vibrio vulnificus* serovar E to eel innate immunity. *Fish Shellfish Immunol* **24**: 134–141.
- Wang, H.W., Chung, C.H., Ma, T.Y., and Wong, H.C. (2013) Roles of alkyl hydroperoxide reductase subunit C (AhpC) in viable but nonculturable *Vibrio parahaemolyticus*. *Appl Environ Microbiol* **79**: 3734–3743.
- Weinberg, E.D. (2009) Iron availability and infection. *Biochim Biophys Acta Gen Subj* **1790**: 600–605.
- Whitesides, M.D., and Oliver, J.D. (1997) Resuscitation of *Vibrio vulnificus* from the viable but nonculturable state. *Appl Environ Microbiol* **63**: 1002–1005.
- Wolf, P.W., and Oliver, J.D. (1992) Temperature effects on the viable but nonculturable state of *Vibrio vulnificus*. *FEMS Microbiol Lett* **101**: 33–39.
- Wright, A.C., Simpson, L.M., Oliver, J.D., and Morris Jr, J.G. (1990) Phenotypic evaluation of acapsular transposon mutants of *Vibrio vulnificus*. *Infect Immun* **58**: 1769–1773.

## Supporting information

Additional Supporting Information may be found in the online version of this article at the publisher's web-site.

**Fig. S1.** Categories of gene regulation after by comparing iron-stimulon with Fur-regulon. **(A)** Number of genes differentially expressed (DEG) by *V. vulnificus* per regulation category and replicon (two chromosomes and one plasmid). The categories are represented in a color's code. **(B)** Most significant motif derived from identified putative Fur boxes among virulence and survival-related genes studied returned by the MEME tool (Bailey *et al.*, 2009). The height of each letter represents the relative frequency of each base at different position in the consensus sequence.

**Fig. S2.** Hemolytic activity of *V. vulnificus* strains at short term. Absorbance of the supernatant of a bovine erythrocyte's suspension in PBS (1% vol/vol) incubated with bacterial cells **(A)** or bacterial extracellular products (ECP) **(B)** was measured at 520 nm.

**Table S1.** List of genes included in the iron-stimulon in *V. vulnificus* CECT4999. Only values of fold change  $\geq 2/\leq -2$  were considered, with a p-value cut-off of 0.01 (+, gene up-regulated in iron-rescription; -, gene down-regulated in iron restriction).

**Table S2.** List of genes included in the Fur-regulon in *V. vulnificus* CECT4999. Only values of fold change  $\geq 2/\leq -2$  were considered, with a p-value cut-off of 0.01 (+, gene up-regulated in  $\Delta fur$ ; -, gene down-regulated in  $\Delta fur$ ).

**Table S3.** Comparison of fold change values obtained by hybridization with the *V. vulnificus* array and by qRT-PCR.

**Table S4.** Results of the GLM (general linear modeling) univariate analysis of variance

**Table S5.** Identified putative Fur boxes among virulence and survival-related genes studied.